AD NUMBER

AD909667

LIMITATION CHANGES

TO:

Approved for public release; distribution is unlimited.

FROM:

Distribution authorized to U.S. Gov't. agencies only; Test and Evaluation; 07 MAY 1973. Other requests shall be referred to Air Force Avionics Laboratory, Attn: NVA/698DF, Wright-Patterson AFB, OH 45433.

AUTHORITY

AFAL ltr, 21 Sep 1978

AFAL-TR-72-374

E/O SENSOR PERFORMANCE ANALYSIS AND SYNTHESIS

(TV/IR COMPARISON STUDY)

Robert L. Sendall
Xerox Corporation/Electro-Optical Systems

and

Frederick A. Roseil
Westinghouse Electric Corporation
Defense and Electronic Systems Division

FINAL REPORT

APRIL 1973

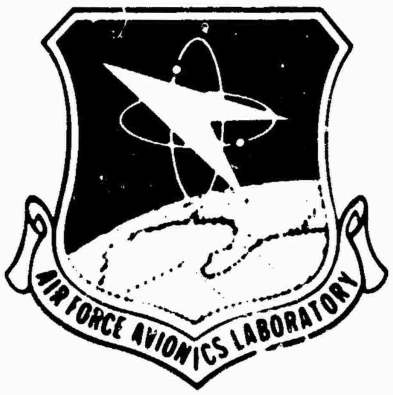

Air Force Avionics Laboratory
Air Force Systems Command
Wright-Patterson Air Force Base, Ohio

NOTICE

When Government drawings, specifications, or other data are used for any purpose other than in connection with a definitely related Government procurement operation, the United States Government thereby incurs no responsibility nor any obligation whatsoever; and the fact that the government may have formulated, furnished, or in any way supplied the said drawings, specifications, or other data, is not to be regarded by implication or otherwise as in any manner licensing the holder or any other person or corporation, or conveying any rights or permission to manufacture, use, or sell any patented invention that may in any way be related thereto.

Copies of this report should not be returned unless return is required by security considerations, contractual obligations, or notice on a specific document.

E/O SENSOR PERFORMANCE ANALYSIS AND SYNTHESIS

(TV/IR COMPARISON STUDY)

Robert L. Sendall
and
Frederick A. Rosell

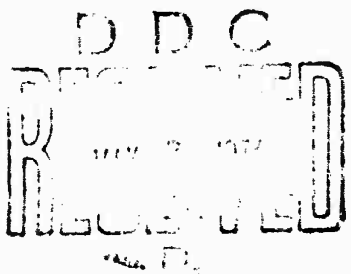

DISCLAIMER NOTICE

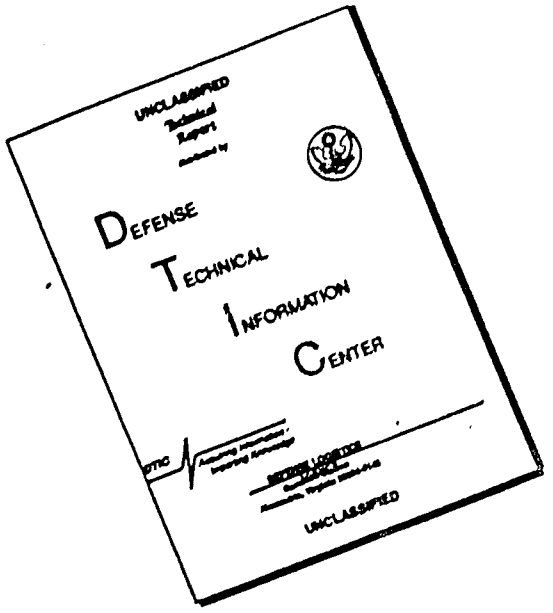

THIS DOCUMENT IS BEST QUALITY AVAILABLE. THE COPY FURNISHED TO DTIC CONTAINED A SIGNIFICANT NUMBER OF PAGES WHICH DO NOT REPRODUCE LEGIBLY.

FOREWORD

The effort documented within this report was sponsored by the Advanced Development Program Office 698DF of the U.S. Air Force Avionics Laboratory, WPAFB, under the direction of Mr. Frank A. McCann, Task Manager. Over the past few years, this office has sponsored a number of programs related to analyzing and evaluating real-time imaging systems. Under contract F33615-70-C-1461 with the Westinghouse Defense and Electronic Systems Division, a series of studies has been oriented toward evaluating and predicting the effectiveness of an operator viewing a noisy TV image. Other contracts with Westinghouse and directed by Mr. McCann have been related to flight and laboratory evaluation of low-light level television (LLLTV) systems. With EOS, laboratory and flight evaluation of a high-performance FLIR has been planned, monitored, and analyzed under contract F33615-71-C-1227, Captain M. Kiya, Project Engineer. In addition, under Project 5227, a High-Performance FLIR study, the tradeoffs associated with the design and performance of a FLIR system were analyzed in detail. This study was completed under contract F33615-70-C-1682 under the direction of Mr. B. Rayner, AFAL/NVT-2.

The effort reported here was a direct outgrowth of and builds heavily upon the foundation provided by the aforementioned programs. It is the intention of this report to discuss active TV and passive IR sensors, in as similar a manner and language as practical, pointing out the many similarities and explaining the few differences.

It was a joint effort primarily executed by Mr. Frederick A. Rosell of Westinghouse Electric Corporation and Mr. Robert L. Sendall of Xerox Corporation/Electro-Optical Systems with parallel and essentially identical contracts. Contract numbers are F33615-71-C-1868 and F33615-71-C-1869.

This report has been reviewed and is approved for publication.

WILLIAM J. DELANEY
Colonel, USAF
Chief Navigation &
Weapon Delivery Division

ABSTRACT

TV (LLTV and ACTV) and IR (FLIR) sensors, as real-time imaging systems for night operations, have become competitive for many applications. While both systems provide TV-type displays for an operator to view and are used in a similar manner, their uncommon backgrounds (evolutions) have resulted in different descriptive parameters and specifications. This report describes the two types of systems in a parallel manner and language so that persons familiar with TV can better understand IR and vice versa. The sources of signal information; i.e., differences in reflectivity for the TV and differences in temperature for the IR are covered so as to provide a better understanding of the differences and similarities of the inputs. The man as the final element of the system is discussed using the theory that the operator is a spatial and temporal integrator. Then with the approach of Otto Schade, Sr., and the result of the psychophysical tests of the coauthor, Rosell, the systems are analyzed and performance prediction equations are derived. While a detection/recognition theory for predicting results against objects of general interest is presented, the three bar object is the basic object for performance definition and detection/recognition theory development. For the IR system, the threshold temperature difference between the bars and spaces of the test object which allows resolution of the bars is called the minimum resolvable temperature (MRT). It is a function of the spatial frequency of the object. In a similar manner, the contrast required for resolution of a 3-bar object is used to define the minimum resolvable contrast (MRC) as a function of spatial frequency for an ACTV system. Analysis is provided to permit the prediction of these performance parameters, and typical curves are provided. Finally, based upon the analysis, methods for comparing TV and IR systems in laboratory/field tests are presented. Suggestions are presented on how tests starting with controlled laboratory tests, then controlled field tests against laboratory objects, then limited controlled field tests against tactical type targets, and finally extensive semicontrolled field tests all using two controlled sensors side-by-side could be used for comparison.

CONTENTS

CONTENTS (contd)

ILLUSTRATIONS

ILLUSTRATIONS (contd)

ILLUSTRATIONS (contd)

TABLES

SECTION I

INTRODUCTION

Television cameras developed for the military have many similarities to cameras used in commercial television broadcast studios but are of much greater spectral bandpass and sensitivity. Since the military TV cameras were developed in parallel with their commercial counterparts, it is only natural that common methods of evaluation and specification evolved as well. While the objectives of TV studio broadcasting and military reconnaissance may be quite different, many of the measurement and description techniques developed are applicable to both. The principal difference is in system specification. In military usage, emphasis is placed on the long-range detection of small objects under poor viewing conditions while in studio broadcasting the emphasis is on obtaining high-quality images of rather large objects at short range under near-optimum lighting and viewing conditions. There is, of course, considerable overlap between commercial and military TV applications.

In this study, we emphasize Active Television, or ACTV, systems which are range gated to reduce contrast degrading atmospheric backscatter effects. By the term active, we imply that an auxiliary scene irradiator, located at or near the television sensor, is used. However, passive TV or PATV, sensors will also be considered.

Real-time thermal imaging systems referred to as FLIR[1] have evolved from the IR family of line scanners, point source detectors, and radiometers. With this hardware evolution, parameters evolved based upon the radiometry and line-scan background.

---

[1] FLIR is an acronym for Forward Looking Infrared which refers to the original application of using the FLIR to look out the front of aircraft. Apparently, the term was first used by Texas Instruments, Inc.

The FLIR is a passive sensor. By passive, we purport that the FLIR senses radiacion which is either self-emitted by the scene or due to natural sources such as the sun, and reflected by the scene.

In more recent times, both military TV and IR systems personnel have been drawing from the technical well of imaging which includes work in optics, photography, and the more analytical TV efforts. Most exemplary and complete is the tremendous published works of Otto Schade (Refs. 1-10) covering a wide variety of imaging analysis, evaluation, and operator interaction.

Since both types of systems provide real-time images and are considered for similar applications, it has become necessary to evaluate their relative merits and compare the systems so that one can make a choice for a specific application. That choice may be to use one of the sensors, both of the sensors in a complementary mode, or neither of these sensors. Because of the different backgrounds, the equipment is usually evaluated in terms of different parameters by people who tend to understand only one of the candidates and therefore the issue has been clouded. While this study may not make such system choice decisions completely clear and automatic, it does establish a uniform language and approach to understanding the similarities and significant differences so that a meaningful comparison can be made for any given set of conditions. Using the analytical approach pioneered by Otto Schade, a common language does evolve. Therefore, the purpose of this study is to provide a common set of evaluation parameters where possible and explain and discuss required differences. In addition, system performance analysis equations are derived in parallel for TV and IR maintaining similarity for more complete common understanding. It is intended that anyone versed in either IR or TV can easily acquire the other discipline from this report. It is important, however, that since considerable emphasis is placed upon providing a parallel TV/IR discussion, many

special cases and subtleties have been glossed over. Because of this, the reader is referred to the final reports of the previous TV and IR studies (Ref. 11 and 12) which were the basis for this work and provide detailed discussions and derivations in the language of the native technology.

Section II presents a summary of the report and as such is a non-linear reduction indicating particularly significant results and conclusions without the use of equations.

Section III is the main body of the report and contains a detailed technical discussion. This section is organized in the same manner that the system is analyzed. The subheadings indicate the level of detail of the parameters being discussed. Throughout Section III, the pages are divided for separate IR and TV parallel writeups where the material cannot be described effectively by a single, general presentation. That is, when significant differences exist, they are written up as equivalents in a side-by-side format.

Section IV briefly describes a comparison approach in terms of laboratory and field tests based upon the results of Section III. It suggests which parameters need be tested.

Section V discusses some of the detailed considerations of planning a controlled-flight test of E/O Sensors. It is anticipated that this section would contribute to planning such a comparison-flight test.

SECTION II

SUMMARY

IR and TV systems have evolved from different backgrounds and in a competitive atmosphere. Because of this, while the overall systems are very similar, they are viewed differently. Many TV designers tend to misunderstand the IR, and the IR designers tend to misunderstand TV. To a large degree, this misunderstanding is a result of a language and analysis approach barrier.

It is the purpose of this study to provide a common language and parallel, if not common, analysis for describing performance of these systems. It, therefore, results in suggested parameters for laboratory comparison and methods and parameters for field comparison. It also provides the analysis for predicting these parameters.

First, in subsection 3.2, the general approach is to describe where the source of information that represents the input to the sensors is derived. The reasons for choosing contrast (Cm) as the scene parameter for TV and delta temperature (ΔT) as the scene parameter for IR and the effects of the atmosphere on each are discussed. A nominal equivalence based upon the guessed probability of occurrence of Cm and ΔT is suggested. This nominal equivalence means that given a TV system sensitive to a 100 percent contrast target of nominal size and average reflectivity of 15 percent, and an IR system sensitive to a 10^{o} ΔT target of the same size, we might expect to get nominally-equivalent images of general terrain, etc. This assumption is only presented to make possible a nominal equivalence, to indicate the need for more data on the probability of occurrence of ΔT and Cm, and to give a general feel for how the authors believe the typical scene variations are related.

Second, in subsection 3.3, the man as the final element of the system is discussed. It is assumed that the operator is a spatial and temporal integrator, and that he makes decisions based upon the signal-to-noise ratio that results (from this integration) being greater than a threshold. He is an imperfect temporal integrator (low-pass filter) of time constant t_i = 0.1 to 0.2 seconds. He is near-perfect spatial integrator over the image for small (less than 0.5^o) images. The output of the integration process is defined as the perceived signal-to-noise ratio SNR_p. The threshold value for detection has been redetermined by the co-author F.A.R. as 2.8 when associated with a t_i of 0.1 second. The many psychophysical tests by Rosell et al have not only established the threshold but supported and determined the limitations of the theory. This general theory is then applied to a single bar and the single bar of a periodic pattern to predict the detection of aperiodic and periodic objects. These predictions are then used with the John Johnson criteria of 2 lines on target for detection and 8 lines on target for recognition to provide a general theory of detection and recognition for a raster generated display. The compatibility between the SNR_p theory and the Johnson empirical criteria is very satisfying. The fact that raster can (and often does) limit performance is also discussed.

Then, in subsection 3.4, the system is analyzed in terms of how each component contributes to the overall system spatial frequency response (resolution) and signal-to-noise ratio. The signal-to-noise ratio which would be measured electrically in the video channel, SNR_v, is defined and the equations for its prediction from the characteristics of each system component are provided.

An expression for the SNR_p in terms of the SNR_v is derived for any raster generated system. This is the analysis which quantitatively ties the man into the system. This analysis also makes possible the prediction of the input signals required for detection/recognition.

The total system sensitivity is finally defined in terms of minimum temperature difference or contrast required for a bar to just be detected at the display. If the bar is one of a 3-bar pattern, we have minimum resolvable temperature (MRT) and minimum resolvable contrast (MRC). If it is a single aperiodic object, we have minimum detectable temperature (MDT) and minimum detectable contrast (MDC).

In Section IV, these concepts are then expanded to show how laboratory and field predictions and comparisons would be accomplished. The independent variable of spatial frequency which is meaningful in the laboratory is converted to range for a specific target for field comparison. The general problem of how to finally expand the comparison into many varied, real-word situations is discussed. It is recommended that even after initial controlled and limited field tests against bar charts and trucks, more diverse tests be planned. The initial tests will prove and/or modify the analysis so that generally the result of any situation should be predictable. However, it is still felt that flying the same pair of sensors in a well understood installation (calibrated by the limited field tests) would be worthwhile in determining which system really performs better under which conditions and when are they truly complementary. It would be hoped that such a test would result in many surprises which would lead to new applications and systems designs.

Finally, in Section V, a few specific comments are made on how to approach the problem of planning the controlled-flight test. It is heavily influenced by the experience gained from previous 698DF sensor flight test programs.

SECTION III

TECHNICAL DISCUSSION

3.1 INTRODUCTION

In order to compare a TV system to a FLIR, it is first necessary to generally define each and point out the characteristics which cause them to produce different responses to the same object. Both systems are real-time imaging systems presently providing a display similar to home television. Both can be described in terms of the same functional block diagram, shown in Figure 1. The sensor optically images and senses the image providing a coded electrical output which represents the scene. This video is processed electronically to prepare it for display, and then displayed as a visible image. The display is commonly a CRT-type display. Since the systems are so much alike, and since both are viewed by man, the analysis of the systems including the operator can, and in most cases should, be identical. Certainly the same techniques and approach can be used. Because of the completeness and extensiveness (Refs. 1-10) of the optical/photographic/television analysis and evaluation by Otto Schade and because of the verification and extension of the evaluation work accomplished by the coauthor, F.A.R., and because of the application and extension of this analysis to FLIR by the coauthor R.L.S., the techniques and approach of O. Schade will be employed for analyzing both systems.

The major differences between TV and IR systems stem from the different characteristics of the scene that cause the image. Both systems sense electromagnetic radiation received at the sensor. The general case of an imaging system is shown in Figure 2. Both sensors receive radiation from the background, foreground, atmosphere, and the object.

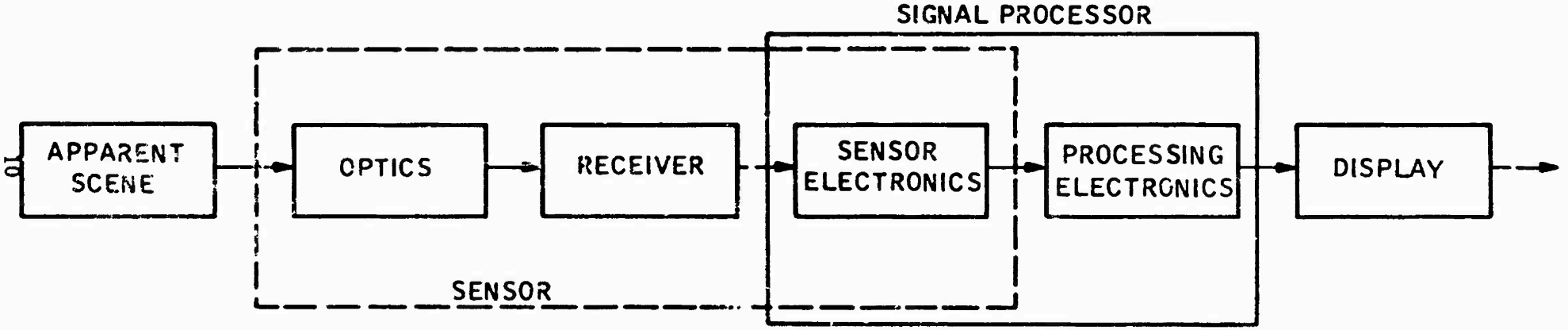

Figure 1. TV/FLIR Functional Block Diagram

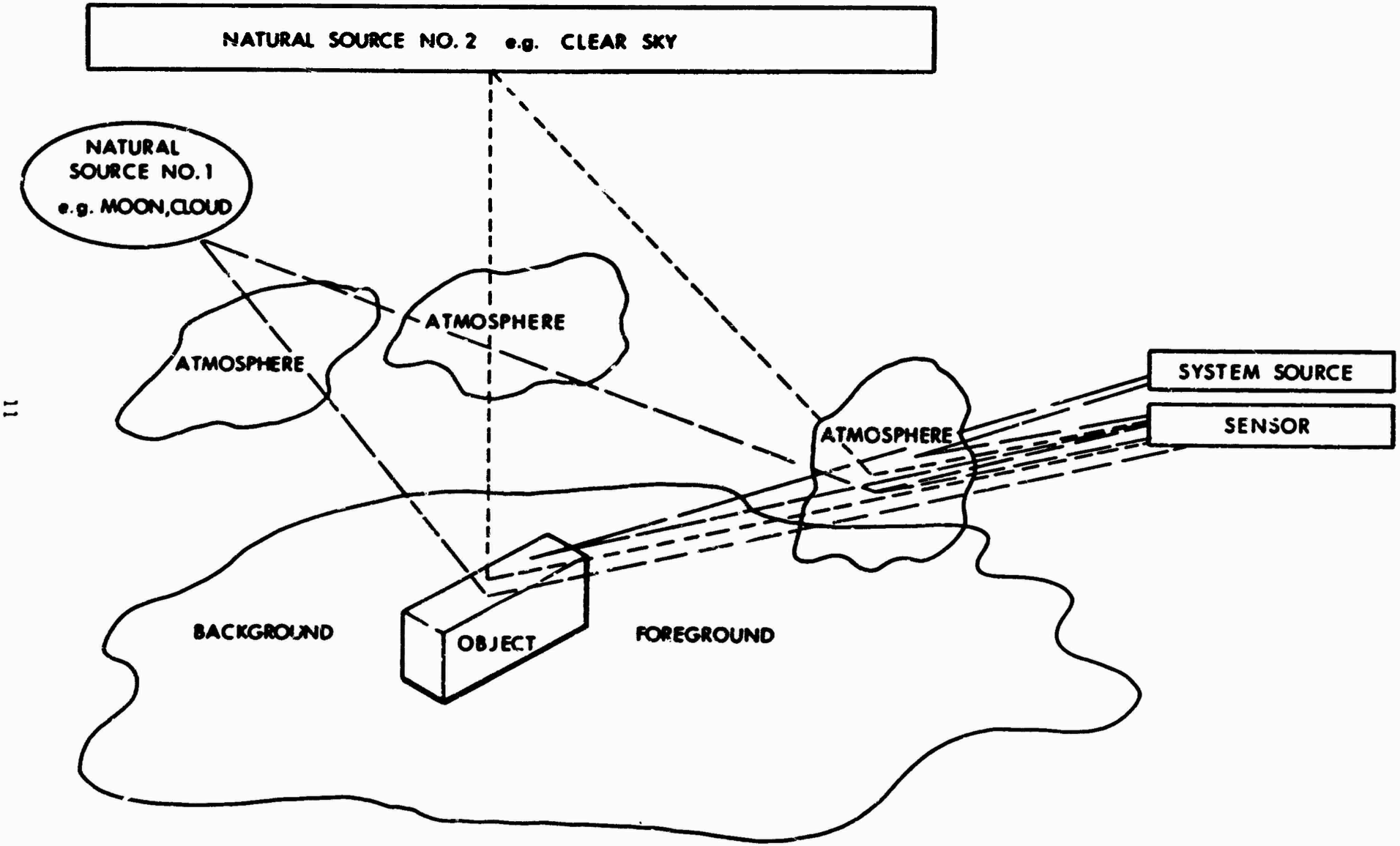

Figure 2. General Imaging Situation

ACTV

Current ACTV systems sense near-infrared radiation at wavelengths of 0.86 micrometer or longer. They derive their images from variations in radiation received. Mainly, these variations are due to variations in scene reflectivity. The radiation reflected from the scene is supplied by an auxiliary scene irradiator or system source located at or near the television sensor. The magnitude of the scene radiation signal is directly proportional to the system source power, differential scene reflectivity, and the one-way atmospheric transmittance. And, it is inversely proportional to the solid angle being irradiated and the square of the range between the sensor and scene.

PATV

Passive TV systems sense visible and near infrared radiation in the 0.4 to 0.9 micrometer band. Images are derived from radiation reflected differently from various objects in the scene. The reflected radiation originates at such natural sources as the sun (moon), stars, and sky.

FLIR

FLIR systems sense longer wavelength radiation either through the 3-5 micrometer or 8-14 micrometer atmospheric window. These systems derive their images from the variations in radiation received. These variations can be due to either variations in the emittance of the scene or variations in radiation reflected from the scene, or both. The radiation reflected from the scene can come from a variety of natural sources (clouds, sky, background, etc.) but is usually less than that associated with an ambient temperature blackbody. The primary scene signal is due to the variations in emittance and can be due to either variations in temperature or emissivity. That is, the scene is the source generating most of the radiation itself due to its inherent temperature. The ambient radiation is that associated with the average scene temperature and emissivity, and the signal is due to variations around the average.

Since radiation characteristics of a complicated scene can assume infinite variety, detailed analysis of any but a small number of representative typical cases becomes prohibitively costly and seldom warranted. The results would be a function of time not only because the radiation characteristics of objects vary, but because of aircraft motion and relative location of scene elements. For flight tests, it is important that scene variables be understood and controlled or measured. The proper choice and orientation of a simple test object makes possible the control of many of the variables and will be found to be imperative for a meaningful flight test. The task of relating a simple test object to military targets, as a function of ambient conditions, is one of the most significant and difficult tasks to be attempted in this study.

To the end of obtaining a simplified situation that has the number of variables reduced for measurement and analysis, the concept of equivalent object and apparent object is introduced. Figure 3 indicates the same situation as before but with the equivalent scene. Figure 4 indicates the apparent scene.

The equivalent scene simplifies the geometry by reducing the scene to a two-dimensional scene, normal to the sensor line-of-sight with both object and background at range R.

TV	FLIR
For TV, the equivalent scene may be considered to have zero emissitity and a constant average reflectivity. The average radiation signal reflected from the scene is the product of the average scene reflectivity and the high light scene irradiance due to the radiation source	The equivalent scene has emissivity equal to unity and therefore 0 reflectivity. The variations in radiation coming from the actual scene are generated in the equivalent scene by variations in temperature. The variation in temperature required

NOTE:

1. SCENE IS DIFFUSE REFLECTOR(EMITTER)AT RANGE R
2. SOURCE PROVIDES HIGHLIGHT IRRADIANCE OF E_H
3. FOR TV SCENE, CHARACTERISTIC IS RELATIVE CONTRAST (REFLECTIVITY)
4. FOR IR SCENE, CHARACTERISTICS ARE ΔT AND BACKGROUND TEMPERATURE, $\epsilon = 1$

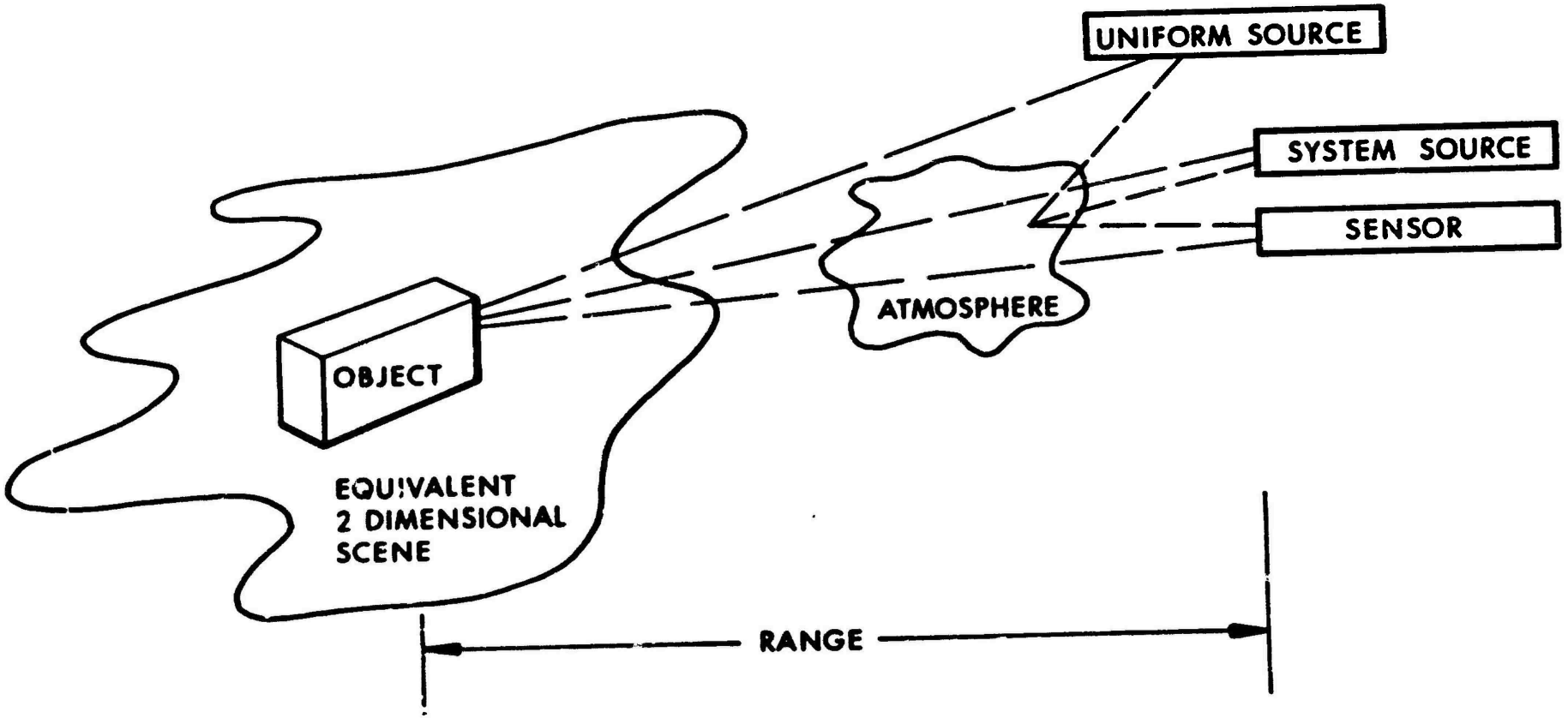

Figure 3. Equivalent Imaging System Situation

NOTE:

1. SCENE IS DIFFUSE REFLECTOR(EMITTER)WITH ANGULAR SUBTENSE
2. SOURCE PROVIDES APPARENT HIGHLIGHT IRRADIANCE OF E_H
3. FOR TV SCENE,CHARACTERISTIC IS APPARENT RELATIVE CONTRAST (REFLECTIVITY)
4. FOR IR SCENE,CHARACTERISTICS ARE APPARENT ΔT BACKGROUND TEMPERATURE, $\epsilon = 1$
5. ATMOSPHERE EFFECTS ARE INCLUDED IN APPARENT PARAMETERS

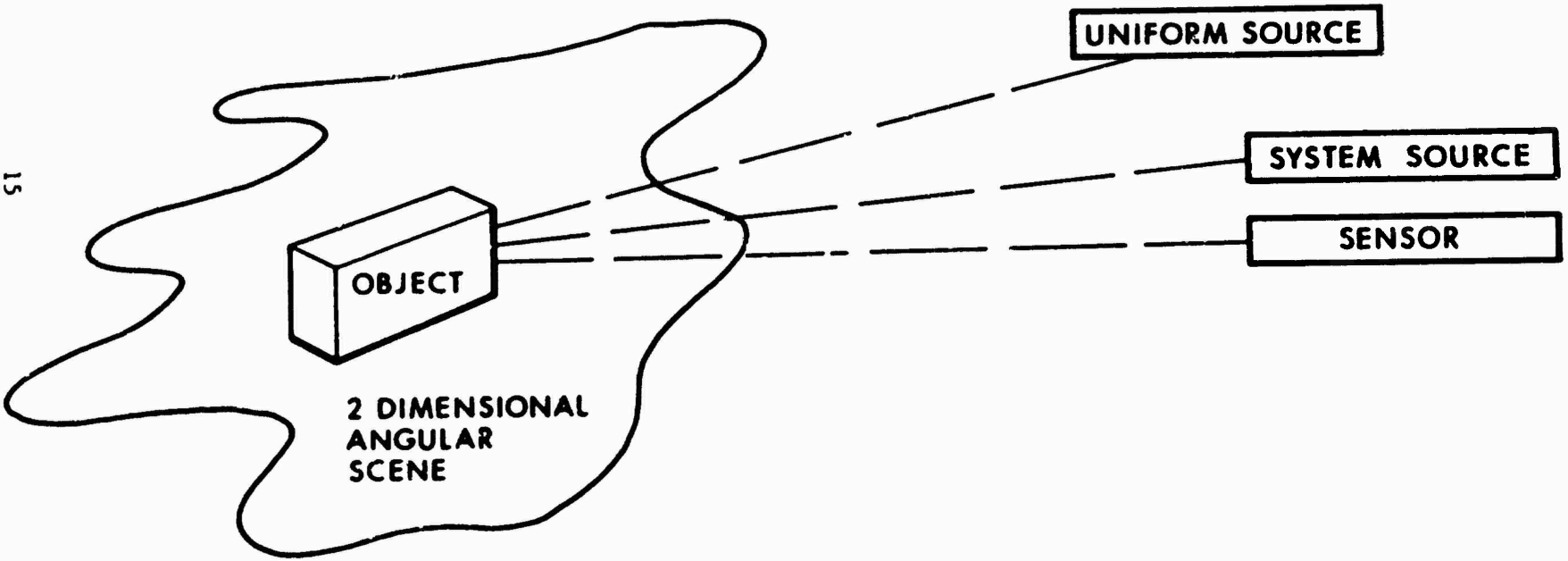

Figure 4. Apparent Imaging System Scene

TV	FLIR
as modified by the atmosphere intervening between the source and scene. The scene is considered to be diffusely reflecting. The variations in the radiation coming from the actual scene are generated in the equivalent scene by variations in reflectivity. It is customary to describe these variations in terms of contrast which is a ratio of the incremental scene reflectivity to the sum of the object and background reflectivity.	to simulate the scene would be a function of the spectral response of the system and differs from the actual temperature except for any blackbody sources in the real scene.
Therefore, the parameters of the average scene are the high light scene irradiance, E_H, the average scene reflectivity, ρ_{av}, and the scene contrast, C_m.	Therefore, the temperature of the background T, and the equivalent ΔT (depends on λ)* over the scene are the parameters of the equivalent scene.

The apparent scene is simply the equivalent scene modified by the range and atmosphere. The range converts the linear dimensions of the equivalent scene to angular dimensions and is an input to the atmospheric model.

Alternately, the apparent scene can be considered in terms of the irradiance (E) versus viewing angle at the input to the sensor. This is the actual signal of interest and in this case, the same nomenclature applies for both systems. However, for the IR system it is more convenient to

*Whenever using equivalent ΔT instead of irradiance we must never forget that it is a strong function of the spectral characteristics of the scene and the sensor.

work in terms of apparent ΔT and a parallel can be drawn for the TV in terms of apparent $\Delta\rho$ and E. In either case a parallel discussion is presented for completeness.

ACTV	FLIR
The atmosphere reduces the average scene radiance due to its two-way transmittance. The atmosphere may also degrade apparent image contrast depending on position of the scene object in the range gate. The apparent scene can therefore be considered to be diffuse with average reflectivity ρ_{av}, apparent modulation contrast C_m, and high light irradiance E_H.	The atmosphere reduces the variations in irradiance and, therefore, the apparent ΔT over the scene. It can also, by re-emitting and scattering, vary the apparent background temperature. The apparent scene has emissivity equal to unity with a background temperature T and ΔT variations as determined by the scene and the atmosphere.

PATV
The atmosphere reduces the apparent image contrast at the sensor by scattering signal out of the line of sight and by scattering scene source radiation into the line of sight. The scene parameters are otherwise the same as for ACTV.

In what follows, these concepts will be discussed so that relationships between real-world scenes and easily measurable and analyzable objects can be established. This will define the imaging system inputs. Then, the man as an element of the total system will be discussed to establish requirements for the outputs of the imaging system. Finally, for both systems the imaging systems analysis will be presented so that performance can be defined and predicted from design parameters. The man interface will be so important that it will affect performance measures, but the man as an element will be separated and treated as the final component of the complete system.

It should be realized that for laboratory testing the real, equivalent, and apparent scene are identical except for units. Since testing is accomplished against an apparent scene, it becomes necessary to relate this to the real-world and vice versa.

3.2 REDUCING THE REAL SCENE TO THE APPARENT SCENE

3.2.1 THE REAL SCENE

The real scene is a complex collection of objects, radiation sources, and atmospheres which determine the spatial and temporal variations in radiation reaching the sensor. Figure 5 indicates a typical situation.

Both systems sense and display the same basic geometrical outline, view reflections of backgrounds in the reflecting areas (such as ponds), and see areas that look like shadows although the IR "shadows" are usually not real time but history-developed temperature gradients. In the large, the scene (and therefore the system display) can look very similar. In the small, however, the details of some objects appear quite different in terms of relative emphasis.

This difference in emphasis is linked to the dynamic-range requirement for the system. The modulation for the general scene for TV is proportioned to the average or highlight brightness, except for a few point sources such as headlights. Therefore, AC and DC vary together. However, for the IR, the modulation is not really proportional to the average value, and there exist large area sources which have significantly great modulation with important small details. Because of this, the AC and DC gain versus display dynamic range question becomes important.

Another important difference is the effect of brush or camouflage that tends to break up the outlines but not totally block the object. In this case, the lack of real shadows and the tendency for the object to be its

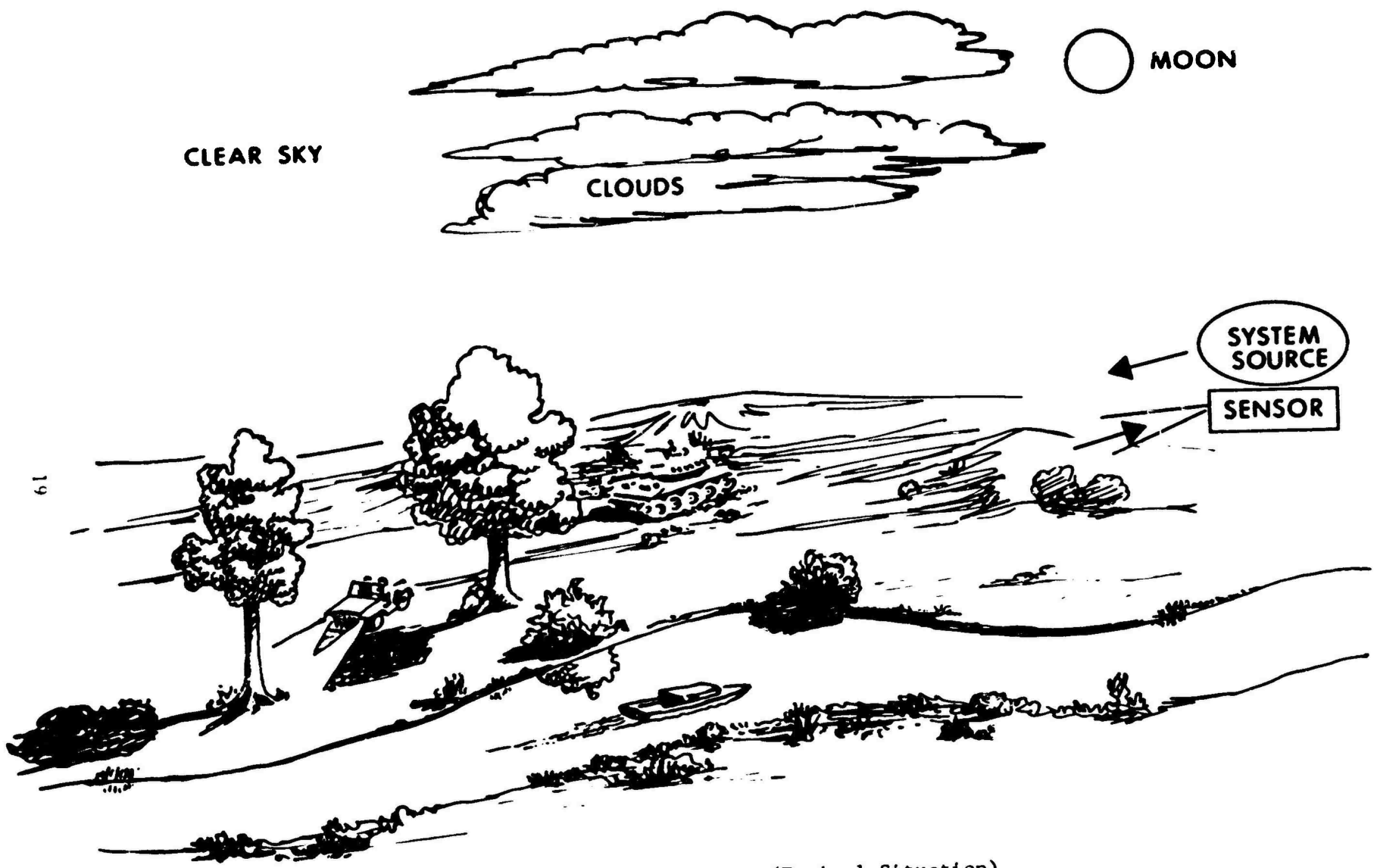

Figure 5. Real Scene (Typical Situation)

own source in the IR causes the IR system to provide a more distinguishable image. On the other hand, foreground clutter can sometimes be range-gated in ACTV to gain the same end.

Of course, the effects of the atmosphere, the moon, etc., are different.

TV	IR
The scene to be viewed consists of a source or a number of sources of radiant energy, an atmosphere intervening between the source and an object, the object itself and its background, and the atmosphere intervening between the object and the observer or electro-optical sensor. The sources may be either natural such as the sun, moon and stars, or auxiliary such as a searchlight. At times, the sources can be a combination of natural and auxiliary sources. However, for the sake of simplicity, we will consider sources to be either predominately one or the other and will analyze the cases separately since a slightly different approach is indicated in each case.	The IR system viewing the scene in the large, produces a TV-like image. It is interesting that trees and bushes generally appear significantly warmer (especially tree trunks) than the grassy ground. At night, the reflection of trees in the water tends to appear even warmer. This could occur for a variety of reasons: 1) the undersides of leaves may stay warmer than the top surfaces due to the fact they cool by radiation to a warm ground rather than a cold sky, 2) the emissivity of the leaves' undersides may be higher because of dew, 3) the sensor viewing the undersides of leaves off the water sees a cavity effect inasmuch as the water adds radiation and the reflection from the underside of a leaf sees another leaf, etc., so as to cause a blackbody effect while the top of the leaf reflects the sky.
A wide variety of natural sources can exist including the sun, stars,	In general, water appears cold due to the high reflectivity (low

TV	IR
moon, and skyglow. Unnatural sources, such as city light reflected off low clouds and even scene floodlighting when the floodlights are not at or near the sensor location, will nevertheless be considered as natural sources on the basis that the scene radiance passes only once through the atmosphere from the object to the sensor rather than twice as is the case for the auxiliary source. The two primary classes of natural sources are those which mainly provide diffuse scene irradiance and those which predominantly provide directional scene radiance. Clear night starlight and heavy overcast sunlight or moonlight represent diffuse sources while clear day sunlight and clear night moonlight would be examples of directional sources. There are obviously cases where both classes of source exist together and are of near-equal importance such as in light overcast sun or moonlight or when the moon is new or when	emissivity) especially at glancing angles. Looking down, as with a line scanner, the reflectivity may be less and can make the water appear warmer. If strongly overcast with a warm cloud layer, the water would appear warmer. It has been shown that clouds can cause daytime shadows that cool areas or can be seen by reflection (off metal, etc.), providing an apparent increase in temperature.[2] Of course, the actual temperature of the various objects is important and a function of time. Most objects in the scene get their energy (heat) from the sun (absorb heat during the day and lose it at night). The process depends upon the atmospheric conditions, the degree of overcast, and the general air temperature. If, as at Eglin Air Force Base, Florida, there is high relative humidity, cloud cover, and an air mass where temperature is almost constant, the temperature of objects in the scene tends not to

[2] Experiment for Captain Kiya, WPAFB, by Dale Green of EOS, Reported in Reference 13.

TV	IR
either the sun or moon are low on the horizon sky.	vary from day to night. Everything stabilizes at air temperature as though the whole system were inside a blackbody.
In diffuse light, the detectability of objects would be expected to be relatively independent of viewing angle since the lighting is nearly uniform in all directions, and the objects are shadowless or nearly so. The average scene constrasts also would be expected to be lower than in the case where lighting is directional. With the directional lighting, one expects sharp contrast shadows but object features may become unrecognizable except at certain viewing and source angles. For example, a black and white bar pattern on a panel may be clearly discerned when the moon is behind the observer, but with the moon behind the panel, the panel appears black.	The physical characteristics of the scene objects also affect the thermal inertia of the objects. Objects with low emissivity tend to take on the temperature of the air with a lag determined by the thermal mass (of the object) and the thermal conductivity. Materials that conduct poorly are apt to have surface temperatures which determine their radiation characteristics and which vary quite greatly. Objects with high emissivity are more likely to have their temperature strongly influenced by the physical characteristics of the scene objects and the radiation characteristics of the sky and atmosphere.
Naturally-irradiated scenes can assume infinite variety depending on the relative aspect angles between the scene object, observer, and the source or type of source. And, it becomes most	For the various natural objects, the IR scene varies with aspect angle, foreground, and background as well as atmosphere. The following summarizes the important parameters and their general relationships. The emissivity of the various objects is constant with time (except

TV	IR

difficult to divide the number of objects into a reasonable number of cases for analytical purposes. Hence, it is usual to assume that the source is either primarily directional or diffuse. If directional, it is assumed that an equivalent diffuse source can be defined.

The irradiance levels to be expected, whether day or night, are generally tabulated for typical scenes. Usually, the irradiance levels are measured with photometers which are compensated to have a spectral response similar to that of the unaided human eye. The resulting curves such as that shown in Figure 6 may or may not be relevant to electro-optical sensors which can have an entirely different spectral bandpass. The subject is discussed in some detail in Reference 12. However, it is assumed that by some means a natural source and scene object can be approximated by an apparent source and object of known geometry and radiance level. Usually, the apparent object and its background are assumed to be diffusely reflecting.

for dew, etc.) but a function of aspect angle. Therefore, it is a function of time when the sensor is moving. The temperature is a strong function of time as sky conditions, air temperature, and the effects of the sun vary with time. The apparent temperature of various areas of the scene is a strong function of the actual temperature, emissivity, and background. Man-made objects exhibit similar but different characteristics. They often have their temperature determined by heat sources other than the sun. When the sun and natural conditions determine the temperature variations on man-made objects, they present a very natural TV-like image. When they have temperature differences due to localized heating, the image can be very unnatural.

A truck, for example, looks like a truck when heated by nature. The cavity under the truck may appear hot if viewed from an angle, since by multiple reflection, this has emissivity of unity (cavity effect). In general, it appears as a truck often having dark metal areas due to low-emissivity surfaces reflecting the sky.

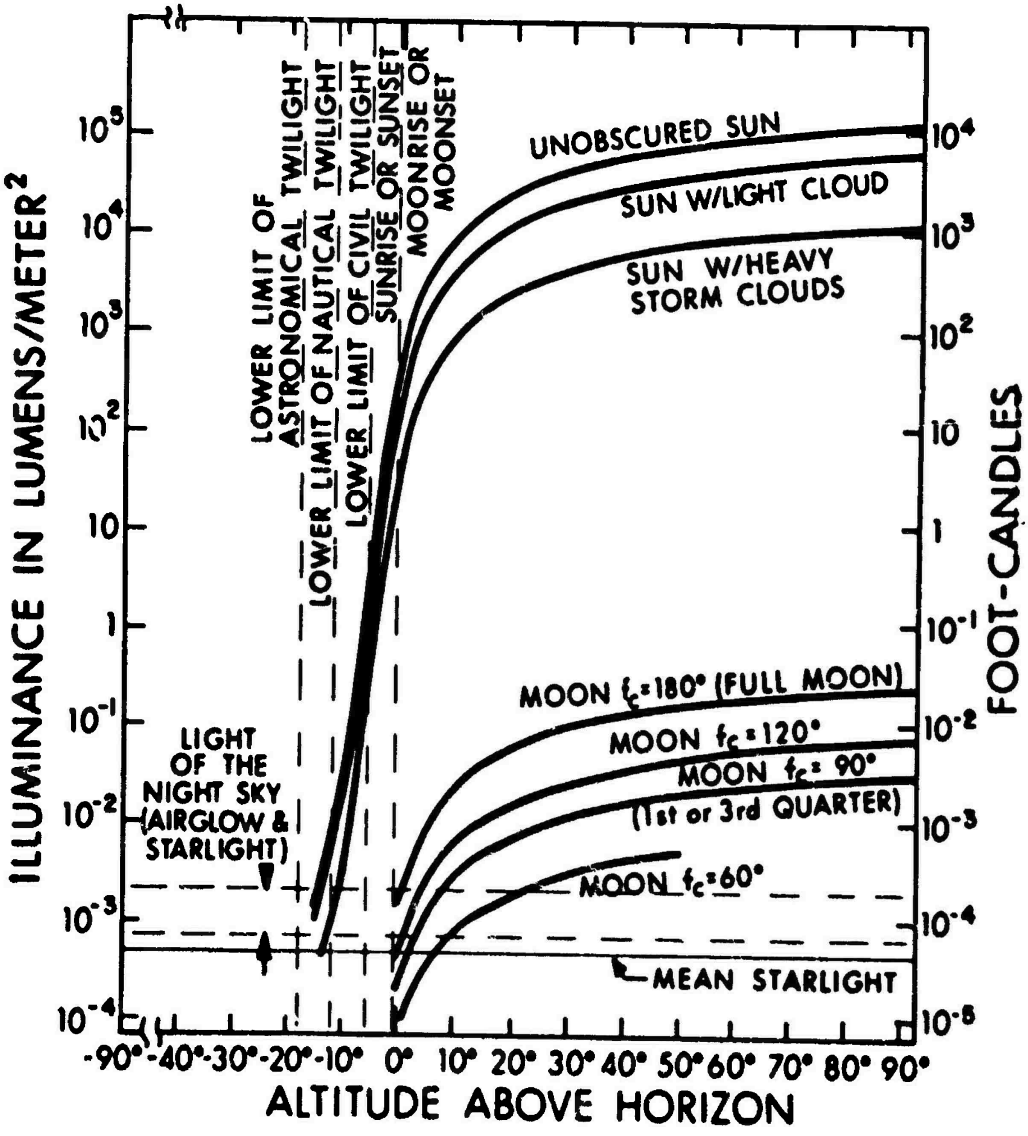

Figure 6. Illuminance Levels on the Surface of the Earth due to the Sun, Moon, and Light of the Night Sky

ACTV	IR
For ACTV, the scene is usually front lighted but may also be back lighted* depending upon the position of the range gate. Unlike natural directional sources, the ACTV scene is shadowless or nearly so. Bodies of water and glassy areas appear nearly black as do roads and streams which appear in strong relief. Specular reflections from man-made objects appear to be much more commonly encountered.	While idling, the engine and exhaust become very hot, exhibiting localized areas of radiation which tend to saturate the display. If the system is displaying hot as white, the extreme brightness can aid detection but degrade recognition. The localized heating would cause the hood of the truck, in fact the whole engine area, to appear very bright. By reversing polarity to hot as black, the picture often appears more natural.
Bright lights, which ordinarily saturate the passive sensor are of little consequence to the active sensor. Similarly, the horizon sky, which quite often prevents imaging just below a horizon treeline for the passive sensor (when the horizon is in the field of view), is ignored by the ACTV although the treeline can still be discerned.	If the truck is moving down a road, again there is localized heating, but not of the same type. The hood is often cooled by the airstream and, therefore, does not appear hot. The exhaust will still be hot and the under carriage will now be very warm providing a hot but usually non-saturating signature. The tires now appear hot.
The variation of scene irradiance from foreground to background, expected to be a problem with ACTV, has been a less serious problem	Similar comments can be made regarding other man-made objects. Tanks have such a large mass they nearly always appear warm, the exception being when parked in snow. Even after not running for days and then being exposed to rain, a tank can stand out as a uniform warm blob with the proper outline.

*Be silhouetted

ACTV	IR
than expected. ACTV systems are of course independent of natural scene light levels so long as the natural scene lighting is not too large. However, daylight operation in the active mode is precluded with the currently available exposure duty cycles and sensor, on-off, gating ratios obtainable.	If it is started, the engine and exhaust become unnaturally warm. After running around, the bogie wheels and treads as well as the rest of the tank, heat to provide a very natural picture except the whole tank is very warm and therefore bright when operating in a white hot mode.
While ACTV systems now in use, appear to have a significant advantage over PATV in night operations, they have not been significiently used to obtain a good feeling for their overall imaging qualities or capabilities. In general, image contrasts are much higher as one would expect due to the atmospheric range gating, but also are much higher in general than was expected even taking into account the generally higher scene reflectivities in the near infrared.	Buildings and bridges tend to look the way one would expect. For example, where obvious heating is dominant (i.e., smoke stacks) they tend to be bright, but otherwise look natural (i.e., TV-like). The notable exception is the metal roof of a Quonset hut which tends to have low-thermal inertia and low emissivity, and at night, reflects the sky, thereby appearing cold. Man-made objects, on or near water, have reflections which, at glancing aspect, can be very strong and even confusing. Other flat areas, such as roads, can also exhibit reflections. Roads and waterways at glancing angles often appear cooler due to reflecting the sky. An artificial temperature gradient or inversion is not uncommon.

3.2.2 THE EQUIVALENT SCENE

The real scene is a complete collection of objects irradiated by sources which vary in time both with regard to location and intensity. As was previously stated, this is too complicated to analyze for the general case. The first step in simplifying the situation is to define an equivalent scene of reduced complexity. The objects in the equivalent scene are two dimensional: they are normal to the sensor at the proper range; and they subtend the same angles to the sensor as did the actual objects.

TV	IR
The equivalent TV objects have zero emissivity so that their radiation characteristics are solely determined by their equivalent reflectivity and the average scene irradiance level. Each object in the scene is considered to be diffusely reflecting and each area in the scene is characterized by the high light irradiance level and its appropriate equivalent reflectivity.	All equivalent IR objects have emissivity of unity so their radiation characteristics are determined solely by their equivalent temperature. There are no reflections. Instead, the area of the scene has an appropriate equivalent temperature.

3.2.3 ATMOSPHERE

In both the cases, TV and FLIR, the equivalent scene is modified by the atmosphere providing the apparent scene. The radiation signal is attenuated as it passes through the atmosphere and the atmosphere adds a uniform masking radiation between the viewed object and the sensor. Small-scale changes in the index of refraction of the air (turbulence, scintillation) in the scene-sensor path degrade the geometrical fidelity of the received information.

In fact, the atmosphere is probably the most significant uncontrolled parameter in the electro-optical performance prediction relationship and can cause the greatest variations in predicted ranges. There are two reasons for this. First, it is difficult to predict the weather at most locations. Second, knowing the weather conditions at ground level it is often not possible to predict the slant path effect on performance.

Since this is such an important part of predicting actual performance, detailed discussions with appendices are presented with this report. A discussion on how the relative effectivenesses of the two systems might be compared for different atmospheres is presented in Section IV.

ACTV	IR
For an ACTV system, the effect of the atmosphere is strongly related to the source and its mode of operation with the system (i.e., range-gated or not). The system source may be a simple searchlight or a complex light emitting diode (LED) array or laser. These sources may be used in conjunction with a simple passive sensor or with a range-gated sensor. The source is considered to be near the sensor and to supply sufficient scene irradiance so as to make the contributions of natural sources, such as the moon, negligible.	Self-emission from the atmosphere and scattering from the ground, etc., cause the atmosphere to add a uniform radiation level to the scene. The primary effect of the atmosphere on FLIR performance, however, is not this background effect but the extinction of the signal (ΔT variations in the scene). At the wavelengths of interest for FLIRs, molecular absorption by the atmospheric constituents is a significant factor. (This has been treated by many models the most commonly used being that of Altshuler.) The first order selection of spectral

ACTV	IR
The atmosphere intervening between the system source and object has two principal effects on active imaging systems. First, the scene radiance is diminished due to scattering of source radiation out of the line-of-sight and secondly, a portion of the source radiation may be backscattered into the sensor's line-of-sight. The apparent scene radiance, due to the extinction of source radiation by the atmosphere, is given by	bands for operation of FLIR sensors is determined by the study of opaque versus "window" regions of atmospheric molecular absorption. The "windows" normally useful for FLIRs are nominally 3 to 5 micrometers and 8 to 14 micrometers.
$$L_s = \frac{\rho_{av} \Phi_s \exp\left(-2\alpha_o \bar{R}\right)}{\pi \Omega R^2} \quad (1)$$	Even within windows, some attenuation takes place at almost every wavelength, and the total amount of precipitable water vapor in the scene-sensor path has a profound effect on the extent of the transmission window.
Where ρ_{av} is the average scene reflectivity, Φ_s is the source power, α_o is the atmospheric extinction coefficient near the object, $\bar{R}$ is the optical slant range, Ω is the solid angle into which the source radiates, and R is the actual range from the source to the sensor. The factor of 2 in the argument of the exponential term expresses the fact that the source radiation is diminished both on its way to the scene and on its return to the sensor. The extinction coefficient is a function of the meteorological visibility and the wavelength of	It is axiomatic that if radiation can be absorbed at any given wavelength, then the absorber can also emit radiation at that same wavelength. Re-emitted energy is usually not a problem at visible wavelengths since when the visible energy is absorbed, it heats the atmosphere and is re-emitted at higher wavelengths. But FLIRs operate on thermal emissions and the air and the objects being observed are at about the same temperature. In the theoretically optimum FLIR, the single-system noise source is directly related to the random emission of

the source radiation. A typical scene radiance vs range characteristics is plotted in normalized form ($L_s/\rho_{av}\ \Phi_s$) in Figure 7 for various meteorological visibilities.

The second major effect of the atmosphere is to decrease image contrast. The contrast reduction in general terms is given by

$$\frac{C_r}{C_o} = \left[1 + \frac{\Phi_b}{\Phi_s}\right]^{-1} \qquad (2)$$

where Φ_b is the total flux returned to the sensor and Φ_s is the total signal flux. In a range-gated system, a short pulse of radiation is sent to the scene by the source. During the time of travel of the radiation to the scene and its return, the sensor is gated off. It is turned on at the precise time that the pulse returns. With a very narrow pulse and range-gate interval, the C_r/C_o ratio is essentially unity. The case for finite pulse durations but a narrow range gate is shown in Figure 8 and the case for a short pulse duration but various range-gate intervals is shown in Figure 9.

photons from the scene and intervening atmosphere. The smaller the spectral bandpass of the FLIR sensor, the less the noise. Including an opaque portion of the atmosphere transmission spectrum in a FLIR's spectral bandpass will therefore add noise without any benefit of additional signal. The specific selection of the spectral bandpass for a FLIR is therefore a compromise, maximizing available signal-to-noise over a wide spectrum of ranges and absolute humidities.

At FLIR spectral wavelengths, Rayleigh scattering is completely absent and Mie scattering, or more properly Mie extinction, has a much different characteristic than it does for visual wavelengths. At wavelengths shorter than approximately 1 micrometer, the imaginary index of liquid water is virtually zero. So, haze or fog droplets are essentially perfectly reflecting spheres (or non-absorbing resonators according to Mie's theory). However, at wavelengths common for FLIR's, the imaginary index of liquid water is significant and an appreciable amount of IR energy is absorbed

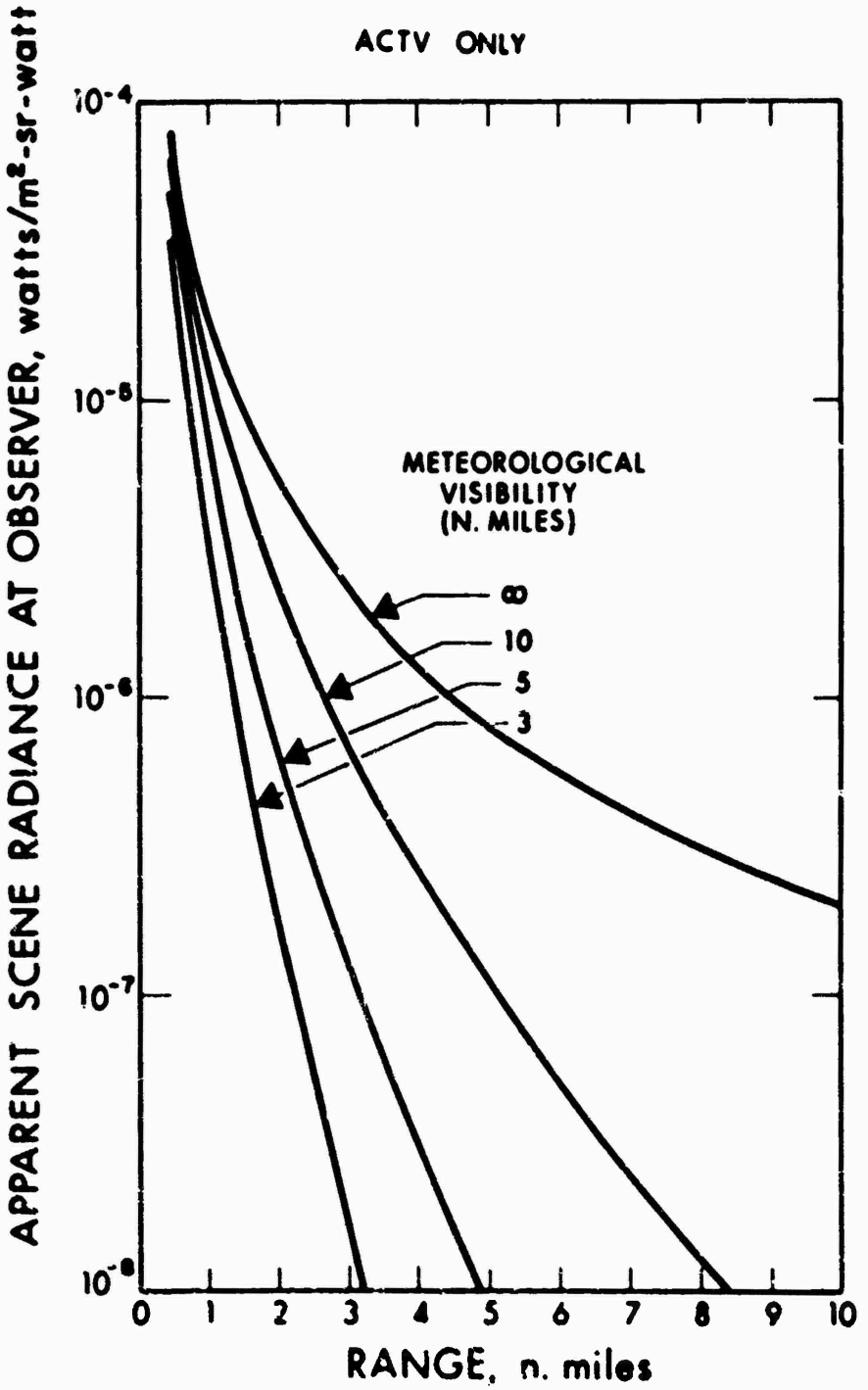

Figure 7. Apparent Scene Radiance at Observer's Location per Watt of Source Power for Scenes of Unit Reflectivity (Field-of-View is 4° x 4° and the Radiation Wavelength is 0.86 micrometers)

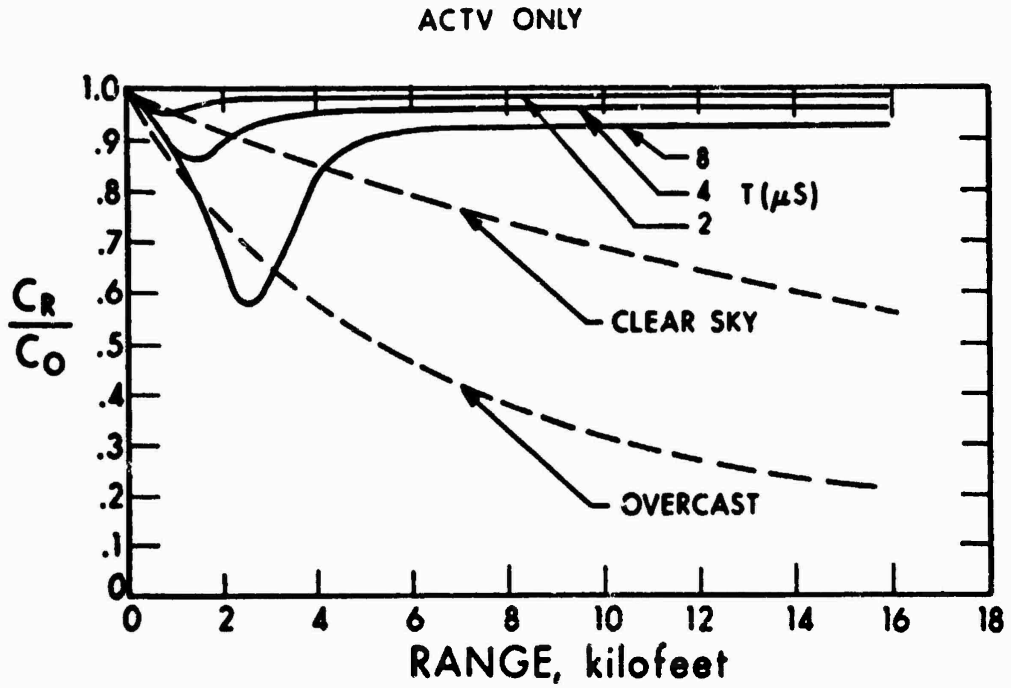

Figure 8. Ratio of Apparent-to-Inherent Contrast for (——) Range Gated Active and (- - -) Passive Sensors for Background Reflectivity of 20% and 10 Nautical Mile Visibility

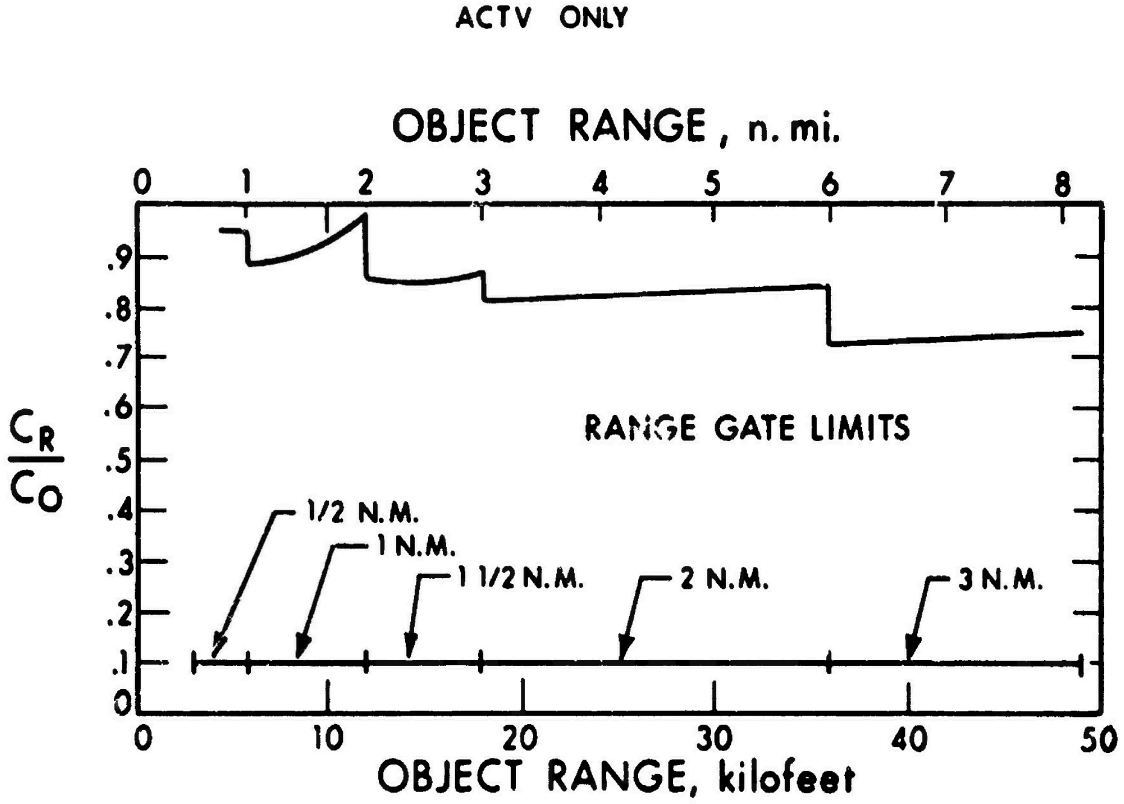

Figure 9. Ratio of Apparent-to-Inherent Contrast versus Range for Objects in the Middle of the Range Gate Limits Visibility at 0.86 micrometers is 10 n. mi. with Average Scene Reflectance = 0.2. T + 2 μs

43693

ACTV

In summary, the parameters for predicting the effect of the atmosphere on range-gated ACTV performance are the average scene reflectivity, meteorological visibility near the scene object, optical slant range, source pulse duration, and the position of the object in the range gate.

PATV

For a passive or PATV, the atmosphere has three principal effects. First, the atmosphere may in effect be the natural source as in the case of the sun just below the horizon. In this case, the light scattered by the atmosphere is the principal source. Secondly, the scene irradiance is diminished due to absorption and to scattering of natural source radiation out of the path between the source and object and finally, a portion of the source's radiant energy may be scattered into the sensor's line-of-sight. The levels of natural scene irradiance are not ordinarily calculated except in special instances but rather, are taken from tables and curves as noted above. The

IR

by the water droplet and re-emitted at the temperature of the air.

This absorption of signal energy and the scattering of signal energy out of the scene-sensor path serve to reduce the effective signal at the sensor. Aerosol extinction, which is a strong function of droplet size and therefore relative humidity, is discussed in Appendix I. In general, however, due to the wavelength dependence of Mie extinction, a FLIR operating in the infrared wavelengths will be less affected by a given haze or fog condition than will a TV sensor operating in the near visible wavelengths.

In summary, the parameters for predicting the effect of the atmosphere on IR performance are relative humidity, temperature, type of air mass, range, and when operating at high altitude (especially 3-5 μm) the other gas constituents. For 8 to 14 micrometer radiation, molecular absorption is a function of the total water in the path. For high-relative humidities, the transmission is dominated by particulate water absorption and

PATV

main effect of atmospheric scattering of radiation into the line-of-sight is to decrease image contrast.

TV

In dealing with atmospheric effects on contrast, it is usual to define two contrasts: the "inherent" contrast and the "apparent" contrast. The "inherent" contrast is the contrast of the object at range zero but along the line-of-sight from the observer's actual position at range, R, to the object. The "apparent" contrast is the actual contrast of the image at the observer's location. (See Figure 10.) The most general law for atmospheric contrast reduction is given in an extremely well written and interesting reference by Middleton (Ref. 14) as

$$C_R = C_O \left(\frac{N_{oo} - N_{bo}}{N_{or} - N_{br}} \right) e^{-\alpha_o \bar{R}} \qquad (3)$$

where N_{oo} and N_{bo} are the object and background radiance at zero range respectively and N_{or} and N_{br} are the corresponding quantities at range, R. Also, α_o is the value of

IR

scattering and is a strong function of particle size and density which is a strong function of relative humidity. As an example of the 8-14 μm transmission is included as Figure 11.

The best known data on atmosphere transmission in the IR was taken by Taylor and Yates. From this data Robert Grube of EOS developed a very simple but useful nomograph which is much more pessimistic than the optimistic predictions one gets with most computer programs based on Altshuler. This nomogram only holds for high-relative humidity and is simply based on empirical fit to the Taylor and Yates data. Figure 12 is a copy of Grube's nomogram reproduced from the High Performance IR Systems Study Report, Reference 11.

The nomograph utilizes two sources of data. First, the precipitable water per unit path length is determined using Hudson's nomograph (Ref. 15). By adding range to this nomograph, precipitable water in the path can be determined as a function of relative humidity, temperature, and range. Second, the relationship

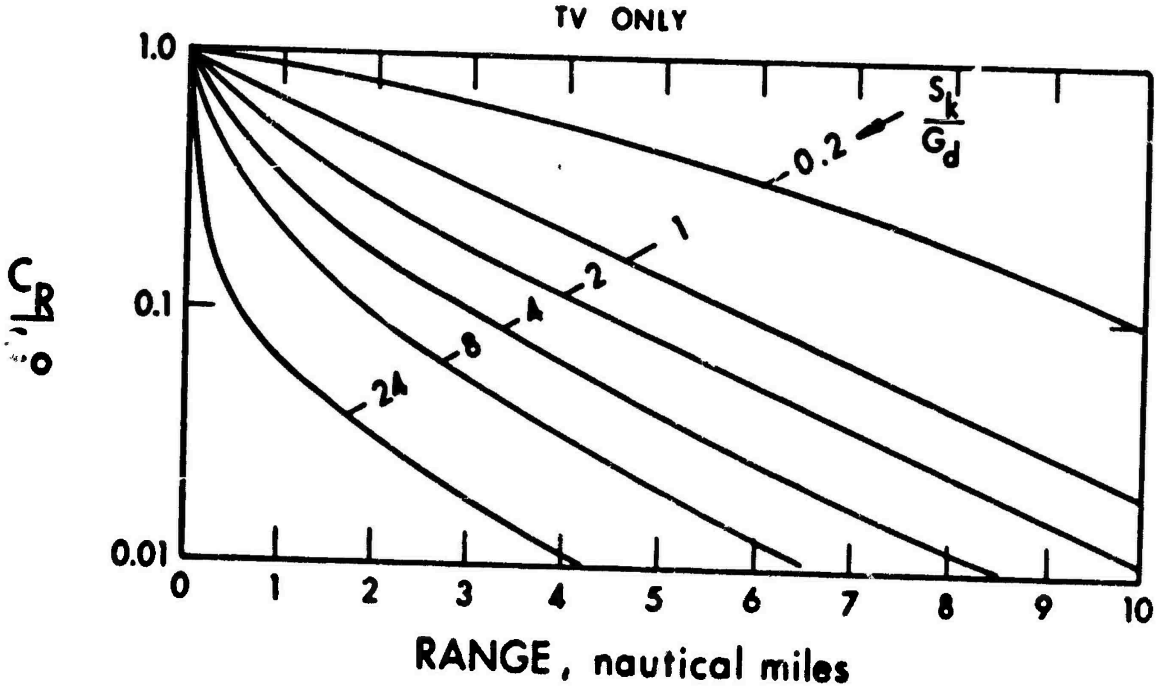

Figure 10. Ratio of Apparent-to-Inherent Contrast versus Range for Various Values of Sky-to-Ground Ratio for a Meteorological Visibility of 10 Nautical Miles

IR ATMOSPHERE

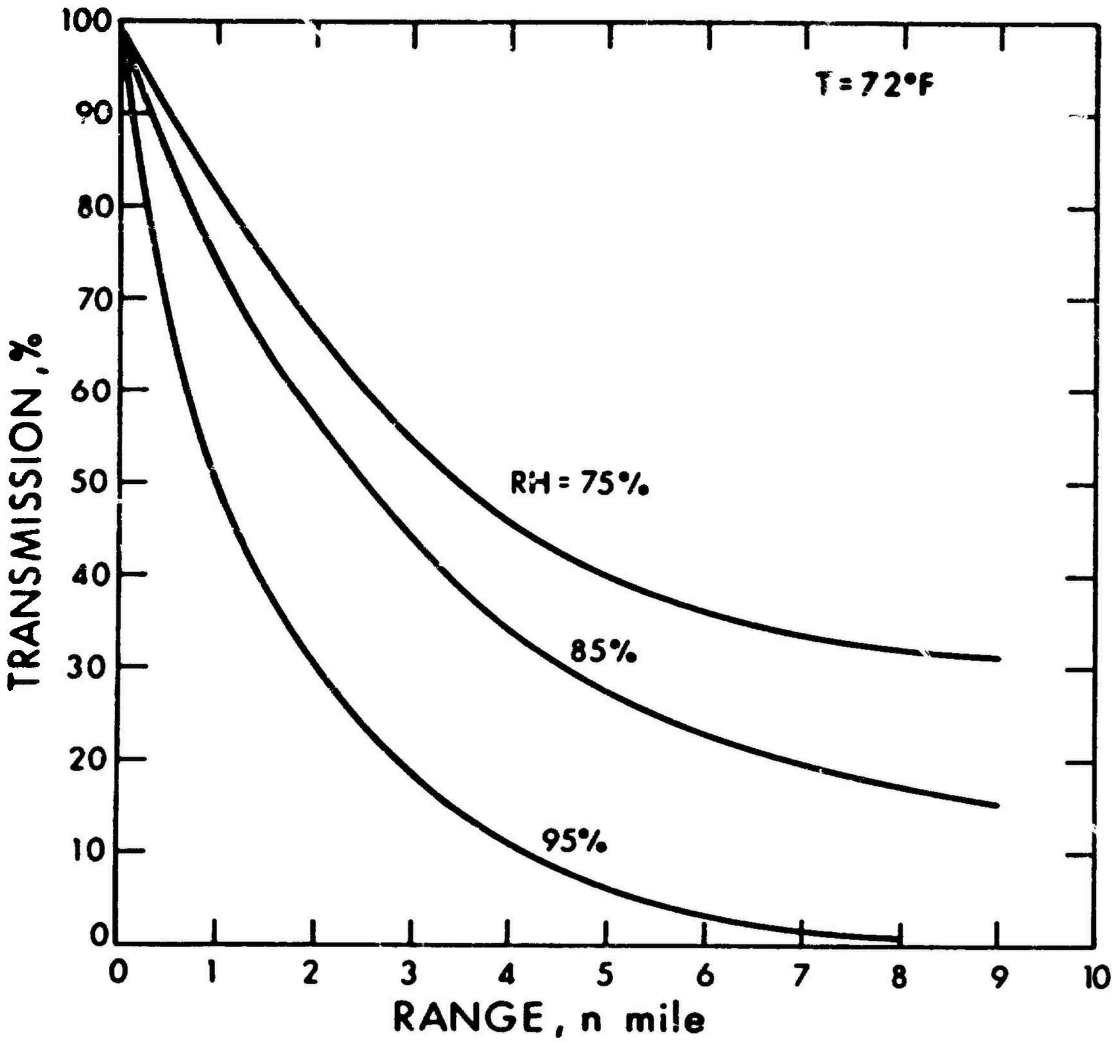

Figure 11. Atmospheric Transmission in the IR

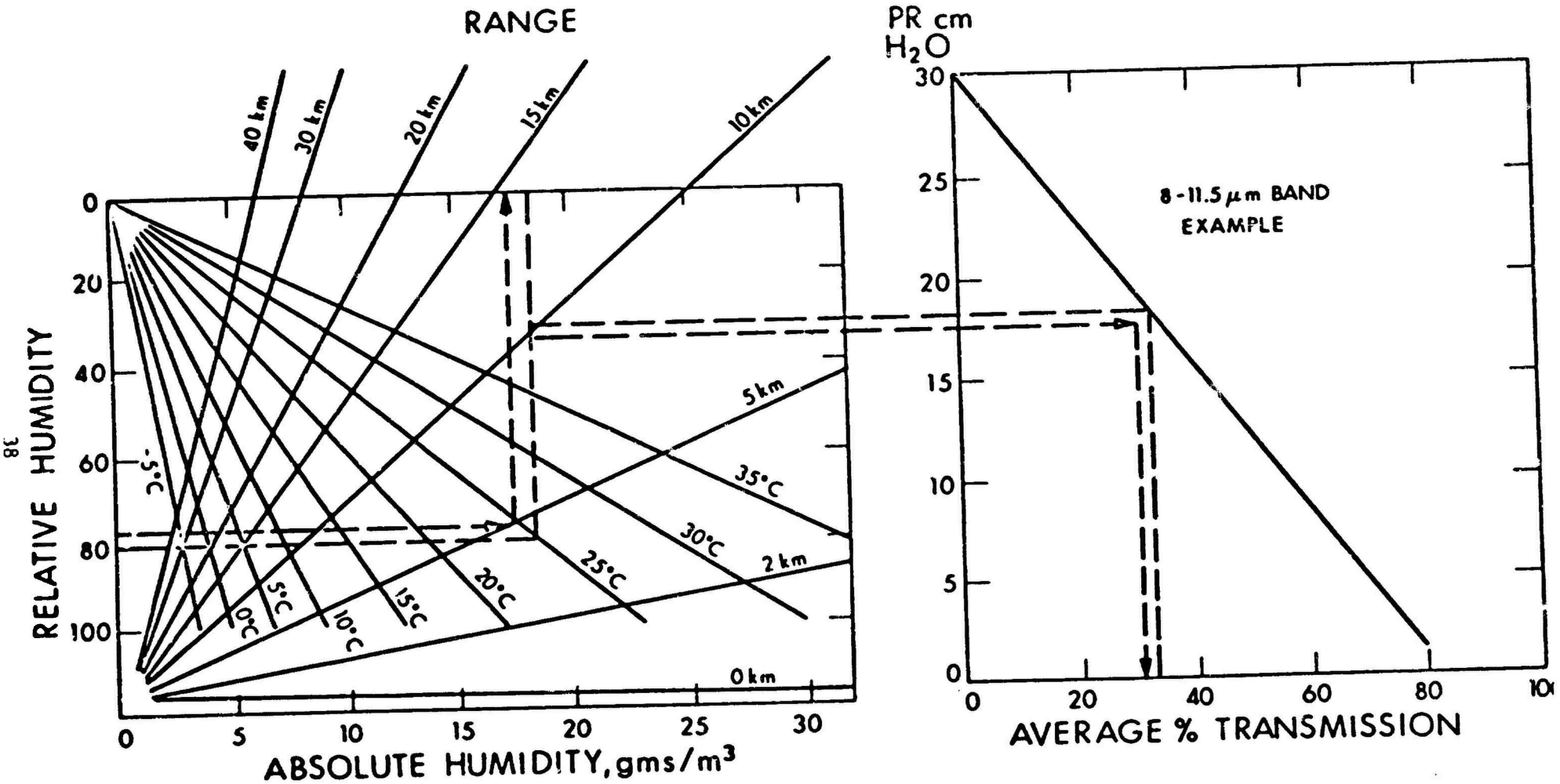

Figure 12. A Quick Look Technique for 8 to 14 μm

the atmospheric attenuation, or extinction, coefficient at zero range and $\bar{R}$ is the "optical slant range" and represents the horizontal distance in a homogeneous atmosphere for which attenuation is the same as that actually encountered along the true path of length R.

The general law of contrast reduction by the atmosphere depends upon the sky condition, viewing angle, source aspect angle, etc. For the special case of downward vision, which is the most important case for aerial surveillance, Middleton gives

$$C_R = C_O \left[1 - \frac{S_k}{G_d}(1 - e^{+\alpha_o \bar{R}})\right]^{-1} \quad . \quad (4)$$

Where S_k/G_d is a quantity dubbed the "sky-to-ground ratio". Its value is estimated to be

$$\frac{S_k}{G_d} = \frac{1}{\beta} \quad \text{(Overcast sky)}, \quad (5)$$

$$\frac{S_k}{G_d} = \frac{0.2}{\beta} \quad \text{(Clear sky)}. \quad (6)$$

where β is the average ground reflectivity.

between precipitable water and average transmission, as derived using Taylor and Yates' measurements, is used to convert precipitable water to average transmission.

The procedure for using the nomograph is as follows: for the example shown, a relative humidity line for 80 percent is drawn to intersect the 25°C temperature line. This determines an absolute humidity of 18.5 grams/m^3. The intersection of this line with the 10 km range line yields a water content of 18.5 precipitable centimeters in the path. The continuation of this line to the folding line provides an average transmission value of 33 percent. The procedure can be followed for other parameters as necessary, providing the pr. cm values fall within the limits shown: 1.3 pr. cm and 28 pr. cm.

TV	IR
In summary, the parameters for predicting the effect of atmosphere on PATV are the viewing direction, average scene reflectivity, sky condition, meteorological visibility, and optical slant range.	

For both TV and FLIR, the geometric fidelity of the scene is degraded as the optical energies pass through the atmosphere from the scene to the sensor. The general term for the effect is scintillation (as in stellar scintillation) although "turbulence" is sometimes applied when the effect is caused by wind.

The driving function for scintillation is energy transfer through the atmosphere. Consider a clear summer night with moderate relative humidity following a hot clear day. A large amount of energy will be leaving the earth's surface and radiating into cold space, traversing the atmosphere in the process. Air is opaque in portions of the infrared spectrum where most energy from a blackbody at usual earth environment temperatures is emitted. Thus, in moving through the atmosphere, the earth-emitted energy is absorbed and re-emitted by successive volumes of air. "Adjacent" volumes of air receive energy from different portions of the earth and so a dynamic system of "cells" (volumes-of-air) is created, each with a different temperature above or below the average air temperature. The index of refraction of air is a function of temperature so the cells have varying index. A plane wave-of-light, entering a volume of cells, will emerge with a modified wavefront.

The cells have various sizes and grow or shrink with time. The temperature differences (and so the scintillation) are strongest near the ground. The cells are blown about with wind.

For small angular areas within the sensor field-of-view, the overall effect of the source to sensor atmosphere path can have two components: a focusing lens effect and a wedge effect. The adjacent small angular area may or may not have the same optical effect. It depends upon the cumulative effects contributed by the cells along the two separate paths. Because of the possibility of wedge effects, energy from a single point of the scene may arrive at the sensor by two different length paths (in number of electromagnetic cycles) and constructive or destructive interference can occur for that point in the scene. The effects of scintillation are therefore exhibited as both geometric and amplitude distortion. (A shadowgraph of heat rising from a candle flame is an example of a related effect.)

If a long-time exposure photograph is made through a scintillating atmosphere, then the apparent effect on the system is as though the photographic system had a low MTF. The effect on a real-time system such as TV or FLIR is also similar to a loss in MTF but, it is dynamic. These dynamic effects on images are only now being subjected to rigorous exploration.

3.2.4 THE APPARENT SCENE

From the point of view of the sensor, it is looking at a two-dimensional (angular) radiation pattern. This pattern can be considered to be the equivalent scene modified by the atmosphere and converted to angular coordinates by the range to the targets. Therefore, the apparent object is an idealized two-dimensional (angular) object that, if viewed through a vacuum, would provide the same image at the output of the imaging system as does the actual object. The parameters used to describe the apparent object are the same as those used to describe the equivalent object since the apparent object is the equivalent object modified by the atmosphere between the object and the sensor. The following gives an indication of the TV/IR difference while discussing the defining parameters.

TV	IR
For a TV system,* the atmosphere reduces the contrast due primarily to the scattering of light from various sources into the view of the sensor. This increases the average irradiance of the scene while having little effect on the signal. In addition, the signal is reduced by absorption and scattering. The parameters for the apparent object are apparent contrast (C_a) with the peak reflectivity equal to unity and apparent highlight irradiance of E_H. All objects in the field are defined as totally diffuse. Alternately, the apparent scene can be defined in terms of the variation in irradiance at the sensor due to the scene as a function of viewing direction.	The IR apparent scene is made up of objects with emissivity equal to unity and varying temperature. The variations in temperature are those which appear to be present. In truth, they are actually determined by: 1) the temperature and emissivity of the object in the scene, 2) the radiation that sources reflect from the scene, and 3) the atmosphere absorption and emission. It must be remembered that it is radiation and not temperature variations that are being detected. Also, that the spectral distribution of the source radiation, the atmosphere absorption, and the sensor sensitivity must be included in the apparent temperature difference determination.

3.3 THE MAN AS THE FINAL THRESHOLD FOR THE SYSTEM

3.3.1 INTRODUCTION

Up to now, we have discussed in detail the input to the system. Before proceeding with the analysis of the hardware, it is desirable to discuss the man as an element of the system since he does in fact act as the final threshold/decision maker.

*For ACTV the amount of contrast reduction is significantly less than for PATV and often negligible.

"On a clear day, one can see forever." While the popular statement is undoubtedly optimistic, it is certainly true that one can see the sun by clear day, and the stars by clear night, at considerable distance. From a more practical viewpoint, the objects of our attention are more likely to be more mundane terrestrial objects at modest range. These objects may be seen with greater or lesser clarity depending on the acuity and sensitivity of the observer and the range, size, and incremental exitance of the object. Sometimes, it will not matter whether the object is seen at a given level of discrimination or not while at other times it may be vital. In general, our concern will tend to favor those conditions under which the observer is highly motivated to observe scene objects with some intended purpose in mind such as navigating in a boat or aircraft, detecting a criminal act, or differentiating between friend or foe. Supposing the observer to have some purpose in searching for scene objects, it follows that he must observe the object at sufficient range if the intended purpose is to be served. For example, it is of little comfort to detect the presence of another aircraft too late to avoid it.

Thus, the range at which an object can be observed with "sufficient clarity" to perform some useful task is of considerable interest. The words "sufficient clarity" should be stressed. In one case, it may be sufficient to merely detect a blob such as a channel buoy. In other cases, a much higher level of object detail is needed. For example, it is of no use to televise and record a burglary if the recording's acuity is insufficient to identify the burglar in a court of law. In the usual case, by range, we imply the maximum range at which we can just barely resolve the object if it is the mere presence of the object in which we are interested. If the object such as the burglar is to be identified, then we would be interested in the maximum range at which the subject's features can barely be discerned. In short, range implies a threshold, but the threshold depends upon the level of object discrimination required. The various levels of discrimination usually defined are detection, orientation, recognition, and identification.

The primary interest herein is in the performance of a man augmented by an electro-optical sensor. The procedure used is to associate a signal-to-noise ratio with an image as it appears on the output of the sensor's display and then, the signal-to-noise ratio required by the observer is determined through experimentation. By relating the signal-to-noise ratio required by the observer to that provided by the sensor, threshold range can be computed. In this analysis, the image signal-to-noise ratio is computed on the basis of an equivalent test object of simple geometry but with characteristics like the real object. The premise is that the detectability of a simple test object can be correlated with the detectability, recognizability, or identifiability of the real object by suitably selecting the parameters of the test object.

For any given system and set of scene variables, the range at which the man can perform his task becomes the parameter of interest. What follows will be aimed at predicting ranges.

The task will therefore be the three related tasks of: detection, recognition, and identification. While detection can be thought of (in most cases) as independent of the others, the other tasks are successively higher order tasks dependent upon the successful completion of the lower order tasks. We can speak of the probability of detection without implying recognition but the probability of recognition implies that the object was first detected. Therefore, we can consider the conditional probabilities:

$P(D)$ = Probability of detection

$P(R/D)$ = Probability of recognition given detection

$P(I/D)$ = Probability of identification given recognition

Actually, the probability of detection will be unity whenever enough information for recognition exists. However, the concept is worth expressing since time may be limiting the search volume and $P(D)$. The probability of identification $P(I)$ then becomes

$$P(I) = P(I/R)\ P(R/D)\ P(D) \qquad (7)$$

We will first consider the simplest case, the one upon which all higher-order cases depend, that of detection.

3.3.2 CONCEPTS

The basis of what follows is that the observer (brain) is a spatial and temporal integrator over the conditions of interest and makes a detection based upon statistical significance, i.e., a spatial distribution of brightness appears statistically significant (brighter or darker) compared with the surround. Because of this, only the perceived signal-to-noise ratio matters. To clarify these statements, we must define spatial and temporal integration, perceived signal, perceived noise, and resolution.

3.3.2.1 Temporal Integration

A temporal integrator is a device which integrates over time. If a constant amplitude input is applied, the output response is proportional to the duration of time over which the input is applied. For the eye, if the total duration of a light stimulus is much less than 0.1 second, the response is proportional to the duration of the input. Extending the duration of exposure can be traded off directly with increasing amplitude. For longer response times, as the duration is extended, the operator's memory gradually fails until no additional integration occurs. That is, the operator acts as an imperfect integrator with an integration time of between 0.05 and 1 second.

The effect of the phenomenon that is of interest here occurs if an observer is presented with a noisy picture in a repetitive fashion. First, if the rate is greater than about 20 fps, it will usually appear to be a continuous presentation. Second, if the noise from frame-to-frame (picture-to-picture) is uncorrelated (independent) while the picture is the same, the picture will appear to have a higher signal-to-noise ratio than any particular frame. This second result occurs because of the effects of

integration on noise. If the noise is random, then the total noise is proportional to the square root of the integration time. Since the signal increases proportionally to time and the noise only as the square root, the signal-to-noise ratio increases as the sqaure root of time or as the square root of the number of frames per integration time.

Film is a good integrator over a limited region of time. Since it is nearly perfect over its linear range, there is relatively no decay of signal and consequently it will saturate if the integration time is too long. However, by using a finite time for the integration and by synchronizing a perfect integrator with a signal, one can indicate the gain due to integration that is available. The actual signal integration time is a function of the display brightness. At high brightness levels, it may be as low as 0.05 second while at low display brightness, it may be much longer but is typically 0.1 second. Section 8.9 of Reference 16 presents an interesting discussion on this subject which indicates that training improves the memory of the observer for some specific cases and that by using long persistence phosphors to increase integration time (memory) it requires a very long phosphor decay time (seconds) to show any improvement in signal-to-noise ratio. There are a number of reasons to believe that the integration time varies with average scene brightness.

An effective integration time of 0.1 second, which is believed consistent with the usual display brightness, will be used here for calculating the improvement in perceived signal-to-noise ratio due to integrating a number of independent frames. Therefore, for a 30 fps system, the perceived signal-to-noise ratio will be $\sqrt{3}$ times the single frame signal-to-noise ratio.

3.3.2.2 Spatial Integration

For our purposes, a two-dimensional spatial integrator is a device which has an output proportional to the integral of the signal over a two-dimensional area. The eye/brain appears to function as a two-dimensional

synchronous integrator, integrating only over the area of the object for objects of angular extent less than 0.5^{o}. It appears that for white noise, the brain perceives a signal-to-noise ratio which improves as the square root of the area of an object as would be the case if the brain indeed integrated over the area of the object. That is, the signal upon which a detection decision is based is proportional to the area of the target and the noise is proportional to the square root of the area of the object.

This hypothesis has been extensively stated and empirically shown for the noisy display case for both film and TV by O. H. Schade, Sr., (Ref. 5). Detection tests by F. Rosell (Ref. 12) have shown that this relation is nearly perfect for targets of different shape and aspect ratio over a considerable range. All this work assumes that the TV or film is linear, i.e., small signals on a brightness threshold are being considered.

3.3.2.3 Perceived Signal

The perceived signal is the signal which the operator appears to use to make the detection decision. It includes the spatial and temporal integration.

3.3.2.4 Perceived Noise

The perceived noise is the noise which appears to affect the operator when he makes the detection decision. It includes the spatial and temporal integration. It is not the noise he acknowledges seeing.

3.3.2.5 The Eye Response Function

The optical part of the eye has an MTF which should be considered as a component. This MTF was measured by F. W. Campbell (Ref. 17) and from

his data we have found the eye to have a resolution as defined in Appendix II as (r_{eye}) equal to 1 to 2 mrad depending on pupil diameter (i.e., brightness level). O. H. Schade, Sr., also determined r_{eye}. Figure 13 represents r_{eye} versus brightness from both sources. In addition r_{eye} as derived from Blackwell's data and theory presented in the following is also presented in Figure 13, - it includes total eye effects.

Since the eye views the display, which has an angular subtense related to the angular subtense of the sensor by the system magnification, the resolution of the eye appears to be improved by the magnification. That is, in object (target) space the eye has a resolution r_{eye}/M where M is the system magnification. M is defined as the ratio of the angle subtended by a target at the eye to the angle subtended in object (target) space. For example, if the system had a magnification of 10, a target subtending 1 mrad to the sensor would appear as 10 mrad to the eye or the eye would appear to have 0.1 to 0.2 mrad resolution in object space.

Figure 14 summarizes the above statements for a system consisting of a sensor and display. Figure 15 then is a plot from this (approximate) analysis showing the effect of display size (magnification), on the total effective resolution. As will be shown, effective resolution (r_{tot}) is inversely proportional to recognition range for a non-absorbing atmosphere and, therefore, it is to be optimized. As the display size (magnification) is increased, the total resolution becomes equal to the system resolution and, therefore, independent of the eye limitation.* When the system resolution equals the eye resolution divided by the magnification, 70 percent of the maximum range is possible. Higher magnification improves r_{tot} (also range) slowly, but lower magnifications degrade performance significantly. This is more clearly shown in Figure 16

*It should be remembered that this discussion of display size does not include the effect of raster or other display blemishes. If these blemishes are pronounced, it may be best to sacrifice total resolution so that the operator is not preoccupied with them. A strong raster line should never subtend more than 0.5 mrad per line at the eye.

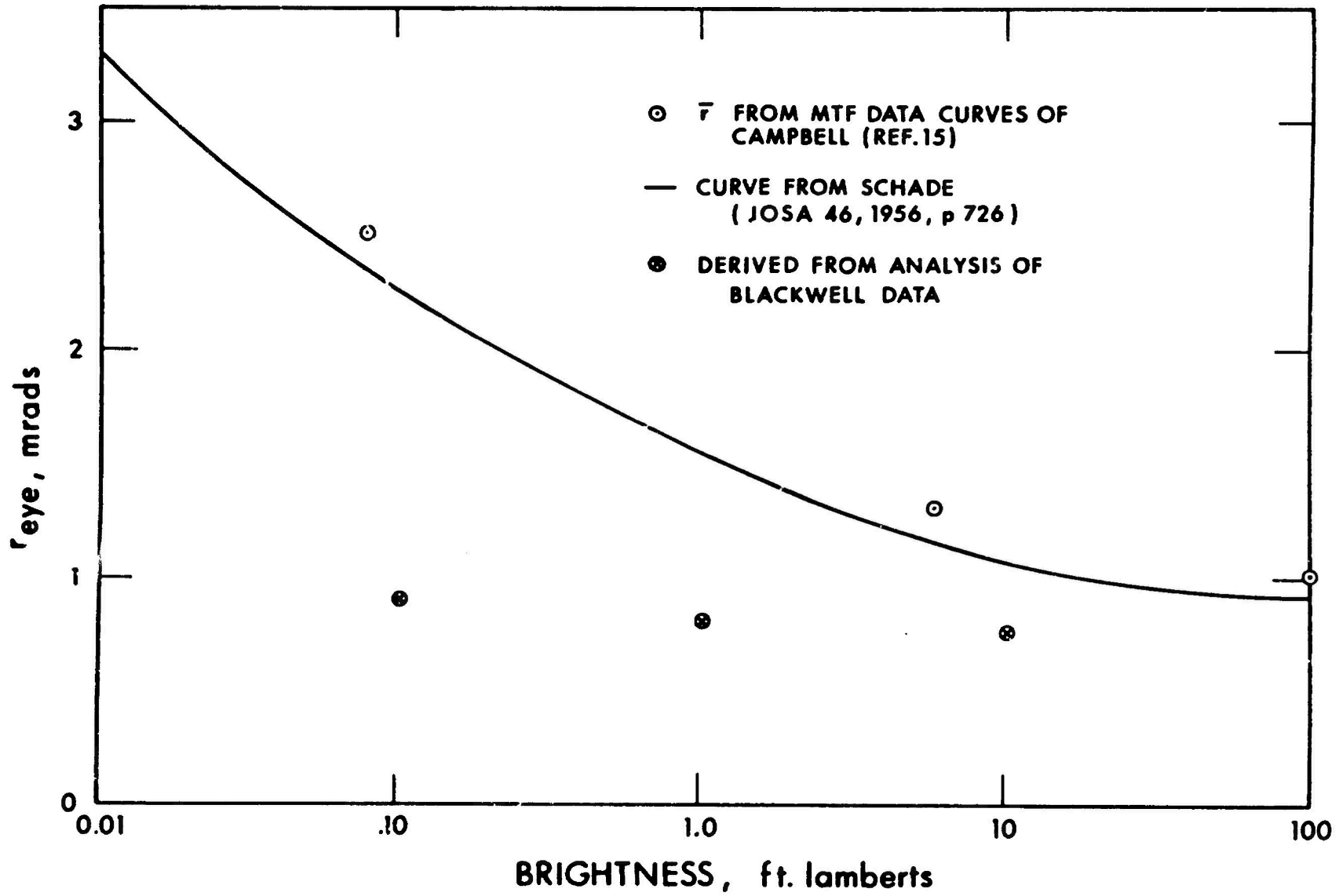

Figure 13. Equivalent Resolution of Human Eye Optics

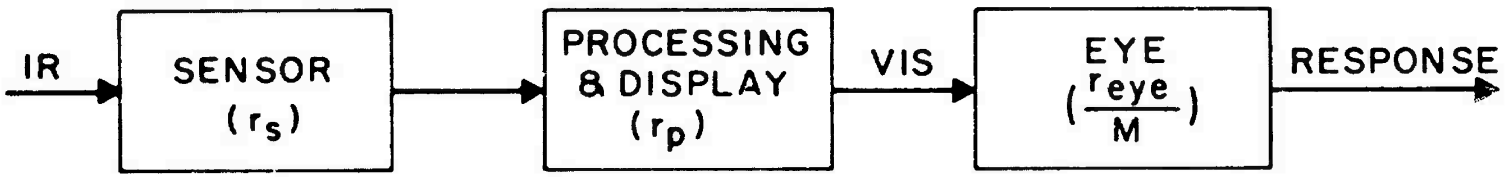

$$r_{sys} \approx \sqrt{r_s^2 + r_p^2}$$

$$r_{toi} \approx \sqrt{r_{sys}^2 + \left(\frac{r_{eye}}{M}\right)^2}$$

Figure 14. Resolution as an Analysis Tool

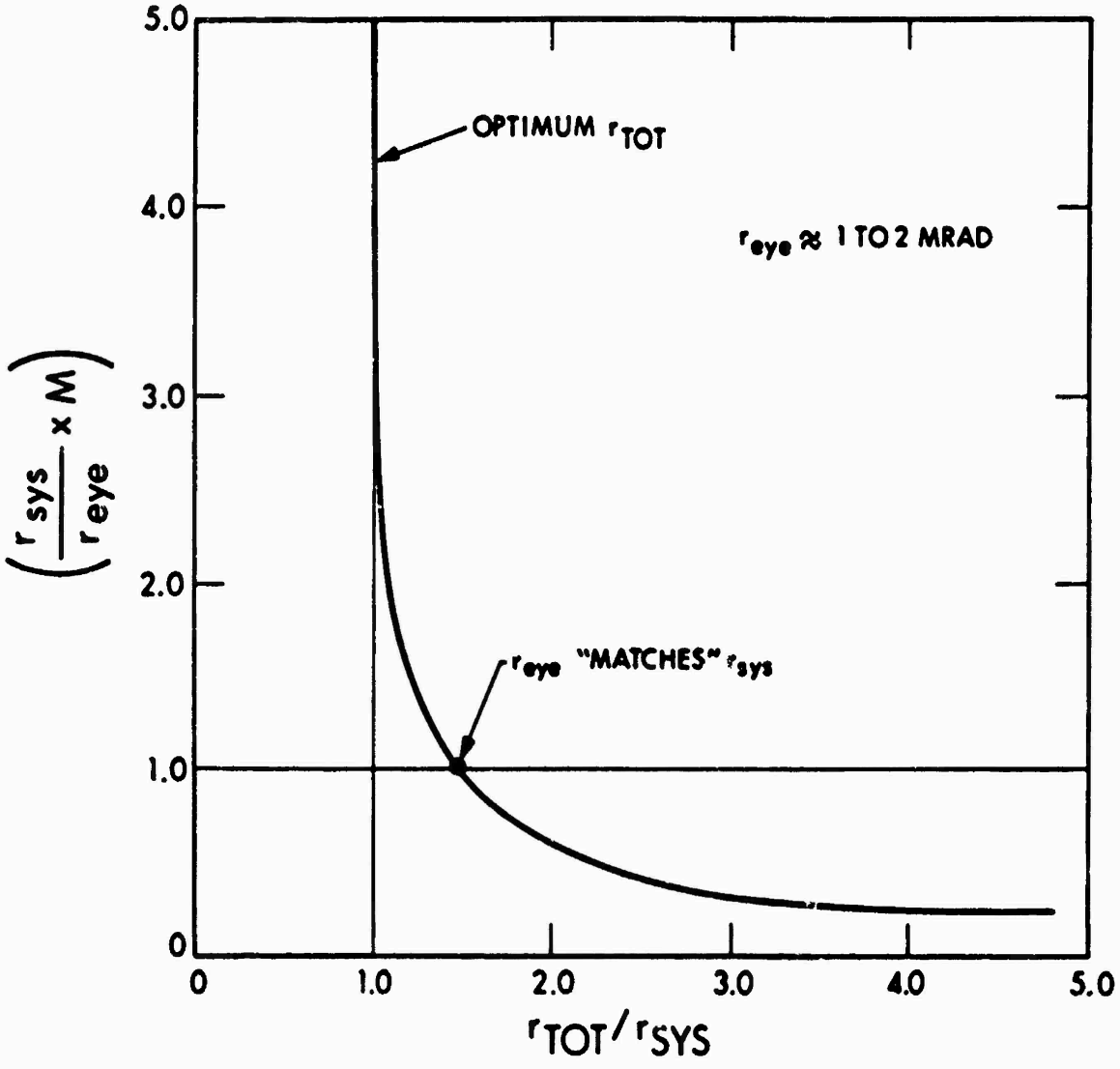

Resolution of eye = r_{eye} = 1 mrad

Resolution of system = r_{sys}

System magnification = M

Resolution of man plus system = r_{tot}

By the definition the resolution of the total (r_{tot}) for a perfect system would be r_{eye}/M. This figure therefore indicates how much of the total resolution is a result of the display being too small i.e., insufficient M. The ordinate is essentially display size.

Figure 15. The Effect of Magnification (Display Size) on Total Resolution

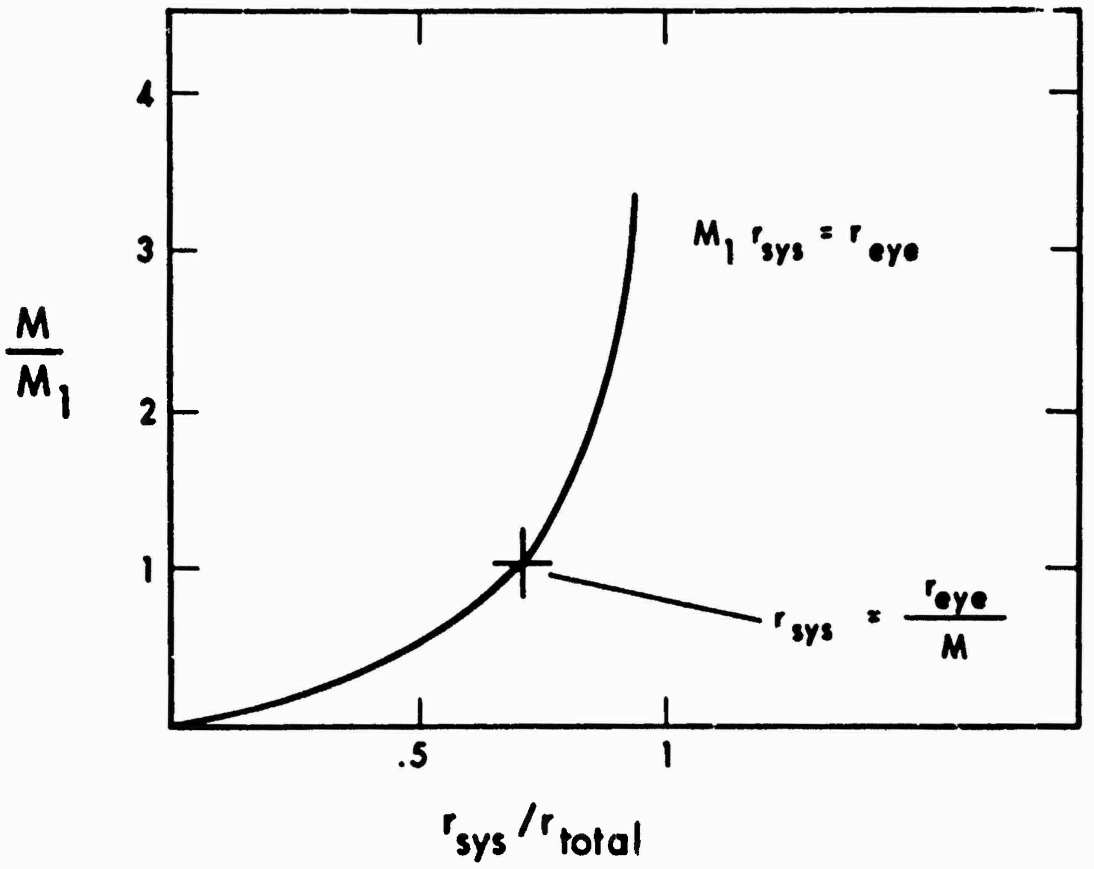

(See Note on Figure 15)

Figure 16. Magnification (Display Size) Required as a Function of the Acceptable Percentage Loss in Resolution Due to the Finite Resolution of the Eye

43697

which is simply another way of showing Figure 15 with r_{eye} = 1 mrad. This curve can easily be applied to existing systems. For a system with an M = 7.5 (e.g., a 6-inch horizontal display at 26-inches to display a 3.3° horizontal field-of-view) and an r_{sys} = 0.25 then, if r_{eye} = 1.5 mrad (brightness ≈ 1 foot-lambert)

$$M_1 = 6$$

$$\frac{M}{M_1} = 1.25 \qquad (8)$$

and r_{sys} would be about 75 percent of r_{tot}. For lower average brightness (r_{eye} = 2 mrad) this would be degraded. If the vibration and other environmental factors are considered, an r_{eye} = 3 to 4 mrad may not be unreasonable.

3.3.3 DETECTION

The probability of detecting an object, given that the operator is looking at the object, includes two non-mutually exclusive cases: non-clutter limited (uniform background) detection and clutter-limited detection.

The first case is where the target is in a relatively uncluttered environment (i.e., on the road) but the ability to detect is limited by random (Gaussian) noise. (Fixed noise and blemishes should be treated separately.) The operator is viewing the display, trying to detect an anomaly in a relatively uniform area. Ship or headlight detection may be an ideal example. The "noise free" (contrast limited) situation is a special elementary subcase of this case and will be discussed first. The analysis of this first case provides the basis for most of the detection and recognition theories presented in this study and therefore will be given the greatest attention. It is based upon the work of

O. H. Schade, Sr. (Ref. 5), H. L. De Vries (Ref. 18), H. R. Blackwell (Ref. 19), and others (Refs. 19 through 23) and simply applies their theories and/or empirical results to the operation of an electro-optical system.

The second case is when the difficulty in detecting is caused by a need to recognize the target from the clutter. This is the case where false targets and/or camouflage have rendered detection to a condition of recognition. This is an extremely complicated case requiring the system and man to extract and possibly filter enormous amounts of information from the scene and object. For this case, it is anticipated that detection may be by prebriefing and context. Such cases are often presented as visual puzzles and the analysis of these cases can be very difficult, but an empirical model has been advanced by J. Johnson (Ref. 24) as part of his unified detection/recognition theory and will be used with interpretations. A special subcase of this second case is the situation where a raster acts as clutter interfering with detection. This will also be discussed.

3.3.3.1 The Man as a Detector, Theory A--Non Clutter

3.3.3.1.1 Noise-Free

Much work has been done investigating the effectiveness of the unaided man as a detector. One of the more well known experimentalists is H. R. Blackwell. Between 1945 and 1957 he made a comprehensive series of measurements of contrast thresholds at various object sizes, background luminances and exposure times. And, while more recent work can be quoted, this examination clearly covers the parameters of interest. The objects were disks presented against uniform backgrounds of luminance B and contrast $\Delta B/_B$.

Measurements were made by the "temporal forced-choice" method. Observers were required to look at a continuously-presented background.* The object was presented, for its stated duration, in only one of four possible temporal intervals, each of 2 seconds duration. The observer had to indicate that he had discriminated the presence of the object by correctly identifying the interval in which it appeared. That contrast level which corresponds to detection 50 percent of the time is known as threshold contrast. Measurements were made for visual angles of 0.3 to 17.5 mrad, exposure times of 0.01 to 1 second, and backgrounds from 0.001 to 1000 foot-lambert. Table I shows the results. Figure 17 shows the variation of brightness threshold with object size and background brightness for 1-second exposure. (Reference 11.)

This plot indicates many interesting aspects on how the operator actually functions. For a brightness of 1 foot-lambert, the operator appears to do spatial integration over either the optics blur (later discussions will clarify this statement) or the target up to an object size of about 3 mrads at which size the integration tends to fail and ΔB becomes constant (as it does with temporal integration). In fact, this relationship seems to occur for all brightnesses with the failure occurring as a maximum integrated signal is reached. Assuming that the noise is photon noise, (when the brightness is high) as discussed by A. Rose, (Ref. 20) it is proportional to $B^{1/2}$. This indeed appears to be the case down to a brightness of less than 0.1 foot-lambert where some internal noise (in the eye-brain) seems to take over and ΔB becomes unaffected by the average brightness. Therefore, detectable brightness curves for 0.01 and 0.001 foot-lambert are near identical to the 0.1 foot-lambert case.

It is interesting that while the breakpoint for the long exposure data is at 0.9 mrad (indicating r_e of the eye = 0.9 mrad) the short exposure

*The background or noise is presented continuously while the signal is only presented in a flash. Therefore, S/N improves directly with exposure time until the integration starts to fail.

TABLE I

CONTRAST THRESHOLDS AT VARIOUS OBJECT SIZES,
BACKGROUND LUMINANCES AND EXPOSURE TIMES
(BLACKWELL 1957)

VA mrad	B ft-L 1000	100	10	1	0.1	0.01	0.001
			t = 1 second				
0.29	0.113	0.159	0.234	0.555	2.38	18.9	189.0
0.58	0.0296	0.039	0.0585	0.139	0.594	4.72	47.2
1.17	0.0112	0.0128	0.0181	0.0398	0.167	1.33	13.3
2.92	0.00863	0.00863	0.0110	0.0179	0.0662	0.526	5.26
17.52	0.00745	0.00745	0.00877	0.0110	0.0312	0.248	2.48
			t = 1/3 second				
0.29		0.230	0.315	0.726	2.92	21.4	212.0
0.58		0.0574	0.0787	0.181	0.731	5.36	53.0
1.17		0.0173	0.0244	0.0516	0.205	1.51	14.9
2.92		0.0105	0.0139	0.0216	0.0774	0.568	5.61
17.52		0.00746	0.00914	0.0112	0.0340	0.249	2.46
			t = 1/10 second				
0.29	0.221	0.346	0.581	1.38	5.81	42.6	413.0
0.58	0.0575	0.0865	0.145	0.345	1.45	10.65	103.0
1.17	0.0196	0.0262	0.0422	0.0977	0.397	2.91	28.3
2.92	0.0117	0.0146	0.0198	0.0380	0.129	0.946	9.20
17.52	0.00855	0.00938	0.0114	0.0164	0.0392	0.287	2.79
			t = 1/30 second				
0.29		0.676	1.25	3.42	15.2	108.0	1065.0
0.58		0.169	0.313	0.855	3.80	26.9	254.0
1.17		0.0516	0.0889	0.239	1.07	7.57	71.4
2.92		0.265	0.0373	0.0889	0.337	2.38	22.5
17.52		0.0146	0.0169	0.0308	0.103	0.103	6.85
			t = 1/100 second				
0.29	0.955	1.92	3.48	10.3	51.5	340.0	3030.0
0.58	0.269	0.479	0.871	2.5	12.9	85.1	759.0
1.17	0.0995	0.146	0.249	0.716	3.49	23.1	206.0
2.92	0.0669	0.0764	0.103	0.255	1.12	7.40	65.9
17.52	0.0368	0.0385	0.044	0.0855	0.346	2.29	20.4

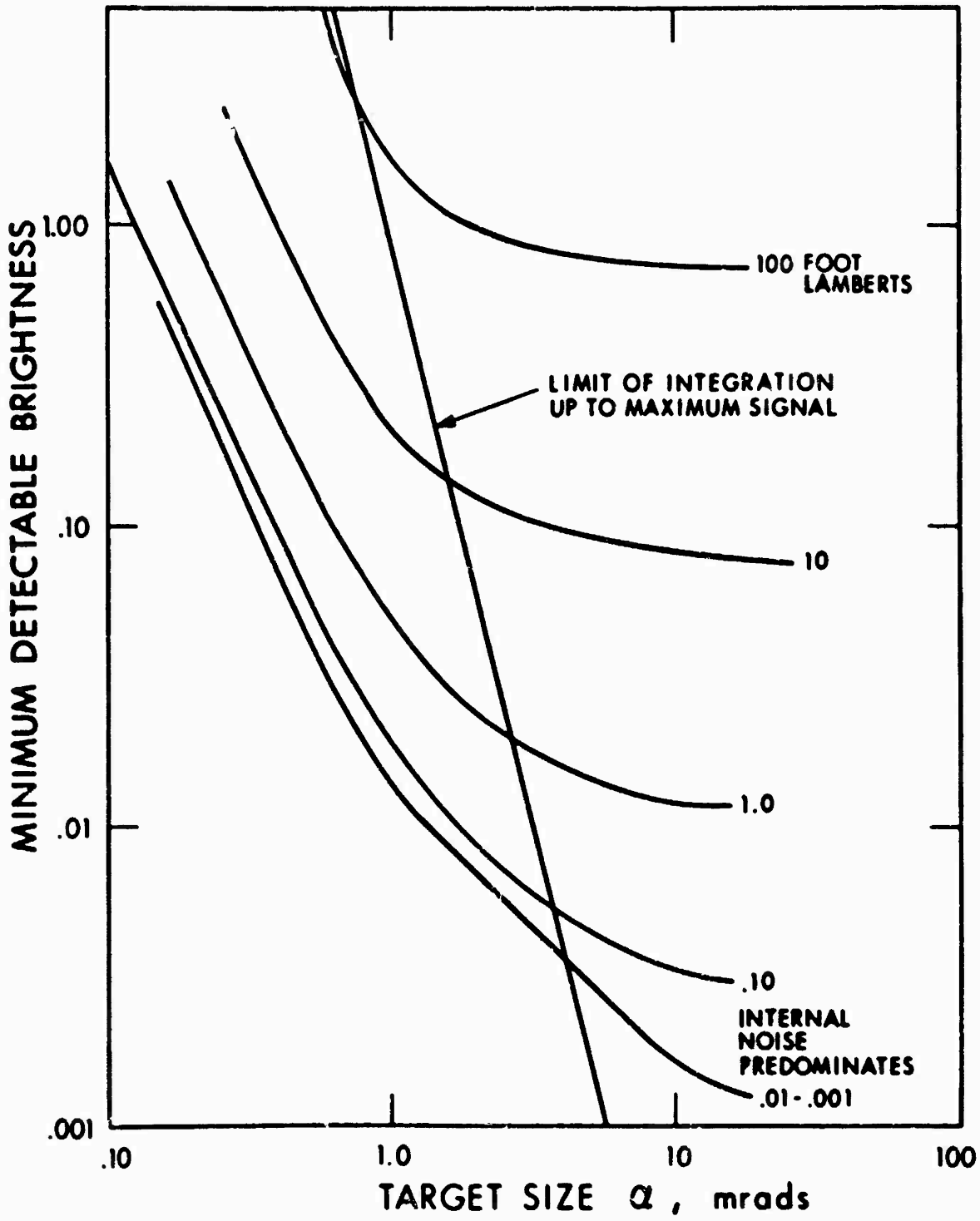

Figure 17. Variation of Threshold Brightness with Respect to Target Size and Background Brightness

data breaks at 1.5-2 mrad indicating that eye resolution is poorer. This may be attributable to retinal enhancement for 1-second times that cannot occur when exposure is only 0.001 second; i.e., eye jitter is not fast enough. This could mean that the eye may perform poorer with TV or FLIR than with photographs.

3.3.3.1.2 Noisy Image Case

There is a difference between detecting disks on a uniform background which represents a noise-free scene and detecting objects in a noisy scene such as a televised scene. It has been the effort of O. H. Schade, Sr., and more recently the coauthor, F.A.R., to extend the experiment to the noisy image case. Their efforts have again shown the brain to act as a spatial and temporal integrator with a fixed threshold based upon perceived signal-to-noise ratio.

While delaying the proof until a later section it is worth stating that the display signal-to-noise SNR_d* ratio is (see subsection 3.4.6.8.1) related to the video signal-to-noise ratio, SNR_V as measured in a TV camera's electrical channel for simple aperiodic objects (squares, rectangles, etc.) as

$$SNR_p = \sqrt{2t\,\Delta f_V\,(a/A)}^{-1/2}\,SNR_V \qquad (9)$$

where t is the observer's integration time, Δf_V is the video bandwidth and a/A is the image area normalized to the entire raster area. The relationship between the SNR_p and SNR_V was first suggested by Coltman and Anderson (Ref. 20) and provides a convenient method of generating noisy test images for use in psychophysical experiments. It should be noted that the above equation only holds for images from sensors with ideal MTF's but that useful threshold signal-to-noise ratios that can be extrapolated to non-ideal cases, can be derived.

*$(SNR)_d$ is the $(SNR)_p$ for an optimum display.

A typical result of psychophysical experiments using rectangles as test objects is shown in Figure 18. Here, we show the probability of detection versus SNR_d for four different rectangles. In the experiment, the test objects could appear in four different locations on the display. The observer response was forced and the probabilities obtained were corrected for chance. The largest rectangle subtended 0.13^o x 6.02^o at the observer's eye, implying that the observer can spatially integrate over very large angles.

In a second series of experiments, squares were used. The threshold SNR_ds obtained (50 percent probability of detection) are shown in Figure 19. The thresholds are seen to be quite constant for squares of angular subtense from 0.1 to 0.5^o but increase for smaller squares and larger squares. The increase for the smallest square is attributed to the MTF of the eye. The results for the large squares are in apparent contradiction to the results obtained in the previous experiment. The proposed explanation is that the eye has a differentiating effect on images. The long thin rectangles are nearly all edge and the eye can make use of the total image. For large squares, the eye can make use of only the perimeter of the square. This effect and the results of a large number of other psychophysical experiments including those discussed below are detailed in Reference 12.

In summary, the threshold display signal-to-noise ratios required for isolated aperiodic objects on a uniform background are quite well known. The average value of the threshold is about 2.8 using Eq. 9 and a value of 0.1 second for the observer's integration time.

While isolated aperiodic objects amid a uniform background are sometimes of interest as in the case of detecting aircraft against the horizon sky, it is more usual to be searching for objects amid some degree of clutter.

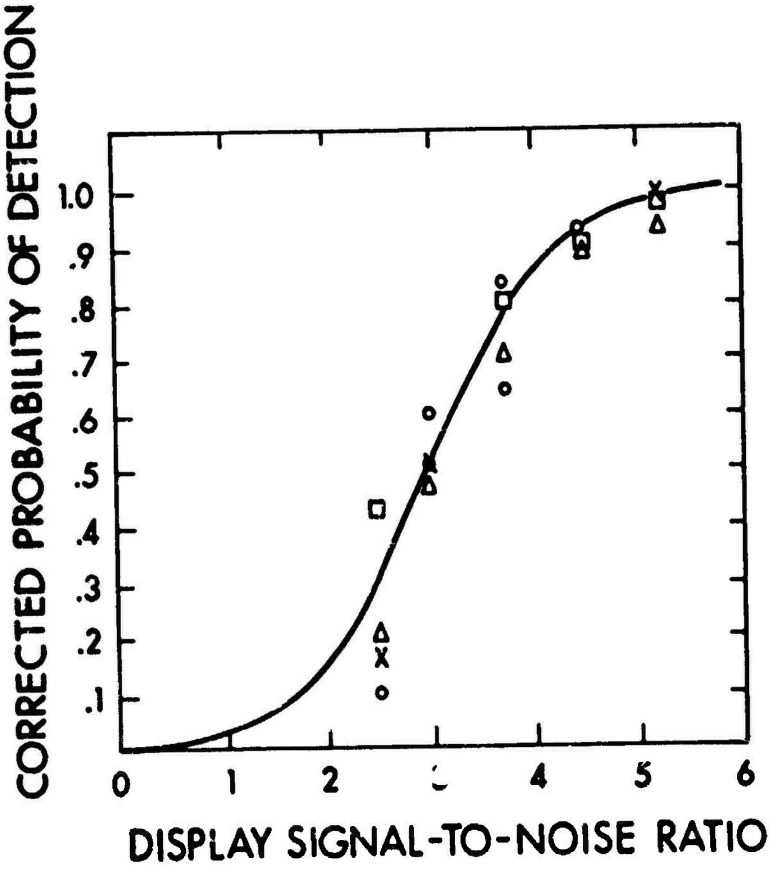

Figure 18. Corrected Probability of Detection vs SNR_d required for Rectangular Images of Size o 4 x 4, □ 4 x 64, Δ4 x 128, and, x 4 x 180 Scan Lines. Televised Images at 30 frames per second and 525 Scan Lines D_V/D_H = 3.5

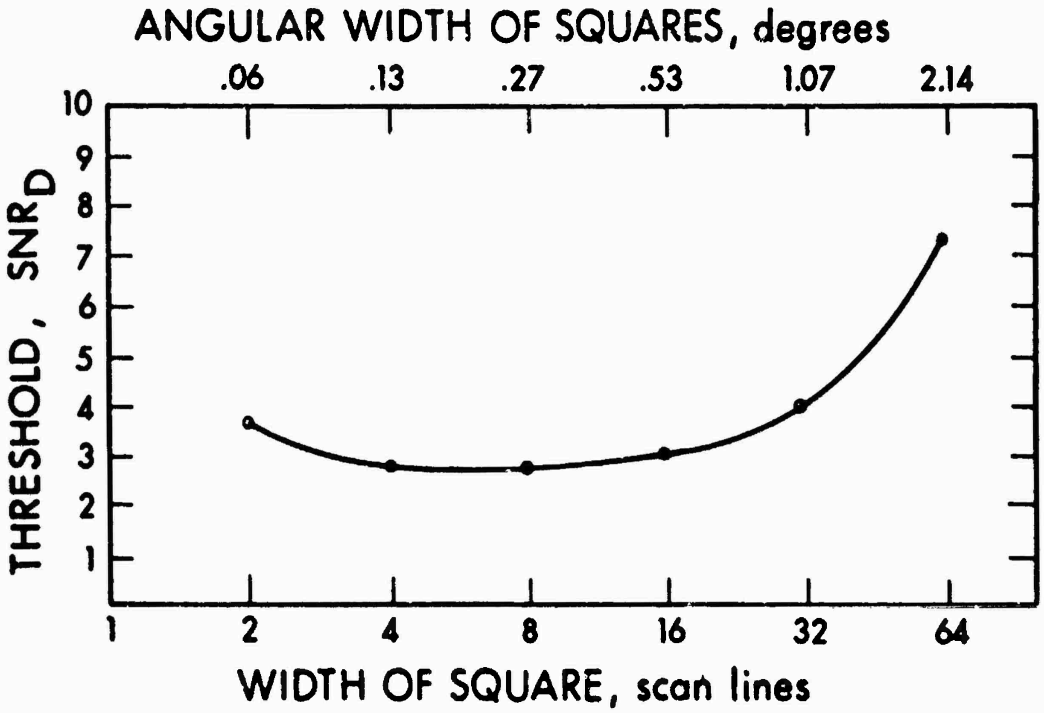

Figure 19. Threshold SNR_d required to detect Square Images of Various Size and Angular Extent

3.3.3.2 The Man as a Detector, Theory B--Clutter Limited

As we noted, uniform backgrounds are seldom encountered. Usually there will be background clutter which can range from comparatively simple to highly complex. For objects amid modest clutter, it has been suggested that detection just occurs when the object just subtends one cycle of the spatial frequency (or 2 TV lines) which can just be resolved. In this criterion, we replace the object by an equivalent bar pattern as described in the next section. The equivalent bar pattern should have the same incremental signal as the object and the width of one bar should be half the minimum object dimension. This concept was first proposed by J. Johnson of the Ft. Belvoir Night Vision Laboratory (Ref. 24) and was shown to have some validity through a series of experiments.

As will be shown in the sensor analysis, the isolated object criterion is essentially identical to the Johnson one-cycle criterion for targets subtending angles much greater than the resolution (defined in subsection 3.4.3.2) of the system and that it leads to predicting much larger ranges than the Johnson criterion as the targets become small. While the ability to detect very small targets requires the aperiodic theory, it should be remembered that raster and other limits tend to reduce the ranges obtained thereby further supporting the one-cycle criterion. In general, it is felt that the one-cycle criterion is clearly too harsh for objects amid a uniform background and may even be too harsh for objects amid comparatively simple clutter, such as a vehicle on a road. On the other hand, the one-cycle criterion would not be nearly stringent enough for objects in severe clutter which would be the case in detecting small vehicles amid trees of size similar to the vehicles.

Very few definitive psychophysical experiments exist for this detection case. As an interim measure, we suggest the following criteria. For objects amid a uniform background, use the theory A. For objects amid a slight amount of clutter such as a vehicle on a large, paved highway

or an aircraft on a runway, use both the isolated image and one-cycle criteria and average the range. For objects in modest clutter such as vehicles in a field with low brush, use the one-cycle criterion. For objects in severe clutter, use the recognition criterion of subsection 3.3.4. As is readily discerned, considerable judgment must still be exercised in predicting detection ranges.

3.3.3.3 The Man as a Detector, Theory C--Raster Limit

While theories A and B describe the limits of detection for non-raster limited systems, it is important that a strong raster can confuse or preoccupy the operator almost to the same degree as severe clutter. Based upon the authors' experience, we hypothesize that this raster effect does not provide a new criterion as much as it provides a limiting image size beyond which theories A and B no longer hold. That is, as long as the image is many raster lines, the raster does not effect the previous criteria but depending upon the strength of the raster (i.e., 100 percent or 10 percent modulation and varying dead-time duty cycle) there is an image size which for smaller images the results become confused and the operator will not function efficiently. For a strong raster (100 percent modulation and 50 percent on, 50 percent off) the image is about 6 times the raster line width. For a weak raster (3 percent modulation and small-spatial duty cycle) this would be for an image about 2 raster line widths.

3.3.4 RECOGNITION AND IDENTIFICATION

The purpose of most electro-optical equipments is to augment an observer so that he can discern a scene object at longer range than with his unaided eye.

The acuity with which an object is seen depends upon range. When we speak of range, we generally mean the maximum or threshold range at which the object can be barely discerned with the needed acuity. And, the needed acuity depends upon the level of discrimination desired whether mere object detection, or object recognition or positive object identification. Typically, the process is as follows. At very long range, a scene object appears first as a blob. Moving ever closer, the object begins to take some shape such as a rectangle. Closer yet, the observer becomes able to classify the object as to type and finally positively identify the object. J. Johnson (1958) has arbitrarily divided these levels of object discrimination into four categories presented in Table II.

TABLE II

LEVELS OF OBJECT DISCRIMINATION

Classification of Discrimination Level	Meaning
Detection	An object is present.
Orientation	The object is approximately symmetrical or unsymmetrical and its orientation may be discerned.
Recognition	The class to which the object belongs may be discerned (e.g., house, truck, man, etc.)
Identification	The target can be described to the limit of the observer's knowledge (e.g., motel, pick-up truck; policeman, etc.)

It is readily evident that a higher degree of visual acuity is needed to identify an object as opposed to just detecting it. To obtain a quantitative feel for the problem, J. Johnson performed a series of experiments using electro-optical sensors. In these experiments, an attempt was made to correlate the detectability of a bar pattern of a given spatial frequency with the level of object discrimination. The procedure was to

increase the object range until it was just barely detected (or recognized, etc.). Then, a bar pattern was placed in the field-of-view and its spatial frequency was increased until it could barely be resolved at the same range. The spatial frequency of the pattern was specified in terms of the number of lines in the pattern subtended by the objects minimum dimension as illustrated in Figure 20 where the object, for the recognition case, subtends 8 lines.*

Johnson's results, tabulated in Table III below, are not unexpected. If the observer could only just resolve a coarse pattern corresponding to 2 bars per minimum object dimension, the level of object discrimination was limited to detection. With higher acuity, a bar pattern of higher spatial frequency could be discerned and the level of object discrimination increased in turn.

TABLE III

JOHNSON'S CRITERIA FOR THE RESOLUTION REQUIRED PER MINIMUM OBJECT DIMENSION VERSUS DISCRIMINATION LEVEL

Discrimination Level	Number of Resolvable Lines* per Minimum Object Dimension
Detection	$2.0^{+1.0}_{-0.5}$
Orientation	$2.8^{+0.8}_{-0.4}$
Recognition	$8.0^{+1.6}_{-0.4}$
Identification	$12.8^{+3.2}_{-2.8}$

*Not line pairs

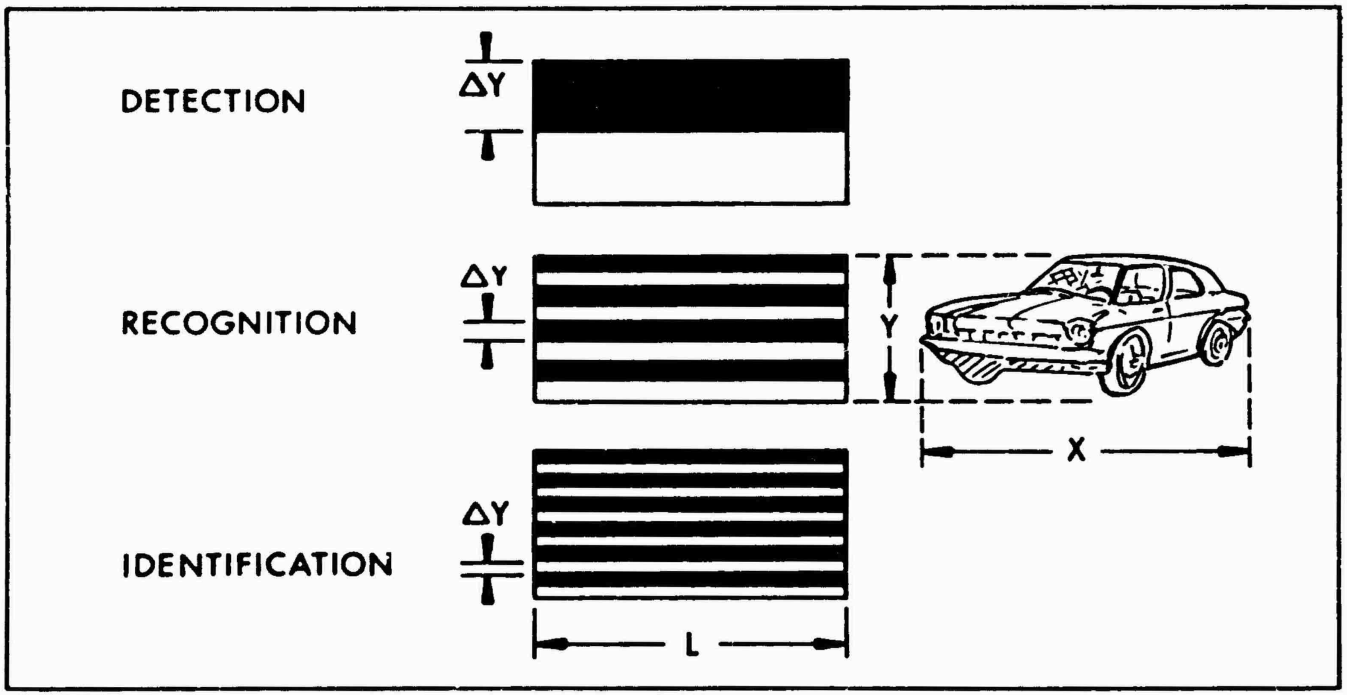

Figure 20. Resolution Required per Minimum Object Dimension to Achieve a Given Level of Object Discrimination Expressed in Terms of an Equivalent Bar Pattern

The preceding table has been widely used and misused by systems designers from the time of its publication to the present. The misuse stems from the neglect of additional requirements imposed by J. Johnson, to wit, that the "signal-to-noise" ratio and image contrast must also be sufficient. However, it was not too clear how these quantities were to be measured and calculated. Thus, the further requirements were neglected in many cases. However, many competent designers did use the sensor's threshold resolution versus scene irradiance curves in estimating the level of discrimination. Since the threshold curves do contain image signal-to-noise as a factor in their measurement, estimates made on this basis turn out to be reasonable if not precise.

Most sensors are characterized by an absolute limiting resolution. If the sensor sensitivity at a given incremental scene irradiance is sufficient to realize the limiting resolution but is not sufficient to perform the desired discrimination task, further increases in scene irradiance level will be to no avail. The only solution is to move closer. On the other hand, if resolution were sufficient at a given irradiance level, a decrease in scene irradiance level could cause the sensor/operator combination's acuity to fall below the level required for the desired level of object discrimination.

In the foregoing data, we have implied that image signal-to-noise ratio, image contrast, and sensor/observer resolution are independent quantities, whereas, in our view, these quantities are functionally related, i.e., the image signal-to-noise ratio is proportional to the image size, contrast, irradiance level, sensor sensitivity, etc. In this case, Johnson's requirements reduce to one. Namely, that an object should be discriminated at the desired level if its signal-to-noise ratio at the output of the observer's retina, after processing and interpretation by the brain, is large enough. Obviously, the signal-to-noise ratio as defined in this manner is not directly measurable but as will be seen, can be indirectly measured through psychophysical experimentation.

The quantitative models developed herein are based on simple test images such as rectangles or bar patterns for which an image size or "resolution" can be precisely defined. Through psychophysical experiments, the threshold signal-to-noise ratios (as calculated on the basis of image geometry, measured electrical quantities, and estimated psychophysical parameters) are determined. While the test images are of simple geometry, it is hypothesized that these images and the requirements for their discrimination can be correlated with the discrimination of more complex imagery as encountered in a real-world scene. Such correlation does appear to exist as will be discussed.

Detection is the lowest level of object discrimination since it usually implies only that an object of undeterminable shape has been sighted in the field-of-view. Recognition usually requires shape information but in some cases, shape need not be known if other clues are available. For example, a series of regularly spaced and moving blobs on a road may be interpreted as vehicular traffic. On the other hand, a single, stationary blob on a road may be the shadow of a tree, a puddle, a truck or any number of other objects. While a blob on a road has a reasonable probability of being a vehicle, the same blob in a field or among a sparse forest can be almost anything. Thus, there are obviously many degrees of discrimination even within a discrimination level. A single criterion, such as that based on resolution and signal-to-noise ratio, is unlikely to be sufficient to cover every case. Rather, a number of cases must be considered and subclasses formed as noted in the detection case above.

However, J. Johnson's hypothesis and definitions are reasonable and have some basis in experimental fact. Thus, we elected to adopt his premises. For this purpose, we assume the image to be detected or otherwise discriminated to be of size X x Y as shown in Figure 20. To correlate the detectability of a bar pattern with a level of object discrimination,

we divide the minimum dimension, Y, of the image by a factor k_d which is numerically equal to the number of resolvable lines per minimum object dimension given in Table III, e.g., for recognition, $k_d = 8$.

As a first step, the discernability of bar patterns was investigated as a function of their signal-to-noise ratio. In performing these experiments, we hypothesized that to discern the presence of a bar pattern, the observer must discern a single bar in the pattern and, hence (after O. H. Schade, Sr.), the SNR_D is calculated on the basis of the area of a single bar using the equation (to be derived)

$$SNR_p = \left[\frac{2t\ \epsilon\ \Delta f_v}{\alpha}\right]^{1/2} \frac{1}{N} (SNR)_v\ R_{sf(N)} \qquad (10)$$

where the terms are as in Eq. 9 except that R_{sf} is the mean square wave transfer function and ϵ is the bar aspect ratio as introduced in subsection 3.4.6. The experiments were performed using TV-generated images and thus the bar patterns were only bar patterns at low spatial frequencies and nearly pure sine waves at high spatial frequencies. However, this is of consequence for the SNR_p calculation since the appropriate corrections for the equivalent mean square wave amplitude were made.

A typical result is shown in Figure 21 for a bar pattern of spatial frequency 396 lines/picture height and of various bar height-to-width ratios. The threshold SNR_D values for bar patterns of various spatial frequencies and display-to-observer viewing distances are shown in Figure 22. The display height for these experiments was 8 inches.

Recognition experiments were performed using four different types of vehicles: a tank, a van truck, a half track with top-mounted radar antenna, and a tracked bulldozer with derrick. The signal-to-noise ratio was computed on the basis of an area of a bar whose length and width are equal* to the length of the vehicle's image and the width of the vehicle's image

*The coauthor R. L. S. generally prefers using a standard bar chart e.g., AF 3-bar pattern.

43835

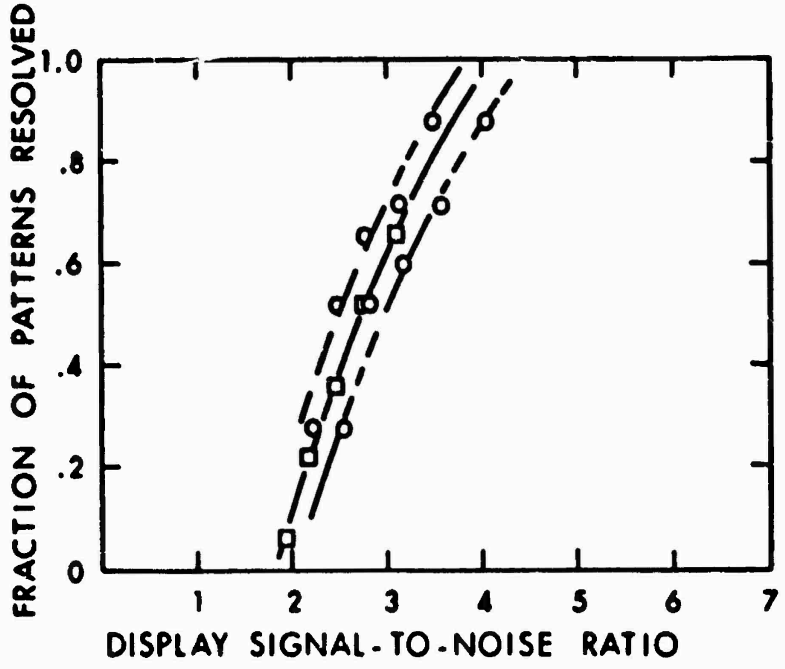

Figure 21. Fraction of Bar Patterns Resolved vs. Display Signal-to-Noise Ratio for a 396 Line Bar Pattern of Length-to-Width Ratio □ 5:1 ○ 10:1, ○ 20:1 Televised Images at 25 Frames/Sec. 875 Scan Lines, D_V/D_H =3.5

43833

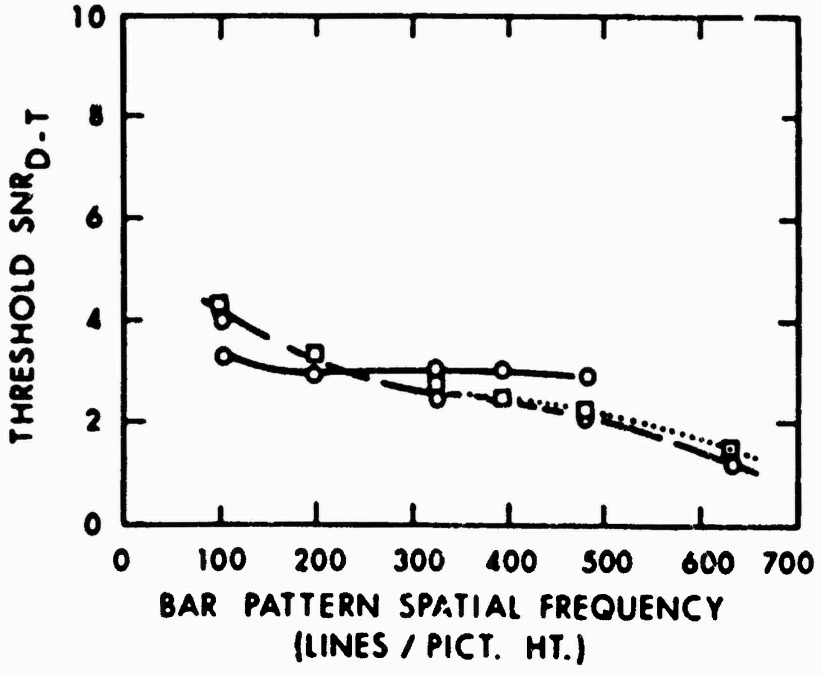

Figure 22. Threshold Display Signal-to-Noise Ratio vs. Bar Pattern Spatial Frequency for Display to Observer Viewing Distances of ○ 14", □ 28" and ○ 56"

divided by 8 in accord with the equivalent bar pattern approach discussed above. The main difference between the calculation of SNR_D for the bar pattern and the vehicular object was that for the equivalent bar patterns, the signal levels were measured in terms of the mean-signal excursion within the bar pattern while for the vehicle, the signal amplitude was measured from the average background level to the peak-signal excursion. Had the peak-to-peak excursion about the average signal within the vehicle area been used, the threshold SNR_p values noted would be somewhat lower. A typical result is shown in Figure 23.

The average threshold SNR_p for vehicle recognition amid a uniform background was 3.3. For the equivalent bar pattern, the threshold SNR_p was 2.9 which is only 14 percent different. Next, a degree of clutter was introduced by means of a background transparency. With moderate to low clutter (grass background) the threshold SNR_p was 4.1 which is 24 percent higher than for a uniform background and with moderate clutter (grass and trees background) the threshold SNR_p noted was 5.0 which is 52 percent higher than the uniform background case.

Next, we progressed to the vehicle identification experiments. The images were tanks: the M47 Patton, the M48 Centurion, the Panther, and the Stalin. Again, an equivalent bar pattern* of length equal to the tank's length and width equal to 1/13 of the tank's minimum dimension was used. The average threshold SNR_p was 5.2 which was identical to that needed for the equivalent bar pattern. With a grass-trees background, the average threshold SNR_D needed was 6.8 versus 6.2 needed for the equivalent bar pattern. The spread, or variance, of the threshold about the average increased as the level of discrimination increased from detection to identification.

In summary, it was hypothesized that the recognizability and identifiability of "real world" objects could be correlated with the discernability of an "equivalent bar pattern". The "equivalent bar pattern"

*Again coauthor R.L.S. prefers standard bar patterns. Other sophistication may be beyond what is warranted by the analysis.

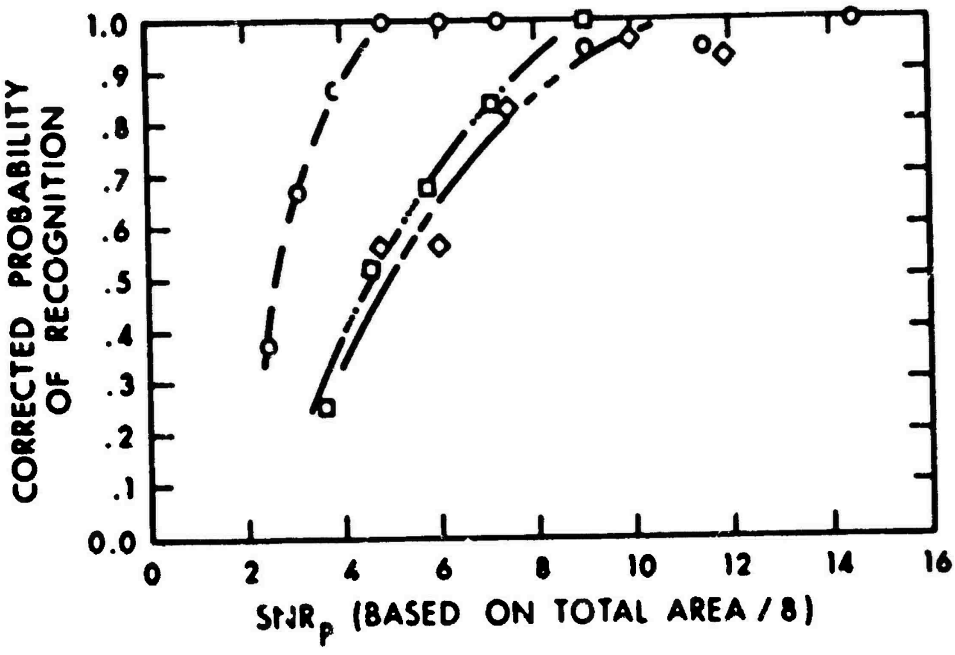

Figure 23. Probability of Recognition vs. SNR_D for a ○ Tank, ◇ Radar Half Track, □ Van Truck and ○ Derrick Bulldozer, Grass Background

was defined (in image space) in terms of a single bar in the pattern of length equal to the length of the image of the "real world" object and width equal to the real world image's width divided by k_d. The factor, k_d, is a number associated with a given discrimination level, e.g., 8 for recognition. When the bar pattern is defined in the above manner, it was found experimentally that the SNR_p required to liminally discern the equivalent bar pattern was very nearly equal to the SNR_p required to recognize the "real world" image when its SNR_p is calculated on the basis of its area divided by k_d. It might be thought that defining the area of the bar in the equivalent bar pattern as 1/8 its area is redundant, but this is not so. The key reason for defining the bar pattern in the manner described is to define the required level of sensor resolution in terms of a spatial frequency. This permits us to take into account the effects of finite sensor apertures. As we noted previously, J. Johnson specified that an image, to be discerned at a given level of discrimination, must be both resolved and have a sufficient SNR. In the above formulation, SNR_p is a function of resolution so that if the SNR_p is sufficient, the resolution will also be sufficient.

We noted an important caution in connection with the method of calculation. The "real-world" objects are not periodic in general but rather, assemblages of aperiodic objects of different sizes. These aperiodic objects which make up the object may be relatively isolated as in the case of the derrick on the tracked bulldozer or more clutter-like as in the case of the half-track. Thus, we cannot say that the equivalent bar pattern approach is the best one. We can only reply that it has been established empirically to be a useful theory.

As a potential solution to the not quite periodic, not quite aperiodic nature of real objects, it might be appropriate to calculate the threshold range for the equivalent bar pattern and then for a single bar in the test pattern assuming that the bar is aperiodic. Then, the threshold

range estimate is taken to be the average of the two ranges. This approach is similar to a recent concept proposed by O. H. Schade (Ref. 25) for estimating the mean resolving power of a sensor system.

3.4 IMAGING SYSTEMS ANALYSIS

3.4.1 INTRODUCTION

In the foregoing subsections 3.2 and 3.3 the input signal and the output interface have been discussed and defined in detail. It is now possible to analyze the system. This subsection, therefore, defines and justifies the performance parameters for each system and provides the analysis for predicting the system performance from the characteristic or design parameters. While it was desired that the development of the performance equations be as parallel as practical, the authors* have not been completely successful at dropping their pet approaches. To the extent that pure logic is possible, the treatment of the problem is identical for the TV and FLIR. Sometimes, experience forces a deviation which is not obviously necessary. In some, but not all, cases the justifications for the deviations are discussed.

3.4.2 FUNCTIONAL DESCRIPTION

Figure 24 is a functional block diagram for either system. The sensor (consisting of optics and receiver) generates an electrical signal from the radiation received from the apparent scene. The output of the sensor is further processed and then displayed as a visible image. A man views the image and makes decisions.

The input to the system is the variation in incidence at the receiver. These variations have already been described as the apparent scene.

*Especially R. L. S.

The output of the electro-optical system is a visible image. This image is a degraded reproduction of a limited field of view of the apparent scene but may be brighter, have more visual contrast, and be magnified. The increased brightness and contrast is due to both spectral conversion (i.e., IR input, visible output) and gain.

In a perfect imaging sensor, all images are transmitted through the sensor with perfect fidelity. In real sensors, the images may be degraded in amplitude, shape, or phase (position), or all three. These degradations are due to finite imaging apertures, geometrical defocusing, spatial nonlinearities, etc. Noise may also be added in the signal processor or display. The distortions and noises introduced combine to reduce image resolution and signal-to-noise ratio.

Also a primary concern are the requirements of the man since he is the final element of the total system, determining the threshold for performance. His pertinent characteristics were discussed in subsection 3.3.

The approach of this analysis will be to determine the signal and signal-to-noise ratio throughout the system for a given input object and range, and then use the man's threshold characteristics to define and predict sensitivity.

Finally, in the next section, range will be treated as the independent variable to determine what object strength is required for the man to complete his task (e.g., detection) at that range.

3.4.3 SYSTEM PERFORMANCE PARAMETERS

Before discussing the analysis of the system, it is advantageous to define which parameters are considered system performance parameters

3.4.3.1 System Field of View

The field of view is a measure of the amount of the scene which is imaged by the system. It is measured as the angular subtense (in object space) of the portion of the scene which is displayed.

3.4.3.2 Resolution (Refer also to Appendix II)

The resolution of the system measures the loss of detail by the system in converting the apparent scene to the displayed image. This could be measured by determining the size of the output from a point or line input. The spot that results from a point input (unit area δ function) is referred to as the point spread function. For a perfect system, this would be an infinitesimal point. Therefore, any spreading indicates a loss of detail. A similar relationship exists between a line input and its output except that this reduces the problem to one dimension and, if as is assumed, separation of spatial variables is warranted, the line spread functions are as complete a measure as the point spread function.

As was stated previously, the analysis is to follow the approach of O. H. Schade, Sr. Therefore, the analysis and measurement will be completed in the frequency domain. This means that for this analysis, Fourier techniques will be used, assuming that (for small signals) the system is linear and space invariant. Instead of using the line spread function as the primary resolution measure, the Fourier transform of the line spread function will be used which is also known as the optical transfer function. The modulus of the transform, when written in polar form, is the modulation transfer function and the argument is the phase transfer function. It is interesting that the modulation transfer function is also the relative sine wave response of the system and can be measured by determining the peak-to-peak output of a sine wave input (normalized to unity at low frequencies).

Because of the difficulty in making sine wave targets, square wave or bar targets have become popular. The relative output peak-to-peak modulation (for a square wave input) as a function of frequency is referred to as the square wave transfer function. It is easier to measure and can be related to the modulation transfer function. (Reference 26.)

It is very important that no single point on the MTF curve has meaning in itself with regard to resolution, any more than any one point on the line spread function does. If a single number is to be used, it should be similar to a bandwidth such as is used in electrical engineering. The bandwidth tends to indicate the region over which the value for the MTF is high. To this end, O. H. Schade, Sr., proposed the equivalent (noise) bandwidth (N_e) as one indicator of the system's image quality. N_e was defined as the integral of the square of the MTF with respect to number of lines. Resolution was defined in terms of the equivalent aperture of width $\delta = 1/N_e$ since the width of a rectangular line spread function is so related to the N_e of such a function.

N_e is a resolution summary number of some importance. As will be shown, it has impact on a given system's probability of detection. O. H. Schade, Sr., and other references indicate that for noise-free pictures N_e correlates with image quality so long as the total MTF curve is monotonically nonincreasing or at least well behaved (smoothly increasing or decreasing).

3.4.3.3 Sensitivity

The sensitivity of the systems will always be discussed as a function of object's angular size (or spatial frequency for cyclic targets) which sometimes will be expressed as range for an object of fixed linear size.

It will be defined in terms of the minimum input signal which will just provide an image of sufficient signal-to-noise ratio to permit an operator to accomplish a set task.

For example, if the task is to resolve the bars of a three bar chart, the sensitivity will be defined as the minimum resolvable radiant exitance difference between bars and spaces. Equivalently for a FLIR the minimum resolvable temperature will be used and for TV the minimum resolvable contrast may be used.

It is important that these sensitivity measures include the complete system including the operator. They are not to be disregarded as subjective measures however, but are human response measures. The operator is not asked if he likes the image or which looks best, but simply what is the threshold input for the task. By definition of how the equipment is to be used, the accuracy of the measure is adequate.

3.4.3.4 Frame Rate/Field Rate

The average rate at which the complete field of view is scanned or displayed will be defined as the frame rate. The rate at which the field appears to flicker will be called the field rate. Standard broadcast TV has a frame rate of 30 frames per second and a field rate of 60 fields per second.

3.4.3.5 Scan Lines Per Picture Height

It is important that both TV and FLIR systems are sampling systems (they sample the image in space by scanning an aperture) and can be sampled data rather than MTF limited. The parameter of importance is the number of independent spatial samples per resolution element in the integration time of the operator, or system if the system integration is longer. It

is easier to refer to the number of independent scan lines per picture height (or field of view) per integration time however, and that will be the approach taken here.

3.4.4 SENSOR

A general sensor is shown functionally in Figure 24. In either system, lenses focus the energy from the scene onto a receiver which converts it to electrical signals for subsequent processing in order to generate a video signal.

TV	FLIR
A typical high-performance television camera is shown schematically in Figure 25. A lens images the scene on the input photosurface of the intensifier which converts the photon image to a photoelectron image. The photoelectron image is accelerated to a phosphor which recreates a visible image of greater radiance due both to the accelerating voltage and phosphor and to any image magnification between the input photo-surface and its phosphor. The amplified image is transferred to a second photocathode which once again creates a photoelectron image. A net signal gain due to phosphor and photocathode is obtained. The new photoelectron image is	In the IR system, no significant temporal integration occurs in the receiver which is typically an array of photon detectors. (See Figure 26.) The image is scanned by optical-mechanical means across this array to generate time varying signals. These detector outputs are then either electrically filtered and time multiplexed to form a video signal or used as parallel video channels to modulate light sources for a display.

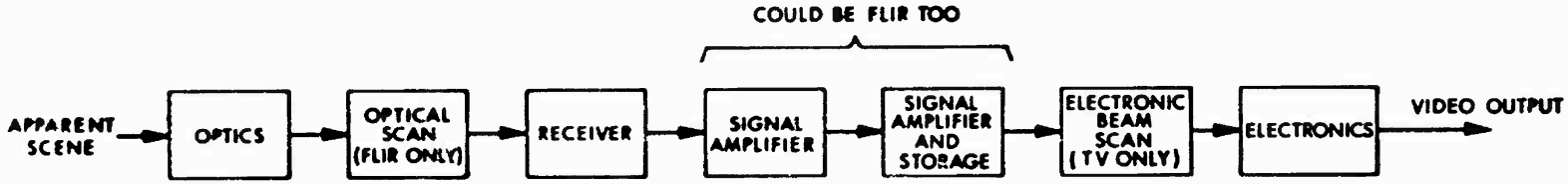

Figure 24. General Sensor Functional Diagram

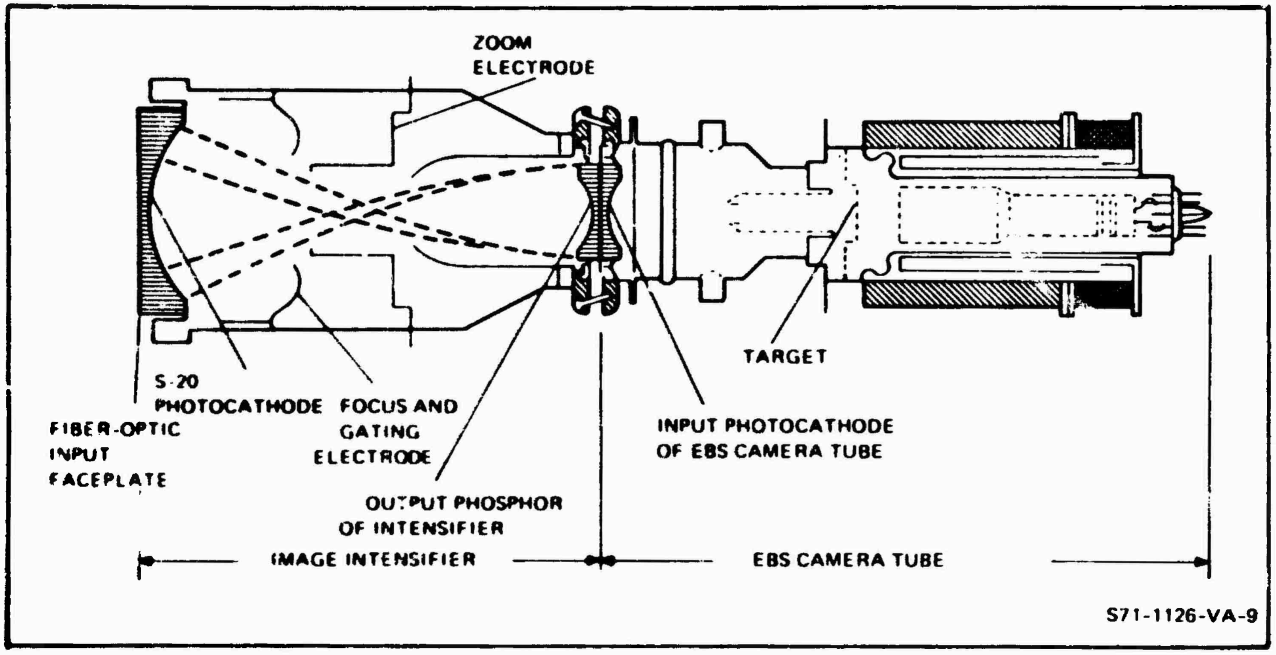

Figure 25. Typical High-Performance TV Camera Diagram

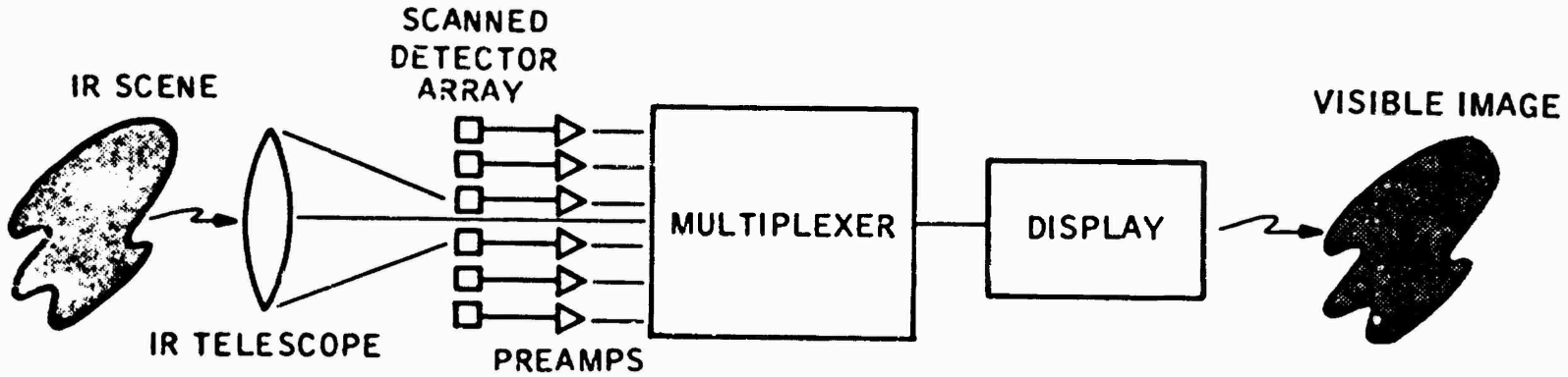

Figure 26. Typical FLIR Schematic

accelerated to a gain storage element, known as the target, where the image is amplified and stored for the period between successive scans by the electron scanning beam. The scanning beam creates a sequential signal which is subsequently amplified and processed for input to a CRT display.

3.4.4.1 Optics

Scene radiant flux is collected and imaged onto the image plane by a lens. For the purposes of illustration and first order analysis, the lens is assumed to be thin and the scene is assumed to be at long range. The first order lens parameters of primary interest are therefore as follows.

3.4.4.1.1 Lens Aperture, D_O

The lens aperture is the effective lens diameter and is sometimes called the clear aperture or entrance pupil. The entrance pupil is the image of the aperture stop from object space (the scene side of the lens). In Figure 27 the iris is the aperture stop and entrance pupil. The maximum diameter of the entrance pupil in the thin lens case is the diameter of the lens itself. (Reference 27.)

3.4.4.1.2 Lens Focal Length, F_L

Parallel light rays from distant objects are focused on the focal plane at a distance F_L from the principal plane of the lens. For a thin lens, this is the plane of the lens. The linear size of an image produced by a lens

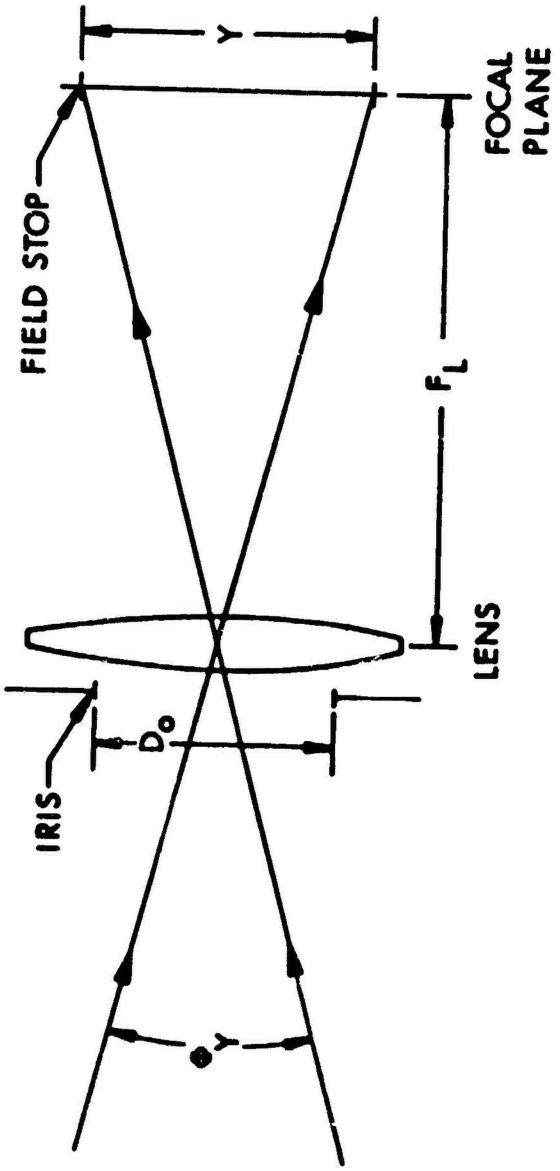

Figure 27. Schematic of the Lens

is related to the angular subtense of that object at the lens by the focal length (i.e., for small angles and large object distances, the angle subtended times the focal length is the image size).

3.4.4.1.3 Lens Focal Ratio, f/No.

The ratio of the focal length to aperture or f_L/D_o is called the focal ratio or "f/number", and is commonly used to indicate the light-gathering ability of a lens. In real lenses, the focal length is not the distance from the entrance pupil location to the focal plane as it is for a thin lens but f/No. is meaningful and related to the angle θ (see Figure 28) by the relationship

$$f/No. = \frac{1}{2n \sin\theta} \tag{11}$$

where n is the optical index of refraction of the material at the focal plane; usually air. Therefore, for an image in air,

$$f/No. = \frac{1}{2 \sin\theta} \tag{12}$$

with a theoretical minimum of 0.5.

3.4.4.1.4 Lens Transmittance, τ_o

The percentage of the energy incident on the lens from a point source that is present in the image includes losses due to absorption, scattering and blockage.

3.4.4.1.5 Lens T Stop, T

The lens T stop is numerically equal to $(f/No.)/\sqrt{\tau_o}$ and is used to relate focal plane incidence to the scene exitance levels.

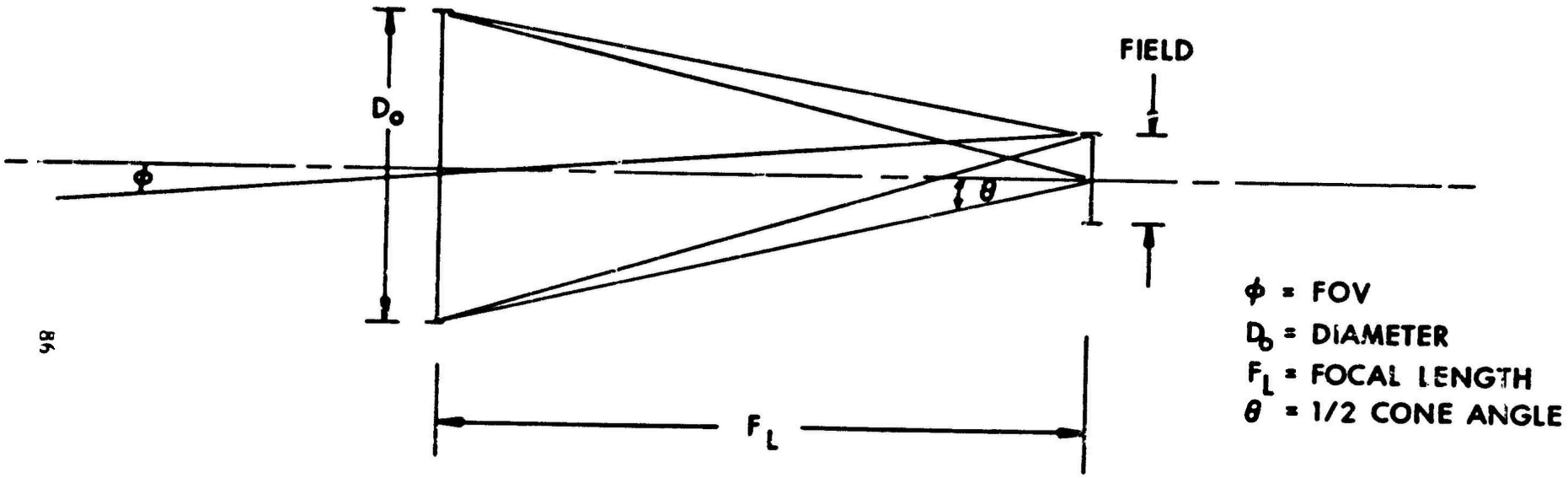

Figure 28. Thin Lens Schematic

3.4.4.1.6 Field Stop

For the thin lens case, the dimensions of the field stop are given by the dimensions of the effective photosensitive area of the receiver. In photography, the field stop is the size of the film being exposed. In TV, it is the area scanned out by the electron beams referenced to the input photosurface. For FLIR, it is the detector array dimension including scanning.

3.4.4.1.7 Field of View ϕ_x, ϕ_y

The field of view is the measure of the amount of the scene that is imaged. It is measured as the angular subtense (in object space) of the portion of the scene that is imaged by the optics onto the field stop.

The sensor field of view is numerically equal to $\phi_x = 2\tan^{-1}X/sF_L$ and $\phi_y = 2\tan^{-1}Y/?F_L$. For small fields of view $\phi_x \cong X/F_L$ and $\phi_y \cong Y/F_L$.

3.4.4.1.8 Lens Point Spread Function, $r_o(x, y)$

The $r_o(x, y)$ is a waveform of an image of a point source. This is sometimes known as the lens impulse response.

3.4.4.1.9 Lens Line Spread Function, r_o (x or $r_o(y)$

The $r_o(x)$ is a waveform of an image of a line source.

3.4.4.1.10 Lens Aperture Frequency Response, $R_o(k_x, k_y)$

The $R_o(k_x, k_y)$ is the lens complex steady-state frequency response to a point source as discussed in Appendix III. $R_o(k_x, k_y)$ is the Fourier transform of $r_o(x, y)$. The quantities k_x, k_y are spatial frequencies. (Refer to Appendix III.)

3.4.4.1.11 Lens Optical Transfer Function, $R_o(k_x)$ or $R_o(k_y)$ or OTF

The $R_o(k)$ is the lens's complex steady-state frequency response to a line source.

3.4.4.1.12 Modulation Transfer Function, $|R_o(k_x)|$, $|R_o(k_y)|$ or MTF

The MTF is the modulus of the optical transfer function.

3.4.4.1.13 Receiver Photosurface Irradiance Level

We next wish to relate the photosurface irradiance level from the scene to that at the scene. Suppose the radiance of a small area a_o on the scene at Range R to be L_s watts/m^2-sr. If the scene is diffuse, that is a lambertian radiator,

$$L_s = \frac{M_s}{\pi}, \tag{13}$$

where M_s is the radiant exitance of the scene in watts/m^2. The flux Φ_o, incident on the sensor's lens will be

$$\Phi_o = \frac{M_s a_o A_o \tau_o}{\pi R^2} \tag{14}$$

Where

$$A_o = \frac{\pi D_o^2}{4}$$

is the effective area of the objective lens and τ_o is its transmittance

$$\Phi_o = \frac{M_s a_o D_o^2 \tau_o}{4 R^2} \tag{15}$$

For an infinity focused lens and small areas,

$$\frac{a_o}{R^2} = \frac{a_i}{F_L^2} \quad , \tag{16}$$

Where a_i is the image area corresponding to a_o.

Therefore,

$$\Phi_o = \frac{M_s a_i T_o}{4F_L^2/D_o^2} \tag{17}$$

and the irradiance at the image from the scene is

$$E_i = \frac{\Phi_o}{a_i} = \frac{M_s T_o}{4(f/No.)} = \frac{M_s}{4T^2} \tag{18}$$

where T is the lens T stop as previously defined. The above equation may also be written as

$$E_i = \frac{\pi L_s}{4T^2} \tag{19}$$

Expressions in terms of both T and f/No. are maintained because historically, the TV-oriented work has used T but the IR analysis, especially of the more recent background limited IR systems, has not. This difference of approach and therefore use of parameters comes about because the IR system's performance is basically independent of f/No. since almost any sized detector is available and as will be shown, the sensitivity is a function of entrance pupil and instantaneous field of view. For the TV system, the area of the photosurface is more of a system parameter making focal length and f/No. more important. That is, for a photon-limited

system, either the instantaneous field of view and optics pupil or the f/No. and photoreceiver diameter can be considered to be the important parameters. The IR took the first two, the TV took the second two. If f/No. is maintained in the equation, then F number is useful to introduce.

The signal for either system is the modulation on the average irradiance rather than the absolute value per se. In this case, we work in terms of the ΔE caused by a ΔM or ΔL. For large targets

$$\Delta E_i = \frac{\Delta M_s}{(2f/No.)^2} \quad \tau_o = \frac{\Delta M_s}{4T^2} \tag{20}$$

but for small targets the amplitude of ΔE_i decreases faster than the relative amplitude of ΔM_s due to the transfer function of the optics. For sinusoidally periodic scene modulation, the image modulation is reduced by the MTF of the optics at that frequency,

$$(E_i)_{p\text{-}p} = |R_o(k_x)| \frac{(M_s)_{p\text{-}p}\,\tau_o}{(2F/No.)^2} = |R_o(k_x)| \frac{(M_s)_{p\text{-}p}}{4T^2} \tag{21}$$

where p-p indicates peak-to-peak of the sine wave. Similar relation ships for other functions exist and require other transfer functions such as square wave, flux, and pulse.

In actuality, ΔM_s may not be the significant or commonly-used scene parameter. For the FLIR, it is convenient to work in terms of an equivalent blackbody ΔT (Refer to Appendix IV). And for TV, it may be convenient to consider the scene irradiance and Δ_o (diffuse reflectivity difference). Therefore, while ΔE may be used for commonality of analysis, the final results will use more conventional parameters.

3.4.4.2 Photon Receivers (Radiation Detectors)

The radiation detector is placed at the focal plane of the optics and receives the image of the apparent scene. It detects the radiation and generates an electrical signal which is then amplified and processed as the video signal. The signal-to-noise ratio resulting from this detection process determines the limiting sensitivity for the system.

This section will first provide a "broad brush" treatment to provide a general feel for the situation as it affects both systems. Then, the details of the photon receiver will be discussed and finally the relationship for calculating the signal-to-noise ratio at the output of the receiver will be derived.

3.4.4.2.1 Introductory Comments

The radiation detector may consist of a photo-sensitive surface which is (in effect) read out by a scanning electron beam as it is for a TV camera or as an array of photo-sensitive detector elements which are continuously read out as they scan the image as is the case for an optically-scanned infrared imaging system (FLIR). In either case, we are interested in photon receivers which will generate a video signal related to the received radiation. In general, the output current is related to the input image by the responsivity which is often separated between its peak value σ_p and the relative function $R(\lambda)$. σ_p is measured in amps per watt and indicates the signal generated per watt of energy at the spectral peak of the receiver. The photon generated current as a function of the area (A) of the receiver flooded with irradiance $H(\lambda)$ watts/cm^2 is given by

$$i = A\sigma_p \left[\int_0^\infty R(\lambda)\, H(\lambda)\, d\lambda \right]^\nu \qquad (22)$$

where ν is introduced for generality and will be discussed later but for now is assumed to be unity.

While the phenomenon is the same for both systems, the nature of the source of the signal and noise has caused different parameters and parameter emphasis to evolve for the two technologies. This section will try to stress the signal imposed differences. To that end, it is easiest to start with the case where the limiting noise is the result of the random detection of photons in the image, the photon noise limited case. For this case, due to the statistics associated with photon arrival/detection, the noise at the receiver output is proportional to the square root of the number of photons incident. The following indicates how the signal-to-noise ratio are generally related to the image irradiance and will make reading the next two sections easier.

TV	IR
For a TV system, the average value of the image irradiance on the photon receiver is proportional to the apparent scene exitance (refer to subsection 3.4.4.1.13) which is proportional to the product of the high light scene irradiance and the average scene reflectivity modified by the atmosphere. These systems are so designed (baffled) that no other source of radiation contributes significant photons to the image. The modulation on this average value varies as the reflectivity in the scene, and is discussed as a percentage of the average value. It is referred to as the ac signal or just the signal.	For the IR system, the irradiance on the photon receiver is the energy in the image plus radiation from all other objects within the field of the detectors and not at cryogenic temperatures. In general, it can be assumed that two temperatures exist, cold and ambient. The result is that the average value of the radiation on the detector is that due to an ambient temperature blackbody filling the field-of-view of the detector. The field-of-view of the detector is limited by cold baffles and is designed to accept signals from the optics while blocking radiation from the sensor housing. The modulation in the image is from the variation in photons over the apparent scene and can be thought of

Because this modulation remains a constant percentage of the average, even though the scene illumination changes, the concept of contrast has become a integral part of the TV signal vocabulary. Contrast is defined by the equation

$$C_m = \frac{L_{max} - L_{min}}{L_{max} + L_{min}} = \frac{\Delta L}{2 L_{av}} \qquad (23)$$

where L_{max} and L_{min} are radiances of the object and background depending on which is the brighter. With the above definition contrast is always positive and can range in value between 0 and 1 only. This is an analytical convenience. Positive and negative contrasts are equally detectable. When image contrasts are much greater than unity, they are separately considered.

For a linear photoelectron noise limited receiver working in this environment, the signal will be proportional to ΔL and the noise is proportional to $L_{av}^{1/2}$. Since both ΔL and L_{av} have essentially the same spectral

as occurring due to (small) temperature variations about the ambient. Since the sources generating the modulation may be at long range viewed through the atmosphere, while the ambient will have contributions from shorter ranges (the atmosphere and even inside of the sensor) the spectral characteristics of the modulation are not the same as the spectral characteristics of the average signal. Additionally, the average signal is essentially constant over the scene and even with time, while the modulation may vary considerably. Finally, the absolute value of the average irradiance has little or no importance to the image of the IR system. These three facts have caused "contrast", as used as a meaningful parameter in the visible scene, to be meaningless in the IR. There is no constant relating the (modulation) signal to the average dc value, (i.e., to the photon noise).

There is, however, a parameter which has intuitive meaning and tends to relate to signal, and since noise is constant, to signal-to-noise ratio. This parameter is the change in temperature from the average, ΔT. It

TV	IR
distribution and are related to the reflectivity ratio of the target scene by the contrast, it only becomes necessary to work in terms of the average photo current and the contrast, with the contrast being a constant of the apparent scene, and the product of the irradiance and the average reflectivity resulting in an average photocurrent being the dependent variable. Therefore, since the peak signal can be related to the average signal by the contrast and the noise is proportional to the square root of the average current, the peak signal-to-rms noise ratio at the output of the receiver is proportional to the product of the contrast and the square root of the average current.	is true that the system actually detects the change in irradiance which is proportional to ΔT only for specific targets, atmosphere, and spectral response but it is a meaningful laboratory signal parameter when coupled with the system spectral response and it is a more meaningful parameter for defining the response of an IR system than contrast would be. (e.g., while 3 to 5 and 8 to 14μm systems, with the same ΔT sensitivity, appear similar, the contrast would be very different.) Appendix IV relates ΔE to ΔT.
$SNR \propto 2C_M (i_{ave})^{1/2}$ (24)	For an IR system, as has been mentioned, the noise is generally constant with conditions. For some systems the noise is determined by the system or preamplifier. For others, it is determined by the IR detector. With many detectors, the system may be operated in a photon* noise limited condition. That is, the noise is derived from the random arrival/detection of photons (from the ambient temperature blackbody within the field of the detector).

*Coauthor F.A.R. would prefer to refer to this a photoelectron noise and consider it to be the result of detection only rather than arrival/detection. The treatment presented is more consistent with the thinking in the IR community.

TV	IR
	The signal, on the other hand, is the change in image irradiance generally related to small variations in scene temperature. Consequently, the signal out of the detector is calculated separately from the noise, based upon the signal generated when a variation occurs over the total area of the detector.

3.4.4.2.2 Photon Receivers

This subsection describes in more detail some of the idiosyncrasies of receivers and the parameters used.

TV	IR
The photosurface is usually a continuous surface of photoemissive materials which creates a photoelectron image proportional to the photon flux incident on the surface. The characteristics of the detector which are of importance are its spectral responsivity and its area.	The detectors are generally photon detectors (either photoconductive or photovoltaic) generating a signal current proportional to the photon flux incident on the surface. The characteristics of the detector which are of importance are the spectral responsivity, spectral detectivity, impedance, and frequency response.
The photosurfaces used in high-performance camera tubes are generally combinations of a number of photoemitters with the overall spectral response reflecting spectral responsivity contributions	The spectral responsivity is the ratio of the signal-out to signal-in. It is generally specified as the Amps/Watt or the Volts/Watt that can be obtained from the detector as

from each of the individual photoemitters. The spectral responsivity is generally specified in Amps/Watt. Quantum efficiency of the photosurface is less than unity at any wavelength.

To achieve high sensitivity, multiple reimaging processes may be involved. For example, an image intensifier may be added as discussed in subsection 3.4.4 which provides gain through image minification and through the gain of the phosphor. Additional gain may be provided in a gain-storage target. A primary function of the gain storage target is to store the amplified photoelectron image for the period between successive charge readouts by the scanning electron beam. Through the image storage, the utilization efficiency of the photoelectron image generated by the input photosurface becomes unity.

The purpose of providing gain before image storage is to amplify the photoelectron noise to a level well above that of the TV camera tube's internal or external

a function of the frequency of modulation of the radiation. Responsivity is important since it is one of the parameters which indicate how difficult the preamplifier design will be. A low-responsivity detector may be difficult to use as it may be difficult to amplify the output without generating significant amplifier noise. However, by knowing the spectral responsivity, the output signal for any input signal can be determined. The current responsivity is determined by the quantum efficiency and the gain of the detector. The quantum efficiency indicates how many photoelectrons are generated per photon. The gain indicates how many signal electrons are generated per photoelectron. In photodiodes, the gain is unity and the quantum efficiency typically 50 percent over the spectral band of interest. In a photoconductor, gains of 10 or more are possible depending upon the bias voltage, size, and the carrier lifetime in the element. This gain occurs because the photocurrent is changing the relative impedance of the photoconductor which in turn generates a signal current through a load resistor. The interested

preamplifier, and to reduce the read-in and read-out time constants at low-image irradiance levels. As the image irradiance levels are increased, the read-in and read-out time constants and preamplifier noise become of little concern and it is advantageous to decrease gain prior to read-out in order to keep from saturating the storage target and to improve image signal-to-noise ratio.

A photoemitter will have a dark current which represents additive noise. This noise is usally negligible for most currently used high-performance TV cameras. Where it is a problem, it is usual to cool the photosurface to bring the dark current within acceptable bounds.

Most low-light level television cameras now in use have their sensitivity limited by the noise generated in the photon-to-photoelectron conversion process when the cameras are operated at maximum sensitivity as is the case for FLIR. Unlike the FLIR, the

reader is referred to R. D. Hudson, Jr. (Ref. 15). Photon detectors tend to be constant photon efficiency devices and therefore have a photon spectral response which is constant out to the cutoff wavelength (Bandgap determined). This results in a spectral response in terms of watts which is proportional to wavelength out to cutoff. The frequency dependence of the responsivity is determined by the lifetime and mobility of the photoelectrons, and can generally be represented by a single time constant indicating the corner frequency for a 6 dB per octave rolloff, a simple low-pass filter.

The impedance of a detector is a significant parameter for preamplifier design and an indicator of the quality of the detector but does not affect this analysis.

The spectral detectivity, $D^*(\lambda, f)$ is the most important single detector performance parameter since it determines the ultimate sensor sensitivity. $D^*(\lambda, f)$ is the signal-to-noise ratio per unit area (for 1 Hz noise bandwidth at frequency f) for a 1 watt

TV	IR
photoelectron noise is a strong function of the scene irradiance rather than being nearly constant.	of λ micrometer energy input modulated at frequency f. This definition, using area normalization, was prompted by the fact that most detectors generate noise voltage (or current) proportional to the square root of the area and thus the signal-to-noise per watt for any area detector can be calculated based upon D*(λ, f) and the bandwidth of interest.
Thermal radiation from the surround of the photosurface is not sufficient to affect visible and near infrared photosurfaces. However, it is necessary through good optical design practice to prevent stray light from being reflected off lens surfaces and sensor walls which may degrade the image contrast.	Most detectors used in the advanced FLIR systems have their sensitivity limited by the noise generated by the random detection of photons which is proportional to the square root of the number of photons received. For these detectors, the D*(λ, f) is therefore a function of the total photon flux (in the spectral region of interest) incident of the detector. In fact, the sensitivity of such a detector operating as a photoconductor is related to its quantum efficiency by the relation

$$D^*(\lambda) = \frac{\lambda}{2hc}\left(\frac{\eta}{Q}\right)^{1/2} \qquad (25)$$

where:

λ = the wavelength of signal radiation

h = Planck's constant

c = speed of light

Q = the rate of arrival of photons on the detector

η_q = the responsive quantum efficiency of the detector.

For a pv or photovoltaic detector, this expression is improved by a factor of $\sqrt{2}$ since the photon generated electrons are swept out of the detector (across the junction) before recombining and causing recombination noise. One could consider the pv detector to be an ideal photon counter.

Improving the D* of the detector improves the limiting S/N ratio determining element. While photon (background) noise-limited detectors are the theoretical limit for a FLIR device and are available, much can be done to optimize their use. It is obvious that one will use the best quantum efficiency obtainable; and, also that one would use photovoltaic detectors all things being equal. In addition, Q should be minimized while maximizing the incremental signal above background. There are two methods for reducing the (background) photon flux (Q) on the detector: spatial shielding and

TV	IR
	spectral shielding. Spectral shielding simply means placing a non-emitting (cold) spectral filter in front of the detector elements. This reduces the radiation received to that present in the region of interest, i.e., spectral bands with no signal such as atmosphere absorbtion regions should be filtered out for field optimization. Spatial shielding means limiting the field-of-view of the detector elements to maximize the signal-to-noise ratio. The optimum case is when the total field-of-view of the detector is the collecting optics. For this case, the background photons collected are proportional to the $\sin^2\phi$ or $\left(\frac{1}{2\ f/No.}\right)^2$. (Refer to subsection 3.4.4.1.3) and D* is proportional to 2f/No. Defining D** as the D* when a perfect detector ($\eta_q = 1$) is exposed to radiation from a full hemisphere; (2π steradians) then for an optimally-shielded detector $D^* = 2f/No. * D^{**} * \eta_q^{1/2}$ (26)

Since a detector is seldom optimally shielded due to practical considerations, it is convenient to define a shielding efficiency as the ratio of the effective D* experienced in the system to that obtainable with optimum shielding. A value for η_s of 0.70 is good in most conventional designs. η_q is a function of the detector material chosen and its quality. A value for η_q of 0.16 is common for Ge:Hg while values of 0.4 are reported for HgCdTe.

When shielding detectors, it is important to remember that as noise due to photons is reduced, other noise sources may become dominant. There is always a practical limit where further shielding will not improve the detector D*. When using narrow spectral filters, the limit for useful spatial shielding can be considerably reduced. For some detectors (not background limited) nothing is gained by shielding below the wide open case. With the definition of (cold) shielding efficiency chosen, it is possible to extend its meaning to cases for non-background limited or marginal background-limited cases. (This has not generally been

done in the past but is considered a useful extension by the authors; it is not a necessary extension for this analysis.) That is, with the detector operating in air (or vacuum) as is the general case for FLIR systems let

$$\eta_s = \frac{D^* \text{ shielded}}{[D^* 2\pi]\, 2f/No.} \qquad (27)$$

η_s has a useful general efficiency meaning for design; that is how close to the shielded background limited case the system is. For a totally background-limited case, it indicates how efficient the cold-shielded design is. For a partially background-limited detector, it indicates the effect of both the geometrical design of the shield and the fact that the system is designed around more shielding than is useful and faster optics are desired. For a non-background limited system, it indicates that the detector will function most efficiently with fast optics, i.e., for all cases in air when $f/No. = 0.5$ $\eta_s = 1.0$. (It should be noted that for immersed detectors $\eta_s > 1$ is possible.) Figure 29 indicates the total effect of this notation by the BLIP lines and the non-BLIP line plus one partially BLIP case. In general, it is easier to obtain high η_s with faster optics.

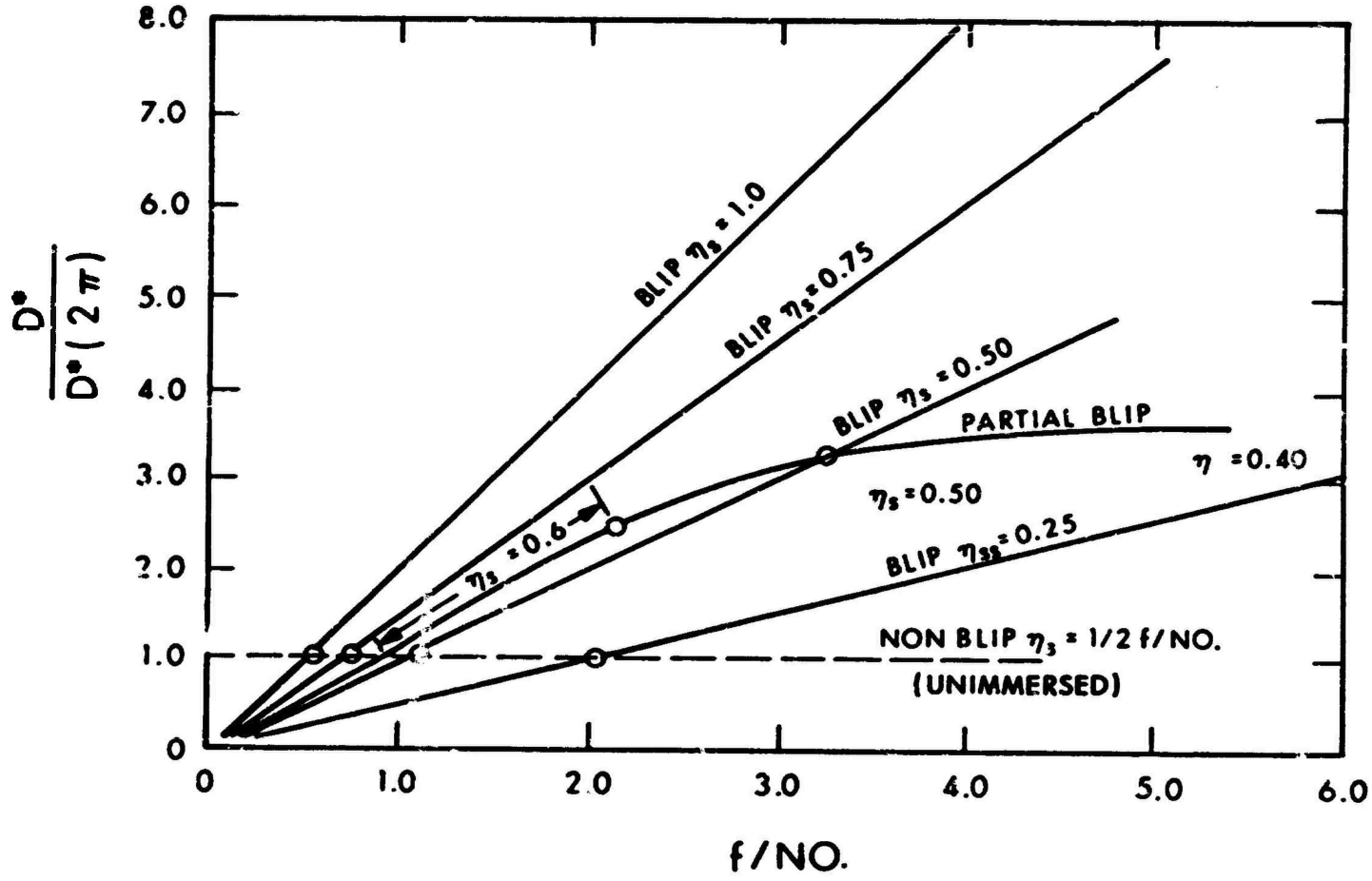

Figure 29. Normalized D* (D* improvement factor) versus System f/No. for Various Shielding Efficiencies

On the other hand, the partial BLIP curve indicates a typical case. For f/No. <0.8; $\eta_s = 1.0$. For $0.8 <$ f/No. < 2; $\eta_s = 0.6$. Above this f/No., the detector is no longer limited and η_s drops off with increasing f/No. but only drops to 0.4 at f/5. Generating this curve for a detector will better clarify the total system efficiency tradeoffs to be made since, in general, the optical transmission (or efficiency) will also vary with f/No., i.e., for a given detector the product $T_o \eta_s$ can be optimized by optical design.

One other degree of non-idealism creeps into some detectors and that is non-white noise. The most common non-white noise is 1/f noise which has a noise power spectral density inversely proportional to frequency. There are many theories on how this noise is generated. For this analysis we will not be concerned with how it is generated only that it is generally well behaved and may be present in detectors which otherwise appear to be photon-noise limited.

3.4.4.2.3 Signal-to-Noise Ratio at Output of Photon Receiver

Because of the differences in signal, noise, and the parameters common to the two technologies, this analysis will be done in parallel. The main common point is to indicate that the signal for each system is a function of the source and system spectral characteristics.

For TV, the variations in source spectrum have a major effect on the quoted systems numbers and therefore a tungsten source operated at 2854°K is often used in making laboratory measurements. The total response per watt being grossly different for other sources, optimizing for the wrong source can give misleading results. Analysis in terms of input photocurrent is quite general however, and is much more useful when different types of sources are expected.

For IR systems, the source spectral characteristics are not so important as the nominal spectral response bandwidth ($\Delta\lambda$). In the laboratory with zero atmosphere, the signal increases almost proportionally to $\Delta\lambda$ while the noise only increases as $\Delta\lambda^{1/2}$. In the field, the atmosphere limits the region over which signal can be gained but has no such effect on the noise. It has not been uncommon to see systems optimized for the laboratory to pass acceptance tests (i.e., large $\Delta\lambda$), and thereby, made to perform poorly in the field. Not only did they perform more poorly than apparently equivalent systems (smaller $\Delta\lambda$) but more poorly than those systems would if properly optimized.

Therefore, in what follows while the analyses may appear different, one should be sensitive to the common problem of performance confusion caused by the desire to drop the wavelength dependence.

TV	IR
The signal-to-noise ratio at the output of the photosurface is as given in Eq. 24 in subsection 3.4.4.2.1 A video signal-to-noise	Combining the results of subsection 3.4.4.1.13 on the irradiance at the optical image plane and the above subsections on detectors, we can

TV	IR
ratio as discussed in parallel for the FLIR has no meaning until after the signal is stored and read out by the electron scanning beam in the signal processor. After scanning, a video signal-to-noise ratio can be defined.	immediately determine the large target signal-to-noise ratio at the detector output which we will call signal-to-noise ratio video channel $(SNR)_C$.
	From the definition of $D^*(\lambda)$,
	$$(SNR)_C = \int \frac{D^*(\lambda)}{\sqrt{\Delta f}} \Delta H_{i(\lambda)} (A_d)^{\frac{1}{2}} d\lambda \quad (28)$$
	where Δf and A_d are defined in the next paragraphs.
	A_d is the area of a detector element and is related to the instantaneous field of view of the sensor for that element by the focal length of the optics. This sensor instantaneous field-of-view (δ) is an important parameter of an IR system. Using δ_x and δ_y to indicate the instantaneous field-of-view in two orthogonal directions
	$$A_d = F_e^2 \delta_x \delta_y \quad (29)$$
	Δf is the noise bandwidth for the noise measurement. This bandwidth, to a great extent, is often arbitrary for an imaging system since the final operator-determined bandwidth is the important one and indeed a deliberately wide bandwidth may be used in the

sensor so as not to reduce the system MTF. Consequently, for the purpose of uniformity, an electrical bandwidth equal to the reciprocal of twice the minimum dwell time of an image point on the detector is recommended. Δf however is not the electrical bandwidth but the noise bandwidth of the sensor. That is, it is the bandwidth based upon the noise spectral density at some arbitrary frequency which, when multiplied by that power density, will provide the correct noise power. For this reason, the noise spectrum of the sensor and the D* at one frequency must be known. If $\sigma(f)$ is the noise voltage spectral density and $\sigma(f_o)$ is the value of $\sigma(f)$ at f_o (the frequency at which the D* was measured) and if $G(f)$ is the transfer function of the bandwidth determining electronics

$$\Delta f = \left\{ \int \left[\frac{\sigma(f)\, G(f)}{\sigma(f_o)} \right]^2 df \right\}^{1/2} \qquad (30)$$

For white noise, the noise bandwidth and electrical bandwidth are similar, e.g., for a single RC low-pass filter the electronic bandwidth

$$\Delta f_e \text{ equals } \frac{2\Delta f}{\pi} \quad . \qquad (31)$$

TV	IR
	For non-white (but gaussian) noise the concept of Δf is useful for sensor measurement prediction but the relative noise spectral density function must be determined for complete system performance prediction.
	Continuing with the analysis, we use the discussion of subsection 3.4.4.1.13 for the signal at the detector input $$\Delta H_i(\lambda) = \frac{\Delta W_s(\lambda)}{(2f/No.)^2} T_o(\lambda) \qquad (32)$$ and from subsection 3.4.4.2.2 $$D^*(\lambda) = D^{**}(\lambda)\ \eta_s\ (\eta_q)^{1/2}\ 2f/No. \qquad (33)$$ then $$(SNR)_C = \frac{\delta_x \delta_y \eta_s \eta_q^{\frac{1}{2}} D}{2(\Delta f)^{1/2}} \int_\lambda T_o(\lambda) D^{**}(\lambda) \Delta W_s(\lambda) d\lambda \qquad (34)$$

3.4.4.3 Signal Processor

The signal processor is functionally illustrated in Figure 30. The photon receiver output must be matched with a low-noise preamplifier, amplified to a usable level, and then prepared for display. For either system the preparation for display involves modification of the frequency response and the amplitude response of the system.

Modifying the frequency response may be to limit the noise (bandwidth) or may be to provide high-frequency boost to improve the system MTF. In this case, the phase shift that can be introduced must be considered and the OTF optimized.

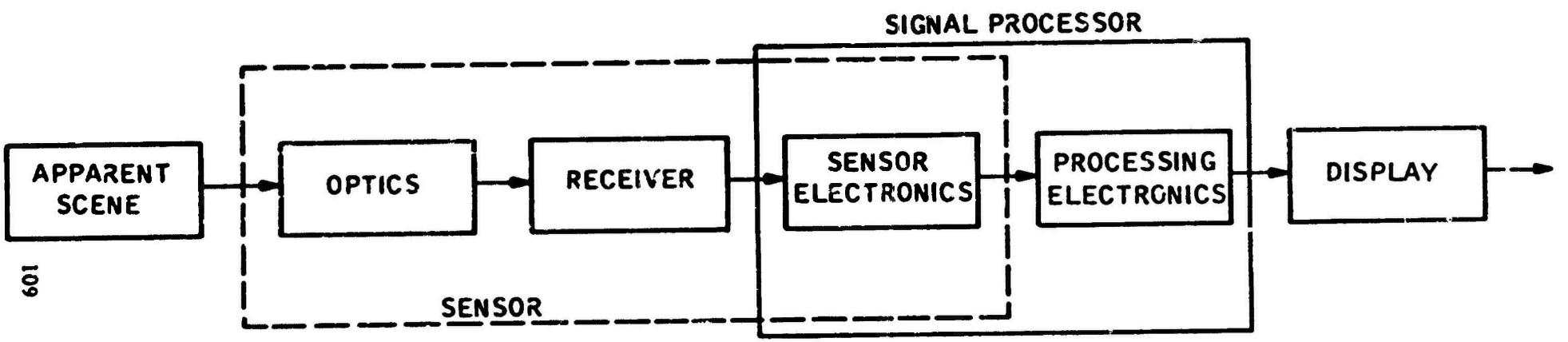

Figure 30. Imaging System Block Diagram, Signal Processor Function

The amplitude function relates the input signal amplitude to the output amplitude. At the very least, the electronics must control the gain (contrast), dc level (brightness), and the saturation characteristics. In addition, it can be used to make the total system linear or deliberately nonlinear.

TV	IR
In a high-performance television camera, the photoelectron image generated by the input photocathode is accelerated to a phosphor by a potential difference of up to 15 kV. The phosphor recreates a visible image. With the maximum voltage applied, the phosphor produces approximately 1000 photons/electron. This amplified image is then transferred to a second photosurface via fiber optics with an efficiency of about 50 percent. The second photocathode then reconverts the photon image with an efficiency of from 5 to 10 percent so that the net gain of the phosphor, fiber optic, and second photosurface is between 25 and 50. This gain may be considered noiseless except as the MTF of the phosphor particles and fiber optics affects noise.	It is not important in this analysis whether the outputs from an array of detectors are time multiplexed, delayed and summed, or parallel processed. (See Figure 26.)
The amplified photoelectron image is then accelerated to the	Multiplexing is used to provide a fast scan in a direction parallel to the detector array length while the array is slow scanned in a direction normal to its length. Since the multiplexer is a time sequential sampling switch (nonlinear) it is necessary that the per channel bandwidth be limited to less than twice the per channel sampling frequency. Otherwise, unwanted signals will be generated within the system bandpass. These signals are referred to as "aliases." Another characteristic of the multiplexer is that the time parameter of the signal becomes related to the fast scan direction rather than the slow (detector) scan direction. Hence, time (or temporal frequency) effects on the signal

gain-storage target. Depending on the type of target and accelerating voltage, an additional gain of from 3 to 2000 is obtained. Again, this gain is noiseless. The new amplified electron image is then stored by the storage target for the period between scans of the electron beam. The electron beam scans the gain-storage target point by point in a raster fashion. Because of the signal storage, the signal utilization efficiency is unity.

In the discussion which follows, the MTF effects and some noise sources are ignored in the interests of illustrational simplicity. However, these factors will be included in later discussion. The incremental signal current in the target lead, ΔI, which represents the stored image read out by the beam is given by

$$\Delta I = G_I G_T \Delta_{ip} / e_v e_h \qquad (35)$$

where G_I is the intensifier gain, G_T is the target gain, Δ_{ip} is the

affect spatial distribution of brightness in that direction. The advantages of such a scheme are that the optical scan rates can be reduced and by reducing the information bandwidth requirement for each channel, the signal-to-noise ratio of the sensor and the system improved as the square root of the number of independent channels. The disadvantages result from the large bandwidth required in the final video channel and the low-level low-noise switching. The fact that the bandwidth gets large tends to result in a compromise which leaves the system sampled data limited in two dimensions.

Delay lines and summing are used when detectors are scanned in series using optical scan for both axes of the sensor field-of-view. This technique generates a single video signal which can be processed as though only a single detector had been used and the time parameter relates to space in the direction of the high-speed scan. The advantages of such a scheme are that the signal from each detector will add linearly while the noise adds with random

photoelectron current generated by the input photosurface and e_v e_h are the vertical and horizontal scanning efficiencies respectively. The rms noise current at the target lead is given by*

$$I_{mt} = \left[\left(\frac{G_I\, G_T}{e_v\, e_h}\right)^2 2ei_{av}\, \Delta f_v\right]^{1/2} \quad (36)$$

where e is the charge of an electron i_{av} is the average input photosurface current, and Δf_v is the video bandwidth. The quantity $2ei_{av}\, \Delta f_v$ can be recognized as the mean square photosurface shot noise.

The video signal-to-noise ratio, SNR_v, at the target lead can now be written as

$$SNR_v = \frac{\Delta I}{I_{mt}}$$

$$= \frac{G_I\, G_T\, \Delta_{ip}/e_v\, e_h}{\left[\left(\frac{G_I\, G_T}{e_v\, e_h}\right)^2 2e\, i_{av} \cdot \Delta f_v\right]^{1/2}} \quad (37)$$

In the case where $G_I\, G_I$ is insufficient, the preamplifier noise may be a factor. Assuming for the moment that the preamplifier noise

phase. Therefore, the signal-to-noise ratio again improves as the square root of the number of independent channels and the scanning of many channels by overscan leads to very high uniformity of displayed signal and noise. The disadvantages of the system are that the large bandwidth required right out of the detector pushes the present state of the art limiting the number of picture elements per second and precluding effective scan overlap leaving the system sampled data limited in one direction. Also the scan speeds required are a mechanical design burden.

The parallel processing approach processes each detector channel in parallel driving an array of light sources. In this case, slow optical scan and narrow per-channel bandwidths result. It minimizes the electronic bandwidth required in each channel and introduces the possibility of optical signal processing. By this technique, considerable overscan and overlap can be implemented with relatively low-speed optical scanning. The disadvantage is that each channel is a complete signal processing channel

*For a photoelectron noise limited system

is white and of mean square value, I_{pa}^2, referenced to the preamplifier input,

$$(38)\quad SNR_v = \frac{G_I\, G_T\, \Delta_{ip}/e_v\, e_h}{\left[\left(\frac{G_I\, G_T}{e_v\, e_h}\right)^2 2e\, i_{av} \Delta f_v + I_{pa}^2\right]^{\frac{1}{2}}}$$

Clearly, the preamplifier noise will become negligible if the gain $(G_I\, G_T/e_v\, e_h)$ is sufficient. However, when Δ_{ip} becomes very large, it is an advantage to decrease gain in order to reduce the mean square photoelectron noise.

(i.e., single video channel processing is not possible). And, therefore if many channels are used, the electronics and the requirement for matching and adjustment can become burdensome.

For any of these processes, the first step is an effective preamplifier. To be effective, a preamplifier must provide gain over a significant bandwidth without adding significant noise. For this analysis, it should suffice to say that the more effort that goes into reducing the noise photons on a detector the more difficult the problem can be, especially for the lower responsivity photodiodes. If the preamplifier can perform as desired, it does not affect the performance analysis. If noise is added comparable to the detector noise, it must be included spectrally and a new video signal-to-noise calculated, $(SNR)_c$.

This is most conveniently analyzed by introducing a system detectivity, D^*_{sys}; sometimes called preamp limited D^*. Defining D^*_{sys} as was done for the detector but now working at the preamp output we can

derive an expression for D^*_{sys} in terms of:

- $D^*(f)$ = Detector detectivity as a function of signal frequency.
- NF = Noise factor for the preamp; the ratio of preamp output noise power (referred to the input) to the noise power for an ideal Johnson noise limited input source.
- n_j = Spectral noise density of a Johnson noise source.
- $R(f)$ = Responsivity of the detector; volt/watt.
- A = Area of the detector.
- n_d = Detector noise spectral density.

Using these definitions and remembering that the detector noise equivalent power (per Hz) or NEP is related to the D* by

$$NEP(f) = \frac{\sqrt{A}}{D^*(f)}$$

we can determine the noise voltage (current) at the detector output by

$$n_d = \frac{\sqrt{A}}{D^*(f)} \; R(f)$$

The preamp noise referred to the preamp input (detector output) is given by

$$(n_p)^2 = NF(n_j)^2.$$

The total noise limiting the system in this case becomes

$$n_T^2 = n_p^2 + n_d^2$$

The noise equivalent power for this combination then becomes

$$NEP_T = \frac{n_T}{R(f)}$$

and therefore by substitution

$$D^*_{sys} = \frac{1}{\left[\left(\frac{1}{D^*}\right)^2 + \frac{NF}{A}\left(\frac{n_j}{R(f)}\right)^2\right]^{1/2}}$$

If

$$\frac{NF}{A}\left(\frac{n_j}{R(f)}\right)^2$$

is significantly less than

$$\left(\frac{1}{D^*}\right)^2$$

then $D^*_{sys} = D^*$ and the system is not limited by the preamp. On the

TV	IR
	other hand, if it is significantly greater than $\left(\frac{1}{D^*}\right)^2$ the system SNR is determined by the preamplifier noise and a better preamp or higher responsivity detector should be used or else the SNR_C must be calculated using D^*_{sys} rather than D* in Eq. 34.
	This treatment of alternate noise sources is standard. For an IR system, it is usually possible to design the system so that the noise contribution of the electronics is negligible and this will generally be assumed here. This is a very important consideration since the optimization criteria of the system, in terms of spectral filtering and number of channels, would be changed drastically.
	The video signal-to-noise ratio can be affected in other ways by a multiplexer. A multiplexer can introduce switching spikes, dc offsets from channel-to-channel, and noise folded into the passband because of too low a sampling frequency. These effects will not, in general, be treated here since they should be precluded by design.

3.4.4.4 Sensor Performance

The output of the sensor (sometimes a gimbaled unit) is a convenient point at which to define and measure a set of performance parameters. These performance parameters are then necessary but not sufficient requirements to obtain total system performance.

The measurements of field-of-view and frame rate are rather obvious by the definition.

Resolution is normally measured only in the direction of scan since in the direction normal to scan the system is typically sampled-data limited. This is an exhaustive area of concern and later will be discussed more completely. For now, it is adequate to state that when you scan with an aperture (to read out the image) you are sampling the image continuously in direction of scan and once per scan line in the other direction. If the image has information that contains high-spatial frequencies, it is important that the scan lines be close together, i.e., have a high-sampling frequency. To faithfully reproduce an image, it is necessary that the image contain no frequency above half the sampling frequency and that the display limit the spatial frequency of the output in a like manner (a statement of Shannon's sampling theorem). In practice, this requirement is compromised in the interest of ease of design and the result is what is commonly known as raster effect. This can limit the system at least in one direction. If a mosaic or a multiplexer ar in a FLIR is used, then the system can be sampled-data limited in two dimensions and the concept of MTF and resolution as commonly used applies only for a limited frequency range. In FLIR and TV, we will mean the MTF in the direction of scan except where we are addressing the sampled-data limitation. The resolution at the output of the sensor is determined by either measuring the electrical output for a line input or by measuring the modulation for a cyclic (bar chart) input.

The sensitivity at any point and, in particular, at the sensor output can be determined by measuring the signal-to-noise ratio for a specific input. Alternately stated, the input which would provide an arbitrary signal-to-noise ratio can be determined. When an electrical signal is measured, it has become conventional to measure the peak signal to rms noise since this has meaning especially with regard to electronic thresholds. In an imaging system where it will be shown that the man processes the image as a function of the signal, it is necessary to know the noise spectral characteristics. Therefore, for a sensitivity measurement at the output of the sensor, we use the signal required for a SNR of unity with an (arbitrary) wide noise bandwidth plus a noise relative spectral density curve. Defining arbitrary bandwidth as the reciprocal of twice the point image dwell time instead of, say, a 1 Hz bandwidth will provide an indication of small target sensitivity. And, since most systems will approach the white noise case, will permit easy extrapolation to other target sizes for many systems.

TV	FLIR
In TV system design, video SNRs are measured but seldom used to specify systems although, a maximum SNR capability is occasionally required. A noise equivalent irradiance level concept, similar to the NET concept used in FLIR, could be developed provided that a reference video bandwidth is specified. The utility of such a measure has not been determined.	The signal-to-noise ratio at the output of the sensor for a well designed system is from subsection 3.4.4.2.3. $$(SNR)_C = \Delta T \frac{\delta_x \delta_y \eta_s \eta_q^{\frac{1}{2}} D}{2(\Delta f)^{\frac{1}{2}}} \int_\lambda \tau_o(\lambda) D^{**}(\lambda) M'(\lambda, T)\, d\lambda \qquad (40)$$ For a FLIR sensor, the noise equivalent input of interest is the noise equivalent ΔT or NET, the temperature difference between adjacent large objects which would provide a $SNR_C = 1$.

We can then write

$$NET = \frac{2(\Delta f)^{\frac{1}{2}}}{\delta_x \delta_y \eta_q^{\frac{1}{2}} \eta_s D} \left[\int_\lambda \tau_o(\lambda) D^{**}(\lambda) M'(\lambda, T) d\lambda\right] \quad (41)$$

Δf is a reference bandwidth and a function of the method of scan and the degree of overscan, etc. While NET is a useful number for comparison and analysis, it is important that criteria for choosing the reference bandwidth be understood. It has been almost universally agreed that the bandwidth will be that equal to the reciprocal of twice the image point dwell time on a detector as the image scans over a detector element. While it is conventional to relate the bandwidth to the scan parameters, this will not be done here. Appendix V, however, presents a derivation of NET without the constraints of considering TV comparison. This analysis of the appendix follows more directly in IR terms.

The usefulness of NET is that for a well-designed system, the video signal-to-noise ratio $(SNR)_v$, for an

input of ΔT can be predicted directly. That is,

$$(SNR)_v = \frac{\Delta T}{NET} \tag{42}$$

where the Δf_o = the reference bandwidth.

3.4.5 DISPLAY

The display transforms the input video electronic signal(s) into a two-dimensional visible display. In most cases, the mechanization is a CRT which has the electron beam amplitude modulated by the video and deflected in synchronism with the scan and/or multiplexer of the system.

Variations in the luminance of the display correspond to the amplitude variations in the video signal. Random noise on the video is displayed as "snow" or random variations on the display. It is possible that the display could add noise to the image but generally this is not the case. When the input to the display is noisy the display is considered as part of the signal processing under good conditions. The gain of the system can be turned down however until no noise is noticed on the display (yet the display is bright) and a very high quality image is observed; a high signal-to-noise ratio case. In this situation, the noise from the random generation/detection of photons limits perception by the observer. This case is the basis for the non-noise limited resolvable temperature (RT) concept discussed in reference 11.

For this study, it will be assumed that the display MTF, brightness, size, and dynamic range are its important characteristics and are the same for each system.

3.4.5.1 Magnification M

An important parameter when relating the system to the operator is magnification. The magnification of the system is the ratio of the angle the image of an object subtends at the eye of the observer to the angle the object subtends at the sensor. It can also be considered as the ratio of fields-of-view. That is if the display subtends 20° at the normal viewing distance and the system has a 4° field-of-view, the magnification is 5X. If an eyepiece display is used, magnification is a constant but with a CRT display magnification will vary with viewing distance since it is a function of display size and viewing distance. It is important when comparing systems of the same reported resolution that they be compared at the same magnification or else the observer limitation can cause variations.

3.4.6 RELATING THE PERCEIVED SIGNAL-TO-NOISE RATIO TO THE VIDEO SIGNAL-TO-NOISE RATIO

3.4.6.1 Introduction

It has already been discussed in section 3.3 that the operator makes his detection/recognition decisions based upon what we call the perceived signal-to-noise ratio. Also, it was discussed that system performance is often predicted based upon a more easily measured (and calculated) video signal-to-noise ratio existing within the electronics. Therefore, in systems using a raster generated display it is often desired to know the relationship between the video or electronic signal to noise ratio $(SNR)_v$ and the perceived signal-to-noise ratio $(SNR)_p$.

$(SNR)_p$ assumes that the operator is a spatial and temporal integrator. It also generally includes signal losses due to the MTF of the eye and noise increases due to internal eye noise. For a well designed system operating at maximum sensitivity, the display will be of sufficient size

and brightness that the degrading effects of the eye are negligible and only the integration need be considered.

$(SNR)_v$ requires (assumes) an (often arbitrary) bandwidth and a noise spectral density which must be noted for $(SNR)_v$ to be meaningful. For many situations, white noise and a reference video bandwidth Δf_v can be assumed.

What follows will calculate the $(SNR)_p$ for the general case using the approach of O. H. Schade, Sr. The test objects that will be considered are a simple isolated bar and a simple bar of a repetitive pattern. These two cases will be referred to as "aperiodic" and "periodic."

A more general detection/recognition theory is discussed in subsection 3.7 based upon these predictions and it is shown that this approach is compatible with J. Johnson's criteria.

The first step in the analysis is to relate the temporal variable of the electronic signal to the spatial variable of the display. Then the effects of integration on signal and noise are discussed. Next the size of the image is related to the size of the object and the system MTFs. Then, the perceived signal-to-noise ratio of a single line and single frame of the image is calculated. Finally, the total image and multiple frame integration for the time constant of the operator will be included to predict $(SNR)_p$.

3.4.6.2 Analysis - Relating Time and Space

To relate the temporal and spatial variables, consider the following parameters

- N = Number of bar widths per picture height
- n = Number of independent parallel video lines at the point of measuring SNR_v and Δf. (For TV, this is typically 1)

n_l = Number of scan lines per picture height (Raster frequency)

Δf_v = Noise bandwidth in each video line in Hz

ϵ = Bar height-to-width ratio

α = Display width-to-height ratio

H = Display height (angular subtense)

W = Display width (angular subtense)

x,y = Spatial variables (angular or linear)

t = Time variable

T = Frame time - Average time to display a complete field-of-view

η_{sc} = Scanning efficiency; the percentage of T that is used to scan the image assuming a linear sweep.*

The scanning of the video signal(s) onto the display transforms the temporal variables of the video signal into spatial variables in the displayed image. The time t_l for a single line to scan across a bar of width N^{-1} is given by

$$t_l = \frac{nT\eta_{sc}}{n_l N\alpha} \tag{43}$$

and the reference frequency (and noise bandwidth as discussed later) for this bar defined as $(2t_l)^{-1}$ is given by

$$f = \frac{n_l N\alpha}{2nT\eta_{sc}} \tag{44}$$

The following comments will provide a better understanding of some of the parameters:

*For nonlinear sweeps (e.g., sinusoidal) special considerations are necessary but similar definitions can be developed.

TV	IR
For a TV system, a single video channel (i.e., n = 1) providing n_1 displayed lines per frame is common. Often n_1/η_{sc} is quoted as the number of lines; e.g., 525. α for TV is typically 4/3.	For IR, there may be n parallel channels (at least at the point of measuring $(SNR)_v$ and somewhat independently n_1 lines. Even in a multiplexed system, it is often desirable to relate the temporal variables of the multiple parallel (or series) channels to the spatial variables of the display.

3.4.6.3 Analysis - The Effects of an Integrator

Before getting into the analysis it is necessary to realize what an integrator does. A perfect integrator continuously sums the values of a function for a set period of time or space. There are two effects of interest: the low frequency gain is proportional to the duration of integration; the response to high frequencies relative to low frequencies reduces as the duration is increased. Specifically, the normalized frequency response of an integrator is given by

$$R/_{Ro} = \frac{\sin \pi vu}{\pi vu} \tag{45}$$

where v is the dummy frequency variable (space or time) and u is the duration variable. The low frequency response is proportional to u.

If white noise is being integrated, then the variations in the output of the integrator from integration period-to-integration period (which is the integrator output noise) are predicted from the noise spectral density of the input white noise $\sigma(f)$ by the multiplying by the square root of the noise bandwidth and duration of the integration. The noise bandwidth (in lines or half cycles) of the integrator is

$$N_e = \int (R/_{Ro})^2 \, dv = u^{-1} \tag{46}$$

Consequently, the rms integrator output noise is

$$\langle I_n \rangle = (N_e)^{1/2} \times \sigma(f) \times u \times K \tag{47}$$

where K is a gain/unit conversion constant.

If a signal of constant value(s) were integrated by the same process for period u, the output signal (S) would be

$$S = s\ u\ K \tag{48}$$

The signal-to-noise ratio of such a process would be given by

$$SNR = \frac{s}{(N_e)^{1/2}\ \sigma(f)} \tag{49}$$

which for white noise is

$$SNR = \frac{s\ u^{1/2}}{\sigma(f)} \tag{50}$$

or the SNR is proportional to the square root of the integration duration. It should be noted that the definition of $\sigma(f)$ as noise spectral density implies an integration for the duration of 1 cycle. Therefore, the integration is summing up independent samples of 1 cycle duration and as is commonly noted when the signal is coherent from sample-to-sample, the SNR improves as the square root of the number summed; i.e., the square root of the integration duration.

If the noise is not broadband, then the noise bandwidth is not determined solely by the integration process but also by the spectral characteristics (bandwidth) of the noise being integrated. Consider the case of band-limited white noise which is flat from approximately dc until rolled off

by a filter with noise bandwidth Ne_1. For this case, as the integration duration becomes small compared to Ne_1^{-1}, the bandwidth is not affected by changing u. Indeed, by extension of the theory discussed in Appendix II a good approximation for the total bandwidth is given by

$$(N_{en})^{-2} = (N_{e2})^{-2} + (N_{e1})^{-2} \tag{51}$$

where

N_{en} = total noise bandwidth out of integrator
N_{e2} = noise bandwidth of integrator
N_{e1} = noise bandwidth of noise into integrator

Hence, the noise from an integrator can generally be predicted by the expression

$$\langle I_n \rangle = (N_{en})^{1/2} \times \sigma(f) \times u \times K \tag{52}$$

and the (SNR) by

$$SNR = \frac{s}{(N_{en})^{1/2}\, \sigma(f)} \tag{53}$$

where it should be remembered that N_{en} is the total noise bandwidth for the noise including the band limiting characteristics of the integration.

3.4.6.4 Analysis - The Size of the Image

Since the $(SNR)_p$ is the result of integration over the image, it will be necessary to determine how large the image is as a function of object size. This can be done rigorously using the system MTF (more correctly the OTF) and the Fourier transform of the object. However, it is easier to use the approximations suggested by O. H. Schade, Sr., and discussed

in Appendix II. Therefore, the concept of system and component equivalent apertures of dimensions $(N_{ex})^{-1} \times (N_{ey})^{-1}$ will be used and (as is completely rigorous for gaussian functions and has been shown to be a good approximation for most cases of interest) it will be assumed they add in an rss manner. For an aperiodic object of dimensions N^{-1} by $(N/\epsilon)^{-1}$ the equivalent size of the image will be approximately

$$\frac{N N_{ex}}{(N^2 + N_{ex}^2)^{1/2}} \text{ by } \frac{N N_{ey}}{(N^2 + (N_{ey})^2)^{1/2}} \tag{54}$$

For the periodic case, it is important that the width of the image equals the width of the object. Therefore, the image of a single bar of a pattern would have the dimensions

$$N^{-1} \text{ by } \frac{N N_{ey}}{(N^2 + (\epsilon N_{ey})^2)^{1/2}} \tag{55}$$

Again, it should be remembered that N is the object width per picture height and ϵ is the target object height to width ratio and the system MTFs are such as to warrant separation of variables.

For a bar input, the SNR_p out of such a system is the integral over the image of the bar and over the number of independent frames presented in the time constant of the eye. The easiest method for calculating the integrals is to first calculate the integral for one raster line in the direction of scan and then integrate over the number of lines on the image in the cross scan direction. It is important that the whole theory breaks down and predicts results which are too optimistic when the raster starts to limit. That is, when there are insufficient raster lines per image for spatial invariance to be approximated. In general, there must be at least two raster lines per $(N_{ey})^{-1}$ or the theory only holds for large targets where there are many lines per $(N/\epsilon)^{-1}$. That is while small bright objects can still be seen they are not seen as well as would be expected if the raster criterion is not met.

There are two significant and related differences when considering one bar by itself rather than a bar in a periodic array. In the periodic array, the width of the image equals the width of the object, N^{-1}. In the aperiodic case, the width of the image of the bar is increased due to convolution of the bar object with the system aperture in the x direction N_{ex}^{-1}. This convolution results in an image width of approximately

$$(N_{ex}^{-2} + N^{-2})^{1/2} \quad ; \quad \text{(Refer to Appendix II.)}$$

At the same time, the amplitude reduction of the bar signal is different for the two cases. For the periodic case, O. H. Schade, Sr., introduced the square wave flux transfer function (R_{sqf}) which predicts the effective amplitude of the image. Figure 31 (from reference 5) shows the relative values for the sinewave, square wave, and flux transfer functions for a Gaussian system impulse response. R_{sqf} is given in terms of the sinewave response R by the expression

$$R_{sqf}(N) = \frac{8}{\pi^2} \sum_{n=1}^{\infty} \frac{1}{(p)^2} R(pN); \quad p = (2n-1) \tag{56}$$

while for most frequencies of interest the following approximation is useful.

$$R_{sqf} = \frac{3}{\pi^2} R. \tag{57}$$

For aperiodic images the integral over the output image equals (except for gain) the integral over the input. This was treated in detail in reference 11 (High Performance IR Systems Study) for the case of a FLIR system. Here, the treatment is meant to be more general with a minimum of Fourier transforms and the reader interested in the subtleties is referred to the reference.

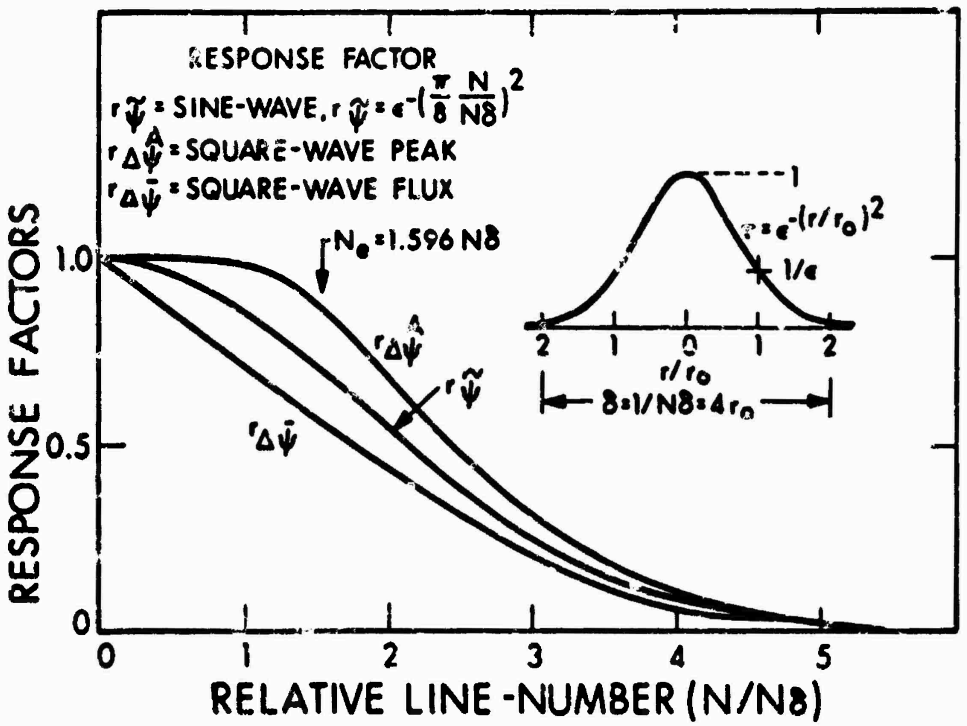

Figure 31. Image Analysis

Using Fourier transforms and realizing that the value of the transform at zero frequency corresponds to the area (volume) under the original function (i.e., the integral of interest) we have

$f_{(x,y)}$ = object function

$g_{(x,y)}$ = image function

$r_{(x,y)}$ = system aperture function (impulse response)

and F, G, and R to represent the Fourier transforms.

Where the symbol * indicates convolution,

$$f_{(x,y)} * r_{(x,y)} = g_{(x,y)}$$

$$FR = G \tag{58}$$

However, the integral over the object A_o is F evaluated at 0,0 and R at 0,0 is unity by definition. Hence,

$$G(0,0) = F(0,0) \tag{59}$$

and except for a gain constant, the integral over the image equals the integral over the object. This particular fact will be used over and over again in what follows since it is easier to integrate the signal over the constant-amplitude well defined object than the blurred (nonconstant amplitude) image.

3.4.6.5 Analysis - Perceived Signal-To-Noise - General

This subsection will discuss a few major points from which the remainder of the analysis will develop. With the above background, consider the system of the block diagram, Figure 32. The signal is modified by each of the transfer functions (apertures) in turn. Therefore, the output

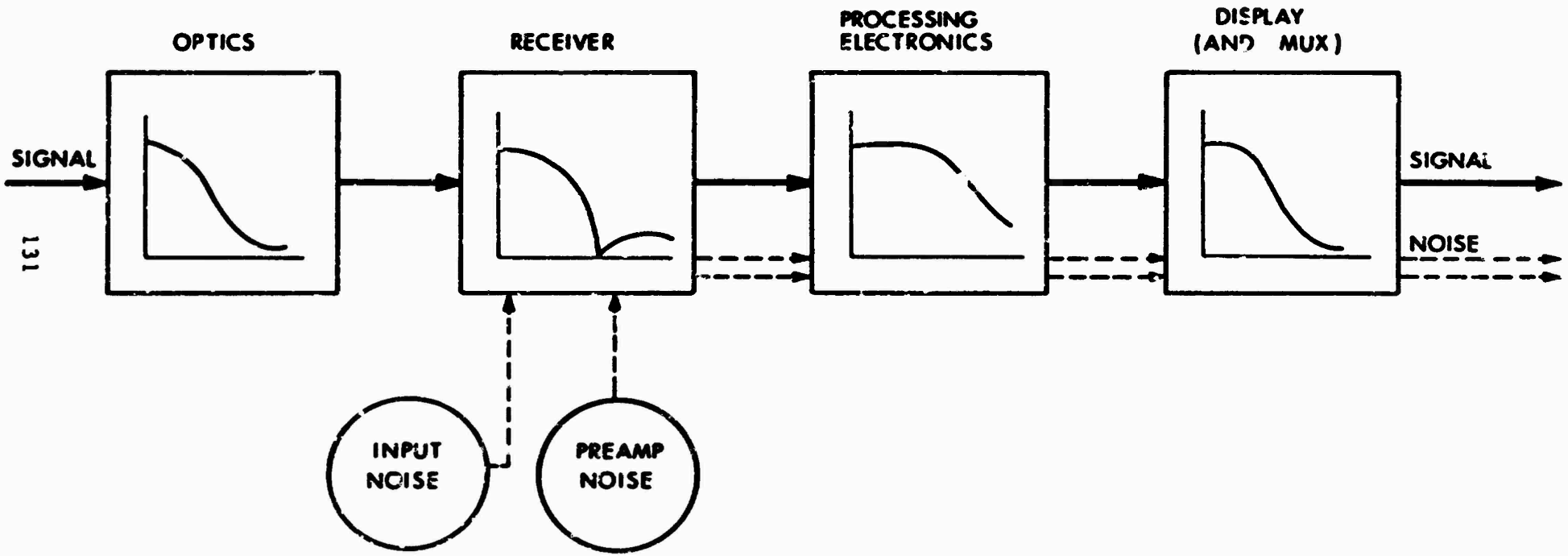

Figure 32. System Block Diagram with Indication of Transfer Functions and Noise

signal is the input signal as modified by the total system MTF or to express it another way, the image is the object modified by the total system transfer function. The noise, on the other hand, is injected at various points throughout the system and therefore is not modified by the total system MTF but only those components following the noise insertion point. It is important, however, that some of the transfer functions do roll off the noise as well as signal and therefore may not degrade performance as much as it would first appear. It is also important that the transfer functions which modify the electrical signals are only one dimensional while the rest tend to be two dimensional.

To simplify the analysis, it will be advantageous to assume that the noise at the point of insertion is white. This is not a real loss of generality because, by inserting dummy transfer functions in the block diagram, the system can be mathematically reduced to this case.

Based upon these observations, it will be advantageous to modify the block diagram to the system of Figure 33. In this diagram, all components which affect only the signal are considered to be the sensor while those components which affect both signal and noise are considered the display. This diagram and set of definitions leads to the following parameters.

$$N_e = \int_0^\infty (MTF)^2 \, dN \qquad (60)$$

N_{ex}, N_{ey} = The N_e of the system in the x, y directions

N_{esx}, N_{esy} = The N_e of the sensor in the x, y directions

N_{edx}, N_{edy} = The N_e of the display in the x, y directions

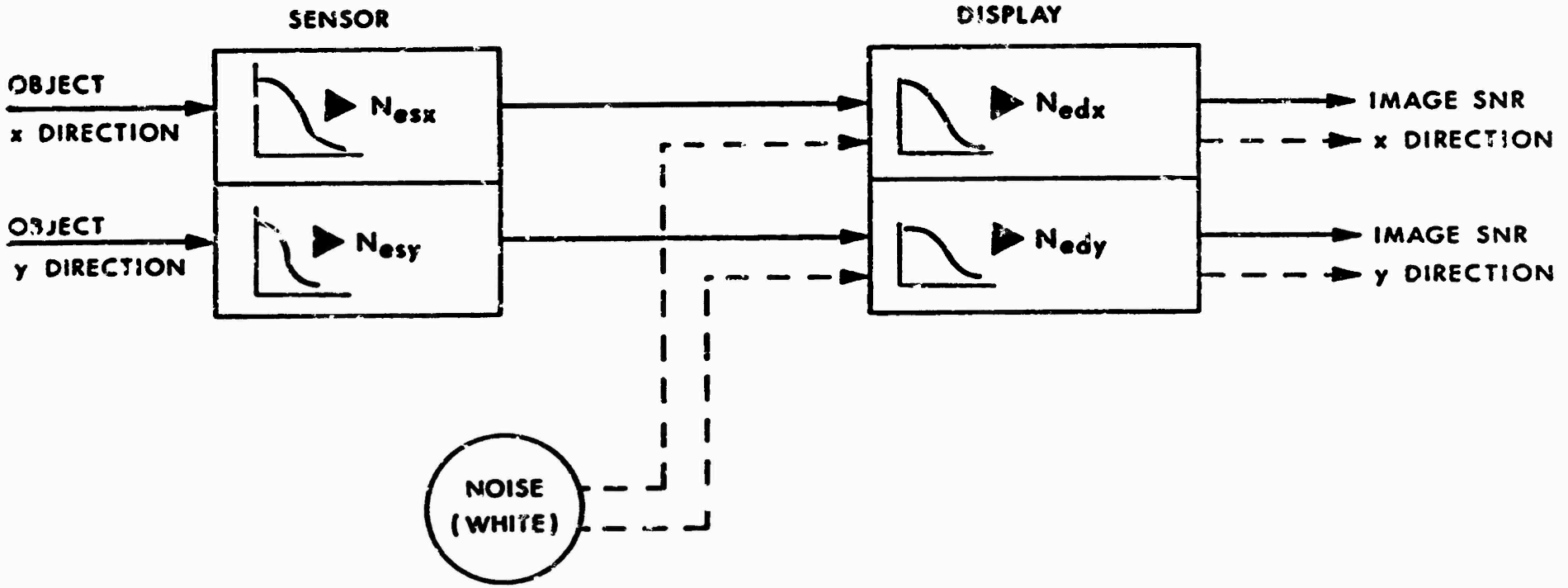

Figure 33. Equivalent System - Analysis Diagram

3.4.6.6 Analysis - Perceived Signal-to-Noise Ratio--Periodic Object

In order to relate the SNR_p to the SNR_v for the case of a periodic object, we proceed as suggested and calculate the per-frame, per-raster line integrated SNR. If i_s is the peak video signal for a large object input, then the integrated signal for one line and one frame I_{s11} would be

$$I_{s11} = K\, i_s\, R_{sqf}\, t_1 \tag{61}$$

where t_1 represents and duration of the integration corresponding to the width of the image and K represents a gain and unit constant.

Using the characteristics of an integrator mentioned earlier, the rms value of the integrated noise for one line and one frame I_{n11} would be

$$I_{n11} = K\, \sigma(f)\, t_1\, (\Delta f_{en})^{1/2} \tag{62}$$

where Δf_{en} is the noise bandwidth of the integrated noise and therefore, includes the effect of integration on bandwidth.

The single frame, single-line integrated SNR then becomes

$$\frac{I_{s11}}{I_{n11}} = \frac{i_s\, R_{sqf}}{\sigma(f) \times (\Delta f_{en})^{1/2}} \tag{63}$$

Considering the necessity of having a reference bandwidth and noise spectral density for defining $(SNR)_v$ we consider a reference video bandwidth Δf_v. Then

$$\frac{I_{s11}}{I_{n11}} = \frac{i_s}{\Delta f_v^{1/2}\, \sigma(f)} \times R_{sqf} \times \left(\frac{\Delta f_v}{\Delta f_{en}}\right)^{1/2} = (SNR)_v \times R_{sqf} \times \left(\frac{\Delta f_v}{\Delta f_{en}}\right)^{1/2} \tag{64}$$

We can relate Δf_v and Δf_{en} to object/image spatial frequencies if we so choose. Using the relations derived above, we have

$$\Delta f_v = \frac{n_l N_r \alpha}{2n T \eta_{sc}} \tag{65}$$

and

$$\Delta f_{en} = \frac{n_l N_{enx} \alpha}{2n T \eta_{sc}} \tag{66}$$

It will be convienient at times to have the Δf_v in terms of electrical frequencies rather than a spatial reference frequency and we can obviously jump back and forth as we please. For now, we will proceed with everything in terms of spatial frequencies. And then,

$$\frac{I_{sll}}{I_{nll}} = (SNR)_v \times R_{sqf} \times \left(\frac{N_r}{N_{enx}}\right)^{1/2} \tag{67}$$

It should be noted that N_{enx} is the total noise bandwidth including the integration over the image in the scan (x) direction and hence

$$N_{enx}^{-2} = N_{edx}^{-2} + N^{-2} \tag{68}$$

where N_{edx} is the bandwidth of the displayed noise, i.e., the bandwidth imposed on the noise by the components following its point of injection.

The single-line single-frame SNR then becomes

$$\frac{I_{sll}}{I_{nll}} = SNR_v \times R_{sqf} \times \left[\frac{N_r}{N N_{edx}}\right]^{1/2} \left[N^2 + N_{edx}^2\right]^{1/4} \tag{69}$$

To obtain the integral over the complete image, we must now integrate over the image in the cross scan or y direction. Since the raster tends

to make the process discrete, the integration becomes a summation and the duration becomes the number of elements (i.e., raster lines) summed.

The integral of the signal over the height of the bar will be the single line integrated signal times the number of lines on the object. The reason for not using the number of lines on the sensor or display image is that the integral over the input equals the intergal over the output and since the object amplitude is constant, the integration is easier over the input. Therefore, the signal integrated over both dimensions equals the single line integral times the lines per object height n_2.

$$n_2 = \frac{n_1 \epsilon}{N} \tag{70}$$

For the noise the integration duration is the number of raster lines on the displayed image which is larger than the object by the effects of the system N_e (aperture). While the low frequency response is proportional to the integration (summation) duration, the integration process reduces the bandwidth of the noise from that representing one raster line (n_1), to that represented by the image and the display apertures. The noise integration duration, n_3, is given by

$$n_3 = \frac{n_1 \left(N^2 + \epsilon^2 N_{ey}^2\right)^{1/2}}{N N_{ey}} \tag{71}$$

and the y direction bandwidth of the noise at the output of the final integration, N_{eny}, is

$$N_{eny} = \left[\frac{N^2}{\epsilon^2 + \left(\frac{N}{N_{ey}}\right)^2 + \left(\frac{N}{N_{edy}}\right)^2}\right]^{1/2} \tag{72}$$

or considering the system to consist of a sensor and display

$$N_{eny} = \left[\frac{N^2}{\epsilon^2 + \left(\frac{N}{N_{esy}}\right)^2 + 2\left(\frac{N}{N_{edy}}\right)^2} \right]^{1/2} \tag{73}$$

where N_{esy} relates to the sensor which puts out white noise.

Since n_1 is the initial noise bandwidth (in lines not cycles) for the cross scan direction, the total bar, single frame integrated SNR can be written as

$$\frac{I_{s1}}{I_{n1}} = \frac{I_{s11}}{I_{n11}} \left[\frac{n_2}{n_3}\right] \left[\frac{n_1}{N_{eny}}\right]^{1/2} \tag{74}$$

which by subsitution from above yields

$$\frac{I_{s1}}{I_{r1}} = \left[SNR_v\right]\left[R_{sqf}\right]\left[\frac{N_r\, \epsilon\, n_1}{N^2}\right]^{1/2} \left[1 + \left(\frac{N}{N_{edx}}\right)^2\right]^{1/4}$$

$$\left[\frac{1}{\left(\frac{N}{\epsilon\, N_{ey}}\right)^2 + 1}\right]^{1/2} \left[1 + \left(\frac{N}{\epsilon\, N_{esy}}\right)^2 + 2\left(\frac{N}{\epsilon\, N_{edy}}\right)^2\right]^{1/4} \tag{75}$$

Having completed including the effects of spatial integration, we then need only to include the temporal integration to obtain the SNR_p for the periodic case. The temporal integration simply results in a gain in SNR equal to the square root of the number of independent frames that occur in an operator time constant; that is

$$SNR_p = \frac{I_{s1}}{I_{n1}} \left[\frac{t_i}{T}\right]^{1/2} \tag{76}$$

Because the equation is so cumbersome and the case where white noise is displayed is often (at least as an approximation) useful, parameters which reflect how the display MTF effects the noise and hence the SNR_D have been defined. The parameters are identically unity when the display MTF losses are negligible. In addition, these functions are usually very weak and may often be ignored. The primary justification for this is for completeness and ease of handling multiple noise sources and injection points. For the periodic case we define

$$\beta_x\ (N) = \frac{\text{Noise Bandwidth Actual}}{\text{Noise Bandwidth for White Noise}} \tag{77}$$

Then with R_{xd} = MTF of the display in the x direction

$$\beta_x\ (N) = \left[\frac{\int_o^\infty \left(R_{xd}\ (Z)\right)^2 \left(\frac{\sin \pi N Z}{\pi N Z}\right)^2 dZ}{\int_o^\infty \left(\frac{\sin \pi N Z}{\pi N Z}\right)^2 dZ}\right] \tag{78}$$

which by our previously discussed approximation is

$$\beta_{(x)}\ (N) = \left\{\left[\frac{1}{N^2} + \frac{1}{N_{edx}^2}\right]^{-1} \frac{1}{N^2}\right\}^{1/2} \tag{79}$$

or

$$\beta_x\ (N) = \left[\frac{1}{1 + \left(\frac{N}{N_{edx}}\right)^2}\right]^{1/2} \tag{80}$$

similarly we define Γ for the Δ periodic case and derive

$$\Gamma_y(N) = \left[\frac{1 + \left(\frac{N}{\epsilon N_{ey}}\right)^2}{1 + \left(\frac{N}{\epsilon N_{eay}}\right)^2 + 2\left(\frac{N}{\epsilon N_{edy}}\right)^2}\right]^{1/2} \tag{81}$$

It is also convenient to define a parameter ϕ which is the ratio of n_1 to N_r; i.e., to Δf_v. Therefore, ϕ becomes the number of raster lines per reference aperture width. If in the future N_r becomes to be defined by N_e of the system (which is often symmetrical) which may be generally meaningful, then ϕ will be the number of raster lines per nominal resolution aperture. This would have significance from a sampling theory point of view. Therefore

$$\phi = \frac{n_1}{N_r} \tag{82}$$

Making these substitutions, we now have for a periodic object a complete expression for SNR_p in terms of SNR_v and a reference spatial frequency (N_r).

$$SNR_p = \left[SNR_v\right]\left[R_{sqf}\right]\left[\epsilon\phi\right]^{1/2}\left[\frac{N_r}{N}\right]\left[\frac{1}{\left(\frac{N}{\epsilon N_{ey}}\right)^2 + 1}\right]^{1/4}\left[\frac{1}{\beta_x}\right]^{1/2}\left[\frac{1}{\Gamma_y}\right]^{1/2}\left[\frac{t_i}{T}\right]^{1/2} \tag{83}$$

or if it is preferred that the reference bandwidth be in temporal frequency (Δf_v);

$$SNR_p = \left[SNR_v\right]\left[R_{sqf}\right]\left[\frac{2\Delta f_v \epsilon \alpha t_i \eta_{sc}}{\alpha}\right]^{1/2}\left[\frac{1}{N}\right]\left[\frac{1}{\left(\frac{N}{\epsilon N_{ey}}\right)^2 + 1}\right]^{1/4}\left[\frac{1}{\beta_x}\right]^{1/2}\left[\frac{1}{\Gamma_y}\right]^{1/2} \tag{84}$$

3.4.6.7 Analysis - Perceived Signal-to-Noise - Aperiodic Object

The aperiodic case can be handled in a similar manner. It must be remembered that the integral of the output is equal to the integral of input and the width of the image is not locked to the width of the object. That is, the integrated signal for 1 line and 1 frame would be

$$I_{s11} = K\, i_s\, t_2 \tag{85}$$

where t_2 represents the duration of the integration over the object with the other parameters defined as above. The integrated noise would be as before

$$I_{n11} = K\, \sigma(f)\, t_1\, (\Delta f_{en})^{1/2} \tag{86}$$

and the single-frame, single-line integrated signal-to-noise ratio becomes

$$\frac{I_{s11}}{I_{n11}} = \frac{i_s}{\sigma(f)} \left(\frac{t_2}{t_1}\right) \left(\frac{1}{\Delta f_{en}}\right)^{1/2} \tag{87}$$

Again introducing a reference bandwidth, we have

$$\frac{I_{s11}}{I_{n11}} = (SNR)_v \left(\frac{\Delta f_v}{\Delta f_{en}}\right)^{1/2} \left(\frac{t_2}{t_1}\right) \tag{88}$$

Since t_2 is related to the object width and t_1 is related to the image width,

$$\frac{t_2}{t_1} = \frac{N_{ex}}{\left(N^2 - N_{ex}^2\right)^{1/2}} \tag{89}$$

And, by the same argument as before

$$\frac{\Delta f_v}{\Delta f_{en}} = \frac{N_r}{N}\left[\frac{N^2}{N_{edx}^2} + \frac{N^2}{N_{ex}^2} + 1\right]^{1/2} \tag{90}$$

or in terms of the sensor N_e, N_{esx}

$$\frac{\Delta f_v}{\Delta f_{en}} = \frac{N_r}{N}\left[\frac{2N^2}{N_{edx}^2} + \frac{N^2}{N_{esx}^2} + 1\right]^{1/2} \tag{91}$$

Consequently;

$$\frac{I_{sll}}{I_{nll}} = (SNR)_v\left[\frac{N_{ex}^2}{N^2 + N_{ex}^2}\right]^{1/2}\left[\frac{N_r}{N}\right]^{1/2}\left[\frac{2N^2}{N_{edx}^2} + \frac{2N^2}{N_{esx}^2} + 1\right]^{1/4} \tag{92}$$

As for the periodic case, the SNR that results from integration over the complete bar image can now be obtained by doing a similar integration over the height of the bar; that is, in the cross scan direction. Again, since the raster tends to make the process discrete, the integration becomes a summation and the duration becomes the number of elements (i.e., raster lines) summed. In all other aspects, the process is exactly as has gone on so far

The integral of the signal over the height will be the single line integrated signal times the number of lines on the object. The reason for not using the number of lines on the sensor or display image is again that the integral over the input equals the integral over the output and the input is of constant amplitude making the integration easier.

Therefore, the signal increases by a factor n_2 where n_2 is the lines per object height.

$$n_2 = \frac{n_1 \epsilon}{N} \tag{93}$$

For the noise, the integration duration is the number of raster lines on the displayed image which is larger than the object by the effects of the aperture of the system. While the low frequency response is proportional to the integration (summation) duration, the integration process reduces the bandwidth of the noise from that representing one raster line (N_1) to that represented by the image and the display apertures. The noise integration duration n_3 is given by

$$n_3 = \frac{n_1 \left(N^2 + \epsilon^2 N_{ey}^2\right)^{1/2}}{\epsilon N N_{ey}} \tag{94}$$

and as was the case before, the bandwidth of the final integrator noise, N_{eny}, is

$$N_{eny} = \left[\frac{N^2}{\epsilon^2 + \frac{N^2}{N_{ey}^2} + \frac{N^2}{N_{edy}^2}}\right]^{1/2} \tag{95}$$

or

$$N_{eny} = \left[\frac{N^2}{\epsilon^2 + \frac{N^2}{N_{esy}^2} + \frac{2N^2}{N_{edy}^2}}\right]^{1/2} \tag{96}$$

Since n_1 is the initial noise bandwidth for the cross scan direction, the total bar single frame integrated SNR can be written as

$$\frac{I_{s1}}{I_{n1}} = \frac{I_{s11}}{I_{n11}} \left[\frac{n_2}{n_3}\right] \left[\frac{n_1}{N_{eny}}\right]^{1/2} \tag{97}$$

which by substitution reduces to

$$\frac{I_{sl}}{I_{nl}} = \left[SNR_v\right]\left[\frac{\epsilon n_1 N_r}{N^2}\right]^{1/2}\left[\frac{N_{ex}^2}{N^2 + N_{ex}^2}\right]^{1/2}\left[\frac{N_{ey}^2}{\left(\frac{N}{\epsilon}\right)^2 + N_{ey}^2}\right]^{1/2} \tag{98}$$

$$\left[1 + \left(\frac{N}{\epsilon\, N_{esy}}\right)^2 + 2\left(\frac{N}{\epsilon\, N_{edy}}\right)^2\right]^{1/4} \times \left[1 + \left(\frac{N}{N_{esx}}\right)^2 + 2\left(\frac{N}{N_{edx}}\right)^2\right]^{1/4}$$

Having included the effects of spatial integration, we then need only to include the temporal integration to obtain the $(SNR)_p$. As for the periodic case, the temporal integration simply results in a gain in SNR equal to the square root of the number of independent frames that occur in an operator time constant, that is

$$SNR_p = \frac{I_{sl}}{I_{nl}}\left(\frac{t_i}{T}\right)^{1/2} \tag{99}$$

As for the periodic case, a set of parameters to reflect how the display MTF affects the noise have been defined.

$$\Gamma_x(N) = \left[\frac{1 + \left(\frac{N}{N_{ex}}\right)^2}{1 + \left(\frac{N}{N_{esx}}\right)^2 + 2\left(\frac{N}{N_{edx}}\right)^2}\right]^{1/2} \tag{100}$$

and

$$\Gamma_y(N) = \left[\frac{1 + \left(\frac{N}{\epsilon\, N_{ey}}\right)^2}{1 + \left(\frac{N}{\epsilon\, N_{esy}}\right)^2 + 2\left(\frac{N}{\epsilon\, N_{edy}}\right)^2}\right]^{1/2} \tag{101}$$

It is again convenient to introduce the parameter ϕ which is the ratio of n_1 to N_r (i.e., to Δf_v); the number of raster lines per reference aperture width. Therefore

$$\phi = \frac{n_1}{N_r} \tag{102}$$

Making these substitutions, we now have for a periodic object a complete expression for SNR_p in terms of SNR_v for the reference bandwidth in spatial frequency (N_r).

$$SNR_p = \left[SNR_v\right]\left[\epsilon\,\phi\right]^{1/2}\left[\frac{N_r}{N}\right]\left[\frac{1}{1+\left(\frac{N}{N_{ex}}\right)^2}\right]^{1/4}\left[\frac{1}{1+\left(\frac{N}{\epsilon\,N_{ey}}\right)^2}\right]^{1/4}\left[\frac{1}{\Gamma_x\,\Gamma_y}\right]^{1/2}\left[\frac{t_i}{T}\right]^{1/2} \tag{103}$$

or if you prefer, with the reference bandwidth in temporal frequency (Δf_v).

$$SNR_p = \left(SNR_v\right)\left[\frac{2\Delta f_v\,\epsilon\,n\,t_i\,\eta_{sc}}{\alpha}\right]^{1/2}\left[\frac{1}{N}\right]\left[\frac{1}{1+\left(\frac{N}{N_{ex}}\right)^2}\right]^{1/4}$$
$$\left[\frac{1}{1+\left(\frac{N}{\epsilon\,N_{ey}}\right)^2}\right]^{1/4}\left[\frac{1}{\Gamma_x\,\Gamma_y}\right]^{1/2} \tag{104}$$

3.4.6.8 Useful Examples

These examples increase in complexity from very idealized to more practical as they go along. It is very important that, especially for LLTV, one realizes there are multiple noise sources injecting noise at various points throughout the system (e.g., photoelectron noise and

preamplifier noise) and that the simple applications shown as the first examples are just that. The final example indicates how the more complicated situation is handled.

3.4.6.8.1 Example I - Psychophysical Test Set Up

The simplest example to consider is a near-perfect (not noiseless) system where in addition to the display size and brightness being sufficient to preclude operator limitations (MTF or noise), the display and sensor are of such quality as not to limit the quality of the image. From a practical point of view, this means that the display and sensor must have broad band MTF curves with values near unity over the frequencies of interest and the raster must be sufficiently fine as to provide many lines per object height. This case lends itself to psychophysical experimentation since well-controlled, electronically-generated video signal-to-noise ratios can be fed to a near-perfect display and then, operator thresholds can be determined. Considerable testing of this type has been completed by F. Rosell, et al. (Ref. 12) and for this use they have referred to the SNR_p as the $(SNR)_D$. Bar patterns were generated electronically and summed with white noise of known bandwidth and rms value to provide a noisy image or well defined bars with known SNR_v.

Using the equation derived above we can derive the equation for determining the SNR_p for this case. The perfect system condition implies

$$N_{ex}^{-1} = N_{ey}^{-1} = 0; \quad R_{sqf} = 1.$$

In addition, since a single video line is used throughout, n = 1. In addition the picture height can be defined as greater than the active area when normalizing N and thereby $\eta_{sc} = 1$. (This is common in TV systems.) Hence for both the periodic and aperiodic object we have

$$SNR_p = SNR_v \left[\frac{2\Delta f_v \; t_i \; \epsilon}{\alpha}\right]^{1/2} \left[\frac{1}{N}\right] \tag{105}$$

For the aperiodic case however it is more convenient to work in terms of the area of the object, a, and the area of the total field A.

$$\frac{a}{A} = \left[\frac{1}{N}\right] \left[\frac{\epsilon}{N}\right] \left[\frac{1}{\alpha}\right] \tag{106}$$

Therefore;

$$SNR_p = SNR_v \left[2\Delta f_v \; t_i \; a/A\right]^{1/2} \tag{107}$$

Obviously, this can be extrapolated to the detection of other simple shapes of area "a" if the integration theory holds. The tests of Rosell et al., seems to indicate it does.

3.4.6.8.2 Example II - Sensor MTF, Perfect Display

While the above example is meaningful for electronically-generated noise, imaging invariably involves optics with limited spatial bandwidth (MTF) which modifies the image before it generates the video signal and, therefore, before the noise (which is time dependent) is added. This example treats the imaging system which has an MTF filtering the signal but not the noise and, therefore, has white noise in the video channel. Again, the perfect large display with adequate brightness is assumed and, therefore, the $(SNR)_p$ is the same as Rosell's $(SNR)_d$. The thresholds for this case were investigated by Rosell et al., by generating the video with a TV camera and then adding controlled white noise.

The video signal to be considered is again that associated with a bar pattern of frequency N but now the input is optical, spatially filtered by the system MTF, and scanned by the sensor to generate the one dimensional electrical signal referred to as video. The MTF involved is two dimensional, separable in k_x and k_y. The scanning raster is of sufficiently high spatial frequency to satisfy the requirement for spatial invariance.

For this case, the operator "sees" a cyclic pattern with edges that are not step functions in intensity but are smoothed. This smoothing is particularly noticeable in the x or cross bar direction.

Again, simple substitutions in the derived expressions will provide the equation for determining the SNR_p. Now $N_{edx}^{-1} = N_{edy}^{-1} = 0$ and therefore $\Gamma_x = \Gamma_y = 1$. $N_{ex} = N_{esx}$ and $N_{ey} = N_{esy}$ and R_{sqf} is approximately the sensor MTF, R_s, times $8/\pi^2$. With n = 1 and $\eta_{SC} = 1$ we have for the periodic case

$$SNR_p = \left[SNR_v\right]\left[\frac{8}{\pi^2} R_s\right]\left[\frac{2\Delta f_v\, t_i\, \epsilon}{\alpha}\right]^{1/2}\left[\frac{1}{N}\right]\left[\frac{1}{\left(\frac{N}{\epsilon\, N_{ey}}\right)^2 + 1}\right]^{1/4} \qquad (108)$$

or for the aperiodic case

$$SNR_p = \left[SNR_v\right]\left[\frac{2\Delta f_v\, t_i\, \epsilon}{\alpha}\right]\frac{1}{N}\left[\frac{1}{\left(\frac{N}{N_{ex}}\right)^2 + 1}\right]^{1/4}\left[\frac{1}{\left(\frac{N}{\epsilon\, N_{ey}}\right)^2 + 1}\right]^{1/4} \qquad (109)$$

Converting to the area notation introduced in Example I

$$SNR_p = SNR_v\left[2\Delta f_v\, t_i \left(\frac{a}{A}\right)\right]^{1/2}\left[\frac{1}{\left(\frac{N}{N_{ex}}\right)^2 + 1}\right]^{1/4}\left[\frac{1}{\left(\frac{N}{\epsilon\, N_{ey}}\right)^2 + 1}\right]^{1/4} \qquad (110)$$

3.4.6.8.3 Example III - Idealized TV - Considering a Single Idealized Noise Source

The idealized TV is a useful case to mention because it generally applies to the TV performance prediction effort that follows.

In a typical TV, both sensor and display have important MTF's. The display in general must have an aperture to discriminate against the raster and the sensor has significant MTF losses as mentioned in earlier sections of the report.

For TV, however, it is common for the raster to be chosen such that the SNR_v is based upon a single video channel n = 1 and so that $\eta_{SC} = 1$. The system square wave flux transform is approximately $8/\pi^2$ the MTF. Then, the following equations apply.

Periodic

$$SNR_p = SNR_v \left[\frac{8}{\pi^2} R_S\right] \left[\frac{2\Delta f_v t_i \epsilon}{\alpha}\right]^{1/2} \left[\frac{1}{N}\right] \left[\frac{1}{\left(\frac{N}{\epsilon N_{ey}}\right)^2 + 1}\right]^{1/4} \left[\frac{1}{\beta_x}\right]^{1/2} \left[\frac{1}{\Gamma_y}\right]^{1/2} \quad (111)$$

Aperiodic

$$SNR_p = SNR_v \left[\frac{2\Delta f_v t_i \epsilon}{\alpha}\right]^{1/2} \left[\frac{1}{N}\right] \left[\frac{1}{\left(\frac{N}{N_{ex}}\right)^2 + 1}\right]^{1/4} \left[\frac{1}{\left(\frac{N}{\epsilon N_{ey}}\right)^2 + 1}\right]^{1/4} \left[\frac{1}{\Gamma_x \Gamma_y}\right]^{1/2} \quad (112)$$

3.4.6.8.4 Example IV - Typical FLIR

The typical FLIR is a slightly different case inasmuch as the SNR_v is usually measured in one of n channels

$$\left(\text{i.e.,} \quad SNR_v = \frac{\Delta T}{NET}\right)$$

and the reference bandwidth is that associated with a detector width. (Maybe in the future N_{ex}^{-1}). The scanning efficiency is typically not unity and both display and sensor MTF losses are significant. The number of scan lines per detector height (ϕ) is a meaningful parameter and becoming better understood. Consequently, the complete equations derived in terms of N_r are applicable and are repeated here with the R_{sqf} approximation.

For Periodic Object

$$SNR_p = SNR_v \left[\frac{8}{\pi^2} R_S\right]\left[\epsilon\phi\right]^{1/2}\left[\frac{N_r}{N}\right]\left[\frac{1}{\left(\frac{N}{\epsilon N_{ey}}\right)^2 + 1}\right]^{1/4}\left[\frac{1}{\beta_x \Gamma_y}\right]^{1/2}\left[\frac{t_i}{T}\right]^{1/2} \quad (113)$$

For Aperiodic Objects

$$SNR_p = SNR_v \left[\epsilon\phi\right]^{1/2}\left[\frac{N_r}{N}\right]\left[\frac{1}{1+\left(\frac{N}{N_{ex}}\right)^2}\right]^{1/4}\left[\frac{1}{1+\left(\frac{N}{\epsilon N_{ey}}\right)^2}\right]^{1/4}\left[\frac{1}{\Gamma_x \Gamma_y}\right]^{1/2}\left(\frac{t_i}{T}\right)^{1/2} \quad (114)$$

3.4.6.8.5 Example V - Multiple Noise Sources and Non White Noise at SNR_v

For this example, consider the system of Figure 34. This system for analysis purposes reduces to the two parallel systems of Figure 35.

By summing the output of these two systems one obtains the effect of the actual system. Since the signals are coherent they add linearly while the noises as the rms. From the previous equations

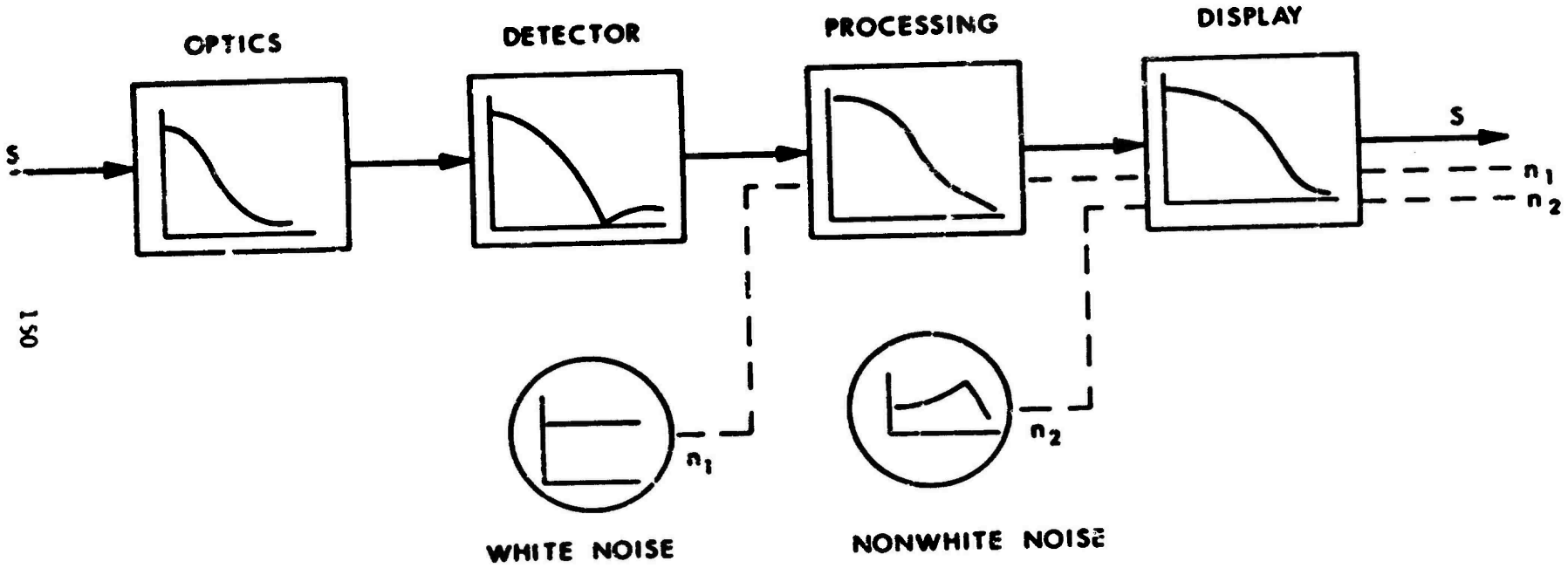

Figure 34. System for Example V

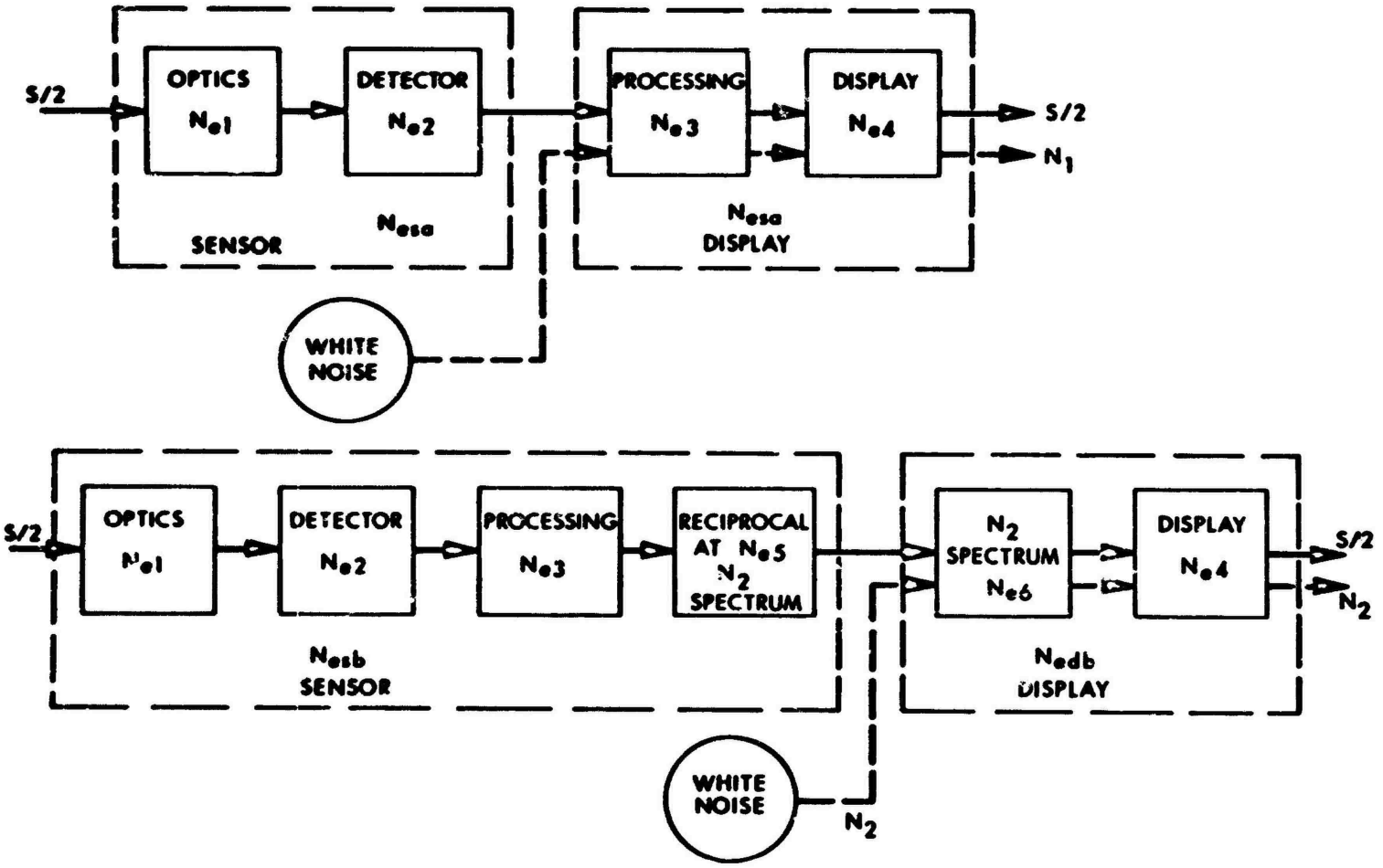

Figure 35. Equivalent System Pair for System of Example V

$$SNR_{pi} = \frac{SNR_{V1}}{\left[\beta_{x1}\,\Gamma_{y1}\right]^{1/2}}\left[H(N)\right]$$

$$SNR_{p2} = \frac{SNR_{V2}}{\left[\beta_{x2}\,\Gamma_{y2}\right]^{1/2}}\left[H(N)\right] \qquad (115)$$

where

$$H(N) = \left[\frac{8}{\pi^2}\right] R_S \left[\epsilon\,\phi\right]^{1/2} \left[\frac{N_r}{N}\right]\left[\frac{1}{\left(\frac{N}{\epsilon\,N_{ey}}\right)^2 + 1}\right]^{1/4} \left[\frac{t_i}{T}\right]^{1/2}$$

letting $S_{p1} = S_{p2} = S_p/2$ and N_{p1}, N_{p2} = Perceived Noise

$$N_{p1} = \frac{S_{p1}}{SNR_{p1}} = \frac{S_p}{2}\left[\frac{\beta_{x1}\,\Gamma_{y1}}{(SNR_{V1})^2}\right]^{1/2}\left[H(N)\right]^{-1}$$

$$N_{p2} = \frac{S_{p2}}{SNR_{p2}} = \frac{S_p}{2}\left[\frac{\beta_{x2}\,\Gamma_{y2}}{(SNR_{V2})^2}\right]^{1/2}\left[H(N)\right]^{-1}$$

Then the total perceived noise would be

$$N_p = \frac{S_p}{2H(N)}\left[\frac{\beta_{x1}\,\Gamma_{y1}}{(SNR_{V1})^2} + \frac{\beta_{x2}\,\Gamma_{y2}}{(SNR_{V2})^2}\right]^{1/2}$$

And the system SNR_p is

$$SNR_p = \frac{S_p}{N_p} = \frac{2H(N)\ SNR_{V1}\ SNR_{V2}}{\left[\beta_{x1}\ \Gamma_{y1}\ (SNR_{V2})^2 + \beta_{x2}\ \Gamma_{y2}\ (SNR_{V1})^2\right]^{1/2}}$$

Or equivalently the following equation represents a fairly general and complicated case for the periodic object.

$$SNR_p = \left[\frac{8}{\pi^2} R_S\right]\left[\epsilon\ \phi\right]^{1/2}\left[\frac{N_r}{N}\right]\left[\frac{1}{\frac{N^2}{N_{ey}} + 1}\right]^{1/4}$$

$$\left[\frac{2(SNR_{V1})\ (SNR_{V2})}{\left[\beta_{x1}\ \Gamma_{y1}\ (SNR_{V2})^2 + \beta_{x2}\ \Gamma_{y2}\ (SNR_{V1})^2\right]^{1/2}}\right]$$

A more general solution would include the influence of gain on SNR_{V1} and SNR_{V2}.

3.4.6.9 Analysis - Perceived SNR - Summary

There are a few assumptions in the analysis which merit repeating. The resulting equations are easily found in the text and at the end of the examples.

The first assumption is that the man is a spatial and temporal integrator that integrates over the image. This provides the definition of SNR_p.

It is assumed that only one bar of a pattern is important to the process.

The approximations using Ne and equivalent apertures rather than extensive Fourier transform analysis are used liberally.

The fact that for aperiodic objects the integral of the signal over the output equals the integral over the input is proven using Fourier analysis and used throughout.

That is for large aperiodic objects, the image amplitude is independent of object size but as the object becomes small and approaches the system equivalent aperture N_e^{-1} the amplitude of the image drops while the image size becomes independent of object size; all this means the integrated signal will decrease proportional to object size regardless of how small the object gets but the noise only decreases with the square root of object size until the object approaches the N_e^{-1} of the system and ther it remains constant.

It is assumed that the systems are linear and spatially invariant. Spatial invariance means not raster limited.

The bar is discussed as oriented across the raster lines. This is not an implicit assumption and has no effect on the analysis. That is ϵ can be less than 1 so long as the other assumptions are met. Indeed these bars could even be diagonal.

The next few sections lean heavily on this analysis and its complete compatibility between TV and IR.

One point not explicitly made in the text is that to handle multiple points of noise insertion parallel systems are mathematically introduced which have different Ne_d and Ne_s but the same N_e and therefore different $(SNR)_v$ and β and Γ. The total system SNR_p can be predicted by appropriate summing of the parallel mathematical systems.

3.4.7 TOTAL SYSTEM SENSITIVITY

In the preceding sections, it was indicated how the video signal-to-noise ratio $(SNR)_v$ could be derived from the component characteristics and how the perceived signal to noise ratio $(SNR)_p$ could be predicted from the $(SNR)_v$ and component MTFs. In subsection 3.3 the requirements of the man were discussed and values for the threshold $(SNR)_p$ for various tasks were provided. In this section, the $(SNR)_p$ in terms of system parameters will be further discussed and the system performance measures defined using these thresholds.

The basic sensitivity is to be defined for both systems, as the minimum signal required from a 3 bar chart, for the chart to just be discernible at the display.

ACTV	FLIR
For active TV, there are necessarily more variables involved than for FLIR and this tends to make the sensitivity definition more involved. The desired parameter is the minimum resolvable contrast (MRC) between the bars and spaces of a three bar pattern with a bar aspect of 5 to 1 and average reflectivity ρ. It is the contrast for which the bar object can just be discerned. Since	For the infrared system, the basic sensitivity is defined as the minimum resolvable temperature (MRT). This is the minimum temperature difference between the bars and spaces of a three bar (5 to 1 aspect) bar chart where the bars and spaces have emissivity unity and a temperature difference about ambient of ΔT. From subsection 3.3, it is clear that when the SNR_p = 2.8 as calculated

the system is active this function of spatial frequency, k, will be a family of functions for different ranges in a vacuum (i.e., no atmosphere). A typical curve is presented in Figure 36.

In order to obtain this parameter we first predict and can measure in the laboratory the minimum resolvable scene radiance (or photocurrent) versus spatial frequencies for various target contrasts shown in Figure 37. Then we predict by straightforward calculation the radiance level that will exist (due to the illuminator) as a function of range in a vacuum (no atmosphere losses) for an assumed average reflectivity ρ (Figure 38). Combining these two measurements and calculations we have the desired MRC function.

In a similar manner, a parameter for the aperiodic case can be defined as minimum detectable contrast; that contrast for a square target which is just sufficient for detection.

based upon $t_i = 0.1$ second that the bars are just discernible. Furthermore

$$SNR_v = \frac{\Delta T}{NET} \tag{116}$$

where the video bandwidth corresponds to the detector width.

From section 3.4.6 we have the expression for $(SNR)_p$ in terms of $(SNR)_v$ and the system component transfer function. If the noise at the point of measuring NET is white the actual transfer functions of the system can be used. On the other hand, if the noise is not white some dummy whitening MTF's must be included. For the IR system, the following equation is the most useful.

$$SNR_p = SNR_v \left[\frac{8}{\pi^2} R_s\right]\left[\epsilon \Phi\right]^{1/2} x \tag{117}$$

$$\left[\frac{N_r}{N}\right]\left[\left[\frac{1}{\left(\frac{N}{\epsilon N_{ey}}\right)^2} + 1\right]^{1/4}\left[\frac{1}{\beta_x \Gamma_y}\right]^{1/2}\left[\frac{t_i}{T}\right]^{1/2}\right]$$

Combining these conditions and setting $SNR_p = 2.8$, $t_i = 0.1$, $\epsilon = 5$, ΔT becomes MRT.

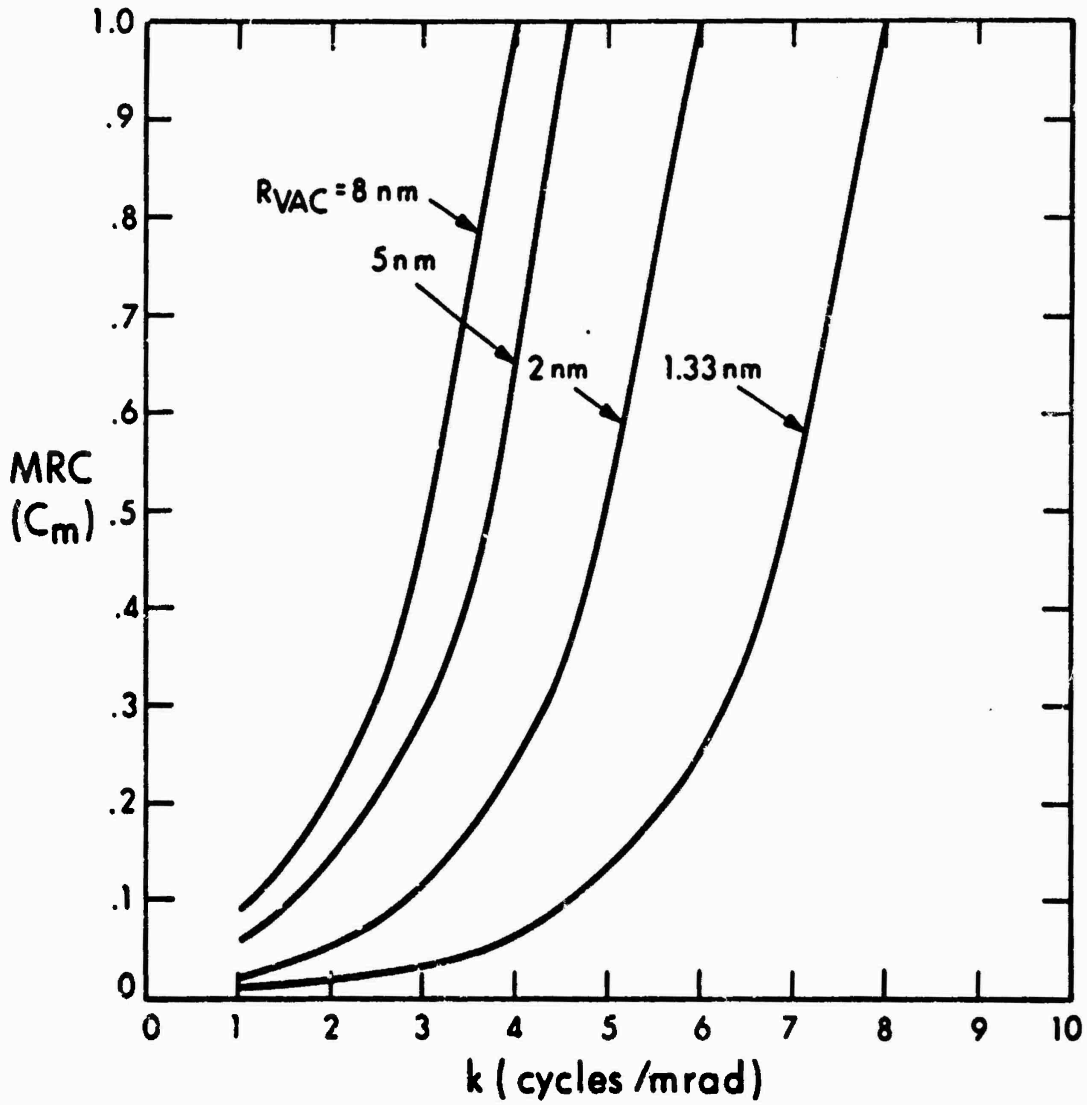

Figure 36. Typical MRC

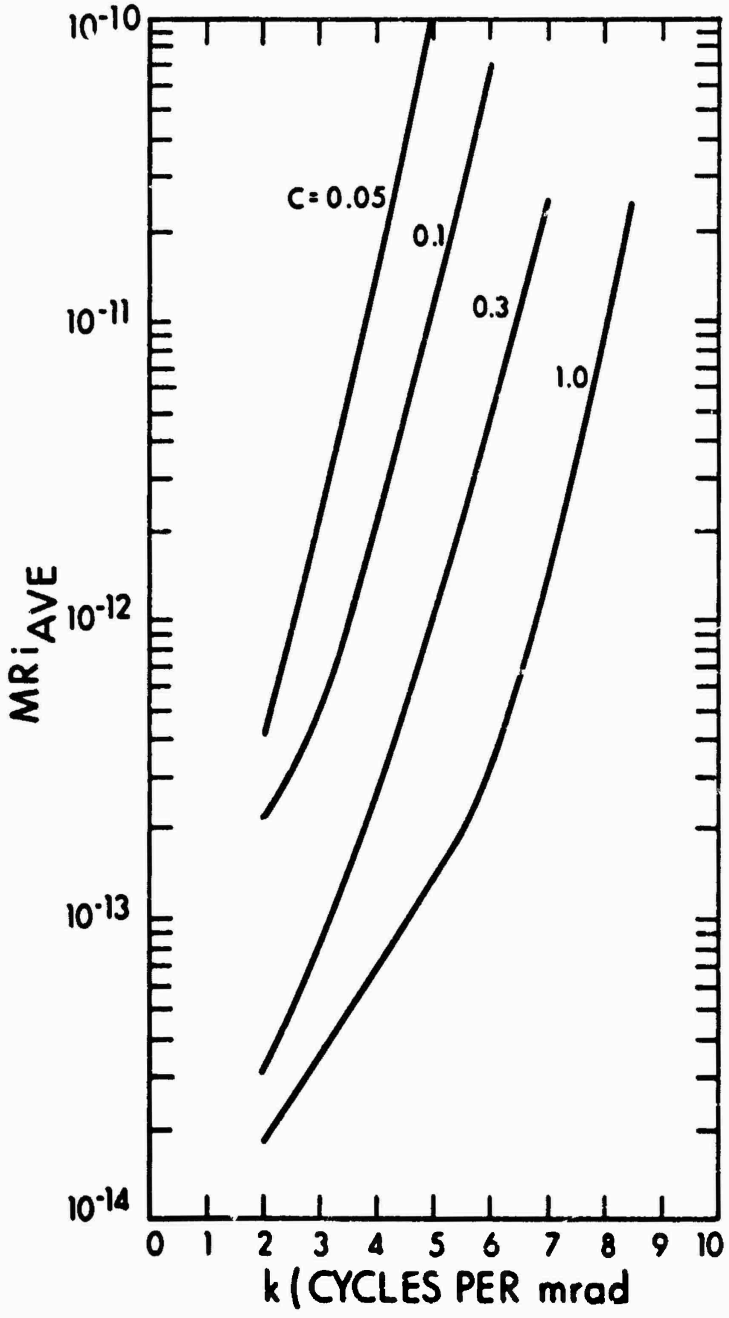

Figure 37. Lab Evaluation - TV

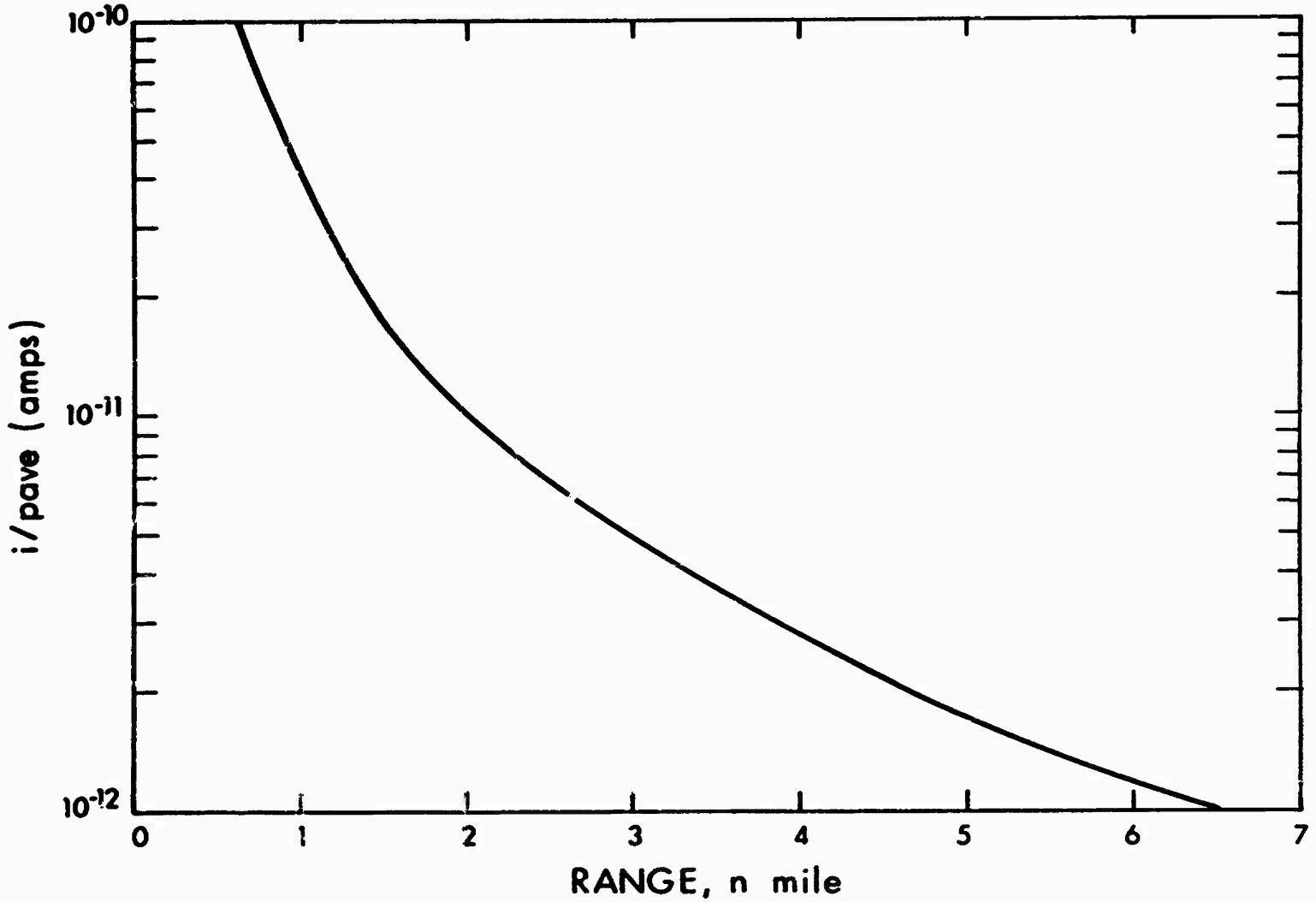

Figure 38. Illuminator Generated Current versus Range for a Vacuum

$$MRT = 4.9 \left[\frac{NET}{R_S}\right] \left[\frac{N}{N_r}\right] \left[\left(\frac{N}{5N_{ey}}\right)^2 + 1\right]^{1/4} \left[\beta_x \Gamma_y \frac{T}{\sigma}\right]^{1/2} \quad (118)$$

Figure 39 is a plot of MRT for a typical system.

For predicting the best possible detection of a square object ($\varepsilon = 1$) and emissivity of unity, we have defined a parameter called minimum detectable temperature (MDT). MDT is the temperature difference required between the square object and its ambient temperature background which makes the object just detectable; it is the aperiodic counterpart of MRT and is predicted by the equation

$$MDT = 8.9 \left[NET\right] \left[\frac{N}{N_r}\right] \left[1 + \left(\frac{N}{N_{ey}}\right)^2\right]^{1/4} \times \left[1 + \left(\frac{N}{N_{ex}}\right)^2\right]^{1/4} \left[\Gamma_x \Gamma_y \frac{T}{\sigma}\right]^{1/2} \quad (119)$$

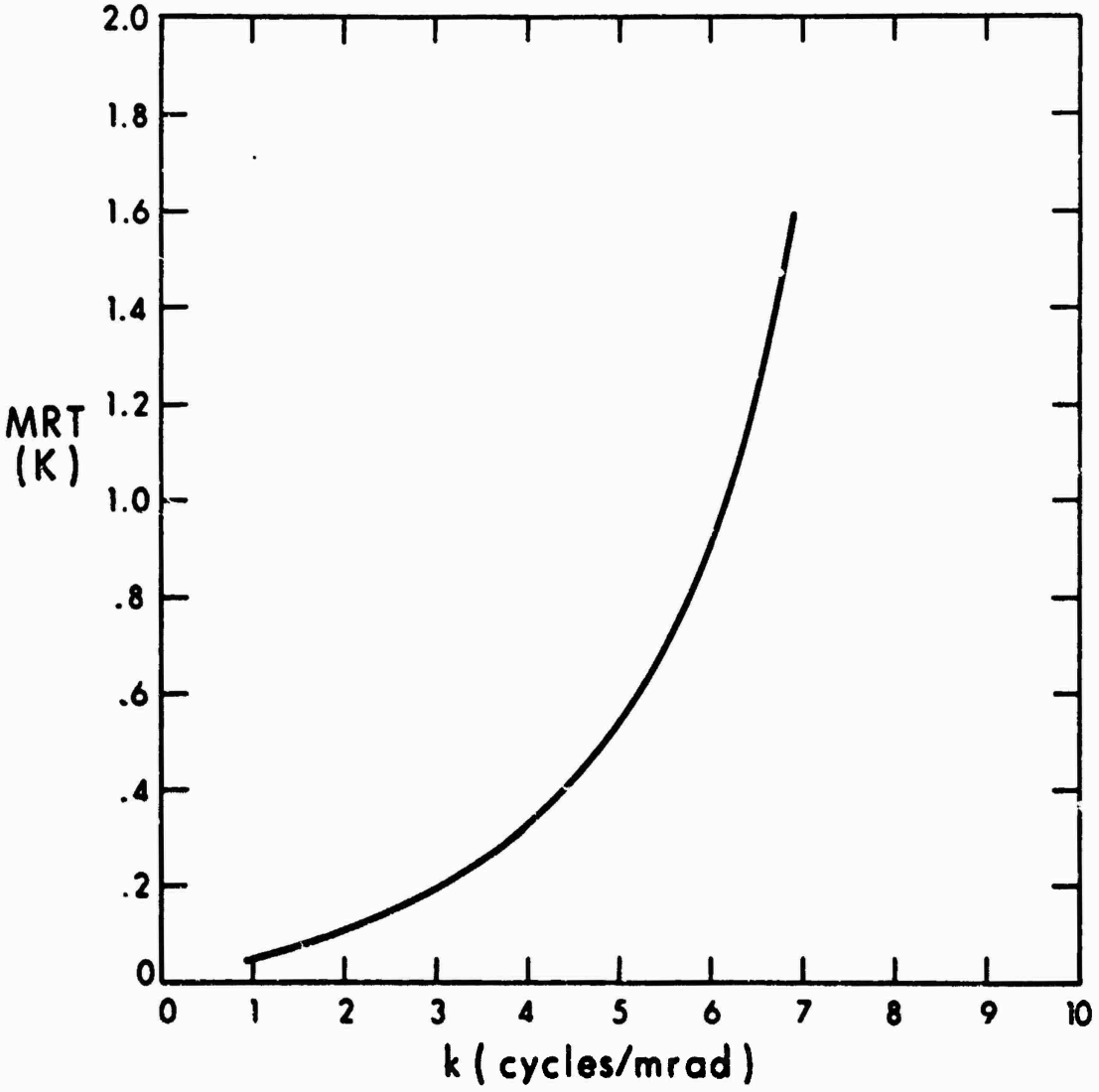

Figure 39. Typical MRT

SECTION IV

TV-IR COMPARISON APPROACH

Now that the characteristics of the scene which generate the images and performance parameters of the systems have been discussed in a similar manner, it is appropriate to discuss how the systems should be compared. It is anticipated that for equal systems they will provide essentially equivalent images under nominal conditions. First, it will be the object of this section to describe what would be considered equivalents and how they might be tested. Then, the section will present discussion on how a flight test might define the conditions where the systems are not equivalent.

If indeed we can quantify the conditions of "equivalence," of "TV best," and of "IR best" then we can evaluate the benefit of having each sensor or both sensors aboard for a specific mission.

The recommended approach to accomplish the comparison is to first make parallel laboratory measurements under well-controlled conditions and compare these data for what is considered nominal inputs for each system. Second, run a controlled-flight test against bar targets and trucks to check the predictions for each system in an actual environment and to check the conditions of nominal equivalence. Finally, it is recommended to fly an extensive flight test under many varied conditions not to check tactical limitations but to establish a data log as to which conditions favor which system and when are they complementary. If indeed the analysis adequately predicts the results of these tests, then the testing can be truncated. However, it is anticipated that surprises and new advantages may spring up from flight testing.

4.1 EQUIVALENCE OF PERFORMANCE PARAMETERS

As a start, the equivalence of individual performance parameters and the effects of variations will be discussed.

4.1.1 FIELD-OF-VIEW

Equal systems will be functioning at the same range which means that for equal ground coverage and acquisition capabilities they should have the same angular field-of-view. This is not the kind of parameter which would affect canned detection/recognition tests since field-of-view has its strongest effects on tactical (search) considerations.

4.1.2 FRAME RATE, ETC.

Both systems should be designed so as to present a non-fatiguing, flicker-free display. The information rate and lag must be equivalent for the systems. Ideally, they will be such that no loss of performance is noted for the dynamic situations to be encountered. If an unequal loss of performance is noted, then a conditions variable of the test to be considered must be the mission dynamics.

4.1.3 RESOLUTION

Ideally, the systems should have the same MTF curves. Short of this, similar curves with near equivalent Ne can be considered equivalent. The ratio of the Ne's for the two systems should indicate the ratio of range non-equivalence under good test conditions (high signal levels).

4.1.4 SENSITIVITY

Sensitivity is the performance parameter which varies with range, atmospheric conditions and target. For that reason laboratory performance

will be defined and then field performance defined separately. The sensitivity must be defined relative to a specific task and target. For the laboratory, the target will be a bar chart and the atmosphere will be idealized to a vacuum for discussing range. In the field, only bar targets and trucks will be considered here but the methodology can be extended to other targets.

For the recce strike task against trucks, it is recommended that the target be a bar target with 1-foot bars. If the modulation from the bars is set to be equivalent to that from a truck under normal conditions, then breakout range on the bars and recognition range on the truck would be about equivalent. Alternatively 4-foot bars could be used for a direct comparison to detection.

4.1.4.1. Laboratory Conditions

ACTV	FLIR
The primary laboratory measure for the TV system without the illuminator is the minimum average scene radiance (or photo current) for the bars of a three-bar chart of contrast (C) to be resolvable on the display. This is plotted versus spatial frequency in cycles per mrad for different values of contrast. This is independent of range as long as no atmosphere is present and can be considered as the laboratory condition for operational ranges. A typical curve was presented in Figure 31.	The sensitivity for laboratory conditions for the FLIR is the plot versus bar frequency (cycles/mrad) of the temperature difference required between the bars and spaces of a three-bar chart (emissivity = 1) for the bars to be resolvable on the display. This is independent of range so long as no atmosphere is present and can be considered as the laboratory conditions for operational ranges. A typical MRT curve was presented in Figure 33.

For an active system, however, the average scene radiance varies as range. In a vacuum, these variations can be calculated and presented for the source power as was done in Figure 38.

From these two functions, it is possible to derive a single laboratory condition sensitivity function which is the minimum contrast required between the bars of the chart for the bars to be resolvable on the display. This function would be plotted as a function of spatial frequency for various values of vacuum ranges. A typical curve is plotted in Figure 36.

For the laboratory conditions, ACTV and FLIR can now be compared by comparing Figures 36 and 39. For true comparison, it is necessary to relate ΔT and C. The authors suggest that two systems with identically-shaped curves would provide equivalent pictures on a typical day if the scale was such that a ΔT of between 2 and 10 degrees corresponds to 100 percent contrast. It is suggested that, as a start, this scale be considered and a new equivalence be determined during the flight test, or possibly a nonlinear scale be determined. This scale says something about the general distribution of ΔT and C in the scene. Based upon this hypothesis, a plot on a single graph where the ordinate is either ΔT of C vs k_x can be generated with the active TV curves being for different typical ranges. Figure 40 is a typical example. From

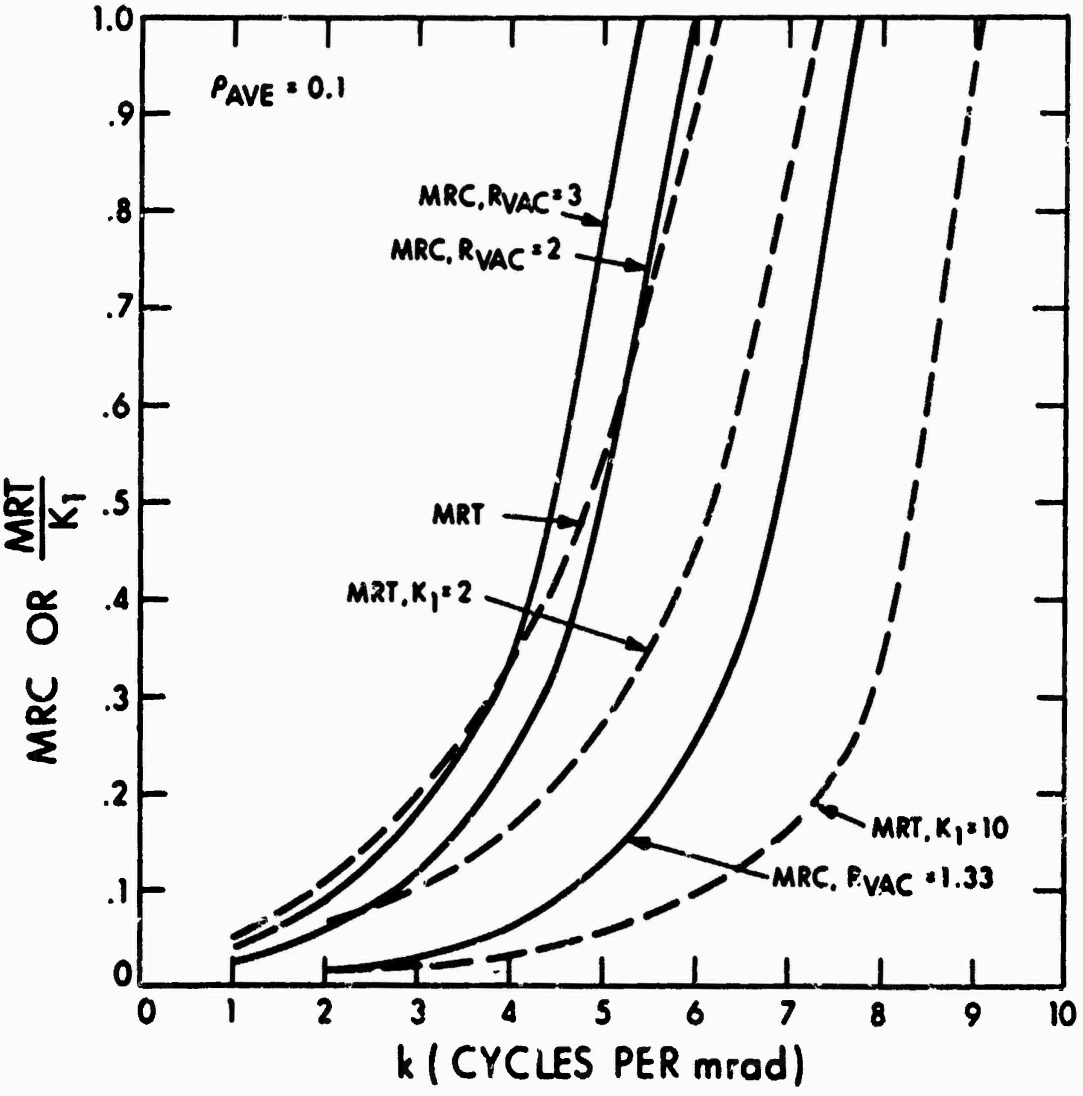

Figure 40. Lab Comparison - TV/IR

this, it can be inferred that the systems would be nearly equivalent at a range of 1.3 n. mi. If on the other hand, the scale was more like 1° = 100 percent contrast, it would be concluded that for small objects the systems would be equivalent at 2 n. mi. range while for large objects they would be equivalent at 3 n. mi. range.

4.1.4.2 Field Conditions

In the field, it is desired that the tasks be increased to include detection and recognition of military objects as well as a quantitative test against a bar chart target. Additionally, the field tests will introduce many uncontrolled parameters associated with the atmosphere, the installation and the military targets. In the field, the primary performance parameter is the maximum range at which a task can be completed be it the task of bar breakout, target detection or recognition.

The existing laboratory functions can be directly used for predicting detection and recognition of various objects with an ideal atmosphere. That is, once the object size is known the angular frequency units on the sensitivity curves can be translated into range units. Since a 6-foot square object is a size of general interest, Figure 41 was derived using our typical FLIR data. This figure presents the ΔT required as a function of range such that: (1) the target be detected based upon aperiodic theory, (2) target can be detected based upon the two lines on target criterion and (3) target can be recognized based upon the 8 lines on target criterion. Raster effects are only alluded to on this figure as providing a degradation at 10 nautical miles but, this assumes a weak raster system.

In a similar manner, Figure 42 was derived for the typical ACTV system discussed.

RANGE PREDICTIONS

SQUARE OBJECT 6'×6'
T_{AVE} = 300°K

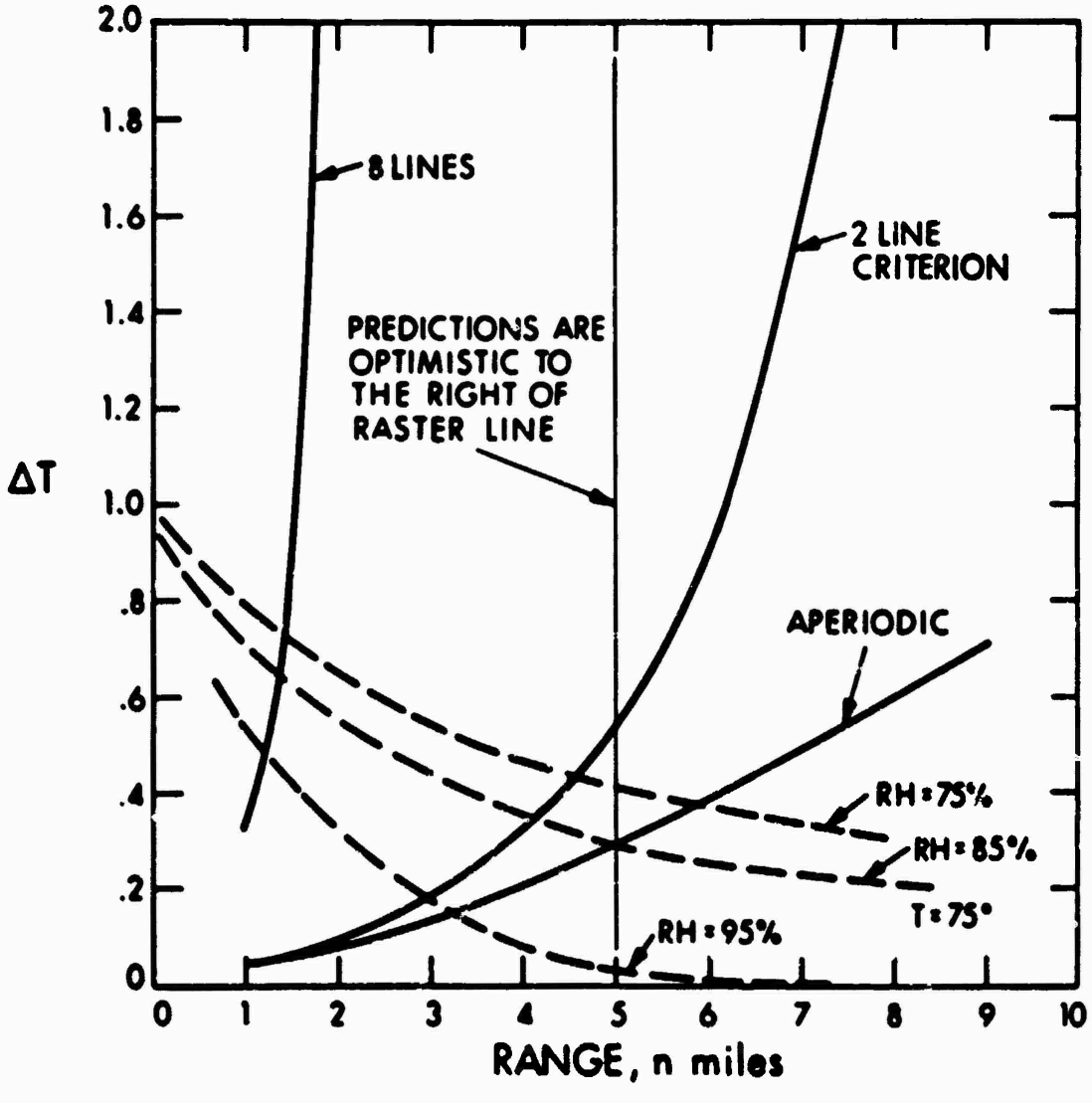

Note: That for a typical FLIR the spatial invariance assumption breaks down below 1/2 the raster frequency and therefore the ranges predicted where there are less than 2 scan lines on the object are very optimistic.

Figure 41. Field Comparison - IR

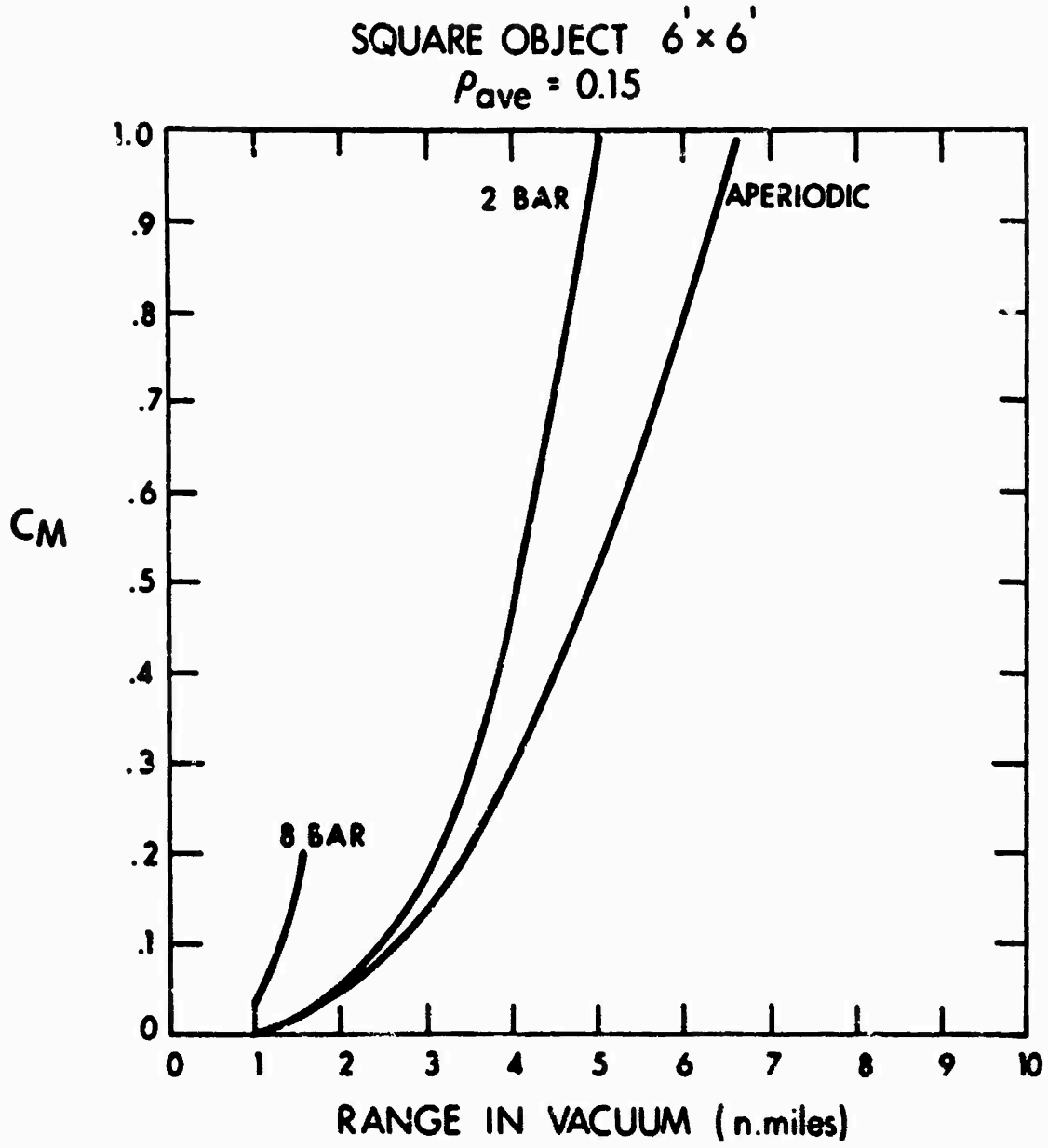

Figure 42. Field Comparison - TV Prediction R_{vac}

Of major importance to the field results will be the effects due to uncontrolled parameters, especially atmospheric effects. To this end, it is recommended that the two systems be compared by plotting range versus atmospheric conditions. As a first cut, however, atmospheric effects for IR are included on Figure 41 and shown more completely for the two line detection criterion in Figure 43.

ACTV	FLIR
For the TV, the atmosphere parameter of interest is visibility. For this comparison, it will be desirable to calculate and plot percent transmission as a function of visibility and range and use this to prepare plots of maximum breakout range as a function of visibility.	For the FLIR, the atmosphere parameters of primary interest are relative humidity and temperature. A separate case, but also of importance is fog. For this discussion, it will be easier to hold temperature constant at a typical value, e.g., $70^{\circ}F$ and consider relative humidity as the variable. In this case, the transmission as a function of RH and range can be calculated, plotted, and used to prepare plots of maximum breakout range as a function of relative humidity. If done for a few representative temperatures ($60^{\circ}F$, $70^{\circ}F$, $80^{\circ}F$, $90^{\circ}F$) every night over a considerable period could be covered for a specific test area. Figure 44 is a typical example.

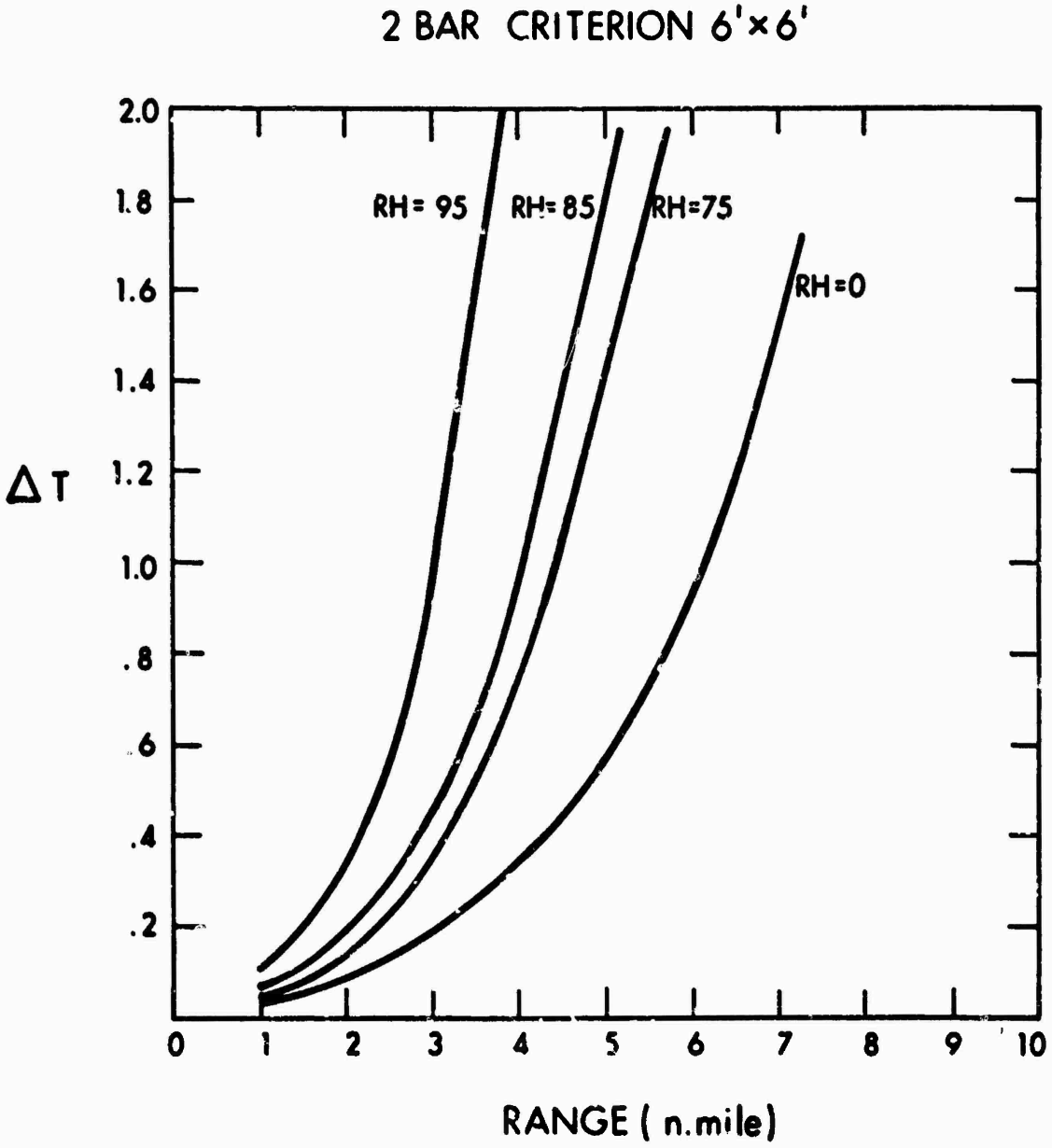

Figure 43. Field Comparison IR Including Atmosphere 75°F

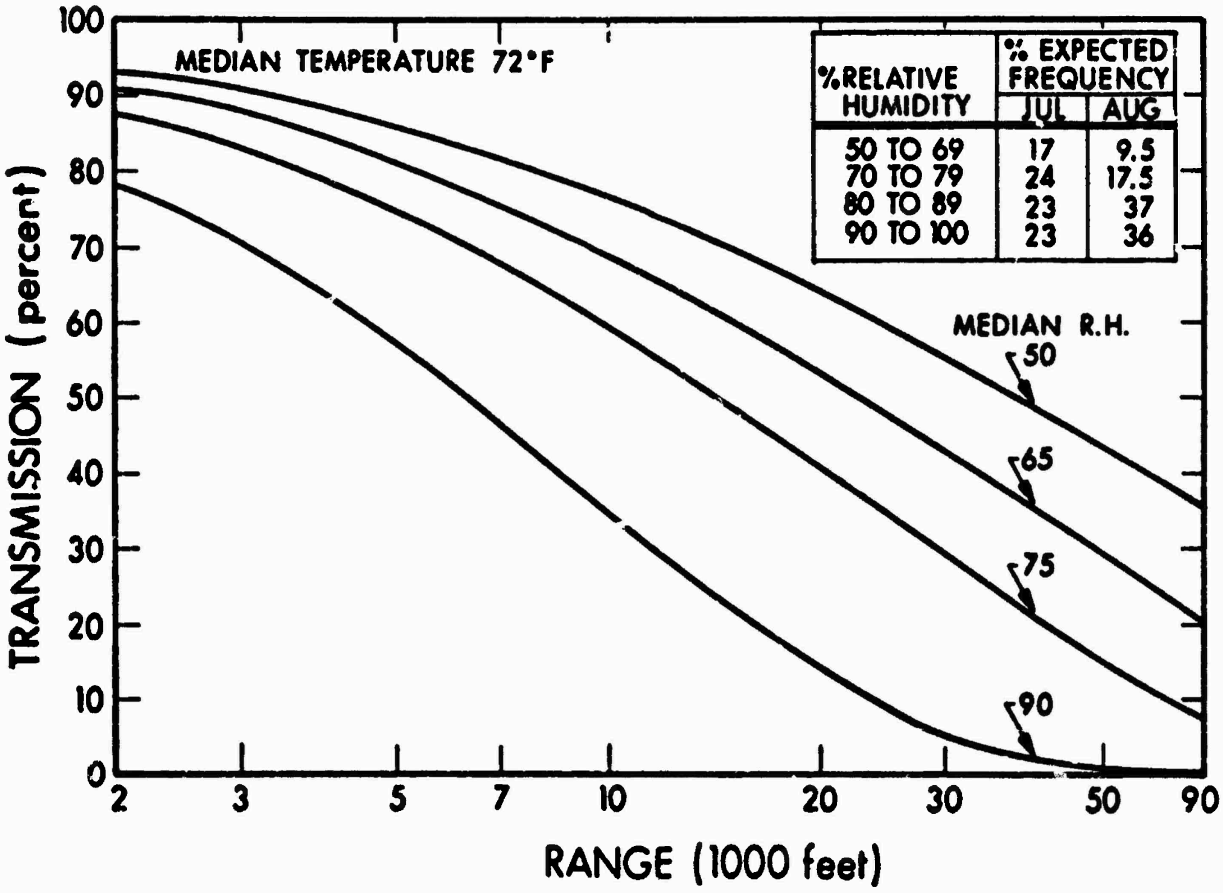

Figure 44. Expected Atmospheric Transmission 8 to 11.5 Micrometers at Patuxent NATC, Maryland, 2200 to 0100 During July and August

For a specific area and period of the year, a nominal RH, temperature, and visibility can be determined for night operation. By combining the two figures above so that the visibility and relative humidity scales are chosen with scales such that the nominal RH and nominal visibility are at the same level and that deviations from either nominal are of similar likelihood, then it is clear that for equivalence at this task both systems should have the same curve. For nominal equivalence, they should have the same range under the nominal conditions. In this case, quantitative comments with regard to other visibilities and relative humidities can be made even to the extent of predicting the relative percent of time useful ranges and exceptional ranges can be expected from each system.

4.2 AN EXTENSIVE FLIGHT TEST

After the analysis, the laboratory tests, and the limited controlled flight testing has been completed and established the general equivalence or nonequivalence of the systems, an extensive flight test will be required to investigate the conditions which favor one system or another. It is expected that if we could fly against all conditions (targets, atmosphere, climate, etc.) for some conditions TV would be best; for others IR would be best, and for some, it would be a toss-up. This statement is depicted in Figure 45. The real question is then depicted in Figure 46. Is one system nearly always redundant or are they truly complementary? Indeed, could we isolate the favorable conditions.

Many parameters define the total set of conditions of interest. Ideally, each condition would be defined by at least the target (its history and details), the atmospheric conditions, the background involved, the climate (region of world), the time of day, and the time of year. It would take many flights with a pair of relatively calibrated systems

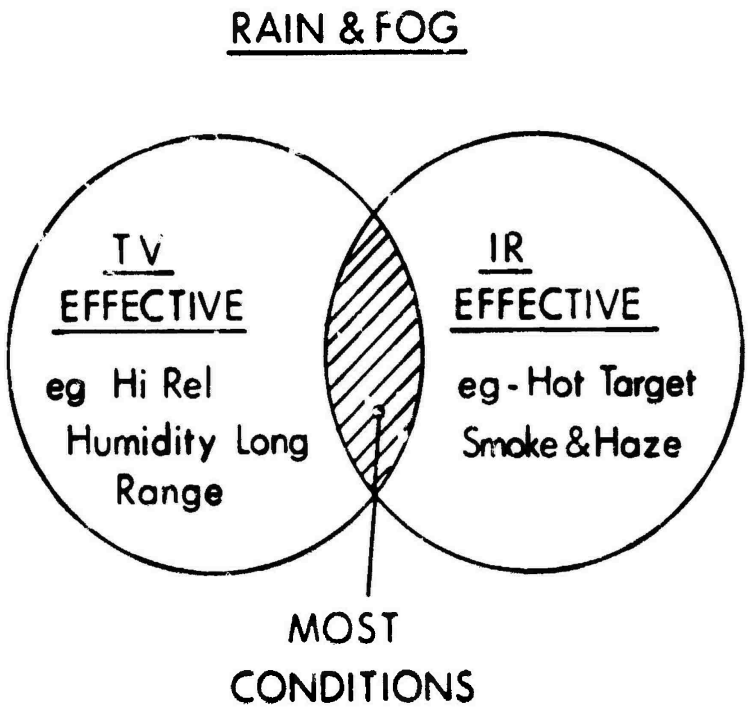

Figure 45. Space of All Conditions

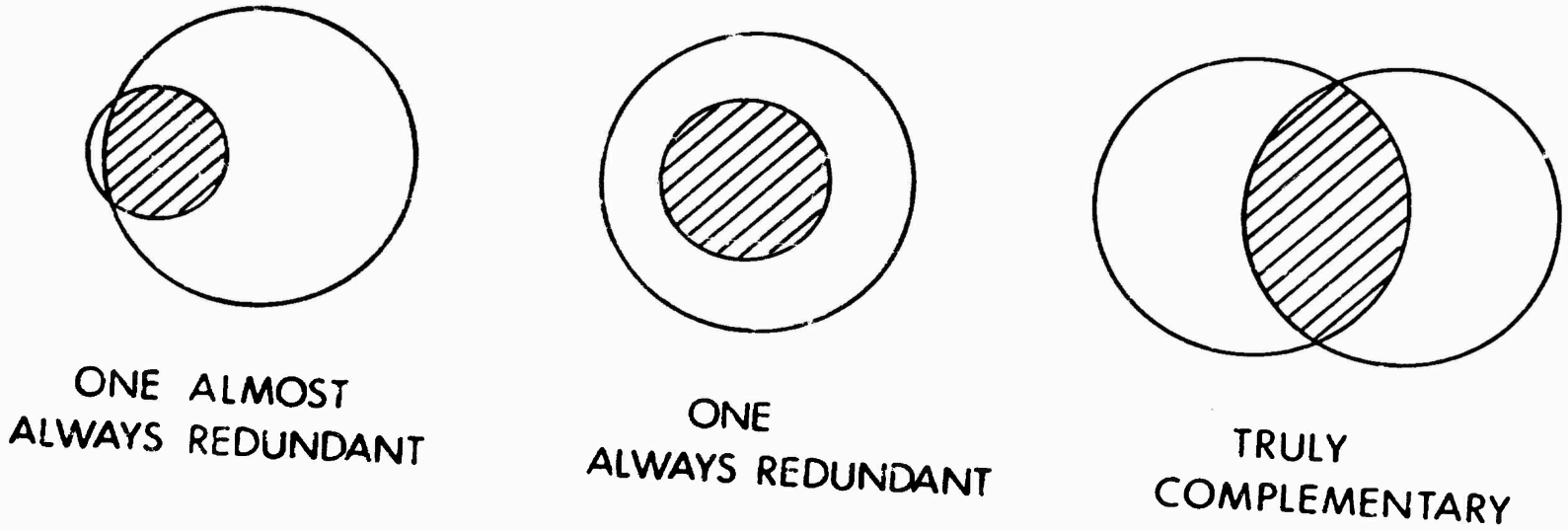

Figure 46. Try and Indicate Conditions

to collect statistically significant data on all of these and possibly other parameters of interest. It should be remembered that these flights are not tactical flights to test the tactical limitations of the installation, etc., but are canned tests against many conditions to determine maximum sensor system range.

To be meaningful, it is important that many different conditions be tested requiring flight in different parts of the world and different times of the year. For completeness, operator comments must be included since the final evaluation may be elusively tied up in the operator's response. The tasks and tests should be kept simple and as constant as possible, i.e., detect/recognize a pre-briefed target.

To be effective, a convenient effective indexing method for keeping and sorting the conditions/data must be developed and computerized. Also, illuminating ways of sorting and presenting the data must be thought out. A few possible methods of sort/presentation are discussed below.

First, a scatter plot of the data by major condition (e.g. a truck, all weather) may be useful. By this, is meant plot TV range (R_{tv}) versus IR Range (R_{ir}) for a task such as detect or recognize. Figure 47 indicates the coordinates and the areas of interest.

Statistics can be derived from the data. For example, for the same conditions as the scatter plots, the probability that the detection range is greater than R can be plotted versus R. By plotting this for each system separately, the relative effectiveness of each can be noted. By plotting a curve based upon the maximum range obtained on each run for the two sensors, an indication of the gain obtained by having both aboard can be measured. Figure 48 is an example of how this might work out.

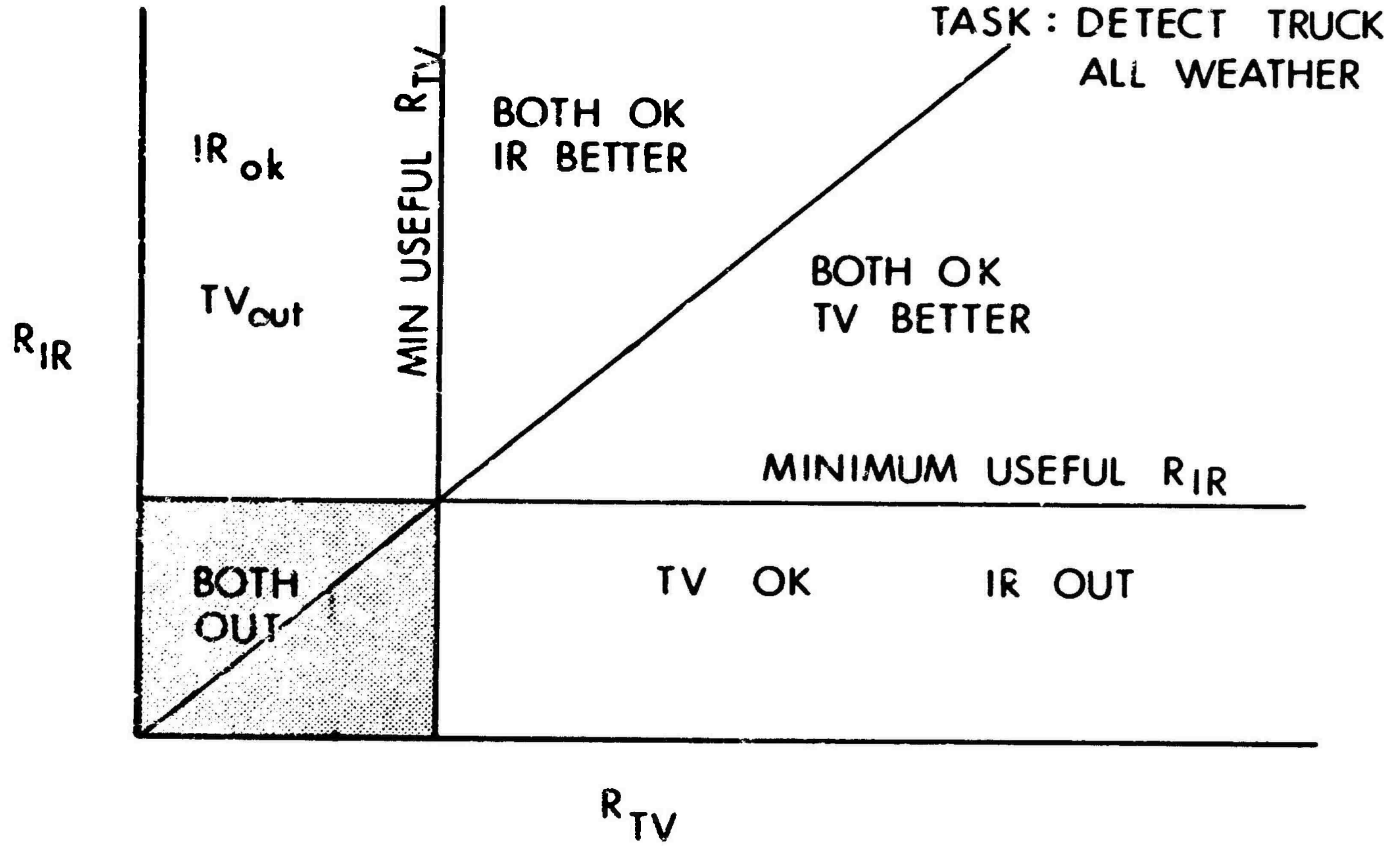

Figure 47. Scatter Plots by Task

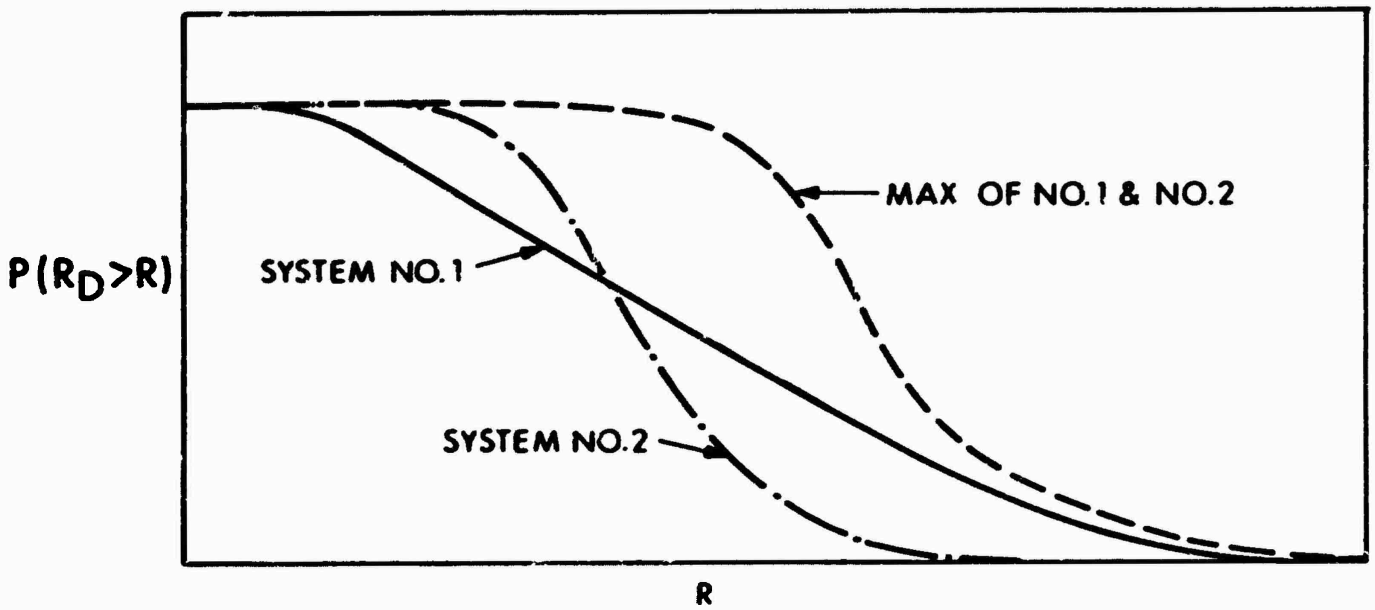

Figure 48. Task Detect Truck - All Weather, Lending Statistical Derivations

Other comparative statistics may prove useful such as plotting the probability density function of $R_{tv} - R_{ir}$ versus $R_{tv} - R_{ir}$ or for R_{tv}/R_{ir} versus R_{tv}/R_{ir}. For example, as shown in Figure 49, it might be expected that when looking at the task of detecting a truck (all weather) that it might be normally distributed for nominal weather but for either very wet or very dry weather, it will be skewed to one equipment or the other.

Finally, perhaps just listing the mean $(R_{tv}-R_{ir})$ and mean (R_{tv}/R_{ir}) for various conditions might provide insight into the relative usefulness. Table IV is an example of how it might work out. An $(R_{tv}-R_{ir})$ mean of 10/0 would indicate that on the average, the TV detects the object 10Km further than the IR but that each recognized the object at the same range. An R_{tv}/R_{ir} of 2/1 would indicate that on the average, the TV detected at twice the range but recognized at the same range.

4.3 CONCLUSIONS ON APPROACH TO COMPARISON

The analysis will provide an indication for the laboratory parameters to be tested and the values to be expected. The laboratory tests will confirm this analysis.

A minimum rigidly-controlled flight test against bars and trucks will confirm the analysis, the atmosphere models, and most importantly, the general concept of equivalence.

Finally, an extensive flight test against many targets under many different conditions will be required to collect sufficient data to be able to make statistically significant statements.

It may become possible to provide sufficiently complete inputs into the analysis to predict adequate results for all conditions suggested in

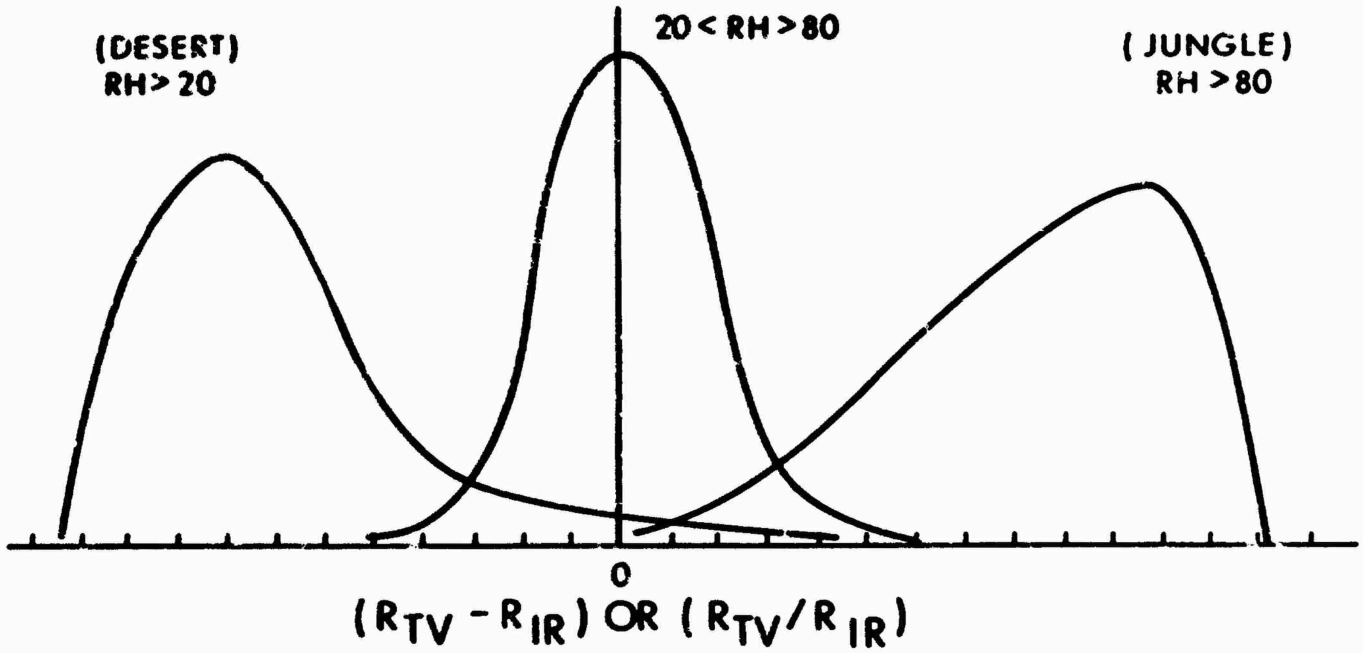

Figure 49. Task Detect Truck - All Climates
Comparative Statistics

the extensive flight test. When this becomes possible, the only advantage of flying rather than analyzing is the relative general acceptance of data over analysis and the useful surprises that can result from a flight test.

TABLE IV

LIST CONDITIONS (VERSUS) (T_{TV} - R_{IR}) MEAN AND (R_{TV}/R_{IR}) MEAN

Condition	(R_{TV} - R_{IR}) mean km Detection/recognition	(R_{TV}/R_{IR}) mean Detection/recognition
Retros - all locations	10/0	8/1
Tanks - Patuxent River	-5/0	2/1
Ship (large)	0/0	1/1
High relative humidity no haze	3/5	2/3

SECTION V

FLIGHT TEST CONSIDERATIONS

The theoretical portion of this study has outlined mathematical relationships for prediction of the range at which targets would be detected (and recognized) under various conditions. Similar mathematical models for prediction of the range at which there is a "breakout" of the individual bars of a standard Air Force three-bar target have also been developed and extensively tested under field conditions. The purpose of the comparative flight test of the TV and IR systems is first to recheck the validation of the individual bar-target breakout models under side-by-side test, and then to validate the individual target detection models under similar conditions for both. If these models can be successfully validated, the individual system performance can be predicted and systems comparisons made.

In subsection 5.1, the parameters which can be measured during a rigidly-controlled flight test to provide model confirmation will be discussed. In subsection 5.2, the controlled parameters will be discussed. These are the parameters which can either be fixed or systematically varied to explore the areas of the applicability of the individual theoretical models. Subsection 5.3 then presents a discussion on those flight test parameters which, although they are uncontrollable, nevertheless affect the results and, consequently, must be measured. All of these three types of parameters are summarized in Table V.

Following the subsections, describing the flight test parameters is a brief discussion of the flight test configuration required to obtain the necessary measurements to confirm the postulated performance models.

TABLE V

FLIGHT TEST PARAMETER SUMMARY

MEASURED PARAMETERS

Bar Pattern Breakout Range	-	Spatial Frequency at Breakout
Vehicle Detection Range	-	Size at Detection
Vehicle Recognition Range	-	Size (and Resolution) at Recognition

CONTROLLED PARAMETERS

Perceived Noise (Display Brightness and Sensor AC Gain Together Set Per-Noise)

Bar Pattern ΔT or C

Bar Pattern Spatial Frequency, k

Operator (which Operator Takes the Reading)

Display Environment Brightness

Vehicle Type (Size)

Vehicle Location

Vehicle ΔT

Vehicle Aspect

Aircraft Flight Pattern

Scene Irradiance

UNCONTROLLED PARAMETERS

Visibility (Meteorological)

Air Temperature

Relative Humidity

Atmospheric MTF (Turbulence)

Background Temperature(s), Radiance

Wind Velocity and Direction

Operator

Equipment Condition

John Hodges, Program Manager of the referenced MAFLIR Flight Test image variable analysis study, provided assistance on the preparation of this section.

3.1 MEASURED RESULTS PARAMETERS

The results parameters of the test program are actually uncontrolled parameters which are dependent on both the controlled parameters and the independent uncontrolled parameters. If there were no independent uncontrolled parameters and the performance prediction theories were absolutely accurate, then the values of the result parameters could be accurately predicted a priori from the controlled parameters of section 4.2.

Object "Breakout" Slant Range/Object Angular Frequency at Breakout

The bar pattern test object used in this program will not be "detected" in the true sense. Rather, the observational task which is tested is the modulation threshold at which the bar frequency is first observed by the operator. In fact, the operator will be able to detect the bar pattern as a whole at ranges far in excess of those being tested. It is desirable that he do so. To achieve good data, it is important that the operator be accurately tracking and centering the target.

To avoid confusion with "detection" as it is defined for tactical targets, the term "bar pattern breakout" has been suggested for the point at which the presence of bars and spaces can first be observed. Since the spatial frequency of the target will be fixed, the relevant parameters to be measured in this test program are the target slant range at breakout, and angular spatial frequency of the target bars and spaces at this range.

To obtain sufficient positional accuracy, phototheodolite or radar tracking of the aircraft is required. In this test, some way must be mechanized by which the theodolite operators can tell when the individual IR and TV target breakouts occur. In the radar tracking case, breakout can be correlated with the aircraft time-position data.

Range at Tactical Target Detection/Range at Tactical Target Recognition

The two primary results to be obtained with the tactical type targets are the slant range at detection and the slant range at recognition.

In most controlled test situations, the term "detection" describes a fundamentally different concept from the term "detection" in a real tactical situation. In a tactical situation, there may be an infinite number of locations for the target and detection depends on cueing effectiveness, the distribution of highly probable target sites (such as roads), etc. These "search" parameters are difficult to duplicate in a flight test program which is controlled sufficiently for a meaningful analysis of the resulting data to be made. Because the exact range at which an operator will become aware of a target will vary, even if he knows the exact location the target will be in (if it is present), multiple measures are required to obtain a mean range useful for theory comparison. Through this repetition, the sensor operator learns to concentrate only on the specific areas where the target might be as called for in the test plan. So long as he can orient himself on the display sufficiently to find these locations, the operator can greatly reduce his search problem, e.g., maximize his probability of looking at the target if it is present on the display. On the other hand, previous flight tests have shown that conditions exist where what eventually is confirmed as the target can be seen on the display before any ground features necessary to determine its location are visible. Then, for test purposes, "detection" is when the operator states with exactitude the location in which he believes the target exists.

Similar problems can occur with the term "recognition." One level of recognition is where the class of target -- truck, jeep, tank, gun -- is determined and another is aspect recognition where the orientation -- nose, side, tail -- with respect to the flight path is determined. Again, only a limited number of situations can be thoroughly tested in a controlled manner. The definitions of recognition must be kept consistent throughout the test program and the reporting of test program results.

As with the bar pattern test object, the slant range can be determined using two phototheodolites provided that tactical target locations are accurately known. Radar aircraft tracking and vectoring will also be used where available.

5.2 CONTROLLED PARAMETERS

The experiment's controlled parameters are those parameters which are believed to be amenable to measurement and precision control.

Perceived Noise

The effect on sensor performance as a function of this parameter is the essence of the experiments to be outlined. Perceived noise is seen from the analytical models to be composed of the separate effects of sensor noise and the photon noise due to display average brightness. The amplitude of sensor noise, as perceived by the observer, is controlled by the sensor AC gain (contrast) control and any internal circuits necessary in an individual equipment required to compensate for the change in some other parameter.

TV	IR
The comments for the parallel IR discussion also apply to TV except that the gain is continually adjusted automatically within the camera and thus, cannot be preset to a constant value. It can be adjusted to some extent however at the monitor.	The operator of real-time thermal imaging equipment has controls to adjust both display average brightness - BRIGHTNESS - and AC gain - CONTRAST - thus adjusting the perceived noise. Under normal conditions, the operator adjusts this to suit his own tastes. However, this operator setting may not be the best setting for optimizing mission performance. It would be expected that brightness and AC gain would be set according to program prior to each run and remain fixed throughout each run. Average brightness should be measured with a photometer prior to each run. The average brightness would be set while the sensor shield is turned backwards so there is a minimum of modulation on the display. AC gain is measured in terms of the change in brightness at the display versus the effective change in target temperature ($\Delta B/\Delta T$) at the aperture measured at nominally low spatial frequency and about the average brightness. Since blackbody emitted power is approximately proportional to the change in temperature at the absolute temperatures and in the spectral bands being considered, this gain term is actually an energy/energy ratio and is a true gain.

Target Temperature Difference/or Target Reflectance Difference

To thoroughly investigate the performance of imaging sensors, a number of spatial frequencies and temperature differences or reflectance differences should be set on the target and the full gamut of perceived noise settings used against each. Unfortunately, the target cannot be set to a wide variety of spatial frequencies with fixed bar aspect ratio so only a small number of patterns will be set. The remaining parameter, which can be used to set angular spatial frequency at the sensor, is target temperature difference (or reflectance). The bar pattern test object at the Naval Air Test Center (Webster Field), Maryland, is capable of presenting similar variable temperature and variable reflectivity bar patterns simultaneously.

Target Spatial Frequency

Because the target breakout range is a function of bar pattern length-to-width aspect ratio and the number of bars as well as spatial frequency, and because specific laboratory data on the sensors will be taken using an Air Force Standard Formal 3-bar target, those pattern combinations which produced three bars with 5:1 bar aspect ratio are recommended for the test program.

Operators

Although it is recognized that the operator performance may be significantly different from one to another, and thus many operators should be used to remove the effects of operator differences, the sample number limitations on a flight test may limit a TV/IR flight test to two operators. They would view each sensor on a randomly-selected basis, but view each type sensor for approximately half of all data runs.

Target Background (Location)

The spatial reflectance, emittance, temperature, and structural content of background against which the tactical type target is located is a parameter of concern since it is the difference in energy, target to background, which is detected. As discussed in subsection 5.1 under "detection", only a few locations are practical in a controlled test situation. These locations must be selected in advance as representative of typical situation -- aspnalt road, dirt road without cover, dirt road with cover, open grass, etc. -- and accurately surveyed. The locations should be laterally close to the nominal flight path to minimize operator tracking requirements. They must be sufficiently far apart along the flight path (3000 to 5000 ft) so that the operator can easily differentiate locations at long range and so that no more than one or two locations are likely to be within "detection range" and on the display at the same time to avoid situations where threshold detection is missed because the operator is looking at other locations at that time. Also, the locations must be easily accessible to good roads so targets can easily be changed.

Spatial reflectance and effective temperature should be measured at specific points about the target and background for each aircraft overflight.

Vehicle Type

The number of types of vehicles (jeep, truck, tank) which can be used in the test is limited by the requirements for multiple measures. In general, only one target can be on range at one time or a detection may be missed while the operator is trying to recognize a target already detected. Also, each vehicle is individual, so the availability of specific vehicles throughout the test period must be assured.

Tactical Target Orientation

It has been shown that the range requirement for target detection, orientation description, recognition and identification is related to the number of sensor resolution line pairs across the target minimum dimension. The orientation of the target with the aircraft flight path must be along surveyed lines and set for each overflight according to prearranged test plan.

Aircraft Speed and Vector

Aircraft speed is one of the parameters to be utilized in determining slant range at target breakout. It is also a weak parameter affecting operator tracking ability and so should be held constant to avoid this source of experimental error. If flight path offset is too great, the target can easily be missed due to sensor gimbal limits.

There is no reason why almost any speed within the capability of the C-131 aircraft cannot be selected. So, the flight speed which the pilot feels comfortable with, for both stability in level flight and maneuverability for executing set flight patterns, should be selected.

Aircraft vectoring against the main target at Webster Field can adequately be handled by the TACAN behind the main target so long as it is working. The main criterion is to minimize the operator's tracking problem by flying directly over the target. For the detection and recognition test, radar vectoring should be considered.

Aircraft Altitude

Aircraft altitude is another parameter which can be fixed with little loss in data generality. Most of the area surrounding Webster Field has a floor of 700 ft. and there is a floor of 1200 ft. in the vicinity. The total area is restricted to military aircraft so any altitude meeting the floor restrictions should be acceptable. Similar conditions probably exist at other potential test areas. The composition of the atmosphere varies with altitude, particularly water vapor, the predominant factor controlling transmission and backscatter. While water vapor must be determined from measurements at the flight level as well as at the ground level, a low angle slant path is desirable. It is recommended that a fixed altitude, as close to 3000 ft. as seems reasonable to the pilot, should be selected but in no case should this altitude be above 5000 ft. Beside affecting the atmospheric composition, higher altitudes exaggerate sensor gimbal limit problems at typical "breakout" and "recognition" ranges when the aircraft is offset from the nominal flight path.

Aircraft Attitude

The operator's tracking ability and consequently the "breakout" range is sensitive to aircraft perturbations. It is suggested that a "commitment" range of 4 n.mi. to target be established. Within this range, the pilot should maintain straight and level flight. For tactical type target detection and recognition, a commitment range of at least 8 n.mi. should be used.

Display Environment Brightness

Light from various sources within the test aircraft which reach the display surface have the effect of reducing the displayed contrast, particularly at low average brightness levels. (This is similar to the experience of watching a movie screen in a lighted room.) The environmental

reduction of displayed contrast can be significant. So, illumination within the aircraft cabin which falls on the display should be kept to a minimum. If it is fixed, it will not have to be measured frequently. However, the brightness of the display surround should approximate the brightness of the display because a very dark display surround has been shown to adversely affect operator performance.

Dark display reflection can be monitored in flight with the same instrument which measures display brightness by simply inserting a white diffuse surface to the side of the display and recording the reflected environment brightness. This reflected environment brightness should be taken with the operator in place and at each of the test average display brightnesses since the display itself will likely be the major source of illumination.

5.3 UNCONTROLLED PARAMETERS

Independent uncontrolled parameters are parameters which are extraneous to the main purpose of the test. If all were either fixed value or absent, the tests could be done with much more precision.

Laboratory tests can remove or precisely control most of the effects of the parameters in this independent uncontrolled category. Therefore, it must be concluded that one of the main reasons for a flight test program is the isolation and analysis of the influence of each of the uncontrolled parameters encountered in flight upon the performance of a particular equipment or class of equipments.

Slant Path Transmission

The uncontrolled parameter with the strongest influence on the test data is the transmission of atmosphere along the slant path between the sensor and the target.

Slant path transmission is determined by a number of subsidiary parameters including range, relative humidity, air temperature, particulate and Rayleigh scattering and barometric pressure.

As discussed in subsection 3.3.2, the transmission in the 8 to 12 micrometer band is almost solely a function of the quantity of precipital water vapor in the slant path. Particulate scattering is included in the Taylor and Yates based transmission estimates given in subsection 3.3.2.

To be accurate, the quantity of precipital water vapor should be integrated along the slant path. For the flight test program, next best would be to take an average of two estimates: one estimate based on ground data at the target, and the other based on data taken at the aircraft. Lacking that, next best is data taken on the ground alone.

Automatic meteorological equipment should be provided at test locations to determine barometric pressure, relative humidity, temperature, and "visibility" at the TV operating wavelength. In general, it has been found that simple meteorological instruments (such as hand held hygrometers for relative humidity through wet and dry bulb temperature difference) are not sufficiently precise for the accurate estimation of transmission.

For the television equipment (operated in active mode), the scene irradiance due to the system source should be continuously monitored and correlated with aircraft range.

ACTV	IR
The primary effect of the atmosphere on an active system is to absorb source radiation both on its way to the scene and its return. The two-way transmittance T is $T = \exp(-2\sigma_o \bar{R})$ where σ_o is the atmospheric extinction coefficient at the source wavelength, and near the scene and $\bar{R}$ is the optical slant range	The atmosphere substitutes its own emitted energy at its own temperature for the target in proportion to one minus the transmission. Since it substitutes for both the cold and the hot bars alike, the target temperature difference is reduced directly by atmospheric transmission, i.e. $\Delta T_e = \Delta T_m \cdot T$ where: ΔT_e = the effective temperature difference at the sensor aperture ΔT_m = the measured temperature difference at the target T = slant path transmission

Target Base Conditions

The target base condition uncontrollable parameters include:

- Cold Bar Temperature
- Target Surround Effective Temperature
- Sky Clear/Overcast
- Recent Precipitation
- Wind Velocity and Direction
- Extraneous Background Lights
- Instantaneous Irradiance Level at Target Due to Intentional Irradience

The first two subsidiary parameters, cold bar temperature and target surround effective temperature, are concerned with the contrast pattern which the overall target presents to the observer of the IR system. The last affects the same quantity for the TV system.

Ideally, the bar pattern should be in the center of a completely uniform field, but this is impossible for the field test. Second best is that the blank space surrounding the bars be large compared with the bar width so that the frequency associated with the leading and trailing cold spaces of the target are well removed from the bar pattern frequency, and the resulting bar pattern frequency spectrum is not radically altered. This condition is generally met with the bar pattern to be used.

The cold-bar temperature can be measured accurately with a radiometer since the bar emissivity is known and high. The surround effective temperature must be estimated with the radiometer by taking a reading of the grassy surround at a grazing angle.

The parameters of sky cover and recent precipitation are concerned with the target apparent emissivity variations. Precipitation on the target may change the emissivity slightly, but the effect is not believed to be serious. Precipitation also has the effect of reducing the thermal contrast of the target with its surrounding which might affect the operators tracking capability.

Because the emissivity of the target bars is not unity, the effective temperature of the surroundings, whether the sky is clear or overcast, also affects the target signature since part of the surrounding energy is reflected from the bar surface to the sensor. For the main electro-optical test target, which has a fixed aspect with its surroundings, these effects can be compensated for by making a measurement of bar space ΔT with the radiometer. The measurement includes any reflection effects

except for a minor directional reflection component. However, for tactical type targets, the surround energy contribution to signature may be significant.

Wind velocity and direction data is a parameter affecting the temperature stability of the target. Fortunately, for the IR tests the prevailing winds in winter and summer do not blow against the target face. Temperatures have been measured to be relatively stable to winds of about 20 knots. Here, the main concern is the variation in bar-space ΔT between the time is is measured with the radiometer and the target breakout on that pass.

For the TV system stimulus, the target has bars with different reflectivities in the visible and near IR spectral region but nearly identical emissivity in the IR spectral region used by the thermal sensor. Thus, both a variable TV bar pattern and a variable IR bar pattern can be simultaneously maintained. Whereas in the case of the IR sensor, the primary stimulus (presented energy difference) is controlled only by the bar-space temperature difference for the TV, the presented energy difference is due both to the reflectivity difference between the bars and spaces and also upon the quantity of direct illumination. Thus, the total angularly integrated TV effective illumination falling on the target must be accurately measured at the target on a real time continuous basis along with a marker which will denote the exact instant of TV target breakout.

The presence of extraneous, strong illumination sources close to the target areas may affect TV operation. Therefore, these must be controlled.

Operator Variables

Since a major portion of the test results are dependent on operator-display interactions, care must be taken in analyzing the parameters affecting operator performance. These parameters include:

- Display Viewing Distance
- Visual Baseline Parameters
- State of Training
- Fatigue, Motivation, etc.
- Operator Impressions

Display viewing distance controls the angular spatial frequency of the target in visual space. Since target breakout and probability of detection of objects can be influenced by visual space size, this can be important.

Viewing distance could be made a fixed, controlled parameter if the display were provided with a hood or a forehead rest to constrain the operator to a fixed distance. If this is not possible, viewing distance should be estimated and reported when different from the average. It is not a strong variable and precise measurement is not absolutely necessary if all tests are clearly noise limited.

Visual baseline operator parameters also enter the performance calculation. For a rigorous statistical study, a number of trained operators should be utilized to obtain the correlation of operator visual parameters with system performance. Unfortunately, it is much too expensive to make a sufficient number of trials during the flight test to support several different operators. The best that can be done is to measure possible relevant visual parameters of two operators, one for each sensor, so that some correlation with later flight test programs or data from other visual investigations can be made. These operator baseline visual parameters should be measured before the test program and after completion of the test program.

Many test programs simply state that their observers have "normal" vision. However, it has been shown, that there can be a significant difference in visual performance by operators who have different but "normal" vision. Accuracy of response and search capability as a function of foveal and peripheral visual acuity were major parameters of the referenced study, and significant correlations were noted. It is suggested that the same battery of acuity tests be given the operator used in this test program. They are:

- Far Binocular Visual Acuity Using Block Letters
- A Landolt C Visual Acuity Test
- A Bausch and Lomb Visual Acuity Test which Involves Recognition of a Checkerboard Pattern
- A Symbol-Discrimination Visual Acuity Test

In addition, accommodation tests should be made since the operator will be viewing the display at a viewing distance of from 10 to 23 inches.

The state of training will also be an important parameter. Although the scene produced by an infrared thermal imaging system is strikingly similar to black and white visual photographs, subtle differences exist, and experience with the sensor being tested and similar equipment is important. It is expected that there will be a trend of improved performance as the test program proceeds, particularly in "tactical" type target detection.

Counter trends may also become evident due to operator fatigue or boredom. It might be expected that there would be a trend of decreased performance due to operator fatigue if all data were ranked in order of the pass number each night. Also, the test program may involve many samples with great similarity so boredom may become a problem.

Operator impressions can be a valuable clue to boredom and fatigue. More important, however, is whether he likes or dislikes the particular display setting he is required to observe as a function of meteorological and target parameters. It will be important to learn whether the operator likes the appearance of the display when it is set to maximize the probability of detection. Past flight test programs have shown that some of the most significant clues to the causes of significant differences in test results and a priori predicted results is obtained through interviews with the operator to determine what he is "seeing".

Equipment Environment Conditions

Uncontrolled equipment environment parameters include:

- Telescope Temperature
- Turret Air Temperature
- Turret Window Temperature
- Aircraft Vibration
- Aircraft Angular Perturbations
- Aircraft Induced Noises

Particular attention must be paid to IR telescope temperature which is a strong parameter affecting focus. Air and window temperature are recorded in case they have some unforeseen effect.

Aircraft vibration is one of the few parameters with an effect difficult to assess. Certainly it must have some effect on performance, but since the level of vibration should be relatively constant throughout the program, no variance data can be obtained.

Aircraft attitude has an effect on operator tracking performance and, thus, perturbations should be kept to a minimum during the test passes. If undue perturbations do occur during a pass, this fact should be recorded.

Aircraft induced noises arise from a number of sources, and must be carefully watched during the course of the test program. Particular offenders are the transmitters on the aircraft which may send noise spikes into the system at inopportune times. If possible, such occurrences should be eliminated by procedural techniques.

Equipment Baseline Conditions

The sensor adjustment is of obvious importance. To the best of their ability, test personnel must be certain that equipment is in excellent and uniform operating condition for each flight. Parameters which may vary should be recorded by logging run-to-run to assure retention of all relevant data. Parameters of importance include:

- Telescope Focus
- Channel Noise Voltage
- Base Line Voltages

Channel noise voltage is measured and recorded during pre- and post-flight with all other aircraft systems operating to provide the base for signal-to-noise ratio at target breakout data.

Various equipment voltages should be monitored and logged periodically throughout the data flights to assure that equipment is as close to the same condition each night as possible.

Tactical Target Base Conditions

Tactical target uncontrolled parameters which are of particular interest are:

- Speed of Travel
- History of Recent Operation
- Predominant Temperatures

It has been found that the thermal signature of a moving vehicle is significantly different from that of a stationary vehicle. Moving air cools the hood while flexing warms the tires of the vehicle. Consequently, recent operating history is a factor in the probability of detection and recognition ranges. Therefore, it is proposed that vehicles used as targets be kept in fairly constant motion until just prior to aircraft overpass. Taking data with the targets moving would probably lead to intolerable errors in slant range measurement and background condition control although the differences in detection range for moving and static targets under various display settings would be interesting.

5.4 FLIGHT TEST CONFIGURATION

There are a number of ways in which the flight test can be configured in order to obtain theoretical performance model conformation. Each way has both merits and faults. Some of the considerations are discussed below.

Mathematically, the detection and recognition of vehicles is less tractable to analysis than is the "breakout" of a regular bar pattern. This is due to the complexity of real-target signatures. The interaction of the parameters contributing to the target detection and recognition signature is not yet fully understood. Consequently, it is

proposed that the fundamental equipment performance model to be confirmed is the performance against a regular bar pattern for various conditions of target bar-space energy difference and equipment controlled settings. From this base, the interaction of tactical type target signatures and equipment parameters can be more easily deduced.

To the author's knowledge, the only Government-owned bar target capable of supporting a simultaneous IR/TV flight test is the large electro-optical test target located at Webster Field, Maryland, and operated by the Naval Air Test Center, Patuxent NAS, Maryland. This target can present various reflectance differences in the visible and near IR and simultaneously present a temperature difference at nearly uniform emissivity in the long wavelength IR region used by the thermal sensor. Although more temperature stability in the bars would be desirable, useful data can be obtained. Because of its uniqueness, the use of this target has been presumed in the discussions in the preceding subsections.

More options exist in the case of the tactical type target detection and recognition tests. Applicable ranges exist at Eglin AFB and in the Panama Canal Zone as well as at Webster Field. It is expected that a desert range at Edwards or China Lake could also be made available. For uniformity of difficult atmospheric transmission weather year-around, the Canal Zone is best, but support of the test is more difficult because of the distance. Also, it is clear that a test program conducted in either uniformly poor or uniformly excellent transmission conditions cannot produce the maximum available information. However, limited tests at the Canal Zone may be useful.

Eglin AFB has a large area available for tactical type target locations, is easily accessible, and has some transmission condition variability winter to summer. Webster Field has a more limited area available for tactical type target locations and a wide range of expected transmission conditions winter to summer. It is also easily accessible. A major advantage of the Webster Field site for detection and recognition tests is that tests can be run simultaneously (serially in any given aircraft pass) with the bar-target tests so that intercomparisons at a single set of atmospheric conditions can be made.

Flight time per data point is of the essence in a flight test program. Experience at Webster Field has shown that approximately three missions per 5-day week can be accomplished. When flying only against the bar target, one data point (one overflight) can be accomplished every 10 minutes. Thus, it is possible to gather as many as 25 data points on a single night and as many as 75 data points average per week of time scheduled at the range.

A flight pattern at Webster Field, which includes both the main target, good tactical type target sites, and meets local flight restrictions, takes approximately 20 minutes to complete. An average of 12 data points of each type on a single night is typical, although longer mission times can increase this number.

At Eglin AFB, sufficient area for test exists so that it may be possible to set up two separate sets of tactical type target sites on opposite legs of a race course pattern. It might be feasible to complete such a pattern approximately every 12 to 15 minutes.

The conditions at the Canal Zone test range are unknown as are the conditions at Edwards AFB and China Lake Test Center. Along with the availability of flight area, the selection of test program configuration also depends on the availability and cost of range instrumentation, target vehicles, support personnel, and data reduction facilities. Therefore, the final selection of flight test site and procedures must receive additional study.

APPENDIX I

ATMOSPHERIC TRANSMISSION ANALYSIS FOR THE IR

I.1 ATMOSPHERIC TRANSMISSION

The transmission of the atmosphere has a profound effect on the design and performance of thermal imaging equipment. Absorption of signal energy along the target-sensor slant path produces a reduction in thermal contrast as viewed by the sensors so that more equipment gain, and a concomitant reduction in displayed dynamic range, is required to see a given temperature difference. Design of future equipment and the evaluation of equipment already built must take into account the effects of this atmospheric absorption contrast reduction as a function of range and meteorological parameters.

Many specific spectral band limits might be selected to meet a variety of equipment mission objectives. To understand the interactions, transmission effects must be studied at several ranges for many atmospheric conditions for each set of band limits. To accomplish this task, a general computer analysis program is required to perform the many calculations.

Two regions of the electro-magnetic spectrum are usually considered in connection with the missions of thermal imaging sensors: the 3 to 5 micrometer band and the 8 to 14 micrometer band. The Infrared Image Test Program Study (Contract F33615-69-C-1199, P005), has been used as a base for much of the 8 to 14 micrometer band work reported here. The investigation of the 3 to 5 micrometer band and scattering effects were accomplished on the High Performance IR System Study (Contract F33615-70-C-1682).

I.1.1 SELECTION OF A TRANSMISSION MODEL

The purpose of the atmospheric transmission study was not to develop an entirely new transmission model, but rather to adapt available models to the specific missions at hand. To accomplish this purpose, possible models were investigated using the criteria that:

a. The model must be already developed
b. The model must accept a range of parameters representative of expected conditions
c. The models must be available and easy to use
d. The results must be believable when compared to measured results

A survey of atmospheric models and measures was made using Anding (Ref. 28) as a primary source. This survey selected three models to be investigated in more detail.

The Yates and Taylor (Ref. 29) measured data are a primary source since it is virtually the only field measured spectral data taken over long pathlengths for a wide variation in conditions. The data are available and easy to use when the specific conditions published are close to the conditions expected; the data are representative of a variety of sea level conditions likely to occur in the Chesapeake Bay region; and the data are accepted as accurate throughout the industry. The major drawback is that the data are difficult to extrapolate to other than the measured conditions. This is particularly true in the 3 to 5 micrometer band where several constituent absorbers contribute to the shape of the usable transmission windows. In the 8 to 12 micrometer band, the transmission is almost totally dependent on the quantity of precipitable water vapor in the slant path, so an extrapolation of the

Yates and Taylor data is relatively straightforward for conditions of moderate relative humidity.

Another model studied in detail was the Altshuler (Ref. 30) estimate. This transmission estimate is developed, readily available, and easy to use. The method was originally developed for quick estimates by hand computation techniques, but it is quite amenable to rapid computer calculation. There are two major difficulties with the Altshuler estimate. First, the fine spectral structure of the constituent absorbers has been averaged so the transmission in small bands cannot be accurately estimated and the band limits of optimum bands are not precisely determinable. Second, at higher concentrations of precipitable water vapor there is a serious discrepancy between estimates for the 8 to 14 micrometer band from Altshuler and the measured data of Yates and Taylor for similar conditions.

During the investigation for the cause or causes of the discrepancy, Mr. Anding was consulted by telephone. Mr. Anding commented that:

> "The Yates and Taylor data has a large scattering contribution at high water vapor concentrations. Altshuler did his analysis using experimental data taken at low water vapor concentrations. Thus, any extrapolation to high water vapor concentrations is likely to be bad Anyone's program will probably have this same difficulty.
>
> Many investigators are currently facing the same problem. They are attempting to obtain long path laboratory data with high concentrations of water vapor. Thus far, all experiments have failed at concentrations of approximately 5 precipitable centimeters due to condensation of the water on the apparatus."[9]

[9] Private Communication with David Anding, Infrared and Optical Sensor Laboratory, U. of Mich., 10 June 1970

A third transmission model that was considered was the University of Michigan transmission computer program. This is a very sophisticated program which can estimate transmission by the various band models as best applicable over a wide variety of slant path conditions with a resolution of approximately 5 wavenumbers. Mr. Anding (Ref. 28) commented that this program begins to underpredict the Taylor and Yates data significantly at water vapor concentrations in excess of 4 precipitable centimeters in the 8 to 12 micrometer band even though the program has a scattering subroutine. However, he reports that the program does much better than Altshuler in the 3 to 5 micrometer band. This model was not pursued primarily because the model is not readily available. Special cases can be obtained through contact with the University of Michigan, but heuristic exploration of parameter variation is not possible.

I.1.2 ALTSHULER TRANSMISSION ESTIMATE

Altshuler's estimate is a series of curves for water vapor, CO_2, N_2O and O_2, plotting spectral transmission as a function of $\log_{10}$ wavelength for a specific level concentration of the absorber. In regions of strong line absorption, these spectral transmission values can be scaled to other equivalent sea level concentrations using the relationship

$$T(\lambda) = \exp\left[-Z(\lambda)\,(W^*)^{1/2}\right] \qquad (120)$$

where:

$T(\lambda)$ = spectral transmission at a given wavelength, fraction

W^* = desired equivalent sea level path of absorber

$Z(\lambda)$ = a number such that

$$T_o(\lambda) = \exp\left[-Z(\lambda)\,(W_o^*)^{1/2}\right]$$

where:

$T_o(\lambda)$ = transmission value given in Altshuler's curves

W_o^* = equivalent sea level path at which the chart data were taken

Under weak-line conditions, in general, where transmission exceeds 95% at sea level, the curves are scaled with curves of the general form

$$T = 1 - K'(\lambda) \frac{W^*}{W^*(95\%)} \tag{121}$$

where:

$W^*(95)$ = amount of equivalent sea level absorber which would produce a transmission of 95% by Eq. 129

$K'(\lambda)$ = empirically derived scaling constant for each absorber.

The equivalent amount of sea level absorber is calculated with the equation

$$W^* = \int_o^x M(x) \left(\frac{P(x)}{P_o}\right)^2 \left(\frac{T_o}{T(x)}\right)^{n+1} dx \tag{122}$$

where

x = slant path length in meters

$M(x)$ = absorber mixing ratio at any specific point on the path

P_o = sea level standard atmospheric pressure (760 mm Hg)

$P(x)$ = pressure at any specific point on the path

T_o = standard condition absolute temperature (15°C, 288°K)

$T(x)$ = absolute temperature at any specific point on the path

n = empirically derived constant depending on the absorber,
$n = 1$ for H_2O, CO_2 and N_2O,
$n = 0.3$ for O_2

By limiting the area of validity of the computer algorithm to approximately horizontal slant paths at altitudes below approximately 10,000 feet, ozone absorption can be neglected and a precise integration of M(x), P(x) and T(x) over the path is not required, so Eq. 131 can be reduced to

$$W^* = M \left(\frac{P}{760}\right)^2 \left(\frac{288}{(273 + T_o)}\right)^2 X \qquad (123)$$

where:

$M(CO_2)$ = 350 ppm x 10^{-4}

$M(N_2O)$ = 0.5 ppm x 10^{-4}

$M(H_2O)$ = 1.225 g/kg x 10^{-4}

This near sea level approximation is considered valid in view of the altitude regimes assumed for many missions.

At the altitudes being considered, the mixing ratios of CO_2 and N_2O can be considered to be constant. The mixing ratio of water vapor, however, is a function of water vapor actually in the path.

The amount of water that air can hold at saturation is a function of air temperature, 3.839 g/Kg at 0°C and 20.44 g/Kg at 37.8°C. (Ref. 31). Over this temperature range, the mixing ratio of water at saturation can be estimated to an accuracy of better than 1 percent by the relationship

$$M = (3.95)\ (1.068)^T \qquad (124)$$

where:

M = mixing ratio of H_2O to dry air, gm/Kg

T = temperature, °C

The algorithm for mechanizing Altshuler's curves by computer was written in two parts. The first step was to convert his data to a form which could be quickly evaluated by a second program over arbitrarily selected band intervals.

Over the wavelength intervals 2.75 to 6.0 and 7.0 to 15 micrometers, the transmission values given in Altshuler's curves were read at 1 percent intervals of the logarithm base 10 of the wavelength in micrometers.

A value for Z (λ) was derived for each point using the relationship

$$T_o(\lambda)/100 = \exp\left[-Z(\lambda)(W_o^*)^{1/2}\right] \tag{125}$$

(See Eq. 120)

$$Z(\lambda) = -\ln\left(T_o(\lambda)/100\right)/(W_o^*)^{1/2} \tag{126}$$

Noting that a linear plot of $\log_{10} Z(\lambda)$ vs $\log_{10}(\lambda)$ results in relatively smooth curves with short intervals between data points, linear curves were fitted between each successive two points of $\log_{10} Z(\lambda)$.

$$Y(\lambda) = \log_{10}(Z(\lambda)) \tag{127a}$$

$$X(\lambda) = \log_{10}(\lambda) \tag{127b}$$

$$Y(\lambda_2) = m\,X(\lambda_2) + b \tag{127c}$$

$$Y(\lambda_1) = m\,X(\lambda_1) + b \tag{127d}$$

$$Y(\lambda_1) - Y(\lambda_1) = m\left[X(\lambda_2) - X(\lambda_1)\right] \tag{128}$$

But in this particular instance, $X(\lambda_2) - X(\lambda_1) = 0.01$, the interval at which data were taken so:

$$m = 100 [Y(\lambda_1) - Y(\lambda_2)] \tag{129a}$$

$$b = Y(\lambda_1) - m [X(\lambda_1)] \tag{129b}$$

Values for m and b are stored in the computer for each constituent absorber and each log wavelength interval. These are the basic data and have to be run only once unless it is desired to add additional wavelength intervals beyond those already processed.

The initial section of the algorithm calculates the temperature and pressure corrected values of the equivalent sea level quantity of the absorber, W*, utilizing Eqs. 123 and 125. Then, starting at the short wavelength band limit requested, the value of the exponent of Eq. 120 is calculated, using the m and b values for interpolation. A test is them made for each constituent to see if the strong-line or weak-line absorption condition prevails:

For water vapor	$T > 93\%$
For CO_2	$T > 95\%$
For N_2O	$T > 80\%$

All at sea level.

If T would exceed the indicated limit, the constituent transmission is calculated by Eq. 121; if not, transmission is calculated by Eq. 120. The spectral transmission for each wavelength is the product of the three constituent transmission values:

$$T(\lambda) = T_{H_2O}(\lambda) \cdot T_{CO_2}(\lambda) \cdot T_{N_2O}(\lambda) \tag{130}$$

The program then increases the wavelength by 0.02 micrometer using the equation

$$X_2 = X_1 + 8.686\ (10^{X_1}) \qquad (131)$$

where:

X = $\log_{10}$ (λ), and calculates the transmission in the next interval until the long wavelength band limit selected is reached

Figure 50 shows spectral data given by this program throughout the 3 to 5 and 8 to 14 micrometer bands.

In formulating this atmospheric transmission algorithm, care was taken to order the calculations in such a way that the program capability is easily expanded, e.g., greater wavelength intervals, 1 to 60 micrometers; altitudes requiring ozone calculations; scattering by haze or fog, etc. Also, the specific response curve of a particular sensor (spectral filter and detector) can readily be incorporated. At the same time, the loops have been ordered to minimize the computation time. The result is an economical tool for investigating the atmospheric transmission effects on thermal imaging sensors within the limits of basic data used.

I.1.3 OPERATIONS ON YATES AND TAYLOR DATA

The Yates and Taylor data consist of a number of reduced transmission curves obtained with a spectrometer set at a resolution of $\lambda/\Delta\lambda = 300$ measured in three sea level paths over the Chesapeake Bay. In this investigation, transmission curves taken of the 5.5 and 16.25 Km range paths were used. Table VI lists the conditions for which data were available. The following sections describe the computer

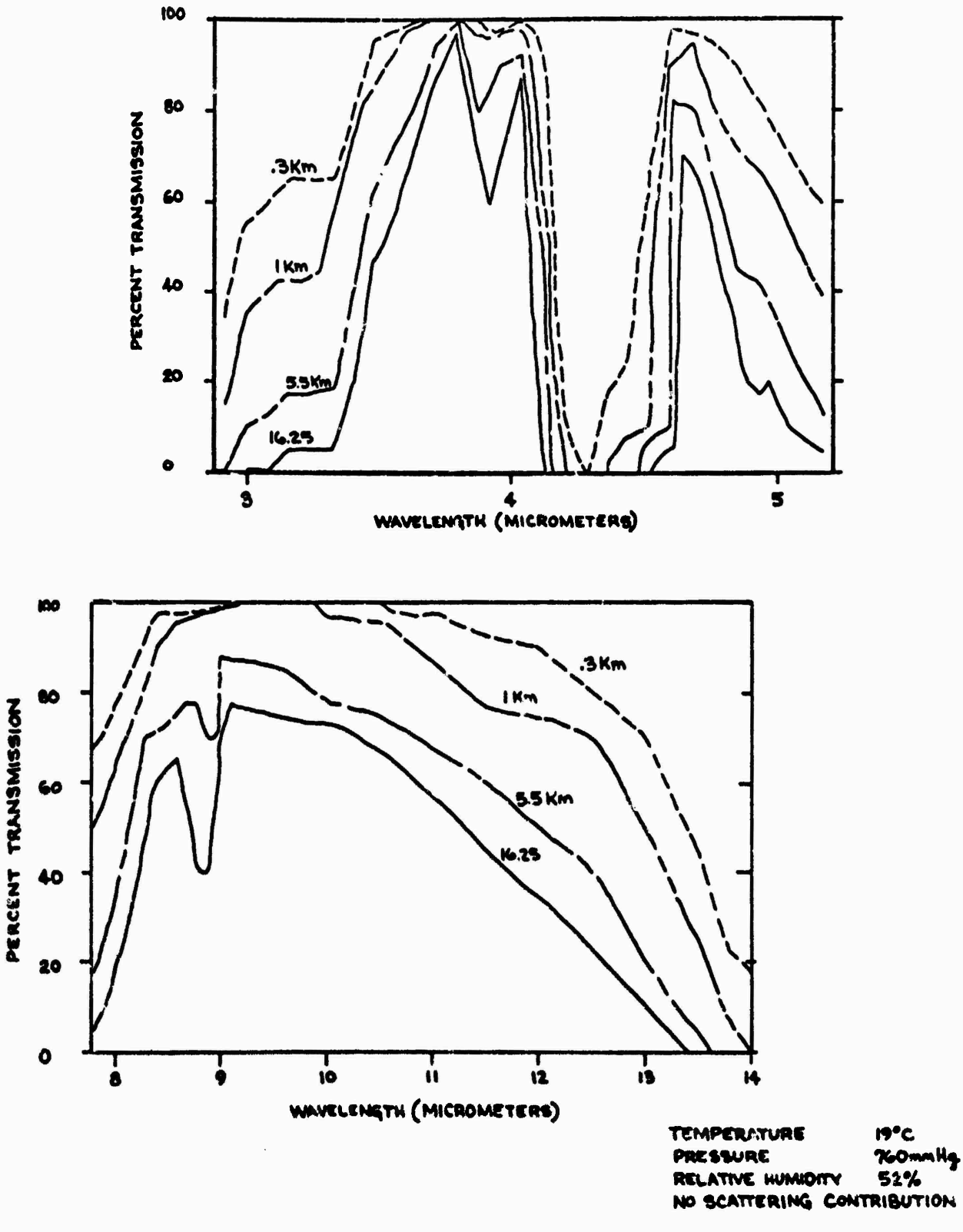

Figure 50. Spectral Data Produced By the ECS Computer Algorithm for Altshuler's Transmission Estimate

algorithms developed to make use of these data. The Curve Numbers listed on the tables are for reference in later discussions.

Integration Algorithm

A simple numerical integration algorithm was developed to obtain average transmission data for the various spectral band limits under investigation. For the 3 to 5 micrometer data, the seven transmission curves listed in Table VI were quantized from graphs at 0.01 micrometer intervals to provide a data file for computer operations. For the 8 to 14 micrometer data, five curves were quantized at 0.05 micrometer intervals.

Average transmissions are obtained by summing one-half the quantized transmission values at the first and last wavelength intervals to the sum of transmission values at all of the intervening intervals, and dividing the result by the number of intervals, e.g.:

TABLE VI

(U) METEOROLOGICAL DATA FOR YATES AND TAYLOR FIELD MEASUREMENTS

Ref. No.	Range km^{-1}	Air Temp. C	Rel. Hum. %	pr. cm. H_2O	δ, 2.17 km^{-1}	δ, 3.5 km^{-1}
1	5.5	1.4	47	1.37	-	-
2	5.5	3.3	66	2.2	0.091	0.062
3	5.5	17.8	51	4.18	0.042	0.031
4	5.5	25.3	73	9.4	-	-
5	16.25	11.7	41	5.2	-	-
6	16.25	20.6	53	15.1	0.038	0.038
7	16.25	23.3	82	27.7	0.046	0.047

$$T_{ave} = \frac{\frac{T_{\lambda 1} + T_{\lambda n}}{2} + \sum_{\lambda_2}^{\lambda_{n-1}} T_{(\lambda)}}{n} \qquad (132)$$

All curves are integrated in parallel. Figure 51 shows a composite result for seven different spectral band limits in the 3 to 5 micrometer band. (The band limits were selected using a photon S/N peaking routine which uses the same data file. The circled entry shows which curve gave the indicated band limits as optimum.)

I.1.4 OTHER ENERGY LOSS MECHANISMS *

Most literature on atmospheric attenuation is devoted to the understanding of gas and water vapor absorption. Although this type of signal energy loss is a very significant contributor to the total loss and a major influence on spectral band selection, the meteorological conditions found in the field during many applications of instruments operating in the 3 to 5 and 8 to 14 micrometer spectral bands demand that other energy loss mechanisms be considered if accurate performance predictions are to be made.

The additional energy loss mechanism usually considered is aerosol "scattering". There exists, however, one absorption mechanism which has been singularly ignored: aerosol absorption. The phenomenon usually referred to as "scattering" is really aerosol extinction, a combination of scattering and absorption. In the infrared, at wavelengths longer than about 3.5 micrometers, aerosol absorption has a

* The remainder of this appendix is taken from: J. A. Hodges, "Aerosol Extinction Contribution To Atmospheric Attenuation In Infrared Wavelengths", Applied Optics 11 (1972) pp 2304 - 2310

TAYLOR AND YATES SIMPLE INTEGRATION PROGRAM 08/26 10:55

THIS PROGRAM NUMERICALLY INTEGRATES IN 0.01 MICROMETER INTERVALS ANY SPECIFIED BANDWIDTH BETWEEN 2.80 AND 5.25 MICROMETERS USING DATA SCALED FROM TAYLOR AND YATES MEASURED CURVES. OUTPUT DATA ARE AVERAGE TRANSMISSION IN PERCENT. COLUMNS 1 TO 4 ARE FOR 5.5 KM RANGE AND COLUMNS 5 TO 7 ARE FOR 16.25 KM RANGE. DATA FOR THE CURVES ARE:

CURVE NUMBER	1	2	3	4	5	6	7
PR. CM H2O	1.37	2.2	4.18	9.4	5.2	15.1	27.7
TEMPERATURE F	34.5	38	64	78	53	69	74
REL. HUM.	47	66	51	73	41	53	82

WAVELENGTH							
2.87,5.07	(40.04)	34.92	37.04	29.10	19.80	18.74	11.20
2.97,5.07	41.29	(36.29)	38.73	30.48	20.72	19.62	11.73
3.32,4.92	45.41	42.39	(48.25)	39.35	25.91	25.42	15.37
3.36,4.16	66.48	61.33	72.67	(66.42)	41.50	44.63	28.55
3.37,4.07	69.51	64.39	75.23	67.72	(45.43)	49.09	31.23
3.38,4.08	69.70	64.54	75.69	68.42	45.50	(49.33)	31.55
3.39,4.09	69.77	64.60	75.99	68.93	45.44	49.40	(31.80)

BAND CIRCLED GAVE OPTIMUM SIGNAL-TO-NOISE

Figure 51. Integration Program for Yates and Taylor Data

double effect: Not only is energy absorbed by the liquid of the aerosol particles but the particles also emit energy at the air temperature producing a masking energy background against which infrared instruments must operate.

Aerosol liquid water absorption can be particularly high under conditions of high relative humidity, a condition where aerosol particles are large. This effect has been discussed by Carlon.[32] He suggested that this energy loss mechanism may be a source of unexplained behavior in many radiometric measurements. Streete[33] has suggested liquid water absorption may be a reason for discrepancy between his data and the data of Yates and Taylor for similar large quantities of precipital water vapor in the path. Streete's data was taken in a longer physical path at lower relative humidities. He obtained considerably higher transmission values in the wavelength band 8 to 10.6 micrometers than did Yates and Taylor.

The estimates for aerosol extinction and absorption are based on the techniques reported by Barnhardt and Streete.[34] A most useful concept in the Barnhardt and Streete technique is the consideration that the distribution of aerosol condensation nuclei can be thought of as a combination of a "maritime" distribution and a "continental" distribution. Any particular case consists of a ratio combination of the two cases. The continental distribution is typically that distribution found near the center of continental masses while the maritime distribution is typically that distribution found far from land. Figure 52 shows the assumed particle densities as a function of radius for the two distributions.

In this appendix, the combination of nucleation distributions is indicated by the fraction continental/continental + maritime. Unity indicates only the continental distribution is present, zero indicates only the maritime distribution is present, 0.5 indicates half of each distribution is present etc.

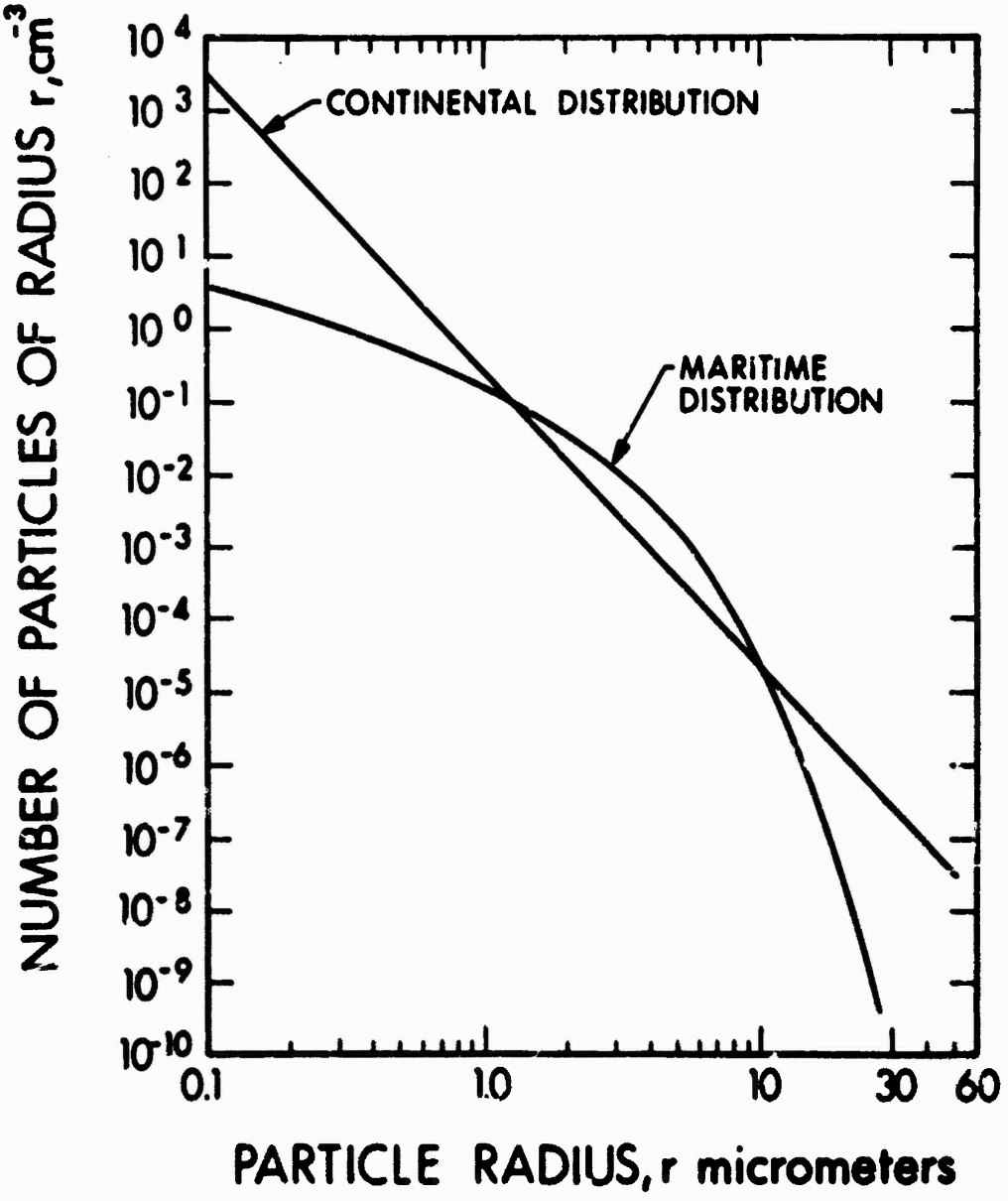

Figure 52. Particle Densities as a Function of Radius for the Assumed Limiting Conditions

39/82

The condensation nuclei distribution is modified by a growth factor which accounts for the accretion of water to the particle as a function of humidity. Growth is not primarily a function of the quantity pr. cm. of water vapor in the path, but rather of the relative humidity. The accretion is slight for relative humidities below approximately 50 percent but is extremely rapid above 80 percent. The growth curve, as reported by Barnhardt and Streete, is shown in Figure 53.

A number of modifications have been made to the basic Barnhardt and Streete estimation technique. Rather than calculating the exact Mie coefficients, the approximate formulas developed by Van De Hulst,[35] as reported in Chu and Hogg,[36] are used. These are corrected by the factors reported in Deirmendjian[37] who states that the correction brings the approximate coefficient within 2 percent of the exact Mie value. Equations for the aerosol extinction and absorption are given in Section I.1.10

The values of the complex index of refraction for water are taken from Chu and Hogg with the values beyond 10 micrometers checked against Centeno's[38] data, the original data source. The real portion of the index is modified as suggested by Barnhardt and Streete to account for the change in index from that of the condensation nucleus (assumed value = 1.54) to that of water as the particle radius grows with occluded water. Figure 54 shows the complex refractive index used in the computer algorithm for a relative humidity of 98 percent.

I.1.5 AEROSOL EXTINCTION AND ABSORPTION RESULTS

The aerosol extinction and absorption computing algorithms have been used in two ways: separately to provide spectral coefficients over a wide range of relative humidities and continental-maritime distribution mixing ratios, and as a part of the overall transmission estimating algorithm.

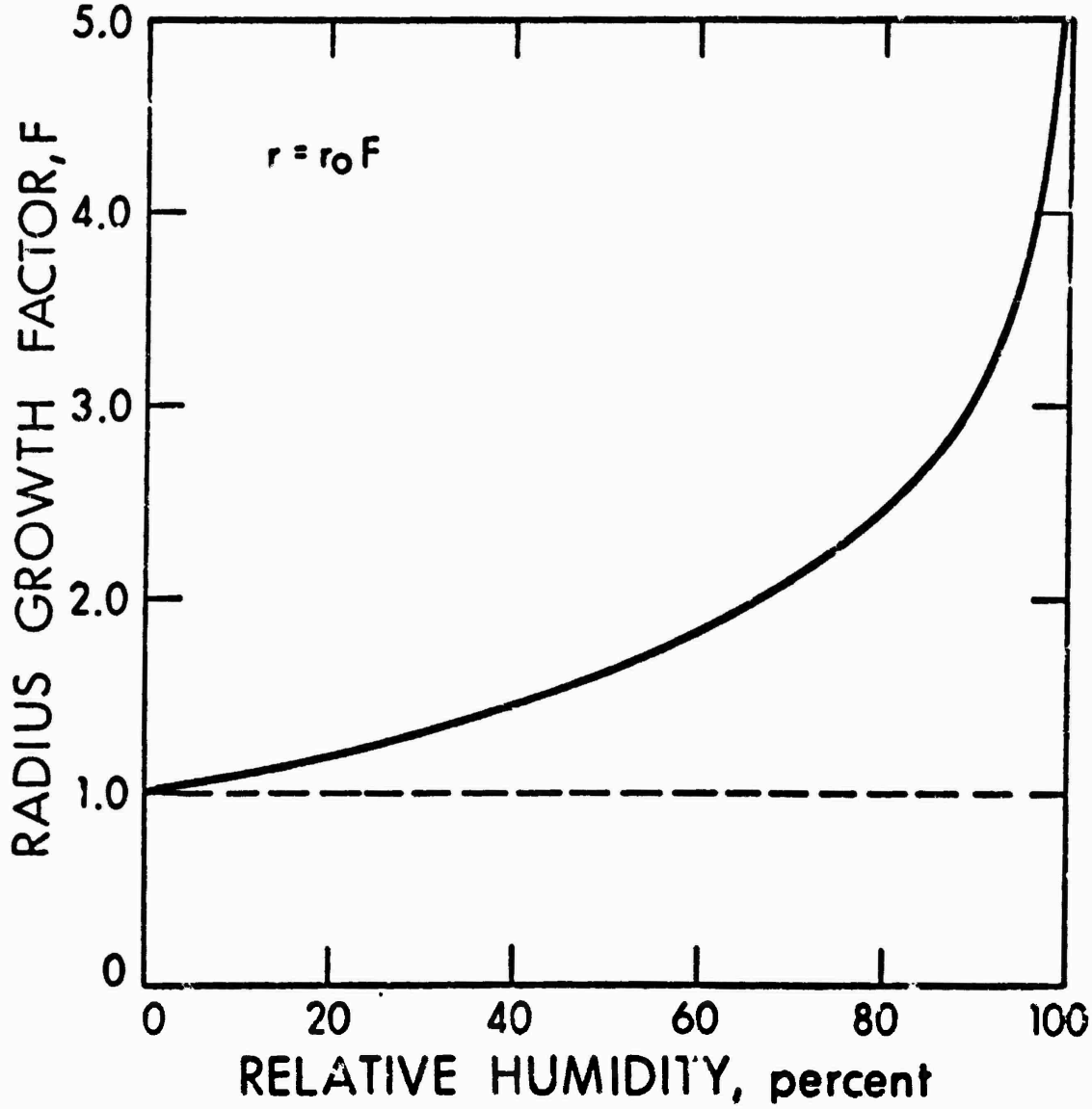

Figure 53. Particle Growth Factor as a Function of Relative Humidity

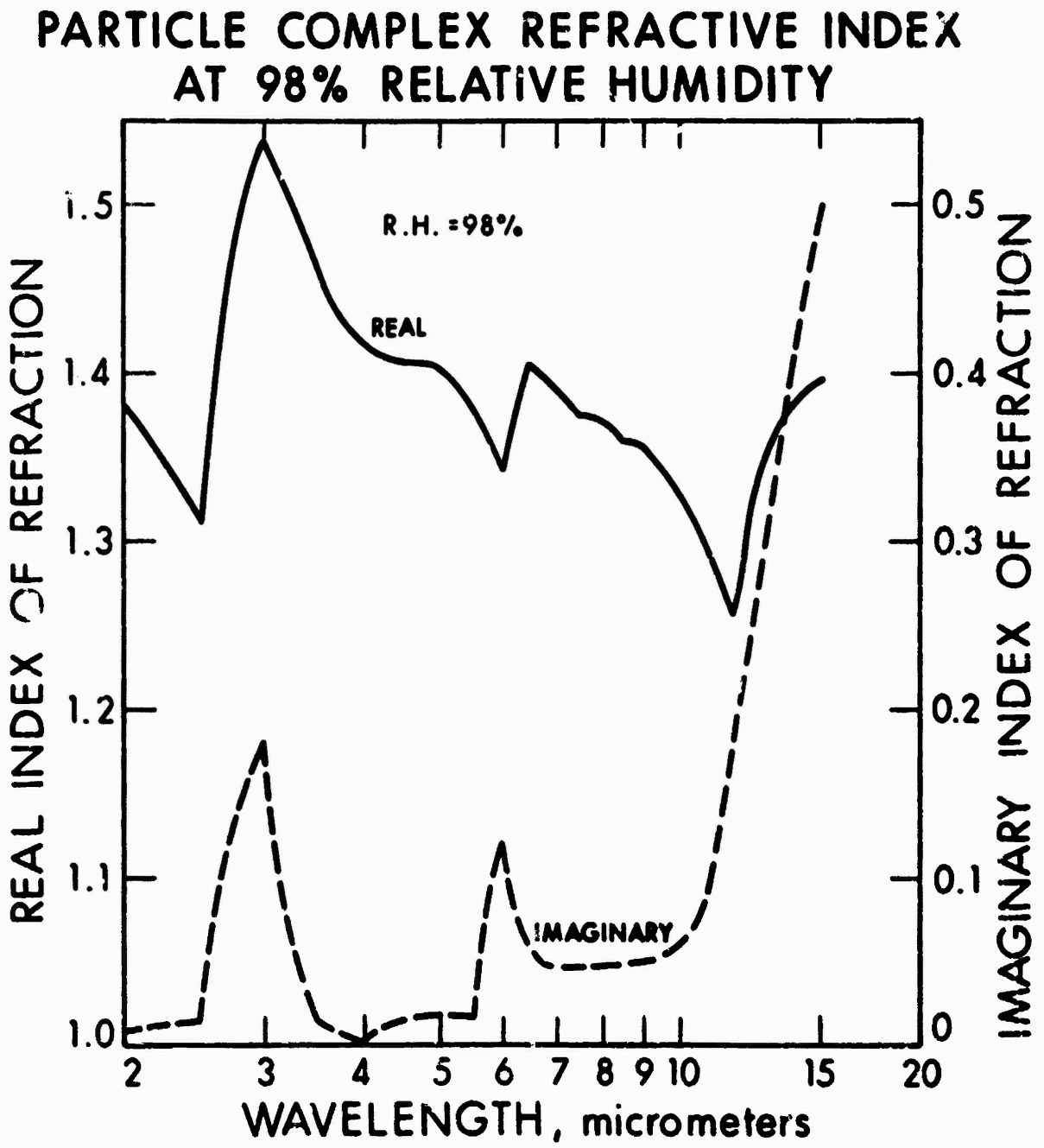

Figure 54. Particle Complex Refractive Index at 98% Relative Humidity

Selected spectral extinction coefficients are given in Figure 55. A most surprising result is that the extinction coefficient near 10 micrometers is almost independent of the condensation nuclei distribution used. This is shown even more dramatically by Figure 56 which is a wider spectrum of the ratio of continental distribution divided by continental plus maritime distribution at a fixed relative humidity of 85 percent. The flatness of the extinction coefficient for the pure maritime distribution is also surprising. These results may, of course, be fortuitous since they depend on interaction of the assumed value of the complex index of refraction of water and the assumed condensation distributions.

Figure 57 illustrates how rapidly the extinction coefficient increases with relative humidity. All of these curves are for the single condensation particle distribution ratio of 0.6

Figure 58 shows the spectral absorption coefficient portion of the extinction coefficient. In general, these curves follow the imaginary portion of the index of refraction. If an imaginary index were assumed for the condensation salt particles, similar to the assumed real index, then the excursion of the absorption coefficient would be moderated at the lower relative humidity values.

The relative amount of energy loss to absorption, as opposed to that lost through scattering out of the observers path, is dramatized by Figure 59 which is the ratio of spectral absorption to spectral extinction.

The curves show that beyond a wavelength of approximately 10 micrometers, the absorption portion of aerosol extinction is quite high. Since the extinction coefficient is also increasing rapidly in this region, it can be concluded that aerosol background emission increases rapidly beyond

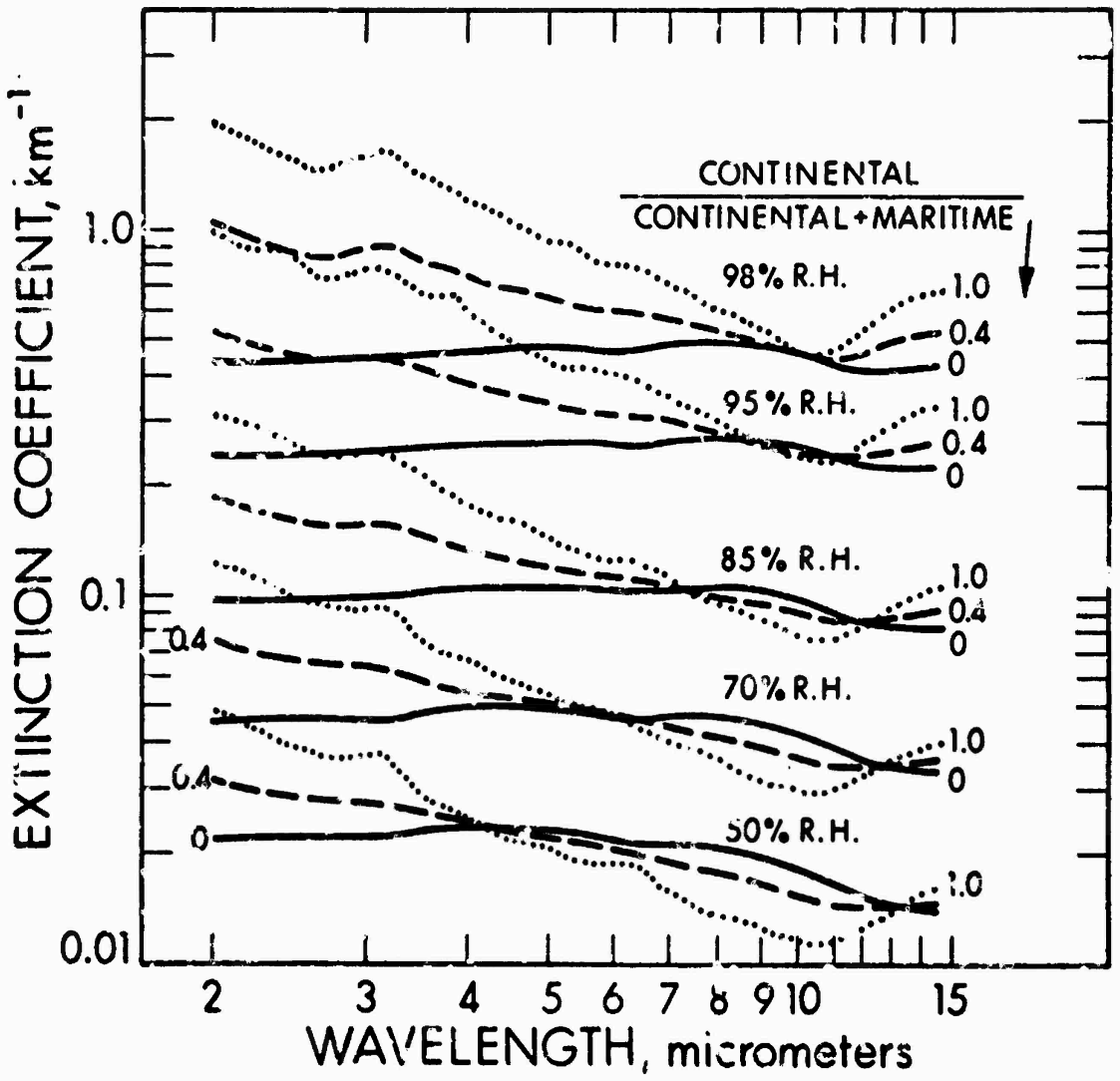

Figure 55. Spectral Extinction Coefficient as a Function of Relative Humidity and Nucleation Distribution

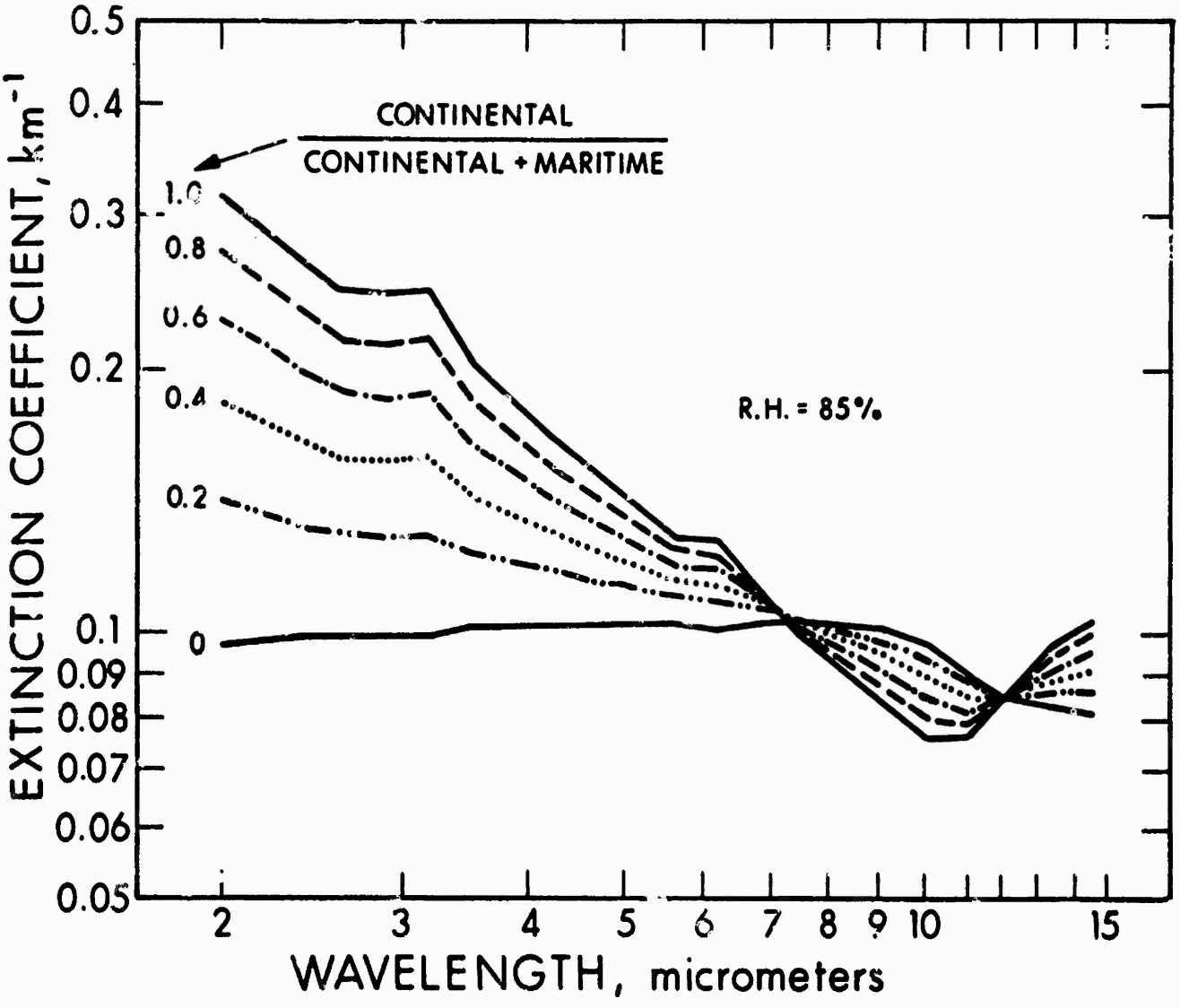

Figure 56. Spectral Extinction Coefficient as a Function of Nucleation Distribution

39787

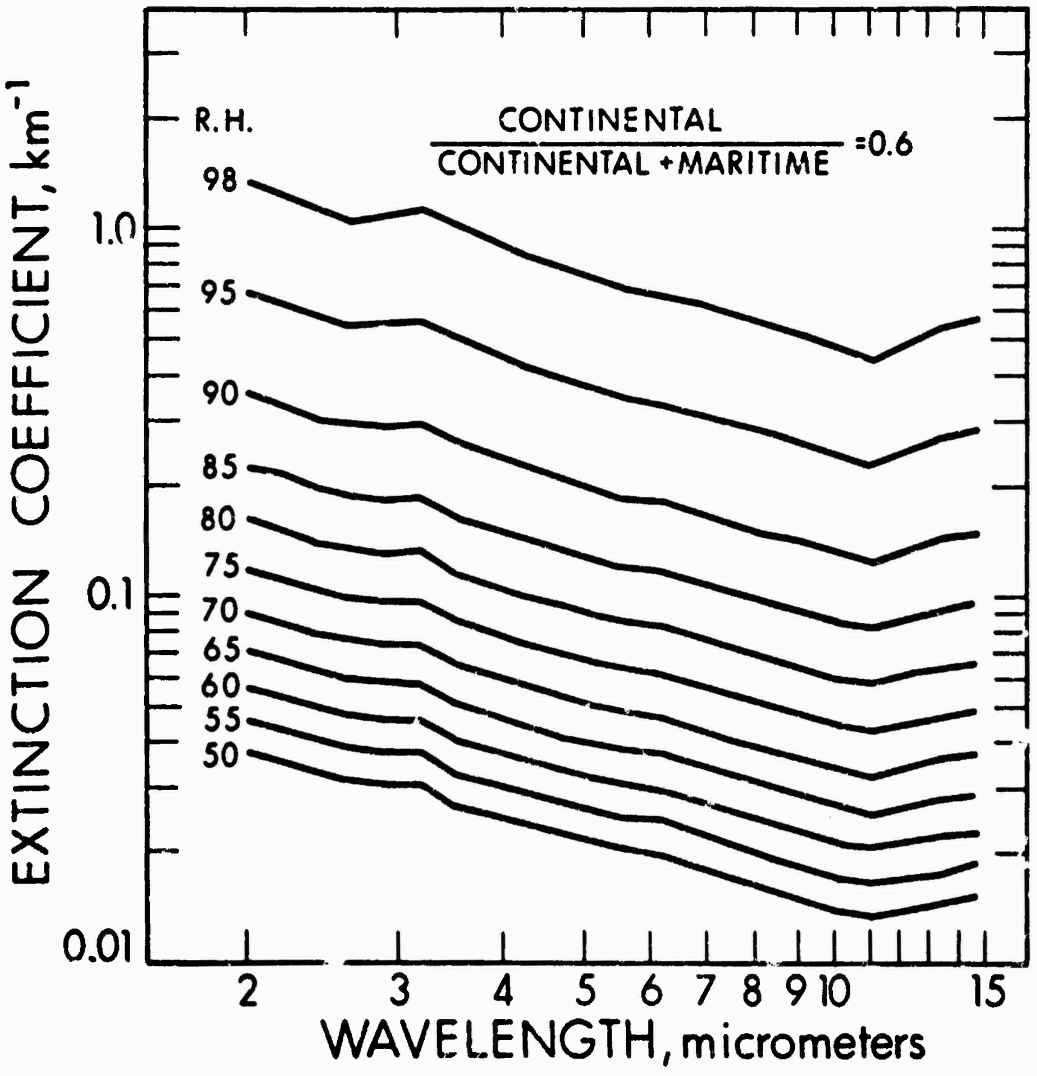

Figure 57. Spectral Extinction Coefficient as a Function of Relative Humidity

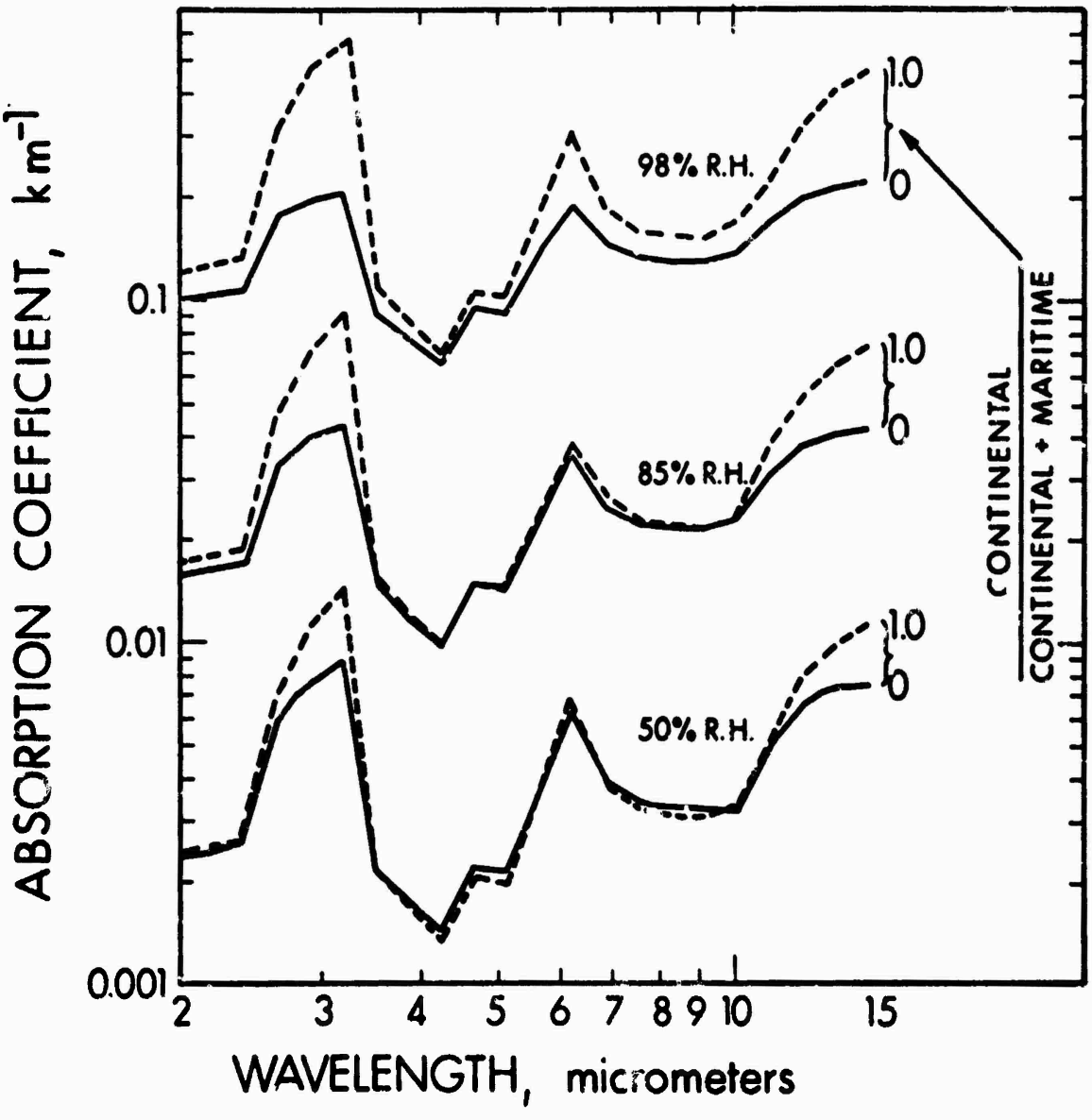

Figure 58. Spectral Absorption Coefficient as a Function of Relative Humidity and Nucleation Distribution

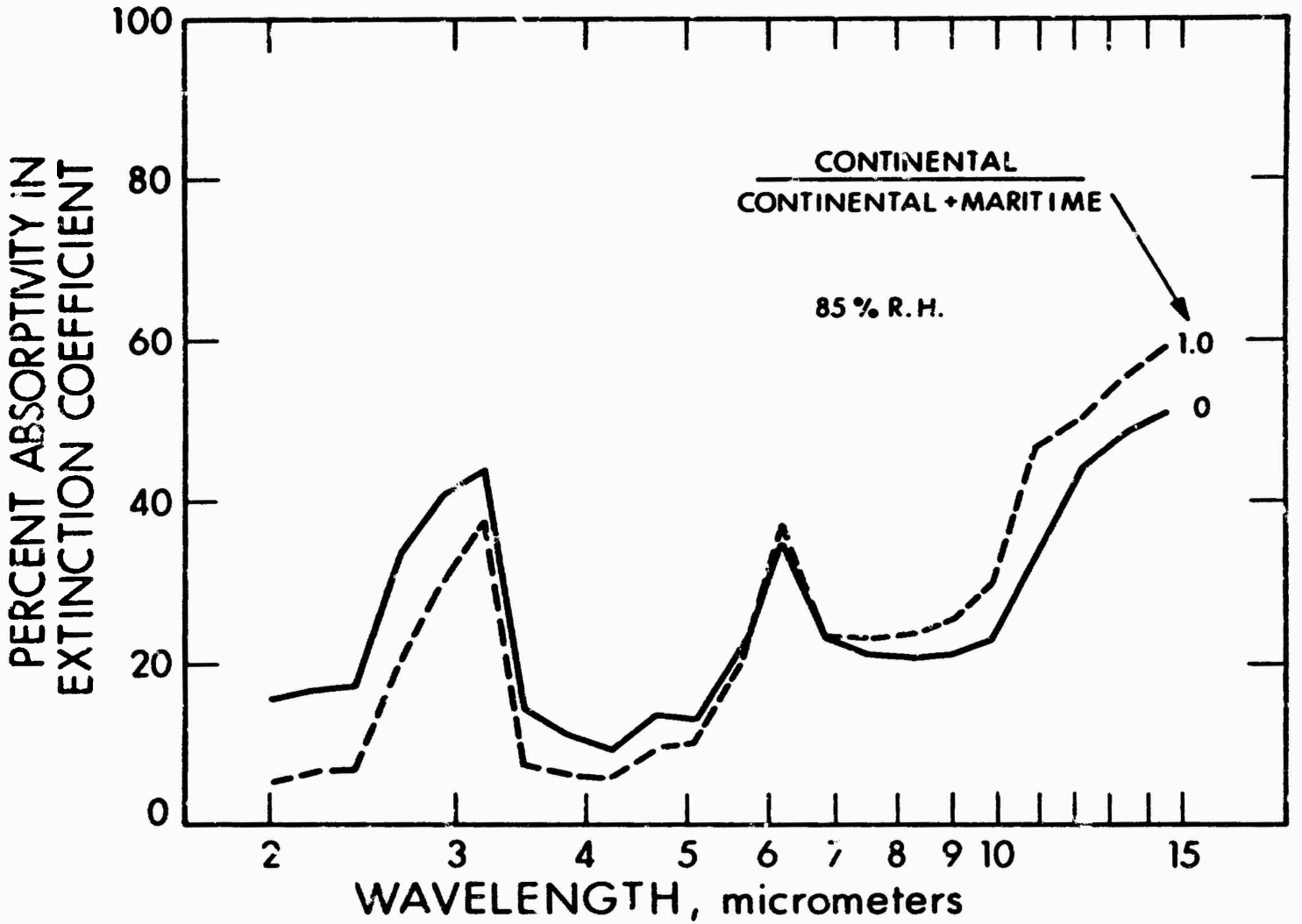

Figure 59. Percent of Extinction Coefficient which is Due to Absorption

approximately 11 micrometers. Similarly, both the extinction coefficient and the absorption portion of the extinction coefficient are higher in the 3 to 3.5 micrometer spectral band.

The shape of Figure 59 indicates that the radiant energy characteristic of a given air mass can change drastically as a function of wavelength. For example, consider a warm air mass overlaying a cool surface. In spectral regions of high scattering and low absorption, the air mass will be scattering energy from the cool surface, while in regions of high absorptivity and low scattering, the energy will be radiated from the warmer air.

I.1.6 COMPARISON OF MEASURED AND ESTIMATED EXTINCTION COEFFICIENTS

Figures 60 and 61 are a comparison of Yates and Taylor measured "scattering" coefficients and estimated extinction coefficients. The measured data in Figure 60 was determined in a 5.5 km sea level path while the measured data in Figure 61 was determined in a 16.25 km path.

Yates and Taylor reported that the "scattering" coefficient". . . determination was based on the assumption that absorption is negligible at certain spectral points away from intense absorption bands, and that in these 'windows' the measured attenuation could be completely attributed to scattering." Samples were taken at the wavelengths of 0.55, 0.60, 0.70 0.80, 0.90, 1.06, 1.26, 1.67, 2.17, 3.5, 4.0 and 4.7 micrometers with the data at 4.7 micrometers judged to be questionable because of the presence of weak absorption bands. In this appendix, only the bands longer than 0.90 micrometers are considered in order to avoid the effects of Rayleigh scattering by atmospheric molecules.

The reference number of Figures 60 and 61 refers to Table VI in Section I.1.3. The Y & T number is the "run number" of the original data. Reference samples 3 and 6 are for the same date, 19 June 1956.

The estimated extinction coefficients are selected by estimating spectral extinction coefficient curves at the indicated relative humidity and at several continental/continental plus maritime condensation nucleus distribution ratios and selecting the ratio that best fits the slope of the measured data beyond 2.0 micrometers. (The two curves for the same day show very different slopes!)

I.1.7 COMPARISON OF MEASURED AND ESTIMATED BAND ATTENUATION

Using the estimated condensation particle distribution ratios determined in Section I.1.6 above, average band attenuations are estimated in the several selected wavelength bands using the meteorological and range parameter values reported by Yates and Taylor. Unfortunately, the measured spectral transmission curves which were transcribed to the earlier computer program for easy integration are not completely coincident with the data for which "scattering" coefficients are reported: Only four curves can be compared in the 3 to 5 micrometer wavelength band and 3 curves in the 8 to 14 micrometer band.

Table VII gives the results of the comparison. The estimates at low relative humidity are in excellent agreement with the measured data. The 3 to 5 micrometer band attenuation estimates tend to be high while the 8 to 14 micrometer band attenuation estimates tend to be low. It seems remarkable, however, that the estimates for both bands are so good considering that the distribution of condensation nuclei consisted of two simple distributions whose ratio is judged by the slope of measured data 2 to 4 micrometers. A small discrepancy in the actual and assumed nucleation particle density distributions

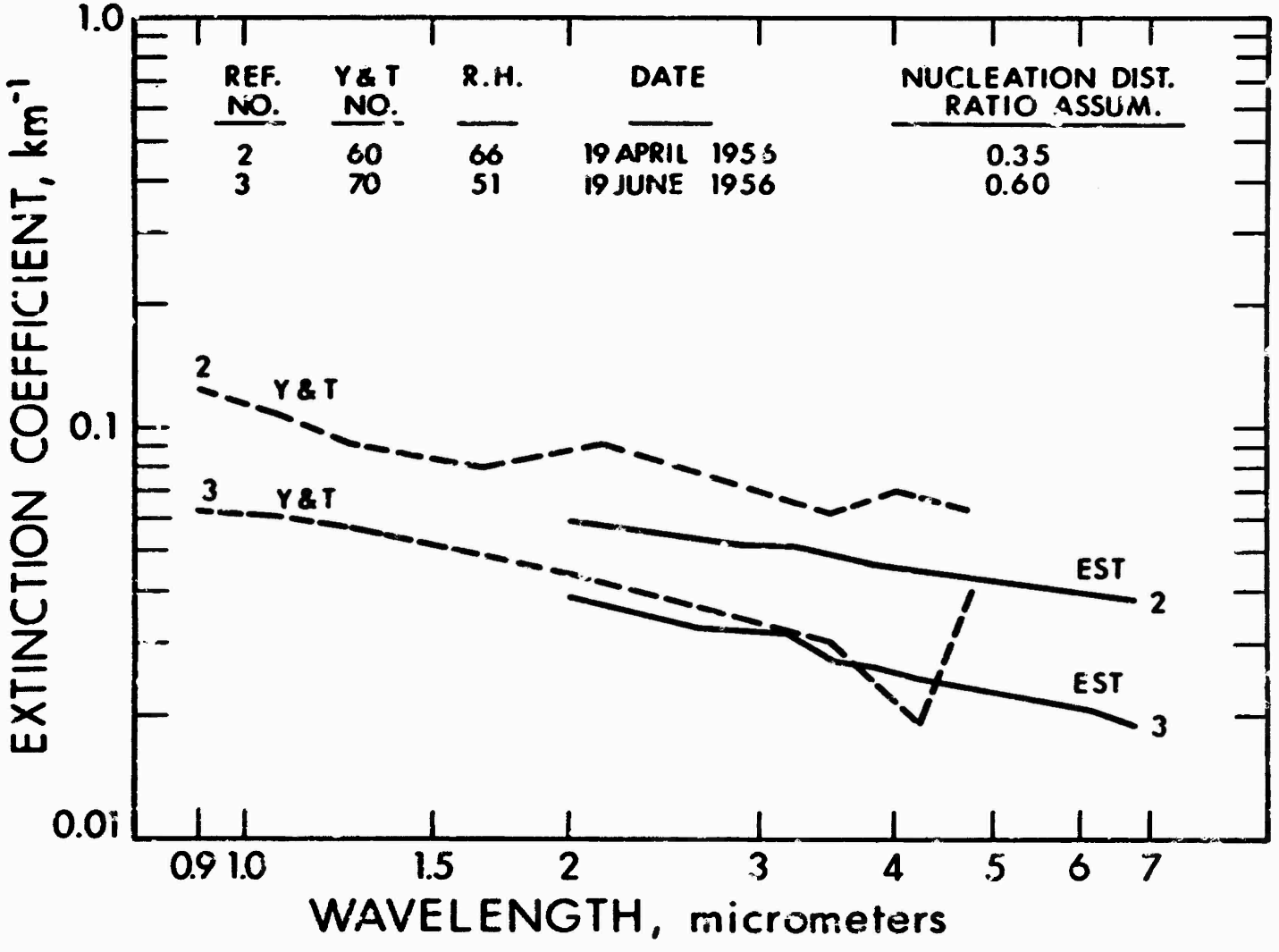

Figure 60. Comparison of Predicted Extinction Coefficients to Yates and Taylor Extinction Coefficients Measured in a 5.5 km Sea Level Path

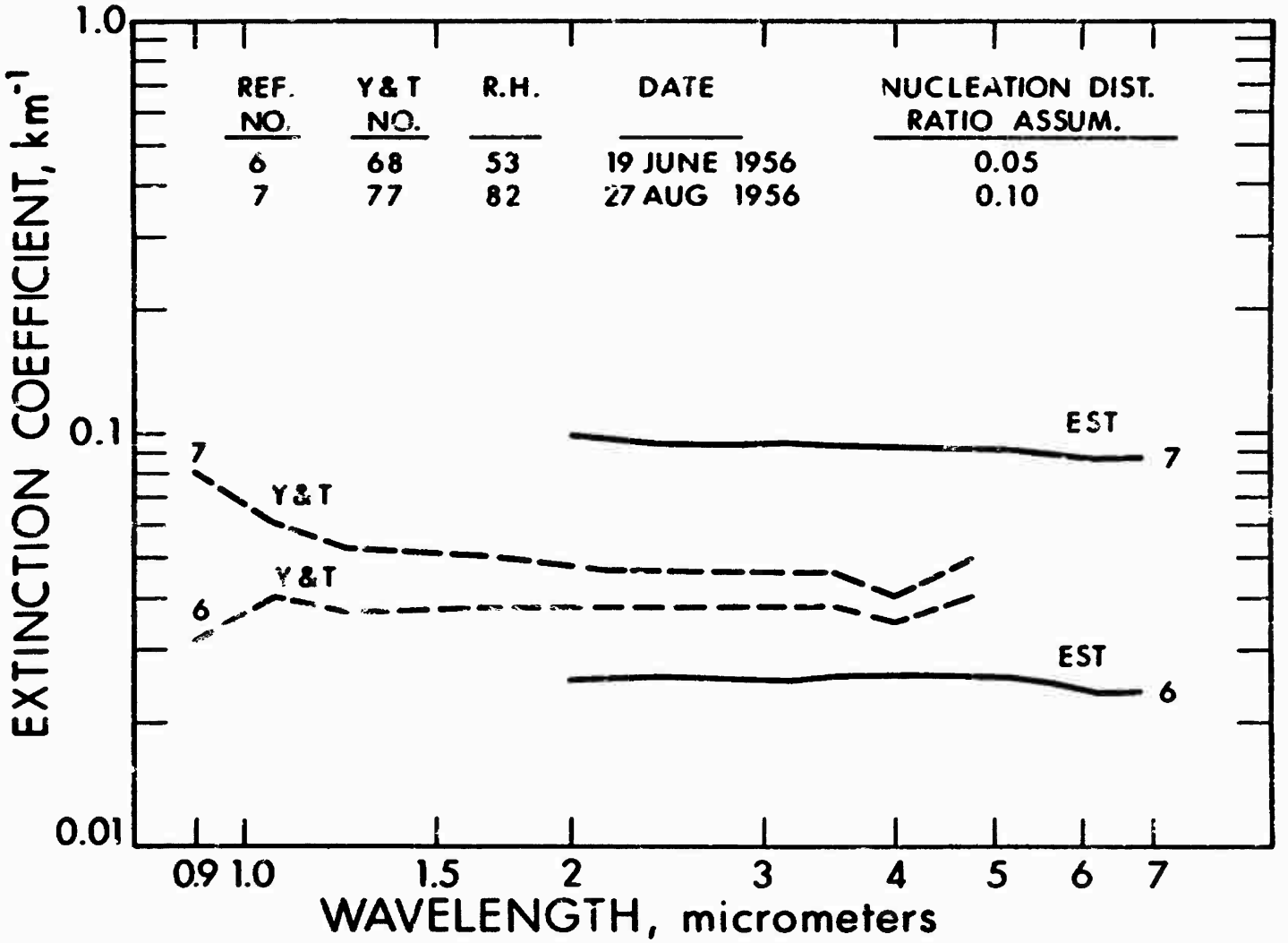

Figure 61. Comparison of Predicted Extinction Coefficients to Yates and Taylor Extinction Coefficients Measured in a 16.25 km Sea Level Path

TABLE VII

COMPARISON OF ESTIMATED ATTENUATION WITH MEASURED ATTENUATION

REF NO.	TEMP °C	RELATIVE HUMIDITY %	RANGE, km	NUCLEATION DISTRIBUTION, $\frac{C}{C+M}$	SPECTRAL BANDLIMITS, MICROMETERS	Y & T MEASURED AVERAGE ATTEN %	ESTIMATED AVERAGE ATTEN %	$\frac{100\,(E-(Y\,\&\,T))}{(Y\,\&\,T)}$ %
2	3.3	66	5.5	0.35	2.87-5.07	65.1	65.4	+0.4
					3.32-4.92	57.6	58.9	+2.3
					3.39-4.09	35.4	32.5	-8.2
3	17.8	51	5.5	0.60	2.87-5.07	63.0	64.5	+2.4
					3.32-4.92	51.8	56.1	+8.4
					3.39-4.09	24.0	27.1	+12.9
					8.00-11.0	30.7	26.9	-11.2
					8.50-11.5	26.2	25.5	-2.7
					8.50-11.0	25.1	23.3	-7.6
					8.85-9.35	19.7	19.6	-0.5
6	20.6	53	16.25	0.05	2.87-5.07	81.3	79.9	-1.7
					3.32-4.92	74.6	73.5	-1.5
					3.39-4.09	50.6	51.2	+1.2
					8.00-11.0	62.1	54.2	-12.7
					8.50-11.5	61.1	52.6	-13.9
					8.50-11.0	58.0	50.6	-12.8
					8.85-9.35	50.2	48.3	-3.8
7	23.3	32	16.25	0.10	2.87-5.07	88.8	93.9	+5.7
					3.32-4.92	84.3	91.8	+8.9
					3.39-4.09	68.2	84.9	+24.5
					8.00-11.0	95.8	84.9	-11.4
					8.50-11.5	96.1	84.0	-12.6
					8.50-11.0	95.4	83.3	-12.7
					8.85-9.35	90.6	83.0	-8.4

can lead to large discrepancies in the shape of the spectral extinction coefficient functions. The differences between measured and estimated transmission for reference samples 2, 3 and 6 are almost all within the experimental error of the original measured data. The last column of Table VII is relative discrepancy in the estimate of total atmospheric absorption.

One possible reason for discrepancy in the results may be the water vapor normalization used by Altshuler[30]. He used Yates and Taylor run 70 data (reference sample 3 in this appendix) to normalize the water vapor absorption curves 9.1 to 15 micrometers. He removed the aerosol contribution to absorption in the data by assuming a uniform "scattering" coefficient of 0.03/km. Figure 60 indicates that the actual extinction coefficient is definitely sloping downward as a function of wavelength. The estimating techniques in this paper would indicate a normalizing extinction coefficient of 0.015/km might be a better estimate. Had an extinction coefficient of 0.015/km been used, then the discrepancies shown for the longer wavelength bands in the last column of Table VII would be smaller.

The data for reference samples 3 and 6 were measured on the same day, yet, two wicely different nucleation distribution ratios are indicated. This implies that the distribution of condensation nuclei can change radically over short distances in time and space. The combined fit for 3 to 5 micrometer band data vs. 8 to 14 micrometer band data for reference samples 3 and 6 could have been improved by abandoning the extinction coefficient slope criterion of Section I.1.6 and increasing the nucleation distribution ratio above 0.60 for reference sample 3 and reducing it below 0.05 for reference sample 6.

The largest difference in measured and estimated attenuation is in the high humidity, 16.25 km path sample. This discrepancy is unfortunate since this is the case of especial interest. Very little data is available for this type of circumstance and not all which has been reported in the literature has been reduced for easy comparison.

There are many possible causes for the discrepancies in Table VII. The assumed nucleation particle distribution may be incorrect, there may have been measurement errors in the original data due to the high attenuation in the path, or the assumed particle growth rate water accretion with increasing relative humidity may be incorrect, etc. Additional comparison with field data would be required to indicate the correct answer.

I.1.8 COMPOSITION OF THE ESTIMATE

The relative importance of each component of the total transmission estimate is given in Table VIII. The table shows clear air absorption for each sample and band limit based on Altshuler's method. The aerosol extinction assumes that there is no gas or water vapor absorption, i.e., it is pure aerosol extinction. Aerosol absorption indicates the fraction of the incident energy on the aerosol particles in the path which is directly absorbed by the liquid water in the particle. The ratio is aerosol absorption to total aerosol extinction may be obtained by dividing aerosol absorption given in Table VIII by the corresponding aerosol extinction. For the two long path cases, the portion of the total transmission represented by aerosol extinction is quite large, particularly in reference sample 7 where the relative humidity is high.

TABLE VIII

COMPOSITION OF ESTIMATED AVERAGE ATTENUATION

REF NO.	TEMP. °C	RELATIVE HUMIDITY %	RANGE, km	NUCLEATION DISTRIBUTION, $\frac{C}{C+M}$	SPECTRAL BANDLIMITS, MICROMETERS	ESTIMATED AVERAGE ATTENUATION %	ALTSHULER CLEAR AIR ATTENUATION %	AEROSOL EXT. %	AEROSOL ABSORPTION %
2	[illegible].3	66	5.5	0.3[illegible]	2.87-5.07	65.4	55.2	22.9	4.5
					3.32-4.92	58.9	47.1	22.3	3.0
					3.39-4.09	32.5	12.1	23.2	3.3
3	17.8	51	5.5	0.60	2.87-5.07	64.5	58.6	13.7	2.6
					3.32-4.92	56.1	49.4	13.2	1.6
					3.39-4.09	27.1	15.2	14.0	1.8
					8.0-11.00	26.9	20.5	8.[illegible]	1.9
					8.5-11.50	25.5	19.1	7.8	2.1
					8.5-11.00	23.3	16.7	7.9	1.9
					8.85-9.35	19.6	12.3	8.4	1.8
6	20.6	53	14.25	0.05	2.87-5.07	79.9	69.5	34.2	6.7
					3.32-4.92	73.5	59.6	34.4	4.6
					3.39-4.09	51.2	25.4	34.6	5.2
					8.0-11.00	54.2	36.[illegible]	28.4	6.1
					8.5-11.50	52.6	34.6	27.5	6.6
					8.5-11.00	50.6	31.3	28.0	6.1
					8.85-9.35	48.3	26.8	29.5	5.8
7	23.3	82	16.25	0.10	2.87-5.07	93.9	72.7	77.8	25.4
					3.32-4.92	91.8	63.0	77.8	18.9
					3.39-4.09	84.9	30.5	78.3	20.7
					8.0-11.00	84.9	44.4	72.8	25.2
					8.5-11.50	84.0	43.1	71.8	26.8
					3.5-11.00	83.3	39.4	72.4	25.4
					8.85-9.35	83.0	34.0	74.2	24.3

I.1.9 CONCLUSIONS

This Appendix has compared atmospheric attenuation estimates computed by relatively unsophisticated techniques with field measured data and found remarkably good agreement. The agreement is sufficiently good to provide a base for estimating infrared equipment performance under adverse environmental conditions -- but without fog -- through approximately horizontal paths near sea level. The results have also tended to confirm Barnhardt and Streete's contention that most nucleation particle density distributions can be thought of as a combination of two limiting distributions, a continental distribution and a maritime distribution. The high aerosol absorption near 10 micrometers emphasizes Carlon's thesis that this contributor to signal energy loss is underrated by most workers in infrared. The results show that relative humidity is as important as absolute humidity for estimating infrared transmission.

The shapes of the spectral extinction curves have been very instructive. They indicate that aerosol extinction at 2 micrometers and 10 micrometers can be equal -- or very different. They also indicate that aerosol extinction at about 10 micrometers under "clear" conditions is little affected by the particle distribution.

The very steep increase in aerosol extinction at wavelengths longer than approximately 11 micrometers may explain why the spectral band-limit optimization predictions based on field measured data tend to be near 9 to 11 micrometers while those based on gas and water vapor absorption only tend to have a "soft" long wavelength limit.

The results also indicate the need, direction and technical requirements for future field measurements of atmospheric attenuation over horizontal, near sea level paths.

I.1.10 EQUATIONS FOR ESTIMATING AEROSOL EXTINCTION AND ABSORPTION

1. Equation of nucleation particle distribution (Ref. 34)

$$N_T(r_o) = \frac{0.6258\ R_N}{r_o^4} + \frac{0.7850\ (1 - R_N)\ e^{-0.772 r_o}}{r_o} \qquad (133)$$

where

$N_T(r_o)$ = the total number of particles in an interval dr_o at a particle radius r_o, $cm^{-3} \cdot \mu m^{-1}$.

r_o = nucleation particle radius, micrometers

R_N = $\dfrac{\text{Fraction of particles from continental distribution}}{\text{Fraction of particles from continental distribution} + (1 - \text{fraction continental}) \text{ particle in maratime distribution}}$

2. Growth factor due to relative humidity (Ref. 34)

$$F = 1 - 0.9 \ln\left(1 - \frac{R.H.}{100}\right) \qquad (134)$$

where

F = particle growth factor due to accretion of water

R.H. = relative humidity, percent

3. Particle index of refraction (Refs. 34, 36, 38)

$$n(\lambda) = 1.54 + n_w(\lambda) \ln\left(1 + \frac{R.H.}{100}\right) \qquad (135)$$

$$n'(\lambda) = n'_w(\lambda)$$

where

$n(\lambda)$ = real index of particle at wavelength λ

$n_w(\lambda)$ = real index of water at wavelength λ

1.5% = assumed real index of nucleation particle

$n'(\lambda)$ = imaginary index of particle at wavelength λ

$n'_w(\lambda)$ = imaginary index of water at wavelength λ

λ = wavelength of radiant energy, micrometers

4. Spectral extinction, absorption, and scattering coefficients (Ref. 36)

$$\sigma_{ext}(\lambda) = 10^{-3} \int_{r_o=r_1}^{r_o=r_2} N_T(r)\, C_{ext}(r, \lambda)\, dr \qquad (136a)$$

$$\sigma_{abs}(\lambda) = 10^{-3} \int_{r_o=r_1}^{r_o=r_2} N_T(r)\, C_{abs}(r, \lambda)\, dr \qquad (136b)$$

$$r = r_o F; \quad dr = dr_o F$$

$$r_1 = 0.1 \text{ micrometer}; \quad r_2 = 20 \text{ micrometer}$$

$$\sigma_{scat}(\lambda) = \sigma_{ext}(\lambda) - \sigma_{abs}(\lambda)$$

where

σ_{ext}, σ_{abs} and σ_{scat} = extinction, absorption, and scattering coefficients, respectively, km^{-1}

$C_{ext}(r, \lambda)$ and $C_{abs}(r, \lambda)$ = effective extinction and absorption cross sections, respectively, to radiation of wavelength λ of a particle of radius r, μm^2

10^{-3} = factor to convert units of σ to km^{-1};

km^{-1} = $cm^{-3} \cdot \mu m^{-1} \times \mu m^2 \times \mu m \times 10^{-3}$

5. Extinction and absorption cross section approximations (Ref. 36)

$$C_{ext}(r, \lambda) = \pi r^2 \left\{2 - 4e^{-Z} \cos(\beta) \sin(\rho - \beta)/\rho + \left[\cos(\beta)/\rho\right]^2 \left[\cos(2\beta) - \cos(\rho - 2\beta)\, e^{-Z}\right]\right\} \quad (137a)$$

$$C_{abs}(r, \lambda) = \pi r^2 \left\{1 - \frac{e^{-2Z}}{Z} + \frac{(e^{-2Z} - 1)}{2Z^2}\right\} \quad (137b)$$

$$\rho = \frac{4\pi r}{\lambda}\left[n(\lambda) - 1\right]$$

$$Z = \rho \frac{n'(\lambda)}{\left[n(\lambda) - 1\right]}$$

$$\beta = \text{ATAN}\left\{\frac{n'(\lambda)}{\left[n(\lambda) - 1\right]}\right\}$$

6. Corrections to cross section approximations (Refs. 35, 37)

a. $\rho \leq 5(n - 1)$ no correction necessary

$$C_{ext_a}(r, \lambda) = C_{ext}(r, \lambda) \tag{138a}$$

$$C_{abs_a}(r, \lambda) = C_{abs}(r, \lambda) \tag{138b}$$

b. $5(n - 1) < \rho \leq 4.08$

$$C_{ext_b}(r, \lambda) = [1 + (1 - 1/n)\rho/4.08] C_{ext_a}(r, \lambda) \tag{138c}$$

$$C_{abs_b}(r, \lambda) = [1 + (1 - 1/n)\rho/4.08] C_{abs_a}(r, \lambda) \tag{138d}$$

c. $\rho > 4.08$

$$C_{ext_c}(r, \lambda) = [1 + (1 - 1/n)\ 4.08/\rho] C_{ext_a}(r, \lambda) \tag{138e}$$

$$C_{abs_c}(r, \lambda) = [1 + (1 - 1/n)\ 4.08/\rho] C_{abs_a}(r, \lambda) \tag{138f}$$

7. Attenuation due to extinction, scattering or absorption.

$$A = 1 - \exp\left(R \int_{\lambda_1}^{\lambda_2} \sigma(\lambda)\, d\lambda\right) \tag{139}$$

where

A = fraction of initial signal attenuated

R = range, km

λ_1, λ_2 = wavelength bandlimits, micrometers

APPENDIX II

COMMENTS ON RESOLUTION

II.1 INTRODUCTION

The following paragraphs discuss the concept of resolution and show how resolution is treated analytically.

Historically (Rayleigh) resolution implies the ability to separate two closely spaced point targets. High resolution means they can be separated when close together and the resolution number (e. g., 0.25 mrad) is meant to indicate how far apart two point sources must be to be identified as two separate targets. This type of definition had some meaning when viewing bright sources with the eye aided only by optics and as people began using optics for imaging, high resolution became synonymous with good image quality. (Image quality is the subjective measure that a picture looks good.)

As systems become more involved using film, image tubes, and electronics, the limitations in dynamic range and the ability to arbitrarily adjust clipping level, etc., made this definition lose value. In truth, if two point sources of low intensity (nonsaturating) had been used with the system and adjusted for good unclipped noise, a meaningful measure of noise limited resolution probably would have evolved. Instead, early resolution measurements were made to make equipment look good and used high intensity sources. Apparently, as a result, it was decided that for the early IR imaging systems, where it was easy to build optics so good that the detector aperture limited the resolution, the resolution should be the detector size. While two-point sources, one detector width apart, can never be resolved, this would be a theoretical limit. As the system began to have higher performance demands, the optics, electronics, and display began to have more effect than the detector, but the detector size was

still the accepted definition. In this case, the detector subtense had little to do with image quality, ability to detect, or resolution by old definitions, but it still persisted.

The film people, meanwhile, had gone away from point sources for practical reasons and were concentrating on the AF standard three-bar chart; measuring resolution as the bar spacing for the smallest bars that could be resolved by an observer. Some experimenters (Ref. 39) were measuring limiting resolution for different input signal strengths (contrast) and thereby obtaining a measure of required signal for resolution versus bar size or spatial frequency.

As part of the TV/film effort, O. Schade was developing a complete theory of analysis, prediction, and measurement based upon operation in the spatial frequency domain. He defined a function which related the input/output amplitude response as a function of frequency (normalized to low frequencies) as the sine wave response function. This since has been defined as the modulus of the Fourier transform of the line spread function and called the modulation transfer function(MTF).

Schade discussed spatial integration, noise in the image, and signal response; rigorously showing how "limiting resolution" could be predicted for different target strengths and different systems.

II.2 DEFINITION OF RESOLUTION

As an outgrowth of his analysis and experimentation, Schade (Ref. 4) defined for the National Bureau of Standards a summary number to indicated image quality and therefore resolution. This was defined as the equivalent (noise) bandwidth (N_e) of the (optical) system; $N_e = 2 \int (MTF)^2 df$. Resolution was then defined as $1/N_e$.

A number of parameters exist with potential for defining the resolution of a complete system. Some are defined for the space domain and others in terms of the blur function or an equivalent aperture (diameter) for the blur function. If the complete function is not used, then representative values such as the 90 percent point or 50 percent point on the point or line spread function or the one sigma radius of an approximate Gaussian spot are considered. In the spatial frequency domain, we have the MTF curve and derivatives.

The space domain parameters have the advantage that they have intuitive meaning (impulse response function). By just looking at a spread function, most engineers have a feel for the resolution (r) image quality of the device. Unfortunately, the analysis which predicts blur is not as easy as the equivalent frequency analysis. In addition, when the operator was used as the measuring device, he was more accurate at determining the highest frequency he could resolve than estimating blur diameters. With the increased availability of good microphotometers, the measurement of the line spread function is so standard it makes one ask: "Why not use it as the primary measure?"

The frequency domain parameters all stem from the MTF which is an extremely convenient analytical tool, has been measured by many (controversial) techniques relating system relative response to various input (spatial) frequencies, and is analogous to the frequency response transfer functions used in electrical engineering for years.

The parameter most often used is one point on the MTF curve; the limiting resolution (this point is about the 5 to 10 percent point). No one point on an MTF curve is meaningful unless comparing curves of the same shape, and then any unique point is an indicator. For example, the fact that one MTF curve has a zero point at a single frequency while another is 10 percent, does not in itself indicate that the response of either system

to a single small target corresponding to that frequency would be better or worse. The response to a line source is the inverse Fourier transform of the MTF (actually OTF) and depends mostly on the characteristics of that part of the MTF curve which approaches unity. If the MTF drops sharply at low frequencies and then maintains some level - renormalizing may be called for.

Fink (Ref. 40) recommends that for the limiting resolution you choose the frequency where the observer first starts to see a loss in response, not the point he can just see under some conditions. Fink's suggestion, as well as the 70 percent point tend to measure the size of the flat region of the MTF or the bandwidth of the system. No one would consider specifying electronic amplifiers by the 10 percent response, but the bandwidth or 3 db (70 percent voltage) point is common. The area under the MTF curve and the area between the MTF and eye demand function have been recommended as summary numbers similar to bandwidth. Schade (Refs. 40 and 41) recommends the equivalent noise bandwidth (N_e) which is the integral of the square of the MTF. The equivalent aperture or the reciprocal of N_e (in number of lines) is the definition of resolution coauthor R.L.S* has accepted when a single number is needed to describe the resolution of a well behaved system.

There are many reasons for choosing N_e and $\frac{1}{N_e} = r$. First, Schade and other references (Ref. 42) indicate that for noise-free pictures, N_e correlates with image quality so long as the total MTF curve is monotonically nonincreasing or at least well-behaved (smoothly increasing or decreasing).

P. G. Roetling (Ref. 43) proved that N_e is the frequency domain equivalent of acutance which the optical people have claimed correlates with image quality for a number of years (Ref. 44). Many references (19-20)

*Coauthor F.A.R. refuses to accept a single number for an indication of resolution under any circumstance.

have shown that image quality correlates with the ability of interpreters to find targets, i.e., probability of recognition. The coauthor, R.L.S., showed (Ref. 11) that the probability of detection is a function of N_e.

As a tie to the past (and a heuristically pleasing fact) for an IR system with only the square detector limiting the MTF, r equals the detector angular subtense. In addition, it will be shown that r = 1/N is a convenient analytical tool.

Also, it has intuitive meaning by its relationship to correlation or dependence area (length). If a random scene is input to an imaging system, the system filters the scene and close points are correlated. The degree of correlation is predicted by the autocorrelation function of the filtered random scene and is equal to the inverse Fourier transform of the square of the system OTF. This can often be characterized by $1/N_e$ which is about the 50 percent correlation width.

II.3 RESOLUTION AS AN ANALYSIS TOOL

Schade (Ref. 5) indicated that the equivalent bandwidth (in lines/mrad (N) rather than cycles/mrad (f)) and equivalent aperture (resolution of a component of a system was calculated by

$$N_{ec} = \int (MTF)^2 \, dN = 2 \int (MTF)^2 \, df \tag{140}$$

and

$$r_c = 1/N_{ec} \tag{141}$$

where the subscript c implies component. Furthermore, the system bandwidth and resolution would be calculated in a similar manner. If a system is composed of cascading components which are linear, and space

invariant, then Fourier analysis applies and the OTF of the system is the product of the component OTFs. While this is the correct method of treating resolution, a convenient approximation is suggested and discussed by Schade. He shows that for well-behaved functions

$$\left(1/N_{e\ total}\right)^2 \approx \sum_{all\ c} \left(\frac{1}{N_{ec}}\right)^2$$

or

$$\left(r_{sys}\right)^2 \approx \sum_{all\ c} \left(r_c\right)^2$$

where

$N_{e\ total}$ = the total system bandwidth

N_{ec} = component bandwidth

r_{sys} = total system resolution

r_c = component resolution

APPENDIX III

COMMENTS ON SPATIAL FREQUENCY, FOURIER TRANSFORMS AND MTF

III.1 INTRODUCTION

The concept of spatial frequency is a useful concept but can be confusing when first encountered. This is complicated by the fact that authors switch units at their slightest whim. This appendix will try to clarify the concept of spatial frequency and indicate why different units are used.

III.2 DEFINITION

If any characteristic such as exitance varies in a repetitive manner over a surface, it is said to have a spatial frequency. If it is varying in only one direction and is varying sinusoidally with the distance in that direction, it is said to be a one dimensional sinusoidal pattern of a particular spatial frequency. Similar comments can be said for bar charts in terms of square waves of a particular spatial frequency.

III.3 FOURIER TRANSFORMS AND MTF

By a rather beautiful analysis Fourier showed that any function can be uniquely described either by its value as a function of the independent variable (say x) or by a sum of sinusoidal variations of different frequency (k) and phase. Given a function r(x) the equivalent frequency representation would be its Fourier transform R(k).

In the perfect imaging sensor, a point object has a point image on the display; in short, all images are transmitted through the sensor with perfect fidelity. In real sensors, the images at the display may be

distorted in amplitude, shape, or phase (position), or all three. These distortions are due to finite imaging apertures such as the objective lens, any fiber-optic faceplates, geometrical defocusing, electron scanning beams, finite detector aperture, electrical bandwidth limitations, etc. The effect of these apertures is to smear image detail in a manner analogous to the filtering of electrical signals by electrical filter networks. This analogy can be put to good use.

To illustrate the effect of apertures, consider the point source object of Figure 62. Due to diffraction, chromatic and geometric aberrations, and imperfect focusing, the point will be imaged by the lens as a blur. Similarly, a line source is imaged as a line-spread function as shown in Figure 62. The line-spread case corresponds most directly to the case most commonly encountered in communications systems, wherein the signals vary only in amplitude and time. Where an image is very long in one dimension compared to the other, it can usually be considered a one-dimensional image, varying only in intensity in a single spatial dimension.

In any event, we will, for the moment, consider an aperture to be analogous to a linear electrical filter, except that it may be two-dimensional. Where two dimensions are involved, we will initially assume that the two dimensions are either independent (so that they can be treated separately) or that they possess radial symmetry (so that they become essentially one-dimensional in character). Many of the apertures that appear in nature are found to have a response to several input stimuli acting simultaneously that is identical to the sum of the responses that each stimulus would produce individually. A system of this type is a linear system. The property of linearity leads to an enormous simplification in mathematical description of such phenomena. In particular, it becomes possible to decompose complicated input signals to simpler signals for which the system response is known and then, to find the total response

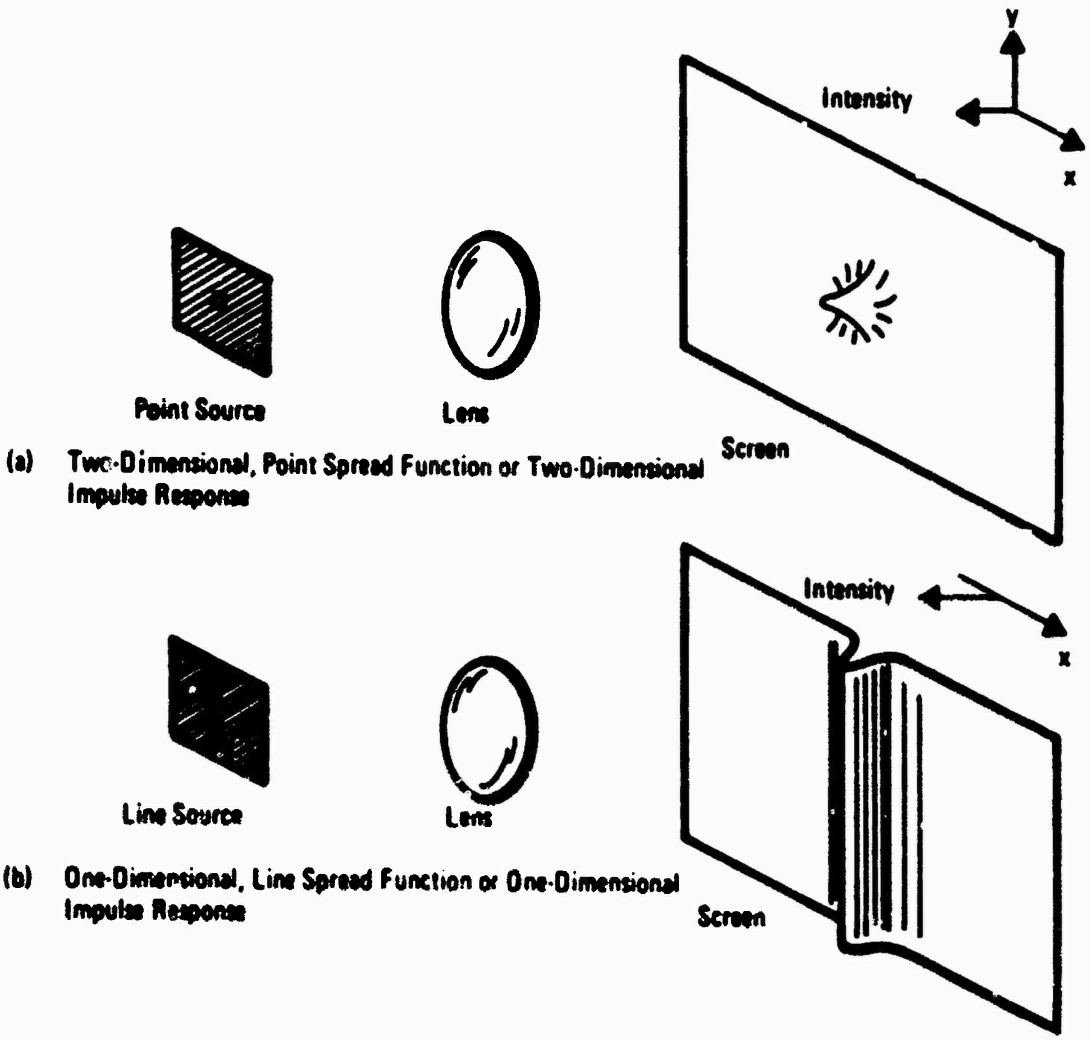

Figure 62. Impulse Response

by summing the individual responses in linear combination. Furthermore, we can then use Fourier analysis in which signals are decomposed to sine and cosine waves.

The statement of linearity implies that the system response to any stimulus can be described by the solution to some appropriate set of simultaneous linear differential equations. The restriction to constant coefficients rules out consideration of linear systems with time or space-varying parameters, but it permits us to apply the principle of superposition.

In general, the linear systems we will deal with are considered to be space and time invariant (sometimes called isoplanatic). By this, it is meant that the system impulse response $r_o(x_1, y_1, \xi, \eta)$ depends only on the distances $(x_1-\xi)$, $(y_1-\eta)$ in which case

$$r_o(x_1, y_1, \xi, \eta) = r_o(x_1-\xi, y_1-\eta) \tag{142}$$

In the case of an imaging system, it is said to be space invariant if the image of a point source changes only in position, but not in functional form, as the image moves about the image plane. In a television sensor, this would imply that corner resolution is the same as center resolution. This is seldom the case, but for analytical purposes, we can divide the image plane into small areas (or isoplanatic patches) within which the system is spatially invariant. The assumption of linearity results in many simplifications.

To proceed, we have observed that image signals in passing through a sensor may be distorted by the various optical elements and reimaging steps involved. Depending on the degree and nature of the distortion, signal strength may be degraded. To analyze these signal effects, we assume that the sensory system is linear in the interval of interest.

Further, as we previously noted, we assume that both the input signal $f(x, y)$ and the system impulse response $r_o(x, y)$ are functions of independent variables x and y and are separable. In this case, we can draw the block diagram of Figure 63 to represent the signal processes. As we have previously observed, the assumption of separability permits us to write the arbitrary functions $g(x, y)$ as

$$g(x, y) = g_X(x) \cdot g_Y(y) \tag{143}$$

and its Fourier transform as

$$F\{g(x,y)\} = F_x\{g(x)\} F_y\{g(y)\} \tag{144}$$

Therefore, the transform is separable into a product of two factors, one a function of f(x) only, and the second, a function of f(y) only. Thus, the process of two-dimensional transformation simplifiers to a succession of more readily calculated and manipulated one-dimensional transforms.

In Fourier analysis, it is convenient to employ a certain set of test signals known as the singularity test functions. The most useful input singularity function is the unit area (or volume) impulse already described as a point image $\delta_o(x, y)$. The system response for this input is designated $r_o(x, y)$. The Fourier transform of the impulse response is designated $R_o(\omega_x, \omega_y)$ and is known as the complex steady-state frequency response. The usefulness of $R_o(\omega_x, \omega_y)$ is that for systems with apertures that are independent in x and y, the response can be measured through use of sinewave image patterns as the input. The output signal amplitude is then measured, and a plot of these amplitudes (as the pattern frequency is varied) represents the magnitude of $R_o(\omega_x)$ or $R_o(\omega_y)$. This function is variously known as the sinewave response or the modulation transfer function (MTF).

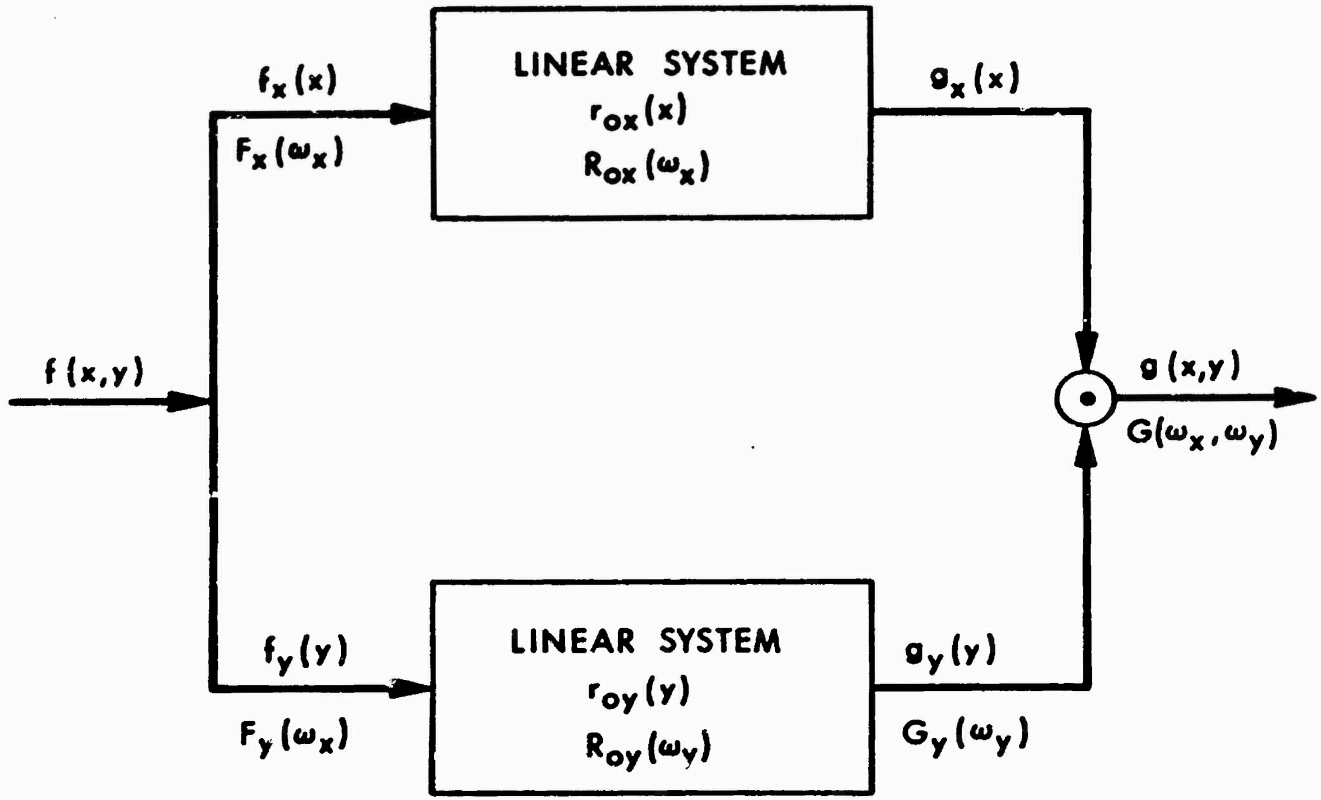

Figure 63. Signal Processor Block Diagram

The MTF or modulation transfer function is the primary method of describing the loss of resolving power due to finite sensor apertures. (See Figure 64.) MTF, in the communications sense is synonomous with the magnitude of the sensor's complex steady-state response $R_o(\omega)$ where

$$R_o(\omega) = |R_o(\omega)| \exp\left[j \phi(\omega) \right] \tag{145}$$

In the above, $\phi(\omega)$ represents a phase or position shift and has been designated by the international Commission for Optics (ICO) as the phase transfer function. The ICO also refers to $R_o(\omega)$, the complex steady-state response as the optical transfer function which seems only partially appropriate to sensors. The ICO recommends changing the word function to curve when referring to curves representing the functions. Also, for specific values of the function at a given frequency, the word function is replaced by factor; e. g., the modulation transfer factor.

MTF is also synonymous with sine wave amplitude response. In the testing of sensors, sine wave amplitude response can be directly measured although the machinery required can be quite complex and costly. Thus, in current practice, it is more usual to employ bar patterns in making tests. The quantity measured is then the square wave amplitude response $|R_{SQ}(\omega)|$. If $R_o(\omega)$ is known, then $R_{SQ}(\omega)$ can be determined directly from

$$R_{SQ}(\omega) = Sq(\omega) \cdot R_o(\omega) \tag{146}$$

where $Sq(\omega)$ is the Fourier spectrum of a square wave wavetrain.

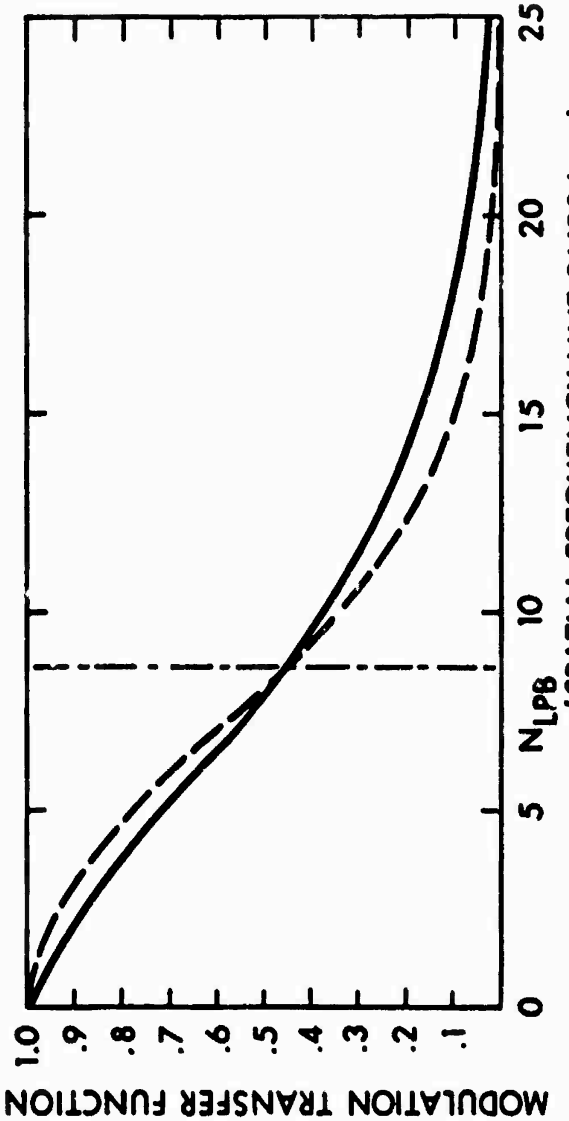

Figure 64. Error Curve (---) Fit to Measured (—) MTF of a 3-Stage Image Intensifier and Equivalent Bandwidth, (N_{LPB}) of the Error Curve

III.4 UNITS OF SPATIAL FREQUENCY

If the spatial coordinates are length such as millimeters then the natural units for spatial frequency are cycles per millimeter. Historically, people have preferred to think in terms of line pairs per millimeter. In photography where the size of the film could be varied and the fineness of the grain was of interest, lp/mm was indeed the logical unit.

For optical lenses lp/mm at the focal plane is also a logical unit. However, if a lens is used as a telescope then the interest is what angular variations in object space can be resolved and cycles per mrad or line pairs per mrad are the most useful. Of course, the focal length of the lens quickly converts one spatial frequency unit to the other.

For IR image systems, which are treated like a total telescope, cycles per mrad were also chosen as the most natural.

For radiometry of distant scenes such as sky backgrounds and the like, the only sensible unit was cycle/angle, e. g., cycles per mrad.

For a photosurface, cycles per millimeter at first appears logical. Since, however, there are going to be many images in the system all with different scale factors, e. g., an optical image on an intensifier reimaged onto a different sized vidicon and then displayed on a large display, a confusion of units could get involved. The answer has been to introduce lines per picture height. Using picture height as the normalizing factor, the effect of each component can immediately be compared with all others and the component MTF's can be a characteristic of the component yet still directly multiplicative with all other component MTF's. If you convert to angle, the numbers only relate to that system.

It is recommended that f be used for temporal frequency (Hz) and k be used for spatial frequency either lp/mm or lp/mrad, and that N be used for spatial frequency in lines per picture height (or width shown by subscript). N can be either for an angular picture height or a linear picture height with equal success.

It is anticipated that the largest confusion results from the choice of lines rather than line pairs. Part of the justification for lines may have been a confusion or interest in TV (raster) lines rather than discussing line pairs. In any case. TV people tend to work in TV lines or just lines and an error of a factor of two is often the result when they mix with other fields reporting in line pairs or conversely.

APPENDIX IV

THE RELATIONSHIP BETWEEN ΔT AND ΔH FOR AN IMAGING SYSTEM

IV.1 INTRODUCTION

The signal for an IR imaging system is caused by the variations in the irradiance (ΔH) on the entrance aperture of the system. While these variations may be caused by other phenomenon (reflections), it is convenient and historically meaningful to consider them to be caused by the variations in temperature (ΔT) of blackbody sources. In the laboratory, targets can be constructed and used at short ranges so that analysis based upon ΔT predicts the results. In the field, systems with the same spectral response can be compared based upon relative ΔT performance and indeed historically a feeling for the required ΔT performance has become established although the apparent ΔT of the scene objects varies from night to night, season to season, location to location, and atmosphere to atmosphere. Since it appears that what changes from time-to-time is ΔT (and indeed we know this is the driving function by observing diurnal effects when many objects reverse their temperature relative to ambient) we become tuned to good IR and bad IR nights based upon the atmospheric transmission and ΔT we would expect from natural objects.

IV.2 ANALYSIS

For the no atmosphere condition the viewing a lambertian blackbody (emissivity = 1) of temperature T, the spectral irradiance at the system aperture can be related to the spectral exitance of the blackbody.

Let:

Parameter	Definition	Typical Units
λ	The wavelength of the radiation	micrometers
T	The temperature of the blackbody	Kelvin
$W(\lambda,T)$	The spectral exitance of a blackbody	watts/cm^2/micrometer
δ	The field-of-view over which the systems is collecting radiation usually the small instantaneous field of view of the sensor defined by the detector	mrads
A	The area of the collecting aperture	cm^2
R	Range from the sensor to the target	cm
$H(\lambda,T)$	The spectral irradiance on the aperture from within a system field of view of δ	watts/cm^2/micrometer

Assuming small angles for δ, the area of the blackbody contributing photons is $(R\delta)^2$ and the solid angle subtended by the system optics is $(A/R)^2$. Therefore, with a lambertian source of temperature T

$$H(\lambda,T) = \frac{W(\lambda,T)}{} \delta^2 \qquad (147)$$

The signal to be generated is the result of varying the temperature of the source from T to $T+\Delta T$ or equivalently to viewing a separate source of $T + \Delta T$ and noting the change in $H(\lambda,T)$, $\Delta H(\lambda,T)$. Since $W(\lambda,T)$ is a Continuous function of T given for a blackbody by the Planck function

$$W(\lambda_1 T) = \frac{2\pi\, hc^2}{\lambda^5 (e^{hc/\lambda kT} - 1)} \tag{148}$$

where:

Parameter	Definition	Units
h	Planck's Constant = 6.62×10^{-34}	watt/sec^2
c	Velocity of Light = 3×10^{10}	cm/sec
k	Boltzman's Constant = 1.38×10^{-23}	watt/-sec/K

The change in $W(\lambda,T)$, for a small change in T by assuming small incremental values for the differential can be directly calculated. That is

$$\Delta W(\lambda,T) \approx dW(\lambda,T) = \frac{\partial W(\lambda,T)}{\partial T}\, dt \approx \frac{\partial W(\lambda,T)}{\partial T}\, \Delta T \tag{149}$$

or equivalently

$$\Delta W(\lambda,T) = W'(\lambda,T)\Delta T \tag{150}$$

where

$$W'(\lambda,T) = \frac{W(\lambda,T)}{\partial T} = \frac{2\pi hc^2}{5} \quad \frac{e}{(e^{hc/\lambda kT}-1)^2} \quad \frac{hc}{\lambda kT^2} \tag{151}$$

$$W'(\lambda,T) = W(\lambda,T) \frac{e^{hc/\lambda kT}}{e^{hc/\lambda kT}-1} \quad \frac{hc}{\lambda kT^2}$$

which for values of interest near $\lambda = 10\mu$, $T = 300^{o}K$ is approximately given by

$$W'(\lambda,T) = W(\lambda,T) \quad \frac{hc}{\lambda kT^2}$$

$$\approx W(\lambda,T) \frac{1.44 \times 10^4}{\lambda T^2} \tag{152}$$

IV.3 CONCLUSION

Accurate calculation of $W'(\lambda,T)$ is tedious without a computer therefore Figures 61 and 62 are considered useful. Figure 65 presents $W'(\lambda,T)$ vs wavelength for a 300K blackbody. Figure 66 presents $W'(10,T)$ (normalized to $W'(10,300)$) vs temperature. From Figure 65, it can be seen that $W'(\lambda,T)$ for a system operating against a 300K ambient and with a spectral passband from 8.5 to 11.5μ would be viewing a source radiating approximately 3×10^{-5} watts/cm^2-stradian for each 1 K temperature difference near 300K. For a typical system with an instantaneous field of view (δ) of 1 mrad, a zero atmosphere irradiance of

$$\Delta H(\lambda,T) = 10^{-11} \text{watts/cm}^2 \text{ per K} \tag{153}$$

would occur.

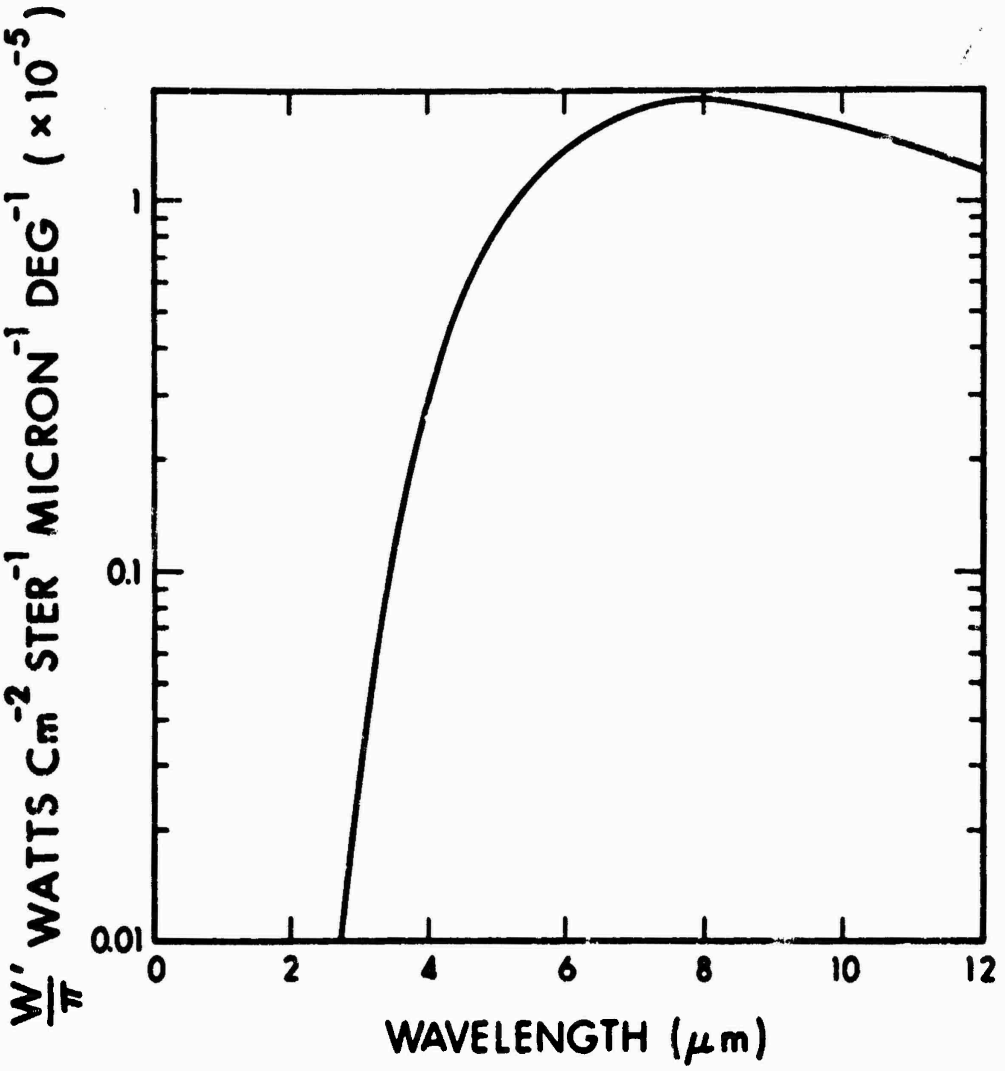

Figure 65. $\frac{W'}{\pi}(\lambda,T)$ for T + 300K

39750

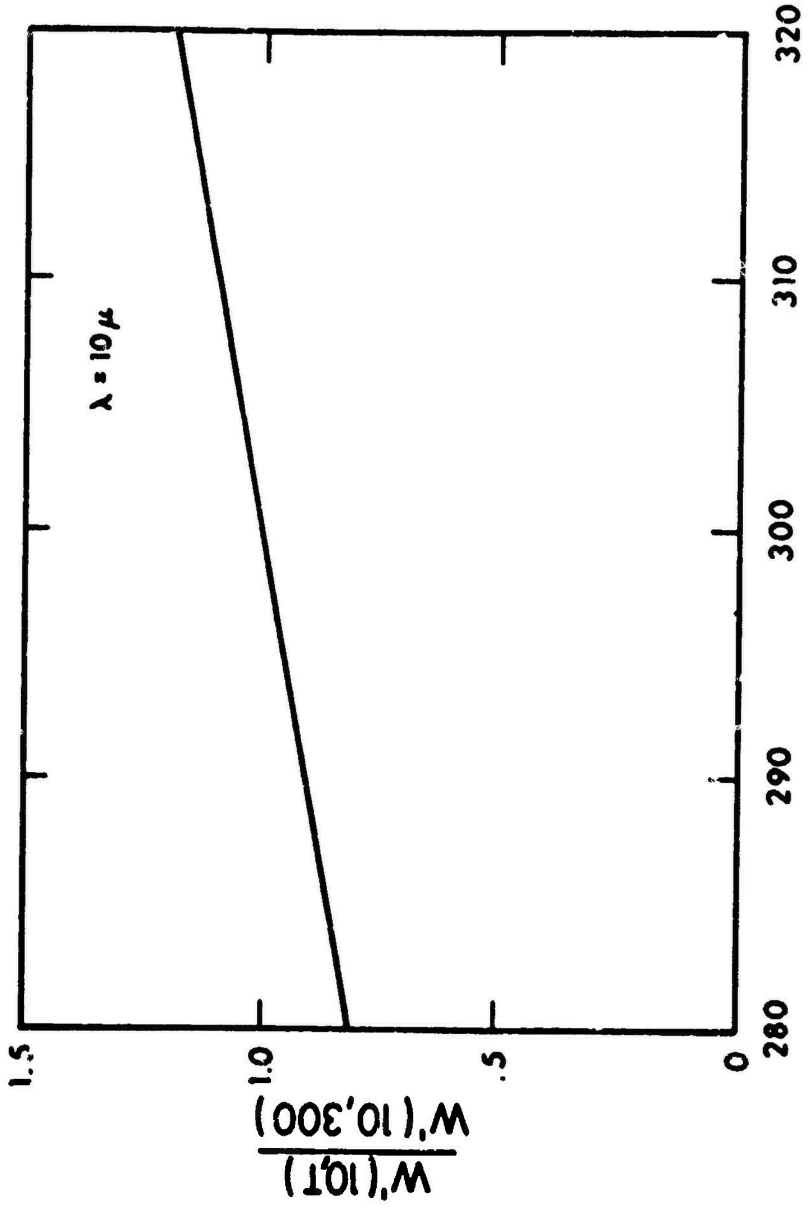

Figure 66. Normalized W' versus T for λ = 10μ

It is interesting that if the ambient temperature changes 10K, $\Delta H(\lambda,T)$ per 1 K would only change by a factor of 10 percent. (See Figure 66). It is not known, however, how actual ΔTs of interest vary with ambient temperature. Therefore, they may compensate for this condition or aggravate it. However, it does not appear very significant.

APPENDIX V

FLIR SENSOR PERFORMANCE EQUATION DERIVATION

INDEPENDENT OF TV ANALYSIS

V.1 INTRODUCTION

A real-time infrared imaging sensor is an electro-optical system which optically scans the instantaneous field of view of a detector array over the total field of view of the sensor in order to generate video information. While the detector elements are continuously detecting the total radiation received in their fields of view as the scene is scanned, they are ac coupled in the electronics and, therefore, only variations in the energy received are represented in the video signal generated.

By synchronously controlling the luminance of a display with the detector signals, a picture is generated where the variations in luminance represent the variations in received power. When scanned at 15 to 30 frames a second, the variations provide a real time picture, with essentially zero storage, which is similar to the daytime scene.

The signal is, therefore, the result of variations in radiant emittance of one area of the scene compared to another which could be caused by either differences in temperature or emissivity (assuming that low emissivity objects reflect a different temperature area, e.g., the sky). It is convenient and historically accepted to discuss the signal as occurring due to temperature variations only. Assuming blackbody radiation and small signals around an ambient (usually 300K) the change in spectral radiant emittance is proportional to the change in temperature.

It should be recognized that two types of equations and parameters exist: one set for analysis of an existing system and the other set for showing tradeoffs and, therefore, aiding the synthesis of a system. The following analysis is to develop an equation to aid synthesis; a much more straightforward approach with interrelated parameters and providing less insight would be used for analysis. An equation for analysis with an abbreviated derivation is given in subsection V.5.

To this end, an equation will be derived between various parameters of the IR sensor. Then the parameters will be grouped to show the relationship between the performance of the sensor, the design adjustable parameters, the design efficiency parameters, and the parameters which are affected by the choice of spectral region.

V.2 DEFINITION OF SYMBOLS

The following set of parameters will be used throughout this analysis. A number of the parameters (shown below with an *) are always a function of either wavelength, λ, or the spectral region, $(\Delta\lambda)$. Spectral values for these parameters will be used until the final equations and then effective values over a $\Delta\lambda$ are used to avoid integrals in the final result. Since it will also be obvious which is intended, no subscripts are added and, therefore, the same symbol may represent either value.

- α = field-of-view of the sensor in the direction of scan
- β = field-of-view of the sensor normal to the direction of scan
- a = instantaneous field-of-view of a detector in the direction of scan
- b = instantaneous field-of-view of a detector normal to the direction of scan
- r_a = resolution of the sensor in the direction of scan
- r_b = resolution of the sensor normal to the direction of scan

T = the average time between scanning points is the FOV (including aver scan)

$\dot{F}$ = frame rate of the sensor equals T^{-1}; not flicker rate

NET = sensor noise equivalent temperature. It is the temperature difference between two large targets which generate a per frame, per detector size resolution element, signal-to-noise ratio of unity at the detector output. It is determined as the temperature difference between two large targets which will provide an electrical peak signal at the detector output equal to the rms noise in a bandwidth corresponding to the detector size. This bandwidth is normally dc to $1/2T_d$.

T_d = the detector dwell time, the time that an image point spends on a detector

Δf = noise bandwidth = $1/2T_d$ by definition

f_ℓ = focal length of IR telescope

f/No. = f/number of IR telescope

d = diameter of the IR telescope entrance aperture

n = number of independent detector elements with field a x b

η_r = resolution efficiency; the effective resolution of the sensor in relation to the detector size

η_d = the ratio of entrance pupil diameter to entrance aperture diameter, aperture efficiency

η_o = optical efficiency; includes both normal transmission losses and blocking at the aperture stop

η_{sc} = scan efficiency; the (minimum) dwell time of the sensor divided by the maximum dwell time possible, i.e., the dwell time of a 100 percent duty cycle zero turn-around, linear scan

η_{cs} = cold shielding efficiency for background limited systems; the degree on which the signal-to-noise ratio of the sensor is optimized with regard to shielding against unwanted background photons

* η_q = quantum efficiency for background limited systems; the effective quantum efficiency of a photodetector

* η_a = atmospheric efficiency; the percent transmission over the desired range

* D^* = detector detectivity; with the final shielded detector receiving radiation as it would in the actual system (f/No. cone), D^* is the per cycle (electrical bandwidth), per unit area signal-to-noise ratio for 1 watt input. It is assumed that the S/N is inversely proportional to

the square root of the detector area. D* is a function of the electrical frequency of test as well as the optical frequency of test (wavelength).

* D^{**} = detector detectivity of a theoretically perfect detector of unity quantum efficiency receiving 2π steradians of background radiation.

* W = spectral radiant emittance of a blackbody of temperature, T

W' = $\partial W/\partial T$, the partial derivative with respect to temperature of the spectral radiant emittance of a blackbody radiator

T = absolute temperature

ΔT = a small change in temperature

ΔW = a small change in spectral radiant emittance

λ = wavelength of received radiation

P = sensor performance

N = number of azimuth scans of an individual detector element per frame in a rectangular raster system

V.3 ANALYSIS

The change in spectral radiant emittance from one target to the next for a ΔT between the targets is, for small signals, approximately

$$\Delta W = \frac{\partial W}{\partial T} \Delta T = W' \Delta T \tag{154}$$

Assuming that the targets are large area lambertian radiators, the change in power on the detector can be written as

$$\left(\frac{\Delta W}{\pi}\right) \cdot \left(\frac{\pi d^2}{4} \eta_d^2 \eta_o \right) \cdot (ab) \eta_a = \Delta \text{ Power} \tag{155}$$

It is interesting that this is independent of range (R) except for η_a, since the area of the source (target) which is effective is abR^2 and the number of steradians of power collected is $\pi d^2/4R^2$.

Since the $D^*/(abf_\ell^2\,\Delta f)^{1/2}$ is the signal-to-noise out of the detector for 1 watt input, we can write the signal-to-noise ratio generated by scanning the above target as

$$S/N = \int_{\Delta\lambda} \frac{D^*}{(abf_\ell^2\,\Delta f)^{1/2}} \times \Delta W \frac{(d\eta_d)^2}{4}\ \eta_o\,\eta_a\,ab\,d\lambda \tag{156}$$

and by setting this signal to noise to unity and substituting for ΔW, we have the ΔT which corresponds to the NET

$$NET = \int_{\Delta\lambda} \frac{4f_\ell\,(\Delta f)^{1/2}}{(d\,\eta_d)^2\,(ab)^{1/2}\,\eta_o\,\eta_d\,D^*\,W'}\,d\lambda \tag{157}$$

from the earlier definition of NET:

$$\Delta f = 1/2T_d \tag{158}$$

T_d can be determined by the scanning parameters and is generally a function of the position in the field as well as the type of scan.

The minimum time an element takes to scan a point in the image is then

$$T_d = \frac{nab}{\omega\beta\dot{F}}\,\eta_{sc} \tag{159}$$

Substituting Eq. 159 into 158 and Eq. 158 into 157 provides Eq. 160

$$NET = \int_{\Delta\lambda} \frac{2\sqrt{2\,f_\ell}\,(\omega\beta\dot{F})^{1/2}}{(d\,\eta_d)^2\,ab\,\eta_o\,\eta_a\,(n\,\eta_{sc})^{1/2}\,D^*\,W'}\,d\lambda \tag{160}$$

In order to reduce the number of interrelated parameters and provide better insight, we continue. By definition

$$f/No. = f_e/d\ \eta_d$$

therefore,

$$NET = \frac{(\alpha\beta\dot{F})^{1/2}}{ab} \frac{1}{\eta_d\ dn^{1/2}} \int_{\Delta\lambda} \frac{2\sqrt{2}\ f/No.}{\eta_o\ (\eta_{sc})^{1/2}\ D^*\ W'\ \eta_a} d\lambda \qquad (161)$$

Although detector instantaneous field of view is an important parameter for determining NET, it is not a measure of the sensor spatial resolution. Many potential measures of resolution exist, however, for the present, it is adequate to state that it contributes to the total system resolution and therefore affects the operator's ability to detect and recognize targets. Without further justification at this time, r_a will be defined in terms of the sensor modulation transfer function (M_a) and spatial frequency, f, as

$$r_a = \left[2 \int M_a^2\ df\right]^{-1} \qquad (162)$$

Similarly,

$$r_b = \left[2 \int M_b^2\ df\right]^{-1} \qquad (162a)$$

when M_b is the sensor resolution normal to the direction of scan. Sensor resolution is related to the detector size by the resolution efficiency, η_r,

$$\eta_r = \frac{ab}{r_a\, r_b} \tag{163}$$

The resolution efficiency, η_r, is a measure of how closely the sensor resolution matches the detector size. In the ideal case, $\eta_r = 1$, the detector size determines the resolution, with all other system components designed such that they do not degrade the detector resolution.

While NET is a common parameter for defining sensor sensitivity because it is relatively easy to objectively measure, it should never be considered independent of $\dot{F}$ or $\Delta\lambda$. It has been shown that because the eye/brain will spatially and temporally integrate, the system sensitivity is proportional to $NET/(\dot{F})^{1/2}$. It must always be remembered that sensitivity in terms of temperature is a convenience that has meaning only when considering the spectral response. We will now regroup the NET equation parameters to show a more intuitively meaningful relationship.

$$(\alpha\beta\dot{F})^{1/2}\, \frac{1}{r_a\, r_b\, NET} = \frac{dn}{\sqrt{2}}^{1/2} \times \eta_d\, \eta_o\, \eta_{sc}^{1/2}\, \eta_r \times \int_{\Delta\lambda} \frac{D^*\, W'\, \eta_a\, d\lambda}{2\ f/No.} \tag{164}$$

To be completely rigorous η_o or $\eta_o(\lambda)/\eta_o$ should be included in the integrand but generally an effective value for η_o can be determined.

Equation 164 is the general equation specifying FLIR Sensor performance and it applies to background limited as well as nonbackground limited systems. For the case of BLIP operation

$$D^* = D^{**}\ (2\ f/No.)\ \eta_q^{1/2}\ \eta_{cs} \tag{165}$$

where D** is the detectivity of a theoretically perfect detector. For BLIP operation, Eq. 165 can be substituted into 164 with the resulting performance equation

$$(\alpha\beta\dot{F})^{1/2} \frac{1}{r_a\ r_b\ NET} = dn^{1/2}\ \eta_d\ \eta_o\ \eta_{cs}\ \eta_{sc}^{1/2}\ \eta_q^{1/2}\ \eta_r \times \int_{\Delta\lambda} \frac{D^{**}\ W'\ \eta_a\ d\lambda}{\sqrt{2}} \qquad (166)$$

V.4 CONCLUSIONS

It has been shown that by a judicious selection and definition of parameters the sensitivity equation for a real time thermal imaging sensor can be presented so that the real sensor tradeoffs are apparent.

All performance parameters have been grouped as a major parameter as

$$P = (\alpha\beta\dot{F})^{1/2} \frac{1}{r_a\ r_b\ NET} \qquad (167)$$

this parameter indicates how resolution can be traded off with sensitivity and field of view.

All of the strongly wavelength dependent parameters are grouped in a major parameter

$$R = \int_{\Delta\lambda} \frac{D^{**}\ W'\ \eta_a\ d\lambda}{\sqrt{2}} \qquad (168)$$

so that wavelength optimization can be systematic. It must be remembered, however, that for strongly diffraction limited systems, η_r is also a function of wavelength and η_d.

The parameters which reflect design efficiency are grouped in a major parameter

$$E = \eta_o \, \eta_{cs} \, \eta_{sc}^{1/2} \, \eta_q^{1/2} \, \eta_r \, \eta_d \tag{169}$$

In general, when this term is not maximized, it must be made up by a larger system with more detectors. It requires resources to make up for the inefficiency.

The design or complexity parameters are grouped in a major parameter

$$C = Jn^{1/2} \tag{170}$$

This is to indicate that the only real freedom a designer has after he has chosen the wavelength and maximized the efficiency is to vary the aperture or add more detector channels. If more performance is required, so is more complexity. That is,

$$P = CER \tag{171}$$

V.5 EQUATION FOR ANALYSIS

For evaluating a specific design it is more meaningful to use equations that have easily determined (measured) parameters. For completeness, such an equation is presented here with an abbreviated derivation.

By definition, for a 1 watt input at wavelength λ, the signal to noise at the output is

$$(S/N) = \frac{D^*}{(A_d\ \Delta f)^{1/2}} \tag{172}$$

where

A_d = detector area (cm)

Δf = noise bandwidth of test

then using the above plus Eqs. 154, 155 and the definition of NET as ΔT for S/N = 1, we have the desired result

$$NET = \int_{\Delta\lambda} \frac{4(A_d\ \Delta f)^{1/2}}{d^2\ \eta_d^2\ \eta_o\ \eta_a\ ab\ D^*\ W'}\ d\lambda \tag{173}$$

REFERENCES

1. Schade, O. H., Sr., "Image Gradation, Graininess and Sharpness in Television and Motion Picture Systems" Part I: Image Structure and Transfer Characteristics, J. SMPTE, Vol. 56, Feb. 1951; pp. 137-177

2. Schade, O. H., Sr., "Image Gradation, Graininess and Sharpness in Television and Motion Picture Systems" Part II: The Grain Structure of Motion Picture Images, J. SMPTE, Vol. 58, Mar. 1952, pp. 181-222

3. Schade, O. H., Sr., "Image Gradation, Graininess and Sharpness in Television and Motion Picture Systems" Part III: The Grain Structure of Television Images, J. SMPTE, Vol. 61, Aug. 1953; pp. 97-164

4. Schade, O. H., Sr., "A New System of Measuring and Specifying Image Definition," National Bureau of Standards, Cir. 526, Apr. 29, 1954; pp. 231-258

5. Schade, O. H., Sr., "Image Gradation, Graininess and Sharpness in Television and Motion Picture Systems" Part IV, A & B: Image Analysis in Photographic and Television Systems (Definition and Sharpness), J. SMPTE, Vol. 64, Nov. 1955; pp. 593-617

6. Schade, O. H., Sr., "Optical and Photoelectric Analog of the Eye," JOSA, Vol. 46, No. 9, Sept. 1956; pp. 721-739

7. Schade, O. H., Sr., "A Method of Measuring the Optical Sine-Wave Spatial Spectrum of Television Image Display Devices," J. SMPTE, Vol. 56, No. 9, Sept. 1958; pp. 561-566

8. Schade, O. H., Sr., "Modern Image Evaluation and Television (The Influence of Electronic Television on the Methods of Image Evaluation," Applied Optics, Vol. 3, No. 1, Jan. 1964; pp. 17-21

9. Schade, O. H., Sr., "An Evaluation of Photographic Image Quality and Resolving Power," J. SMPTE, Vol. 73, Feb. 1964; pp. 81-119

10. Schade, O. H., Sr., "The Resolving-Power Functions and Quantum Processes of Television Cameras," RCA Review, Sept. 1967; pp. 460-535

11. Worthy, N. H.; Kendall, R. L., et al, Electro-Optical Systems, "High Performance IR Systems Study" (S), Technical Report AFAL-TR-71-285, Jan. 1972

12. Rosell, F. A.; Willson, R. H., "Performance Synthesis (EOS)" Westinghouse Defense and Electronic Systems, Systems Development Division, Baltimore, Maryland, Technical Report AFAL-TR-72-279, Aug. 1972

13. Hodges, J. A., "Infrared Image Test Program Study," Report AFAL-TR-70-269, Aug. 1971

14. Middleton, W. Knowles, "Vision Through the Atmosphere," University of Toronto Press, 1952

15. Hudson, Richard D., Jr., Infrared System Engineering, John Wiley & Sons, Inc., New York, 1969

15. Lawson and Uhlenbeck, "Threshold Signals," MIT Radiation Laboratory Series, McGraw-Hill, New York, 1946; Chapters 8, 9

17. Campbell, F. W., "The Human Eye As An Optical Filter," Proc. IEEE 56, 1968, pp. 1009-1014

18. De Vries, H. L., "The Quantum Character of Light and Its Bearing Upon Threshold of Vision, The Differential Sensitivity and Visual Activity of the Eye," Physica X, 1943; pp. 553-564

19. Blackwell, H. R., "Specification of Interior Illumination Levels," Illuminating Engineering 54, 1959, pp. 317-353

20. Rose, A., "The Sensitivity Performance of the Human Eye on an Absolute Scale," JOSA 38, 1968; pp. 196-208

21. Rosell, F. A., "Electro-Optical Aids for the Eye," July 18, 1969, Westinghouse Electric, Aerospace Division, Baltimore, Md.

22. Coltman and Anderson, "Noise Limitations to Resolving Power in Electronic Imaging," Proc. IRE 48, 1960; pp. 858-865

23. Lavin, Herb; Chapter in L. M. Biberman and S. Nudelman, "Photo-Electronic Imaging Devices," 1970, Plenum Press, New York

24. Johnson, J., "Analysis of Image Forming Systems," Proceedings of Image Intensifier Symposium, Oct. 6-7, 1958, pp. 249-273

25. Schade, O. H., Sr., "Resolving Power Functions and Integrals of High-Definition Television and Photographic Cameras--A New Concept of Image Evaluation," RCA Review, Vol. 32, Dec. 1971; pp. 567-609

26. Marshall, Fitz-Hugh, "Infrared Camera Tube Resolution Curve Transformations," Proc. IRIS, Oct. 1965; pp. 29-32

27. Born & Wolf, Principles of Optics, Macmillan, New York, 1964; pp. 186-187

28. Anding, David, "Band-Model Methods for Computing Atmospheric Slant-Path Molecular Absorption," AAVSO P-2449-1, Infrared Optical and Sensor Laboratory, University of Michigan, Feb. 1967

29. Yates, H. W., and Taylor, V. H., "Infrared Transmission of the Atmosphere," NRL Report 5453, Naval Research, Washington, D.C., 8 June 1960

30. Altshuler, T. L., "Infrared Transmission and Background Radiation by Clear Atmospheres," Report No. 615D199, General Electric Co., Dec. 1961

31. Smithsonian Metereological Tables, 6th Ed., 1963

32. Carlon, H. R., "Infrared Emission by Fine Water Aerosols and Fogs," Applied Optics, Vol. 9, Sept. 1970, pp. 2000-2006

33. Streete, J. L., Applied Optics 7, 1545, 1968

34. Barnhardt, E. A., and Streete, J. L., "A Method for Predicting Atmospheric Aerosol Scattering Coefficients in the Infrared," Applied Optics, Vol. 9, No. 6, June 1970, pp. 1337-1344

35. Van de Hulst, H. C., Light Scattering by Small Particles, John Wiley and Sons, New York, 1957

36. Chu, T. S., and Hogg, D. C., "Effects of Precipitation on Propagation at 0.63, 3.5 and 10.6 Microns," The Bell System Technical Journal, May-June 1968, pp. 723-759

37. Deirmendian, D., Quart. J. Royal Meteorol. Soc. 85, 404, 1959

38. Centeno, M., JOSA 31, 244, 1941

39. Scott, F., "Three-Bar Target Modulation Detectability," Photographic Science and Engineering, 10, 1966; pp. 49-52

40. Fink, "TV Handbook"

41. Schade, O. H., Sr., "Image Gradation, Graininess and Sharpness in Television and Motion Pictures," Part II: The Grain Structure of Motion Picture Images," J. SMPTE, 58, March 1952, p. 191

42. Higgins, G. C.; Lamberts, R. L.; Wolfe, R. N., "Validation of Sine Wave Analysis for Photographic Systems," Optica Acta, 6, 1959, pp. 272-278

43. Roetling, P. G.; Trabka, E. A., and Kinzly, R. E., "Theoretical Prediction of Image Quality," JOSA 58, 1968; pp. 342-346

44. Luxenberg, H. R., Kuehn, R. L., Display Systems Engineering, McGraw-Hill, New York, 1968

Security Classification

DOCUMENT CONTROL DATA - R & D

(Security classification of title, body of abstract and indexing annotation must be entered when the overall report is classified)

1. ORIGINATING ACTIVITY (Corporate author)
Xerox Corporation/Electro-Optical Systems
300 N. Halstead, Padadena, California 91107

2a. REPORT SECURITY CLASSIFICATION
Unclassified

2b. GROUP

3. REPORT TITLE
E/O SENSOR PERFORMANCE ANALYSIS AND SYNTHESIS
(TV/IR COMPARISON STUDY)

4. DESCRIPTIVE NOTES (Type of report and inclusive dates)
FINAL

5. AUTHOR(S) (First name, middle initial, last name)
Robert L. Sendall
Frederick A. Rosell

6. REPORT DATE
April 1973

7a. TOTAL NO. OF PAGES
282

7b. NO. OF REFS
44

8a. CONTRACT OR GRANT NO
F33615-71-C-1869

b. PROJECT NO.

c.

d.

9a. ORIGINATOR'S REPORT NUMBER(S)
1189 FINAL

9b. OTHER REPORT NO(S) (Any other numbers that may be assigned this report)
AFAL-TR-72-374

10. DISTRIBUTION STATEMENT
This document may be further distributed by any holder only with specific prior approval of AFAL/DO, Wright-Patterson Air Force Base, Ohio 45433

11. SUPPLEMENTARY NOTES

12. SPONSORING MILITARY ACTIVITY
Air Force Avionics Laboratory
Air Force Systems Command
Wright-Patterson Air Force Base, Ohio

13. ABSTRACT

TV (LLTV and ACTV) and IR (FLIR) sensors, as real-time imaging systems for night operations, have become competitive for many applications. While both systems provide TV-type displays for an operator to view and are used in a similar manner, their uncommon backgrounds (evolutions) have resulted in different descriptive parameters and specifications. This report describes the two types of systems in a parallel manner and language so that persons familiar with TV can better understand IR and vice versa. The sources of signal information; i.e., differences in reflectivity for the TV and differences in temperature for the IR are covered so as to provide a better understanding of the differences and similarities of the inputs. The man as the final element of the system is discussed using the theory that the operator is a spatial and temporal integrator. Then with the approach of Otto Schade, Sr., and the result of the psychophysical tests of the coauthor, Rosell, the systems are analyzed and performance prediction equations are derived. While a detection/recognition theory for predicting results against objects of general interest is presented, the three bar object is the basic object for performance definition and detection/recognition theory development. For the IR system, the threshold temperature difference between the bars and spaces of the test object which allows resolution of the bars is called the minimum resolvable temperature (MRT). It is a function of

DD FORM 1473

the spatial frequency of the object. In a similar manner, the contrast required for resolution of a 3-bar object is used to define the minimum resolvable contrast (MRC) as a function of spatial frequency for an ACTV system. Analysis is provided to permit the prediction of these performance parameters, and typical curves are provided. Finally, based upon the analysis, methods for comparing TV and IR systems in laboratory/field tests are presented. Suggestions are presented on how tests starting with controlled laboratory tests, then controlled field tests against laboratory objects, then limited controlled field tests against tactical type targets, and finally extensive semicontrolled field tests all using two controlled sensors side-by-side could be used for comparison.